Dissertation

submitted to the

Combined Faculties for the Natural Sciences and for Mathematics

of the Ruperto-Carola-University of Heidelberg (Germany)

for the degree of

Doctor of Natural Sciences

Put forward by

Siddharth Hegde

born in: Mangalore (India)

Oral examination: February 4, 2015

Remote Detection of

Life

in Extreme Exoplanetary Environments

Referees: Prof. Dr. Lisa Kaltenegger

Prof. Dr. Michael Hausmann

असतो मा सद्गमय
तमसो मा ज्योतिर्गमय
मृत्योर्मा अमृतं गमय

Asato Maa Sad-Gamaya

Tamaso Maa Jyotir-Gamaya

Mrtyor-Maa Amrtam-Gamaya

From ignorance, lead me to the truth

From darkness, lead me to the light

From death, lead me to immortality

- *Brihadaranyaka Upanishad* (1.3.28)

Abstract

The search for a second genesis of life outside Earth is now well and truly underway with the first rocky exoplanets detected in the central star's liquid water habitable zone. Recent results based on population studies show that small planets are abound in our galaxy. With the next generation of space- and ground-based telescopes on the horizon, it is critical to determine the best candidate exoplanets to follow up on for potential habitability and life.

This PhD thesis shows how colors of extreme Earth-like planets can be used as a first characterization when prioritizing exoplanets for spectroscopic follow up. We build a strong interdisciplinary link between geomicrobiology and observational astronomy, by exploring the color signatures of extremophiles as well as the various extreme niches that those organisms inhabit on Earth. In addition, we provide the first database of surface signatures of terrestrial life for a broad range of pigmented microorganisms, including ones isolated from Earth's most extreme environments. Our spectral library provides a broader and more realistic guide for the search for surface features of extraterrestrial life. The work presented in this thesis provides a first step toward characterizing a second Earth, in preparation for the next generation of space- and ground-based instruments, which will increase the chances of detecting life.

Zusammenfassung

Die Suche nach Planeten um andere Sterne zaehlt schon ueber tausend Planeten und mehrere tausende weitere Kandidaten, wobei kleine Planeten in der Mehrzahl sind. Dies eroffnet die Frage nach potentiellen Planeten, die habitable Bedingungen ermoeglichen und vielleicht sogar Leben beherrbergen. Die naechsten Generation von Teleskopen wird gerade gebaut und wird es uns zum ersten Mal ermoeglichen, solche Spuren auf anderen Planeten nachzuweisen. Daher ist die offene Frage wie man die Beobachtung von vielversprechenden Kandidaten optimieren koennte, um die interessantesten zu beobachten, ein wichtiger Schritt der Forschung.

In dieser Doktorarbeit untersuche ich, wie man die Farben von Extrasolaren Planeten als erste Characterisierung einsetzen kann, um eine Prioritaetenliste der Kandidaten zu erstellen. Die Arbeit verbindet interdisziplinaer Forschung in Mikrobiologie und Astronomie, indem sie die erste Datenbank von Reflektionspektren fuer ein breit gefaecherstes Feld von Mikroorganismen erstellt und diese in die Auswertung einbezieht. Die meisten dieser Mikroorganismen wurden in extremen Umgebungen der Erde gewonnen, um das breite Spektrum von Leben auf der Erde zu zeigen und koennten auf Extrasolaren Planeten unter anderen Bedingungen, die dominante Lebesform darstellen und auch die beobachtbare Reflektion der Oberflaeche eines Exoplaneten dominieren. Diese Doktorarbeit zeigt eine Mogelichkeit Planeten auf Grund ihrer Farben fuer weitere – zeitintensivere - Spektralanalyse zu prioritisieren und dadurch einen Weg, die Suche nach Leben im All zu optimieren.

To my parents
for always encouraging me to follow my dreams

Remote Detection of

Life

in Extreme Exoplanetary Environments

Contents

Table of Contents *i*

List of Illustrations *iii*

Preface *v*

Acknowledgements *vii*

1. Introduction 1

    1.1 The Holy Grail of Modern Astronomy 1

    1.2 Life in extreme environments 7

    1.3 Colors of Solar System planets 11

2. Colors of Extreme exo-Earth Environments 15

    2.1 Abstract 15

    2.2 Introduction 16

    2.3 Extremophiles on Earth 17

    2.4 Detectable surface features 19

    2.5 Results 23

    2.6 Discussion 27

    2.7 Conclusions 30

3. Surface biosignatures of exo-Earths 33

    3.1 Abstract 33

    3.2 Introduction 34

3.3 Materials and Methods 36
3.3.1 Sample preparation 36
3.3.2 Spectrometer system 37
3.3.3 Sample measurements 38
3.3.4 Microscopy 40
3.4 Results 42
3.5 Discussion 45
3.6 Model description 49
3.6.1 Simplifying assumptions 50
3.6.2 Case 1: Sample-substrate system with a light trap back 50
3.6.3 Case 2: Sample-substrate system with a spectralon back 54
3.6.4 Sample reflectance 56
3.7 Conclusions 61

4. Exploring colors of extreme exo-Earths 63
4.1 Abstract 63
4.2 Introduction 64
4.3 Surface reflection features of biota 65
4.4 Results 67
4.5 Discussion 70
4.6 Conclusions 73

5. Summary and Outlook 75

6. *Appendix* 77

7. *Bibliography* 217

List of Illustrations

Figures

1.1 Demographics of observed planetary population, p. 3

1.2 True occurrence of planets orbiting close to G- and K-type stars, p. 5

1.3 Stellar temperature versus insolation flux for Kepler planet candidates, p. 5

1.4 Estimated TESS exoplanet yield, p. 7

1.5 Distribution of known terrestrial life in the physical and geochemical parameter space, p. 8

1.6 Broadband filter photometry (smooth curves) and overlaid low-resolution spectra (non-smooth curves) for Solar System objects, p. 12

1.7 Color-color diagram of Solar System objects, p. 13

2.1 Characteristic reflection spectra of different surfaces on present-day Earth that are known to support extremophiles as well as bacterial mat, lichens, and trees, p. 22

2.2 Color-color diagram based on observed reflection spectra of characteristic surfaces that support extremophiles on Earth as well as bacterial mat, lichens, and trees (using conventional Johnson-Cousins BVI filters). Trees are shown here in black as reference to other VRE studies, p. 24

2.3 Color-color diagram based on observed reflection spectra of characteristic surfaces that support extremophiles as well as bacterial mat and lichens in (a) an aerobic atmosphere and (b) an anaerobic atmosphere, p. 25

2.4 Color-color diagrams and water, p. 28

3.1 Scanning Electron Microscope (SEM) images of sample cells deposited on a filter substrate, p. 39

3.2 Spectrometer system used in hemispherical reflectance measurements, p. 41

3.3 Diversity in reflectance spectra for eight sample organisms for (A) the entire measured spectral range (0.35-2.5 µm), and (B) only the VNIR portion (0.35-1.0 µm) of the spectrum, p. 43

3.4 Template of the sample description page showing the information provided (when available), p. 44

3.5 Effect of cell dehydration on the reflectance spectrum, p. 48

3.6 Spectral characteristics of the filter substrate used (plain, white, Millipore, HAWP02500), p. 49

3.7 Simplified illustration of the light interactions and multiple scattering between the sample layer and the filter substrate, p. 51

3.8 Spectral characteristics of the pressed barium sulfate powder that was used as a reference standard inside of the LI-COR 1800-12 integrating sphere, p. 52

3.9 Figure showing the uncertainty in the sample reflectance spectrum for a minimum (20%) and maximum (79%) fraction of filter substrate that can undergo forward scattering, p. 59

3.10 Figure showing the uncertainty in the sample reflectance spectrum for the minimum and maximum values that can be used for the parameter R_s in Eq. (3.17), p. 60

4.1 Color-color diagram showing the position of remotely detectable surfaces features of life for 137 microorganisms, p. 68

4.2 Color-color diagram showing the position of hypothetical exo-Earths covered with one of 137 diverse microorganisms as well as the Solar System objects with an atmosphere, p. 69

4.3 Color-color diagram distinguishing the different classes of planets, p. 71

Table

2.1 Classification of Extremophiles, p. 20

Preface

The work presented in this PhD thesis was performed at the Max Planck Institute for Astronomy, Germany and at NASA Ames Research Center, CA, USA in the period between April 2011 and December 2014 under the supervision of Prof. Dr. Lisa Kaltenegger, Prof. Dr. Thomas Henning, and Prof. Dr. Lynn Rothschild.

The thesis itself consists of five chapters:

Chapter 1

The first chapter consists of a brief overview on the current status of exoplanet detections and an update on the population statistics based on recent surveys. In addition, I provide a short introduction on the importance of extreme environments to astrobiology and the search for life outside the Solar System. The importance of colors in differentiating the types of planets in our Solar System is also touched upon to serve as a reference for the scientific chapters that follow.

Chapter 2

This chapter is based on the paper:

"Colors of Extreme Exo-Earth Environments" (2013)[*†], **Hegde, S.** & Kaltenegger, L., *Astrobiology*, vol. 13, no. 1, pp. 47-56.

[*] This paper was awarded the "Ernst Patzer Prize" for best-refereed paper by a PhD/early career postdoc at the MPIA/ZAH institutes in Heidelberg in 2013.

[†] The work based on this paper was awarded the "Best Poster Prize" for outstanding research and presentation at the 12th European Workshop on Astrobiology, EANA 2012 in Stockholm, Sweden.

In this chapter we explore the low-resolution characterization of an Earth-analog planet for different surface environments and the known extreme forms of life on Earth that such environments could harbor.

Chapter 3

This chapter is based on the paper:

"Surface biosignatures of exo-Earths: Remote detection of extraterrestrial life" (2014)[‡], **Hegde, S.** et al., *Proceedings of the National Academy of Sciences of the United States of America (PNAS)*, In Review.

We develop the first catalogue of reflectance spectra for a broad range of pigmented microorganisms, including ones that were isolated from Earth's most extreme environments. This catalogue provides a broad scope of surface signatures for life on exoplanets, which could provide different conditions than Earth, allowing for example, extremophiles on Earth to become the predominant life form. Much of the history of life on Earth has been dominated by microbial life, and it is likely that life on exoplanets evolve through single-celled stages first prior to multicellular creatures. Here, we present the first database for such surface features (also see *Appendix* for the complete database presented in this chapter) in preparation for the next generation of space- and ground-based telescopes that will search for a wide variety of life on exoplanets.

Chapter 4

In this chapter, we use low-resolution broadband filter photometry in the visible to near infrared portions of the electromagnetic spectrum to explore how color-color diagrams can help in prioritizing potentially habitable planets for detailed follow up. This work builds upon our previous study (Chapter 2) by including a diverse range of 137 surface biota (Chapter 3), a dataset that was recently added to the literature, in our analysis.

Chapter 5

Here, I summarize my thesis and touch upon some key results.

---

‡ Portion of this work was carried out at NASA Ames Research Center as part of the NASA Planetary Biology fellowship, awarded to Siddharth Hegde in 2013.

Acknowledgements

It gives me immense pleasure in submitting herewith my PhD thesis on the "Remote Detection of Life in Extreme Exoplanetary Environments." I have thoroughly enjoyed myself while working on this fascinating interdisciplinary field of exoplanet research and astrobiology.

I sincerely thank my supervisor Prof. Lisa Kaltenegger for her support and ever caring nature throughout the course of my PhD. In addition, I am also grateful to Prof. Thomas Henning and Prof. Joachim Wambsganss for being a part of my thesis committee and for providing me with valuable advise whenever they got a chance. A special thank you to Prof. Michael Hausmann for taking the time out to review my thesis especially during the Christmas holiday season.

I have been extremely fortunate to work at two institutes and in two vastly different fields in astronomy and microbiology during the course of my time as a doctoral student. Coming from a background in physics and astronomy, my time at NASA Ames Research Center was most fruitful where I gained valuable laboratory experience and insights into the biology world. I thank Prof. Lynn Rothschild for providing me with this opportunity, and for adopting me as part of her "laboratory family."

I am indebted to Susan Ustin and her wonderful team at University of California, Davis for providing me with unconditional access to her laboratory and the spectrometer system. In this regard, a special thanks to Maria Alsina-Marti for hosting my stay while at Davis, and for making me feel at home. They are some of the nicest and most helpful people that I have come across.

I am grateful to Vern Vanderbilt (NASA Ames), Sherry Palacios (NASA Ames), and Jeroen Bouwman (MPIA) for spending endless hours of discussion

with me. I thoroughly enjoyed my constructive debates with them, and it made science that much more fun and exciting for me.

I feel privileged to be a part of two research teams – at MPIA and at NASA Ames. I have learned so much from each of those groups and have made some really good friends for life. I extend my warmest thanks to Alissa Greenberg, Ivan G. Paulino-Lima, Ryan Kent, Sarah Rugheimer, Jesica Navarrete, Ian Crossfield, Yan Betremieux, and Yamila Miguel. I have endured some of my most difficult and testing times, both personal and professional, over the last three and half years, during the course of my PhD. In this regard, I would like to acknowledge the enormous support that I received from Sarah during those darker days of a graduate student's life, when all hope was lost and everything seemed bleak. This PhD has been as much a test and development of character, as it has been of the technical and scientific abilities.

I am grateful to all of the administrative and computing staff at MPIA. They have treated me like the "institute's child" and have forever given priority to all of my endless needs and wants. A big thanks to Ina Beckmann, Heide Seifert, Monica Dueck, Ingrid Apfel, Marco Piroth, Frank Witzel, Britta Witzel, and Ulrich Hiller. They made my life that much easier, which helped me focus on my work.

During the course of my research work, I have been privileged and lucky to receive endless financial support in terms of fellowships and awards. I thank Christian Fendt and the International Max Planck Research School for Astronomy and Cosmic Physics at the University of Heidelberg (IMPRS-HD), the Deutsche Forschungsgemeinschaft (DFG), the Simons Foundation on the Origins of Life, the Marine Biological Laboratory (MBL), the Patzer Foundation, and the National Aeronautics and Space Administration (NASA).

Finally, I would like to thank my parents who have been extremely supportive and patient with me. They have always believed in me throughout, regardless of my low and high points. I do not think much of my work would have progressed or be worth it without their everlasting love and encouragement.

Siddharth Hegde

Heidelberg, December 2014.

1

Introduction

ARTHUR C. CLARKE, in the year 1951, imagined a historian of the year 3000 looking back and writing:

> *"To us a thousand years later, the whole story of Mankind before the twentieth century seems like the prelude to some great drama, played on the narrow strip of stage before the curtain has risen and revealed the scenery. For countless generations of men, that tiny, crowded stage --- the planet Earth --- was the whole of creation, and they the only actors. Yet towards the close of the fabulous century, the curtain began slowly, inexorably to rise, and Man realized at last that the Earth was only one of many worlds. ...(T)he childhood of our race was over and history as we know it began ..."*

These words were written long before satellites had been launched into space and much before most of the technology used in detecting planets was developed.

1.1 The Holy Grail of Modern Astronomy

Are we alone in this Universe? Or are there other worlds out there that are similar to ours? The question has puzzled philosophers and scientists alike since the dawn of the ancient Greeks. The Greek philosopher Aristotle was of the opinion that the Earth was unique in the cosmos, while Epicurus thought otherwise, and believed that the number of worlds like the number of atoms was truly infinite. It took twenty-four centuries of debate and discussion before astronomers could finally answer the question that would prove the great Aristotle wrong!

Extrasolar planets, exoplanets, exo-Earths, super-Earths – these are current terms often used in the astronomy community while answering a question that is over two millennia old – Are there planets similar to ours out there in this Universe? The first breakthrough came in the year 1992 when two radio astronomers discovered planets orbiting around a pulsar (PSR 1257+12), a star in its final stage of stellar evolution (Wolszczan and Frail, 1992). That was odd and was least expected. How could a planet have survived a supernova explosion resulting in a pulsar? This was heartening and stirred much excitement among the scientific community. Surely, if planets are found orbiting such inhospitable environments, then they must be commonly found elsewhere orbiting around normal main sequence stars?

It was not long before two astronomers announced, in October 1995, using precise radial velocity measurements, that they had discovered a planet orbiting around 51 Pegasi, a Sun-like star! What was astonishing though, was not that a first planet discovery about a main sequence star had now been made, but the remarkable fact that this planet was about 0.47 times the mass of Jupiter and was orbiting its central star in only 4.2 days, that is eight times closer than Mercury is to our Sun (Mayor and Queloz, 1995). This did not resemble any planet in our Solar System, leave alone our home – planet Earth, since such close proximity between 51 Pegasi and its companion would leave the planet in scorching heat with surface temperatures upward of 1300 K.

The field has grown dramatically since then, and exoplanet discoveries are being reported at an unprecedented rate. As of this writing (December 2014), the exoplanet archive is host to 1854 planets associated with 1163 unique stars with 473 of those host stars harboring multiple planets (cf. http://exoplanet.eu/). In addition, over 4000 planet candidates are awaiting confirmation (cf. http://kepler.nasa.gov/). In particular, NASA's 10th Discovery mission, Kepler, launched in 2009, has changed the demographics of observed planetary population considerably. Fig. 1.1, top, shows a plot of mass (or minimum mass for non-transiting planets) versus orbital period for all non-Kepler discoveries with symbols color-coded representing the different discovery methods used. For the same figure, bottom, shows addition of Kepler planet candidate discoveries. The axis has been transformed from mass to radius for the plot at the bottom. For non-Kepler planets where the radius is unknown, they are estimated by using a polynomial function ($R = M^{0.4854}$) to fit the Solar System planets (Batalha, 2014).

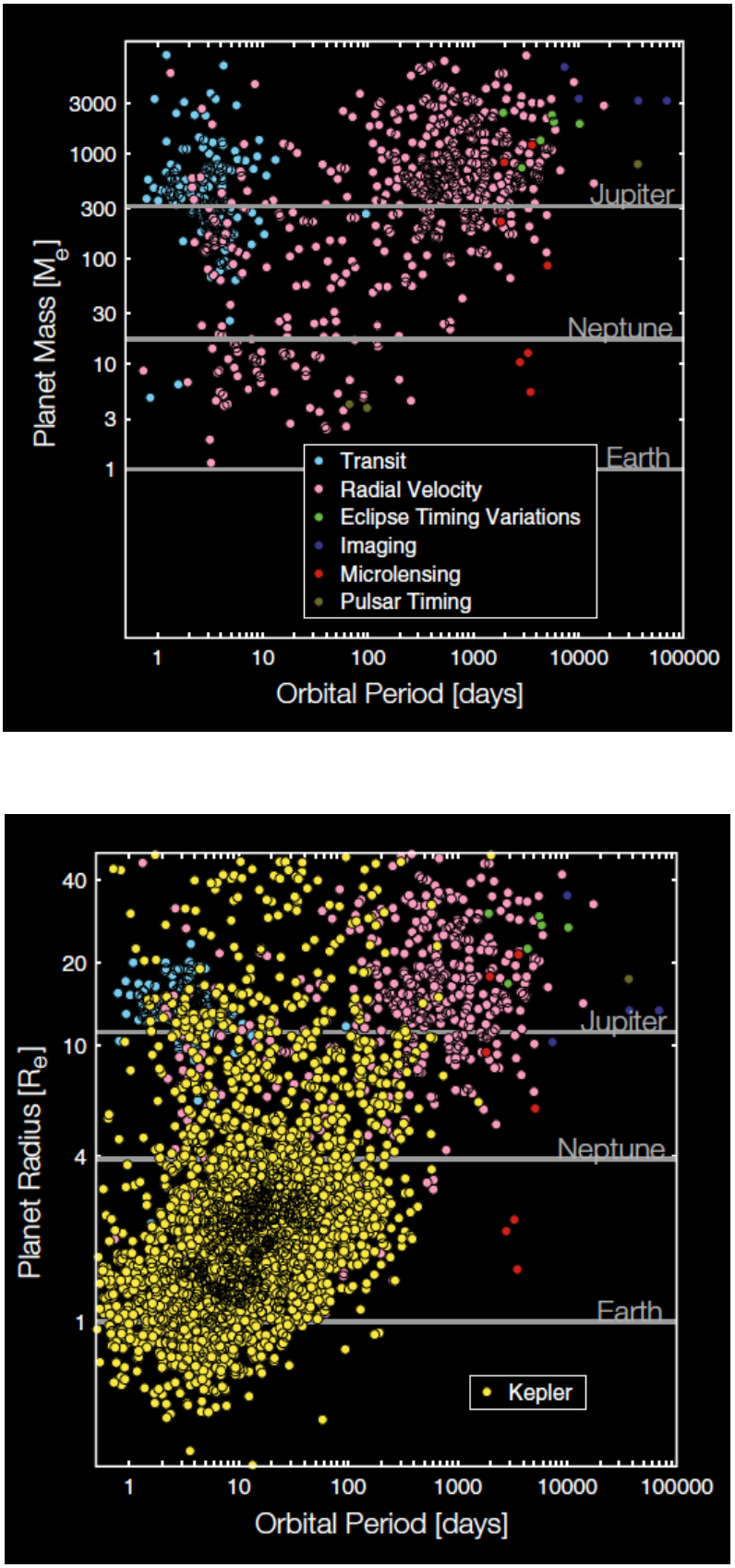

FIG. 1.1: Demographics of observed planetary population. (From Batalha, 2014)

As seen in the figure, Kepler has not only increased the number of planets substantially, but is also exploring an area of parameter space that was previously inaccessible. Furthermore, while 86% of non-Kepler planet discoveries are observed to have masses larger than Neptune, the opposite is true for Kepler discoveries, with 85% of planets having radii smaller than Neptune. Kepler has lifted our blinders to the small planets that are prevalent in our galaxy. Although most of the Kepler discoveries are planet candidates and are still awaiting confirmation, the overall reliability of the data is observed to be between 80-90% (Batalha, 2014), and therefore forms a good base for population statistics. Occurrence rate estimates based on the subsets of Kepler data that have been corrected for observation and detection biases, already indicate that small planets far outnumber the big ones in our galaxy (Fressin et al., 2013; Howard, 2013). This is illustrated in Fig. 1.2, depicting the true occurrence of planets in nature based on observations of transiting systems (top) and radial velocity surveys (bottom) for G- and K-type stars. Kepler has already transformed the discovery space revealing that nature produces smaller planets with relative ease when compared to the bigger ones especially in the warmer regions of a planetary system (see Batalha, 2014, Howard, 2013).

Kepler's primary mission objective is to determine the frequency of rocky planets in the habitable zone (HZ) of their central stars. The HZ, defined as a region around a star where a rocky planet can maintain liquid water on its surface, is a natural requirement when searching for planets with potential habitability. This is because all carbon-based life on Earth requires water as a necessary ingredient for life. The additional requirement that water be present on the surface is for remote sensing of such features in the planetary atmosphere.

Fig. 1.3 shows all Kepler planet candidates that have been analyzed from the first three years of data, in a plot of stellar effective temperature versus insolation flux received by the planet. The wider HZ in the figure (light green) refers to the "optimistic" HZ, with limits defined by insolation fluxes for when both Venus and Mars were thought to have surface liquid water (1.78–0.32 $F_{\oplus}$) (Kopparapu et al., 2014). The narrow HZ (dark green) refers to the "conservative" HZ with limits (1.02–0.35 $F_{\oplus}$) (Kopparapu et al., 2014) as defined by current climate models for an Earth-like planet with differing CO_2 and H_2O

concentrations, taking the planet to the two extremes, that are, the runaway greenhouse and the maximum greenhouse limits.

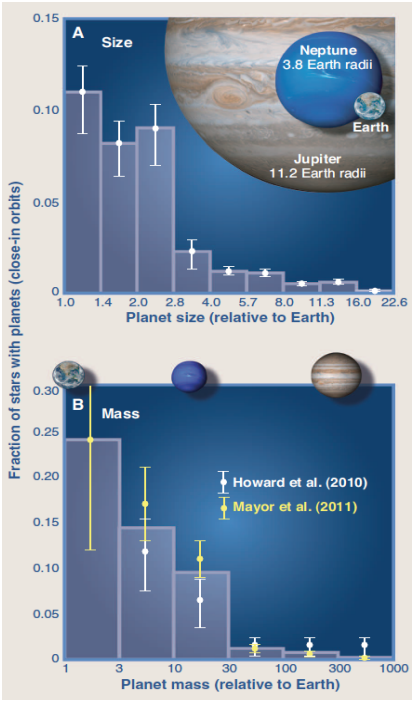

FIG. 1.2: True occurrence of planets orbiting close to G- and K-type stars. (From Howard, 2013)

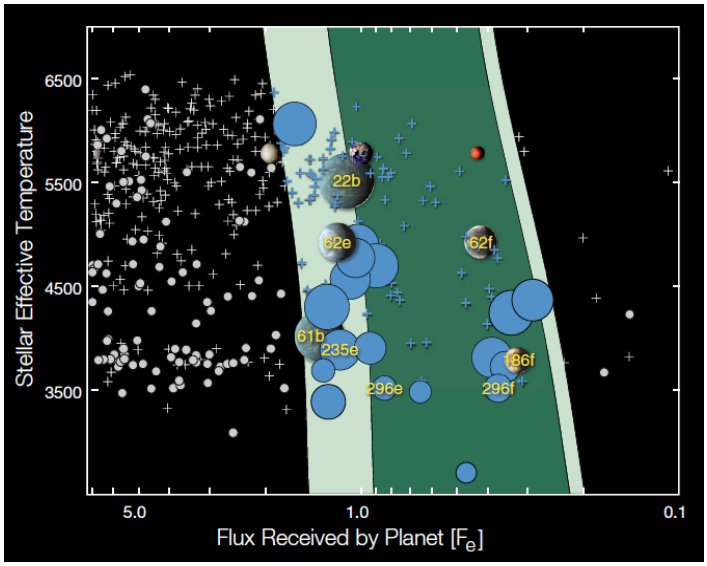

FIG. 1.3: Stellar temperature versus insolation flux for Kepler planet candidates.

Plusses and circles denote planets having radii larger and smaller that 2 $R_{\oplus}$, respectively. Symbols are in blue if they lie inside the HZ. (From Batalha, 2014)

Fig. 1.3 shows about 100 planet candidates that fall within the optimistic HZ, with 21 of those having radii smaller than 2 $R_{\oplus}$. These numbers are expected to rise even further in the coming years with Kepler's analysis phase now underway for the remainder of its most significant data. Statistical estimates based on initial Kepler data indicate that the average number of rocky planets (0.5-1.4 $R_{\oplus}$) in the optimistic HZ of M-type stars is approximately 0.5 (Dressing and Charbonneau, 2013; Kopparapu, 2013; Gaidos, 2013). Extrapolation of this data set to longer orbital periods for a sample of G- and K-type stars yields an occurrence rate of 22 ± 8% for a HZ planet (0.5-1.4 $R_{\oplus}$, optimistic HZ) (Petigura et al., 2013).

Kepler has lifted our blinders to the small planets that are common in our galaxy, and the exoplanet discovery space looks dramatically different now than it did before Kepler. Near-future missions like NASA's Transiting Exoplanet Survey Satellite (TESS, launch in 2017) (Ricker et al., 2014) and ESA's PLAnetary Transits and Oscillations of stars (PLATO, launch in 2024) (Rauer et al., 2014) are expected to further increase the number of small exoplanet detections considerably. While Kepler was designed to address the statistics of how common true Earth analogs are, the primary mission of TESS is to find out where the nearest transiting rocky exoplanets are located. TESS target stars will be a factor of 10 closer (and on average 100 times brighter) than those of Kepler (10^2 versus 10^3 light-yr) (Ricker et al., 2014). It is anticipated that TESS with its all sky survey will provide the best candidate exoplanets around M-dwarf stars that can be readily followed up for in-depth characterization on potential habitability. Fig. 1.4 shows the estimated yield of TESS exoplanet detections. Further ahead, PLATO is a precision photometry survey instrument that will observe patches of sky for several years. As such, PLATO will complement TESS in that it will be sensitive to long-period exoplanets.

All of these suggest that this is a golden era for exoplanet exploration, and that it may not be too far before we happen upon a planet that is similar to Earth or one that is potentially habitable.

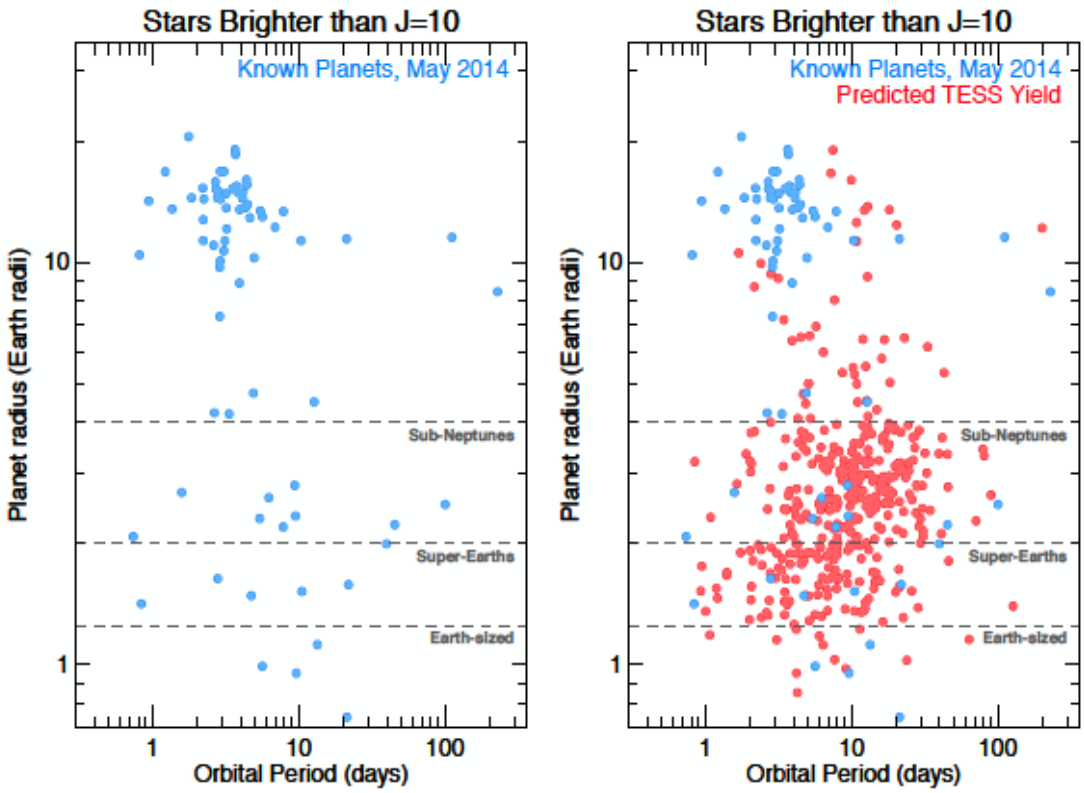

FIG. 1.4: Estimated TESS exoplanet yield.

The figure on the left shows currently known planets including those from Kepler and ground-based surveys. The figure on the right includes estimated TESS detections. (From Ricker et al., 2014)

1.2 Life in extreme environments

Observations of exoplanet discoveries so far showcase a broad range of diversity in terms of their masses (or radius), orbits, and host star type, suggesting that any environment on a planet is plausible within the laws of nature (Batalha, 2014; Seager, 2013). The stochastic nature of planet formation means that small changes in the initial conditions can have a major impact on the evolution of a planet, which may lead to a particular environment (physical or geochemical) being dominant, thereby governing the evolution of life on that planet. Therefore, an environment or niche that is considered extreme on present-day Earth could be predominant on a potentially habitable exoplanet. To increase our chances of detecting extraterrestrial life, one approach, when searching for potentially habitable exoplanets is to explore the environmental limits known on Earth that support extreme forms of life or "extremophiles." Although there is much debate on what "extreme" means, most of the

definitions are anthropocentric (see Rothschild and Mancinelli, 2001 for a detailed account on the philosophical issues). However, the more objective, and scientifically tenable definition currently accepted in the microbiology and astrobiology community is one in which extreme is that condition where it is difficult if not impossible for a carbon-based life form that uses water as a solvent to survive (Rothschild and Mancinelli, 2001). Hence, extremophiles are those organisms that live and thrive under such extreme conditions. As seen in Fig. 1.5, extremophiles cover a wide definition for life and provide us with the minimum known envelope of environmental limits for life on Earth.

A.

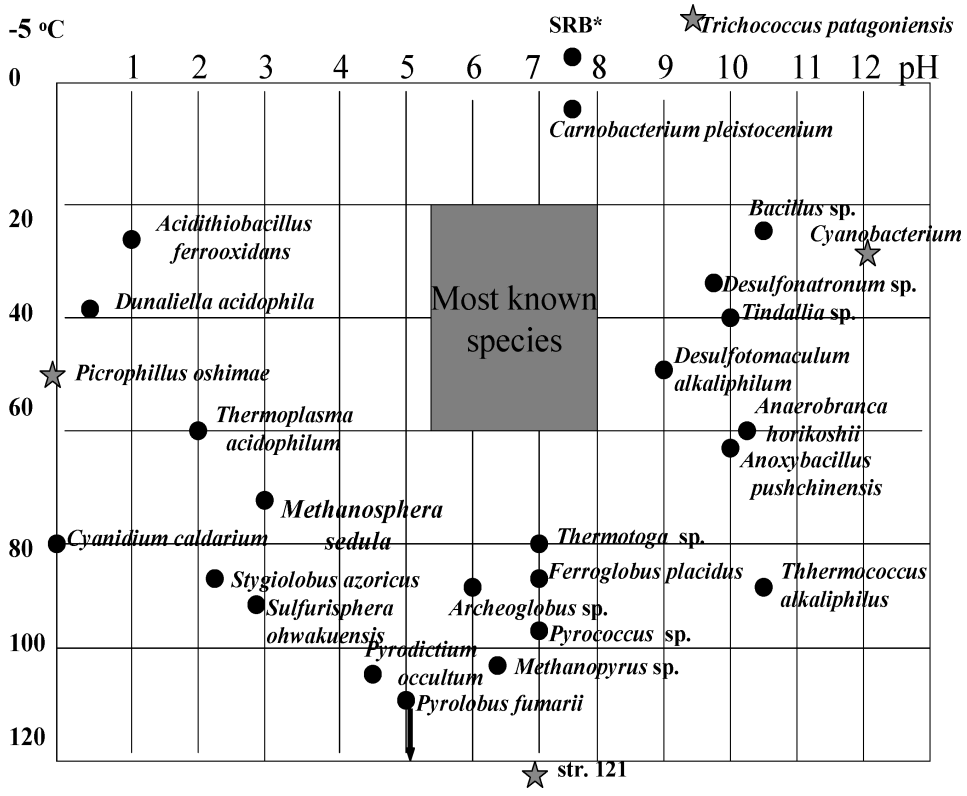

B.

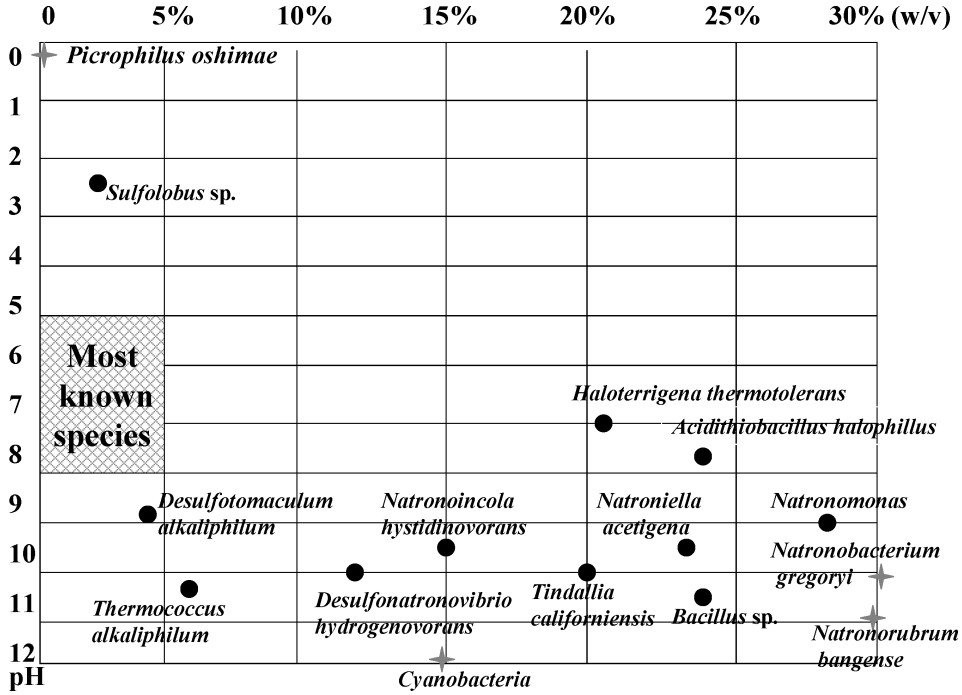
0
5%
10%
15%
20%
25%
30% (w/v)
0
1
2
3
4
5
6
7
8
9
10
11
12
pH
Most known species
Picrophilus oshimae
Sulfolobus sp.
Haloterrigena thermotolerans
Acidithiobacillus halophillus
Desulfotomaculum alkaliphilum
Natronoincola hystidinovorans
Natroniella acetigena
Natronomonas
Natronobacterium gregoryi
Thermococcus alkaliphilum
Desulfonatronovibrio hydrogenovorans
Tindallia californiensis
Bacillus sp.
Natronorubrum bangense
Cyanobacteria

C.

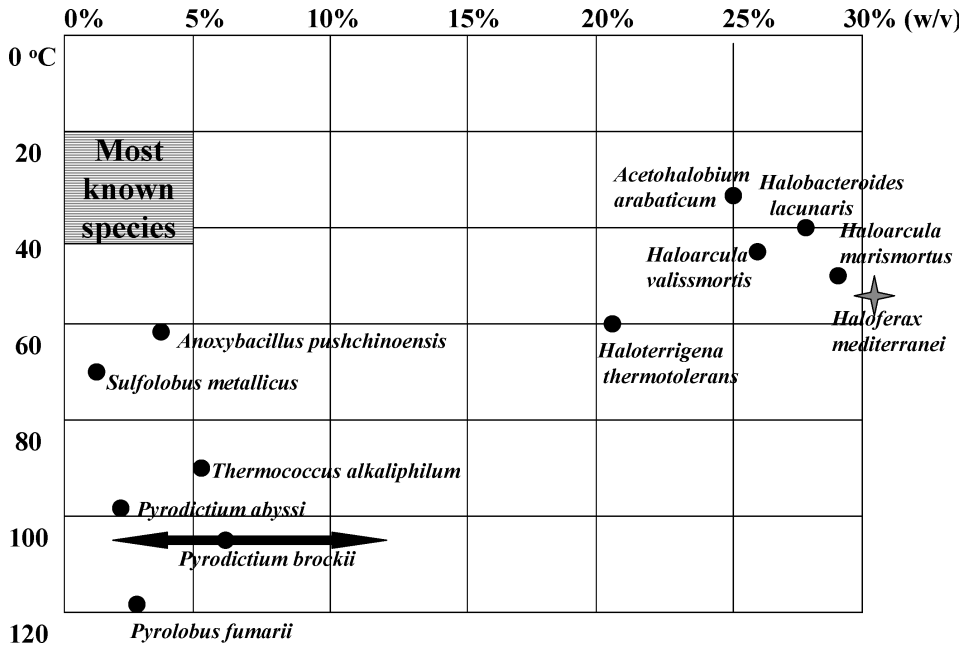
0%
5%
10%
15%
20%
25%
30% (w/v)
0 °C
20
40
60
80
100
120
Most known species
Acetohalobium arabaticum
Halobacteroides lacunaris
Haloarcula marismortus
Haloarcula valissmortis
Haloferax mediterranei
Anoxybacillus pushchinoensis
Haloterrigena thermotolerans
Sulfolobus metallicus
Thermococcus alkaliphilum
Pyrodictium abyssi
Pyrodictium brockii
Pyrolobus fumarii

D.

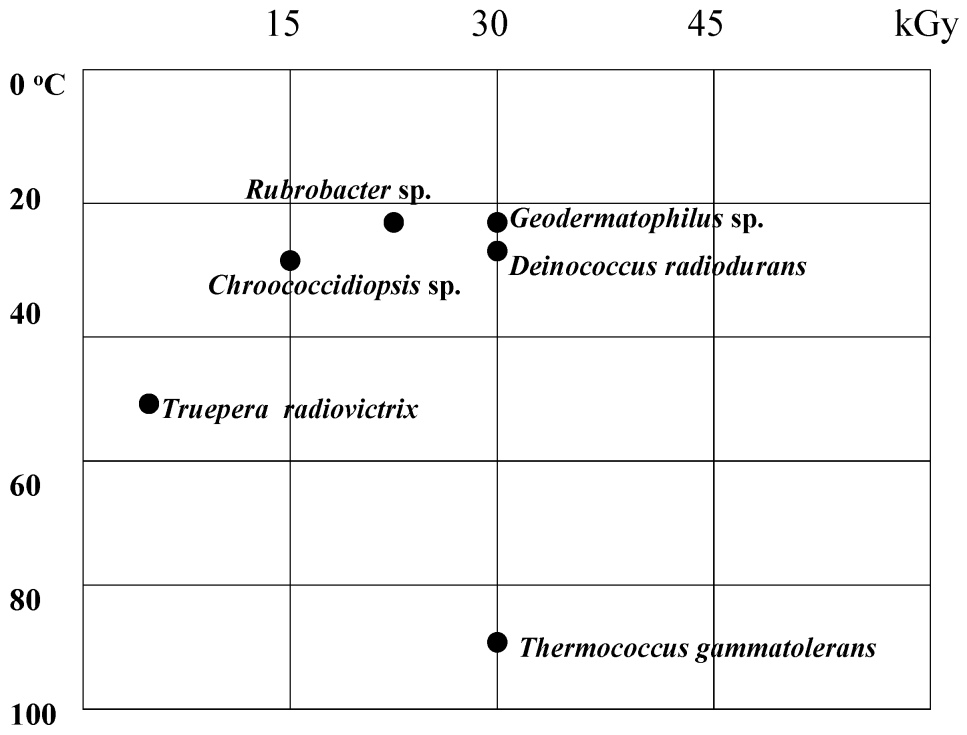

FIG. 1.5: Distribution of known terrestrial life in the physical and geochemical parameter space.

(A) pH versus Temperature; (B) Salinity versus pH; (C) Salinity versus Temperature; (D) Radiation versus Temperature. Asterisks indicate organisms currently known at an environmental limit. SRB = Sulfate-Reducing Bacteria. (From Pikuta et al., 2007)

The reader is referred to Section 2.3 as well as Table 2.1 for a general introduction on the different classes of extremophiles on Earth.

It is critical for an extremophile, like any other organism, to maintain cellular functions in order to carry out metabolic activities. The easiest approach usually undertaken by extremophiles is to keep the external environment out or to remove the problem as quickly as possible. If this becomes difficult, evolutionary responses kick-in, enhancing the repair and protective mechanisms in the organism, or alternatively alter the physiology of the organism (Rothschild and Mancinelli, 2001). Hence, extremophiles help us understand the evolutionary processes on Earth, which is useful when looking for life on potentially habitable exoplanets.

1.3 Colors of Solar System planets

Broadband filter photometry in the form of a color-color diagram provides a powerful and quick first approximation on the physical and atmospheric properties of a planet (see, e.g., Traub, 2003b; Crow et al., 2011). The color of a planet is useful in determining its planet type as proposed by Traub (Traub, 2003b). This is especially true in the visible portion of the electromagnetic spectrum where planet characterizability is excellent as seen in Fig. 1.6 for Solar System objects. The figure shows that the colors for each planet type are unique, with gas giants like Jupiter and Uranus both showing depressed red as well as blue albedos. Venus has a depressed blue albedo but otherwise has a flat reflectance due to its thick atmospheric cloud coverage. Earth has an enhanced blue albedo due to its strong Rayleigh scattering. Rocky objects with a thin or no atmosphere like the Moon, Mercury, and Mars are observed to have a smooth red albedo.

On plotting a color-color diagram using three equal width bands from 0.4 – 1.0 µm, differentiates the rocky planets from the gas giants for our Solar System as seen in Fig. 1.7 (Traub, 2003b). The figure shows that different planet types form groups. For instance, rocky planets with thin or no atmospheres group together in the "red-red" portion of the plot, as dusty surfaces reflect more toward longer wavelengths. At the other extreme of the plot, gas giants with deep molecular atmospheres group together in the "blue-blue" portion as a result of strong atmospheric methane absorptions. Outer planets like Jupiter, Saturn, and Titan are also seen to form a separate group in the plot, since their clouds prevent the methane absorptions from dominating the colors. Finally, Venus and Earth are seen to form their own color space as a result of their differing UV trends. These results for the Solar System objects show that broadband filter photometry in the form of a color-color plot can be used for differentiating the planet types as well as provide a first approximation on planet characterizability.

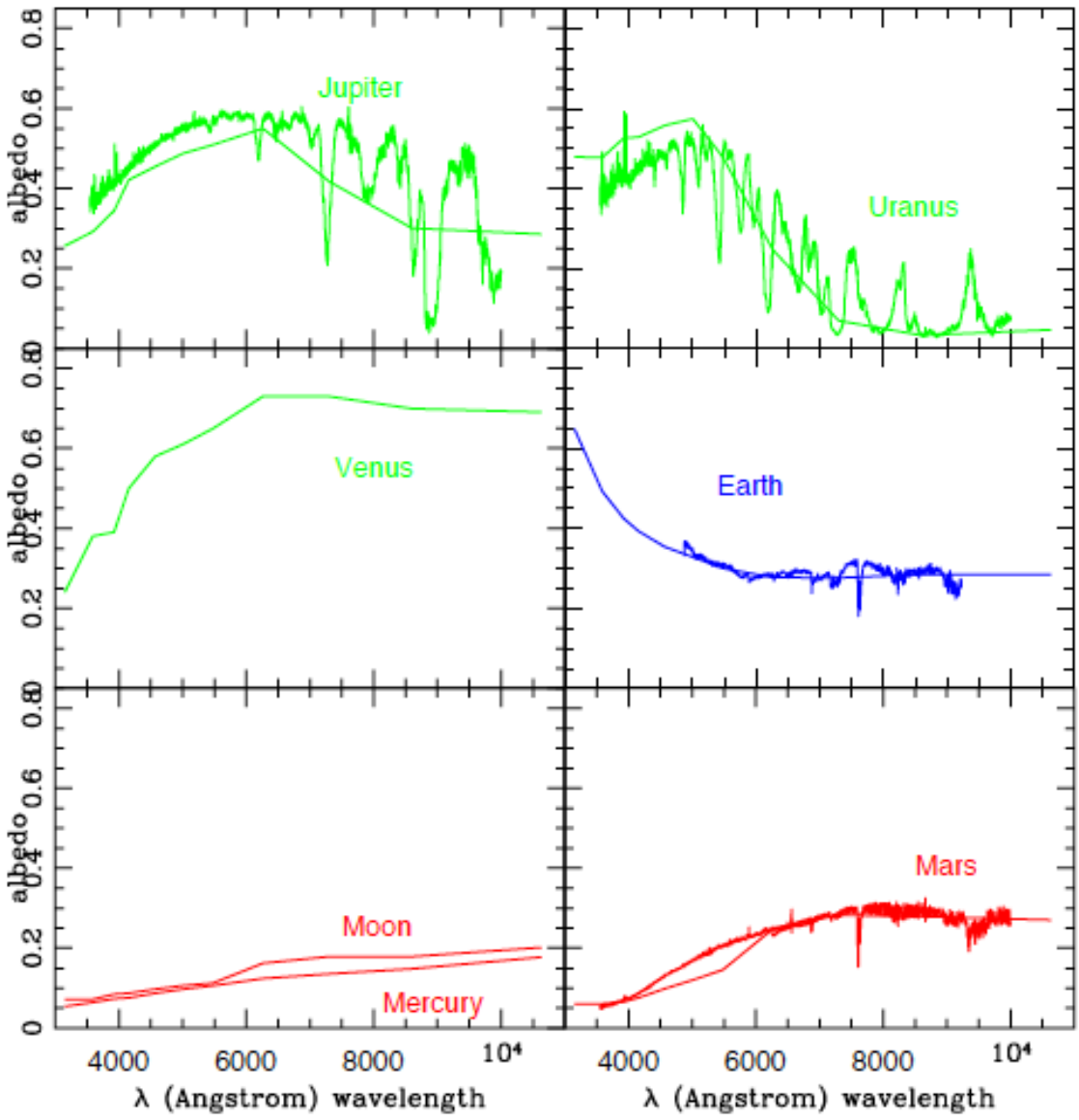

FIG. 1.6: Broadband filter photometry (smooth curves) and overlaid low-resolution spectra (non-smooth curves) for Solar System objects. (From Traub, 2003b)

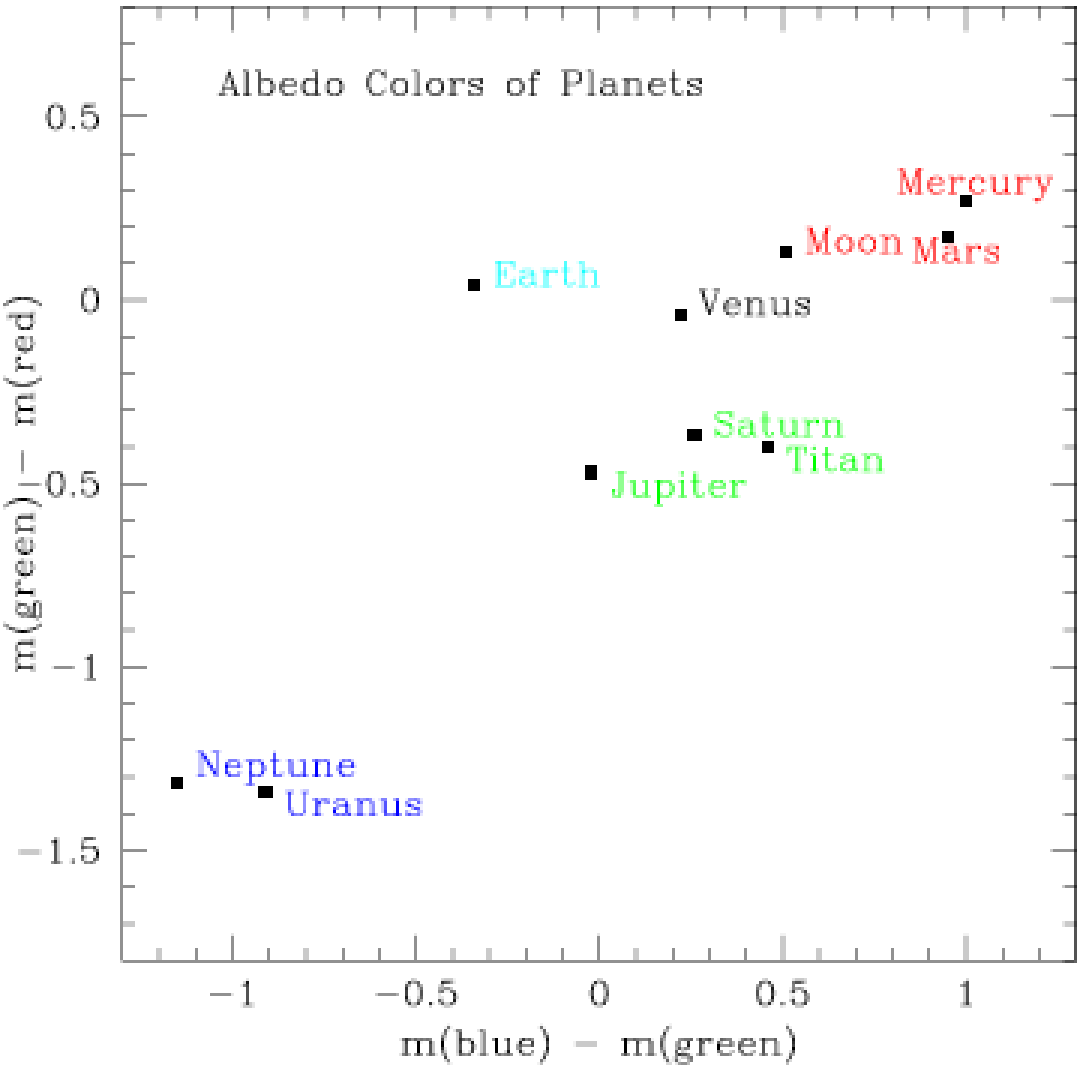

FIG. 1.7: Color-color diagram of Solar System objects.

The colors are obtained using customized filters: Blue=0.4-0.6 µm; Green=0.6-0.8 µm; and Red=0.8-1.0 µm. (From Traub, 2003b)

This PhD thesis focuses on Earth-like planets within this framework to explore how broadband filter photometry in the visible to near infrared portions of the electromagnetic spectrum can help prioritize rocky exoplanet targets for follow up spectroscopic characterization. Chapter 2 focuses on the remote differentiation of exo-Earths dominated by various surface environments found on Earth that support extreme forms of life (From Hegde and Kaltenegger, 2013). Chapter 3 presents the first spectral database of surface reflectance from 0.35 – 2.5 µm for 137 phylogenetically diverse microorganisms, including ones isolated from some of Earth's most extreme environments (From, Hegde et al.,

2014) (Also, see *Appendix* for detailed information on the sample description and reflectance characteristics). Chapter 4 makes use of these measured surface biosignatures by exploring the color signatures of exo-Earths dominated by such life forms for remote detection of extraterrestrial surface life. Chapter 5 concludes by presenting our summary and outlook.

With several big space (JWST) and ground-based (E-ELT, GMT, TMT) telescopes on the horizon that will provide the first opportunity to characterize rocky exoplanets, but will have limited observation time available, it becomes critical to prioritize exoplanets for follow up spectroscopic characterization. The work presented in this PhD thesis provides an initial characterization for rocky exoplanets that will help prioritize targets, and will increase the chances of finding a potentially habitable planet.

2

Colors of Extreme Exo-Earth Environments

From Hegde & Kaltenegger (2013): *Astrobiology, vol. 13, no. 1, p. 47-56*

2.1 Abstract

The search for extrasolar planets has already detected rocky planets and several planetary candidates with minimum masses that are consistent with rocky planets in the habitable zone of their host stars. A low-resolution spectrum in the form of a color-color diagram of an exoplanet is likely to be one of the first post-detection quantities to be measured for the case of direct detection.

In this chapter, we explore potentially detectable surface features on rocky exoplanets and their connection to, and importance as, a habitat for extremophiles, as known on Earth. Extremophiles provide us with the minimum known envelope of environmental limits for life on our planet.

The color of a planet reveals information on its properties, especially for surface features of rocky planets with clear atmospheres. We use filter photometry in the visible waveband as a first step in the characterization of rocky exoplanets to prioritize targets for follow-up spectroscopy.

Many surface environments on Earth have characteristic albedos and occupy a different color space in the visible waveband (0.4-0.9 μm) that can be distinguished remotely. These detectable surface features can be linked to the extreme niches that support extremophiles on Earth and provide a link between geomicrobiology and observational astronomy. This chapter explores how filter photometry can serve as a first step in characterizing Earth-like exoplanets for an aerobic as well as an anaerobic atmosphere, thereby prioritizing targets to search for atmospheric biosignatures.

2.2 Introduction

Several rocky (e.g., Léger et al., 2009; Batalha et al., 2011) as well as potentially rocky (e.g., Mayor et al., 2009, 2011) exoplanets have been detected. Three super-Earths, consistent with rocky planetary models, Gliese 581d, HD 85512b, and Gliese 667Cc orbit their host stars within the habitable zone (Udry et al., 2007; Bonfils et al., 2011; Pepe et al., 2011; Anglada-Escudé et al., 2012). In addition, NASA's Kepler mission has recently announced several potentially rocky exoplanet candidates (see Batalha et al., 2012; Borucki et al., 2011, 2012) in the habitable zone.

A comprehensive suite of tools will be needed to characterize such planets since a mere detection of a rocky planet in the habitable zone does not guarantee the planet to be habitable (e.g., Selsis et al., 2007; Kaltenegger and Sasselov, 2011). For the case of direct detection of exoplanets, detailed characterization in regard to the habitability of Earth-like extrasolar planets or "exo-Earths" is achieved by studying the atmospheric and surface properties of the planet in contention. Filter photometry is a tool with which to initially characterize exoplanets. A color-color diagram distinguishes giant planets from rocky ones for Solar System objects (see Traub, 2003b; Crow et al., 2011, for details).

The position of an extrasolar planet in a color-color plot can in principle show analogies to the Solar System, approximate the basic physical properties of a planet (Traub, 2003a, 2003b), and place constraints on its atmospheric composition (Crow et al., 2011). Exploring surface features of Earth-like planets becomes possible if either no significant cloud cover exists on an exoplanet or the signal-to-noise ratio (SNR) of each observation is sufficiently high to remove the cloud contribution from the overall detected signal (e.g., Ford et al., 2001; Pallé et al., 2008; Cowan et al., 2009, 2011; Fujii et al., 2011).

In this chapter, we focus on Earth-like planets within this framework and especially on remote differentiation of the different environments found on Earth that are known to support extreme forms of life or "extremophiles." Small changes in temperature, pH, or other physical and geochemical factors (see section 2.3) can lead to such environments being dominant on a potentially habitable exoplanet, which could govern evolution of life. These various "extreme" surface environments on Earth have characteristic albedos in the visible waveband (0.4-0.9 μm) that could be distinguished remotely. We

therefore explore the color signatures that are obtained from the surface environments inhabited by extremophiles as well as test our approach by using measured reflection spectra of extremophiles.

Note that detection of such surface features of environments in a reflection spectrum alone is not a reliable detection of life on an exoplanet. This diagnostic can only be used in combination with atmospheric properties (see, e.g., Cockell et al., 2009).

Several groups have focused their attention on the vegetation red edge (VRE) (also known as the chlorophyll signature) to detect direct signatures of life remotely (e.g., Arnold et al., 2002; Woolf et al., 2002; Seager et al., 2005; Montañés-Rodríguez et al., 2006; Tinetti et al., 2006; Kiang et al., 2007a, 2007b). The VRE is a surface feature of terrestrial land plants that has been widespread since about 460 million years ago (Carroll, 2001; Igamberdiev and Lea, 2006; Kiang et al., 2007a) and is characterized by a strong increase in the reflectivity at near-IR wavelength regions longward of 0.75 µm. In this chapter, we expand that approach for different life-forms by including surfaces that provide environmental conditions for extremophiles on Earth over geological times. We consider different classes of extremophiles that have adapted to severe physical or geochemical extremes in order to explore the known limits for habitability on exoplanets. We thereby link geomicrobiology to observational astronomy by exploring the low-resolution characterization of an Earth analog planet for different surface environments and the known extreme forms of life on Earth that such environments could harbor.

In this chapter, Section 2.3 discusses the different types of extremophiles on Earth. Section 2.4 focuses on surface characteristics of different environments that support extremophiles and links those extreme environments to remotely detectable observables. Section 2.5 presents our results with a low-resolution color-color diagram to distinguish the different environments, explores the effect of mixed surfaces, and builds a link to extremophiles for aerobic and anaerobic atmospheres. We discuss our results in Section 2.6 and conclude in Section 2.7.

2.3 Extremophiles on Earth

The search for life on extrasolar planets relies on defining limits for life in regard to its evolution and distribution as observed on Earth. These limiting

factors in turn correspond to physical or chemical parameters, which act as templates while looking for life elsewhere. To provide a wide definition, we therefore focus on organisms that live under extreme conditions on Earth. Extremophiles (literally "lovers of extreme environments") are organisms that live and thrive in very harsh environmental conditions. These environmental "extremes" are defined in terms of physical (such as temperature, radiation, pressure, etc.) and geochemical (desiccation, salinity, pH, etc.) extremes (see, e.g., Rothschild and Mancinelli, 2001). Observations on Earth indicate that life is ubiquitous even in extreme niches as long as there is liquid water, an energy source for metabolism, and a source of nutrients that helps in building and maintaining cellular structures (Rothschild, 2009).

We explore the parameter space of extremophiles to look for signatures of extraterranean life by focusing on extreme environments that those organisms inhabit on Earth.

Table 2.1 shows that multiple organisms have evolved to function at different environmental extremes (e.g., temperature, pH), which suggests that such evolutionary adaptation is not a singular event (Rothschild, 2008) and carbon-based life-forms may evolve in similar environments on extrasolar rocky planets. Regarding temperature extremes, extremophiles are categorized as hyperthermophiles (temperature for growth is $>80^{\circ}C$) that are, for example, isolated from submarine hydrothermal vents, and psychrophiles (temperature for growth is $<15^{\circ}C$) that are, for example, isolated from glaciers. Alkaliphiles grow at a pH >9 and are found, for example, in soda lakes; acidophiles grow at pH <5 and are, for example, found in acid mine drainages. Piezophiles are organisms that thrive under extreme pressure conditions such as the Mariana Trench, which has a hydrostatic pressure of ~1,100 bars (Marion et al., 2003). Halophiles grow under high salt concentrations and can be found, for example, in salt lakes. Xerophiles grow with very little water and reside, for example, in sand deserts, ice deserts, and salt flats like the Atacama Desert in Chile. Endoliths live inside rocks such as sandstone, which protect the organisms by attenuating the UV radiation while allowing the photosynthetically active radiation through its upper translucent surface (Southam et al., 2007) and thereby allowing for photosynthetic metabolism. This phenomenon is often described as "cryptic photosynthesis" due to the effective shielding of any specific reflection signature that could indicate the biota by the overlying rock surface in the reflection spectrum. Rocks protect the organisms residing within

against low temperatures, UV radiation, and severe desiccation (Cockell et al., 2009; Canganella and Wiegel, 2011). Endolithic communities are also found in complete darkness, whereby they receive their energy by reducing sulfate and iron among other metals found in the host rock (Cavicchioli, 2002).

Limits as stated in Table 2.1 for the different classes of extremophiles are based on activity and not mere survival, except for radiation. Radiation-tolerant extremophiles survive high doses of ionizing and UV radiation but do not grow optimally under those conditions, as is seen in laboratory experiments (Venkateswaran et al., 2000; Rothschild and Mancinelli, 2001). Exceptional levels of ionizing and UV radiation rarely occur naturally on present-day Earth, and the tolerance of extremophiles to radiation is suggested to be a by-product of their resistance to desiccation (Mattimore and Battista, 1996; Battista, 1997; Ferreira et al., 1999).

2.4 Detectable surface features

Table 2.1 shows that most extremophiles live in subsurface conditions either as a measure to protect themselves or a means to gain access to the required nutrients provided by the host environment. Therefore, when observing surface features remotely, unlike surface vegetation, one does not generally detect extremophiles in a reflection spectrum unless the extremophilic organism is living close to or on top of the surface environment. In this chapter, we focus on the surface features of environments that support extremophiles residing within them. To complement the approach, we also include the albedos of extremophiles in our study when available, to show the applicability to surface reflection of extremophiles as well. Table 2.1 shows the extreme environment or source that supports the various classes of extremophiles and the surface features that are detectable remotely. The data for these spectra were obtained from the ASTER spectral library (Baldridge et al., 2009) and the USGS digital spectral library (Clark et al., 2007).

Table 2.1

Environmental Parameter	Class	Defining Growth Condition	Environment / Source	Remotely Detectable Observable	Example Organisms
High Temperature	Hyperthermophile Thermophile	> 80 °C 60 - 80 °C	Submarine Hydrothermal Vents Hot Spring	Water	*Pyrolobus fumarii, Strain 121* *Synechococcus lividis, Sulfolobus* sp.
Low Temperature	Psychrophile	< 15 °C	Ice, Snow	Ice, Snow	*Psychrobacter, Methanogenium* spp.
High pH	Alkaliphile	ph > 9	Soda Lakes	Salt	*Bacillus firmus OF4,* *Haloanaerobium alcaliphilum*
Low pH	Acidophile	ph < 5 (typically much less)	Acid Mine Drainage, Volcanic Springs	Acid Mine Drainage	*Picrophilus oshimae/torridus,* *Stygiolobus azoricus*
High Pressure	Piezophile	High pressure	Deep Ocean eg. Mariana Trench	Water	*M.kandleri, Pyrococcus* sp., *Colwellia* sp.
Radiation	-	Tolerates high levels of radiation	Sunlight eg. High UV radiation	Sand, Rocks	*Deinococcus radiodurans,* *Thermococcus gammatolerans*
Salinity	Halophile	2 - 5 M NaCl	Salt Lakes, Salt Mines	Salt	*Halobacteriaceae, Dunaliella salina,* *Halanaerobacter* sp.
Desiccation	Xerophile	Anhydrobiotic	Desert, Rock surfaces	Sand, Rocks	*Artemia salina, Deinococcus* sp., *Lichens, Methanosarcina barkeri*
Rock-dwelling	Endolith	Resident in rock	Upper subsurface to deep subterranean	Rocks	*Lichens, Cyanobacteria,* *Desulfovibrio cavernae*

Table 2.1: Classification of Extremophiles.

"Remotely Detectable Observable" denotes the surface reflection signatures that can be observed remotely for the extreme environments considered here, which support different classes of extremophiles. Adapted from Rothschild and Mancinelli (2001), Cavicchioli (2002), Marion et al. (2003), Pikuta et al. (2007), Rothschild (2009), Canganella and Wiegel (2011).

The direct albedos of the extremophiles obtained from the spectral libraries were limited to a sample of three organisms that is composed of lichens, bacterial mats, and red algae in acid mine drainage (AMD) and have been included in this work. Lichens are composite organisms that consist of a fungus with a photosynthetic partner, usually either a green alga or cyanobacterium (Marion et al., 2003). Lichens are desiccation-resistant and occur at some of the most extreme environments on Earth, such as hot deserts, but are also found on top of rock surfaces. The bacterial mat spectrum used here is composed of two thermophilic species, the photosynthetic bacterium *Chloroflexus aurantiacus* and the cyanobacterium *Synechococcus lividus,* which are found at Octopus Springs in Yellowstone National Park, USA. This microbial mat forms at a temperature of ~65°C (Rothschild and Mancinelli, 2001), which is cool compared to the temperature regimes occupied by the hyperthermophilic organisms in hydrothermal vents [>110°C (Marion et al., 2003)]. The lower temperature still permits photosynthesis, as chlorophyll breaks down above ~75°C (Rothschild and Mancinelli, 2001). Hence, these organisms grow very close to the water's surface such that they receive enough sunlight to carry out photosynthesis; therefore, the reflection spectrum of the microbial mat will have a major contribution to the overall albedo [measured on site with a field spectrometer (Clark et al., 2007)]. The spectrum of red algae in AMD is one where red algae are coating rocks at ~10 cm depth below the surface.

Some surfaces, such as water, can be linked to several extremophiles like hyperthermophiles in submarine hydrothermal vents as well as piezophiles found deep in the ocean. Snow can be linked to psychrophiles living in cold environments in this model. Soda lake, a type of salt lake with a high content of sodium salts, in particular, chlorides or sulfates, can be linked to both alkaliphiles as well as halophiles. AMD links to Acidophiles. Sand is used here as the surface feature for xerophiles and radiation-resistant extremophiles. Finally, exposed rocks like limestone link to endoliths that live inside the rock as well as xerophiles and radiation-resistant organisms, which live on the rock surface. Note that some surface features like water are not a unique indicator for extreme environments and can also indicate environmental conditions that are not extreme. Our aim in this work is to explore a wide range of surfaces that can support extreme forms of life. But the reverse, that these surfaces all need to support life, is not given. By considering the range of extreme environments, we also include non-extreme forms of life in our model.

Information on a planet's potential habitability can only be obtained once atmospheric properties and biosignatures are detected in the planet's atmosphere. The results obtained in this work aim to prioritize targets for spectroscopic characterization. The method presented here provides a first characterization for prioritizing exoplanet targets for follow-up spectroscopy.

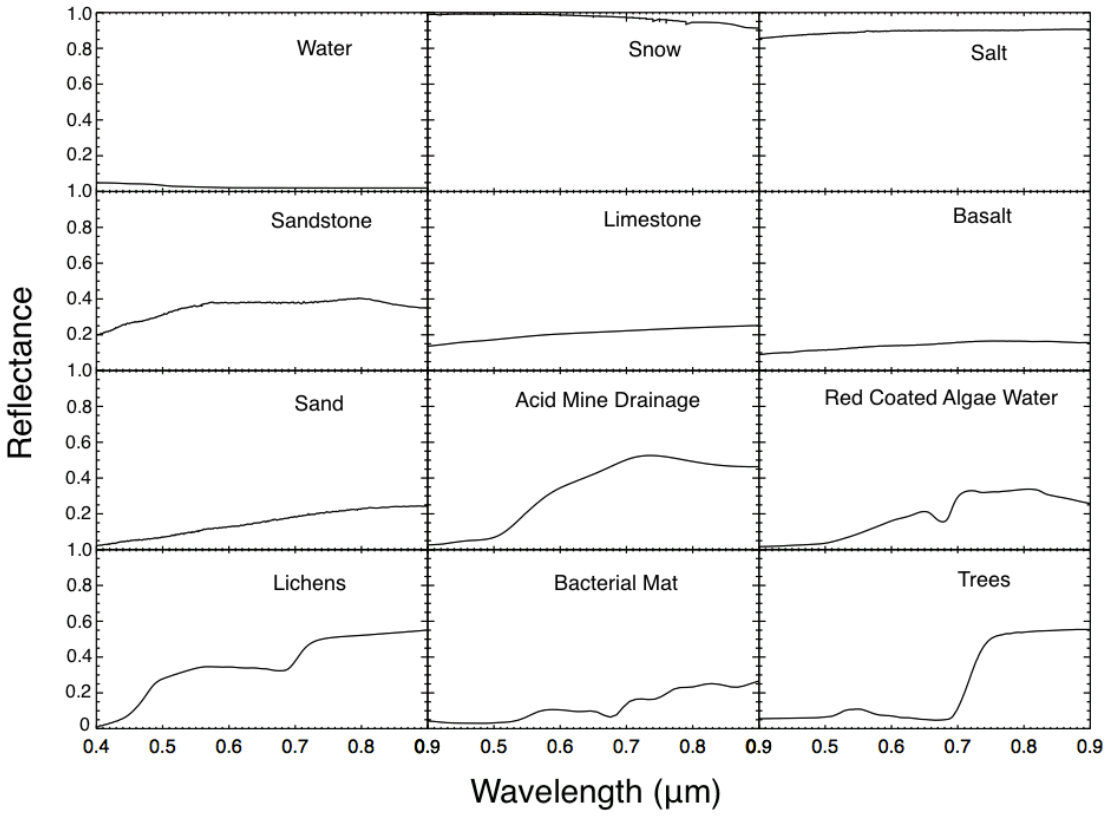

FIG. 2.1: Characteristic reflection spectra of different surfaces on present-day Earth that are known to support extremophiles as well as bacterial mat[1], lichens, and trees[2].

[1] The bacterial mat spectrum used here is composed of two thermophilic species, the photosynthetic bacterium *Chloroflexus aurantiacus* and the cyanobacterium *Synechococcus lividus*.

[2] Data obtained from the ASTER spectral library (Baldridge et al., 2009) and the USGS digital spectral library (Clark et al., 2007).

Fig. 2.1 shows the corresponding surface albedo for water, snow, salt, sandstone, limestone, basalt, sand, AMD, red coated algae water, lichens, bacterial mat, and trees. Apart from the remotely detectable surface features for extreme environments, we also include trees (deciduous) for vegetation (VRE signature), as a reference to other studies for comparison. Other terrestrial land plants occupy a similar position in our color-color diagram.

2.5 Results

Using the albedos of extremophiles as well as different surfaces they reside in as shown in Fig. 2.1, we explore the low-resolution characterization of rocky Earth-like extrasolar planets in the visible waveband (0.4-0.9 μm) by making use of a color-color diagram. Note that here we inherently assume an Earth analog atmosphere and suppression of the stellar light to make this comparison (see Discussion). To assess general detectability, we first assume full surface coverage of a particular surface (e.g., water, snow). Using these approximations, we use a color-color diagram to distinguish planetary environments remotely.

Color is the difference of magnitudes in two filter bands and is defined as:

$$C_{AB} = A - B = -2.5 \log_{10}\left(\frac{r_A}{r_B}\right) \tag{2.1}$$

where, r_A is the reflectivity in band A and r_B in band B.

We use the standard Johnson-Cousins BVI broadband filters, blue (B) = 0.4-0.5 μm, visible (V) = 0.5-0.7 μm, near-IR (I) = 0.7-0.9 μm, here. In principle, any number of filter bands can be used as long as the bandpass definitions are larger than the expected measurement noise and there is a high enough signal available per filter, which would allow finer distinctions.

Fig. 2.2 shows the B-V versus B-I color-color diagram, which distinguishes the environments (shown in Fig. 2.1) clearly. Surfaces with high reflectivities—snow, salt, and rocks that support endoliths, such as sandstone, limestone, and basalt—group together, as indicated by color coding in Fig. 2.2. Trees are shown as a reference to other VRE studies. Trees do not group with the other photosynthesis-based species considered here that contain chlorophyll pigments

like the *Synechococcus*-bearing bacterial mats or lichens (see Discussion). AMD and red coated algae water (i.e., AMD water with red alga living at ~10 cm depth below the surface) group together.

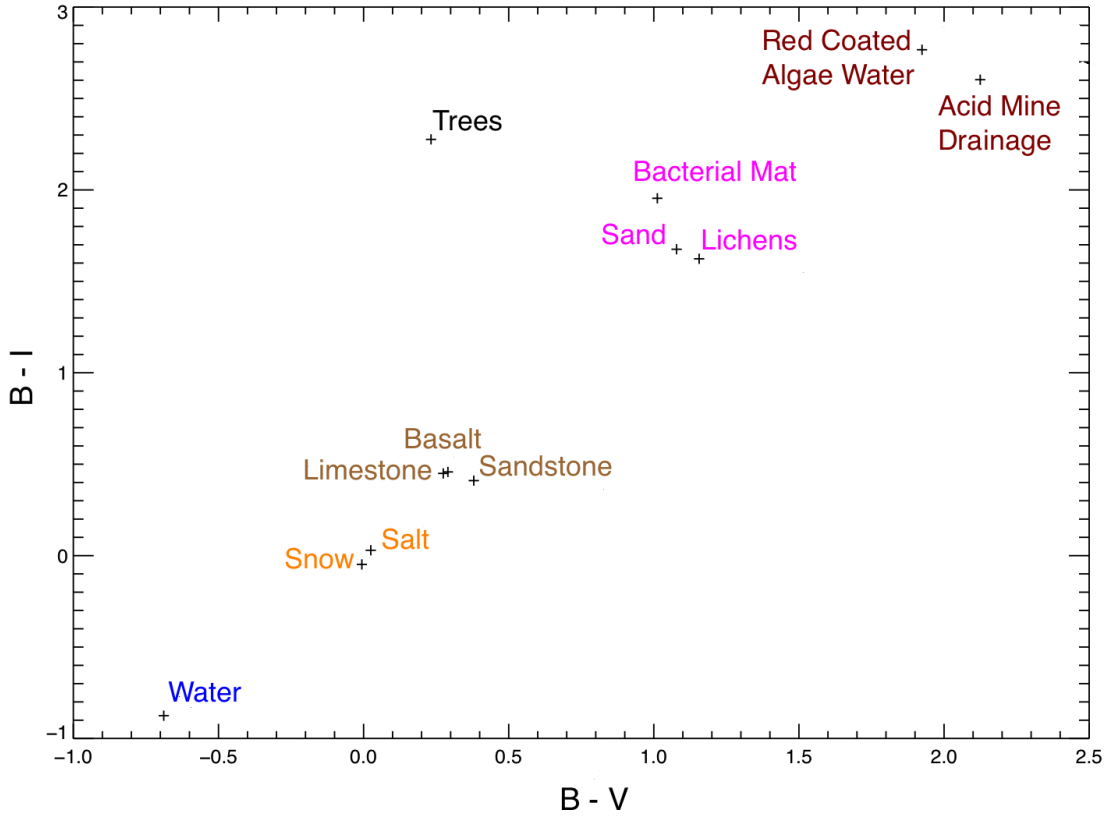

FIG. 2.2: Color-color diagram based on observed reflection spectra of characteristic surfaces that support extremophiles on Earth as well as bacterial mat, lichens, and trees (using conventional Johnson-Cousins BVI filters). Trees are shown here in black as reference to other VRE studies.

Our results indicate that different surface types can be distinguished in a color-color diagram. Highly reflective surfaces like snow, salt, and the different rocks form two distinct groups. AMD and red algae at ~10 cm depth in AMD group together, which suggests that extremophiles living in subsurface conditions can be linked to remotely detectable surface features.

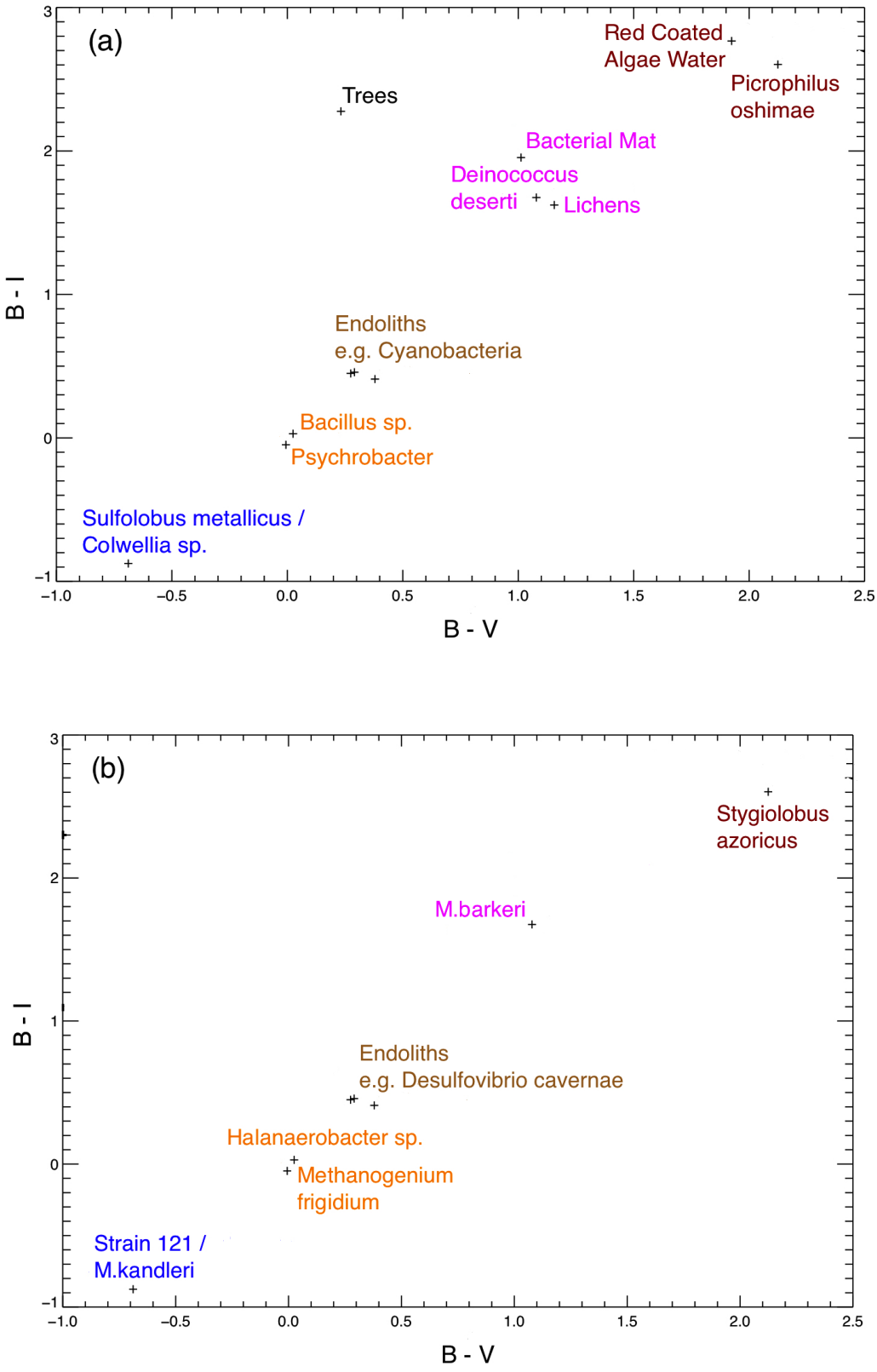

FIG. 2.3: Color-color diagram based on observed reflection spectra of characteristic surfaces that support extremophiles as well as bacterial mat and lichens in (a) an aerobic atmosphere (top) and (b) an anaerobic atmosphere (bottom).

Fig. 2.3 links the remotely detectable surface features to habitability with the use of different kinds of extremophiles that exist under extreme environments on Earth. On the basis of geological evidence, we know that Earth has been anaerobic for parts of the history of life. Significant levels of free O_2 first appeared in the biosphere around 2.4 billion years ago (Cloud, 1972; Holland, 1994, 2006; Pavlov et al., 2001). Life on present-day Earth inhabits environments that range from those that exhibit strictly anaerobic (obligate anaerobes) conditions to those that exhibit strictly aerobic (obligate aerobes) conditions. Fig. 2.3 indicates where the different classes of extremophiles fall, for an environment that is aerobic (a) or anaerobic (b). The VRE surface albedo is shown for reference. Note that the data points for photosynthesis-based organisms have been removed from the anaerobic plot, as they are aerobic in nature.

Our model initially assumes full surface coverage of one particular surface in order to explore the general detectability of surface effects in a color-color diagram. This assumption is valid if changes in temperature, pH, or other physical or geochemical parameters differ slightly from Earth's. Therefore a particular environment that is considered extreme on current Earth could dominate a potentially habitable rocky planet and thereby govern the available environment for life. Fig. 2.2 shows that the surface effects can be detected remotely.

Based on our current understanding, liquid water is one of the main ingredients necessary for life. Water is also the dominant surface fraction on Earth, but its surface coverage on exoplanets is generally not known. Therefore, we explore the parameter space by investigating the effect of water as a second surface on the detectability of different extreme surface environments on a hypothetical exoplanet. Note that one could allow for a wide range of potential combinations of surface types in this parameter space. With water being the necessary ingredient for life, we constrain the number of additional surfaces to water in our analysis (see, e.g., Fujii et al., 2011, for a detailed analysis on the retrieval of different surface features on present-day Earth). Following our initial argument of slight physical or chemical changes on a habitable rocky planet, one surface environment should dominate our extreme exo-Earth model.

To explore the parameter space of the fraction of water on an exoplanetary surface, we calculate a set of color-color diagrams with varying water surface

fraction to explore its effect on prioritization of exoplanet targets for follow-up spectroscopy (see Fig. 2.4*)*. The data point represented in blue denotes the position of present-day Earth: it is modeled by assigning 70% of the planetary surface as ocean, 2% as coast, and 28% as land. The land fraction consists of 60% vegetation, 9% granite, 9% basalt, 15% snow, and 7% sand (following Kaltenegger et al., 2007).

Fig. 2.4 shows that the addition of water surface fraction from 10% to 90% moves the position of the planet in the color-color diagram along a diagonal. We define the region encompassing planets dominated by extreme environments with differing surface fractions of water between contours denoted by region I "extreme Earths." Note that some surface features like water are not a unique indicator for extreme environments and also indicate environmental conditions that are not extreme. Allowing for non-extreme habitable environments, like vegetation, widens the contours of extreme Earths in the color-color diagram (denoted region II) to a wider contour of "habitable planets."

2.6 Discussion

The method presented in this chapter provides a strategy with which to prioritize targets for follow-up spectroscopy once rocky extrasolar planets have been identified either by their physical properties or with the use of a color-color diagram such as those used to distinguish giant and rocky planets in our Solar System (see Traub, 2003b; Crow et al., 2011). Our aim in this work is to explore a wide range of surfaces that can support extreme forms of life. But the reverse, that these surfaces all need to support life, is not given.

As a first-order approximation, we assume here that the planet has a see-through atmosphere such that clouds and hazes do not obscure the surface signatures of the planet. Exploring surface features of exoplanets is only possible if either no significant cloud cover exists on an exoplanet or the SNR of each observation is sufficiently high to remove the cloud contribution from the overall detected signal (see Pallé et al., 2008). This holds true for directly observable surface reflection features of life like the VRE from terrestrial land plants and for the direct and indirect features shown in this chapter.

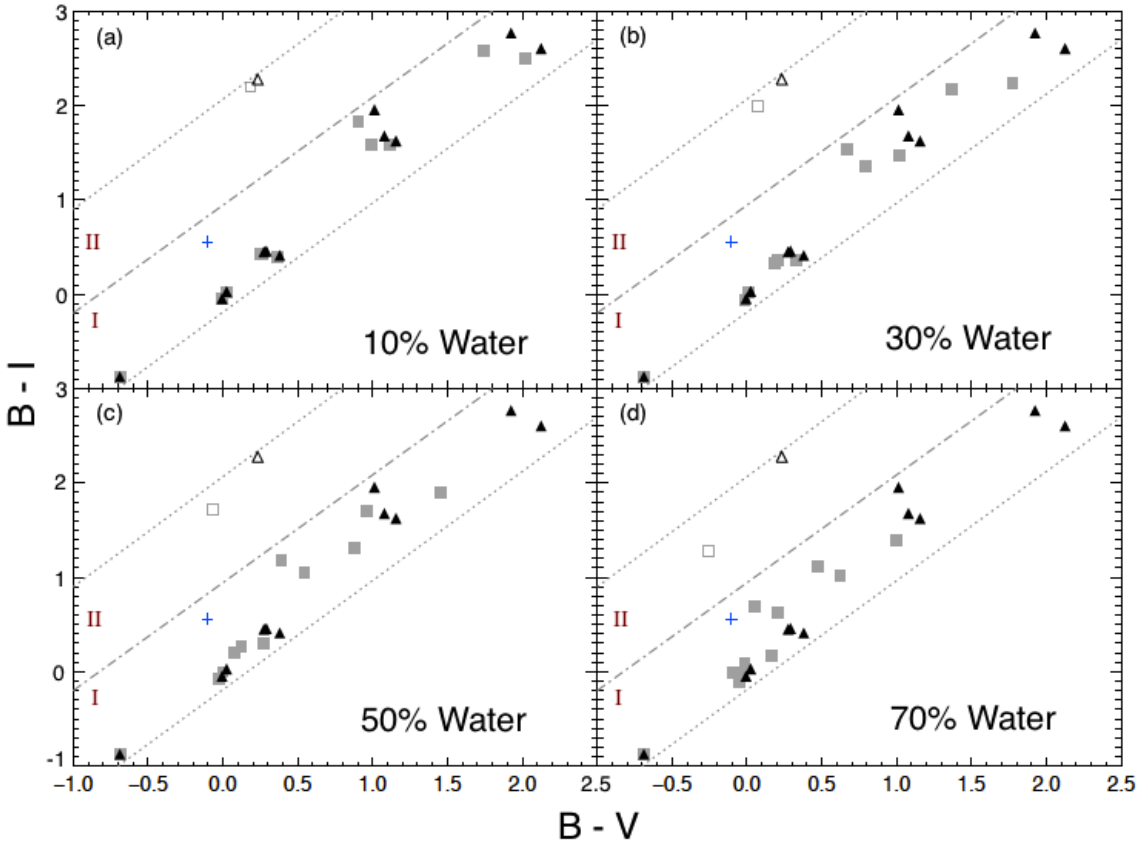

FIG. 2.4: Color-color diagrams (as above) and water.

Filled triangles represent a planet completely covered by a particular surface. Filled squares denote the case when the planet is (a) 90%, (b) 70%, (c) 50%, and (d) 30% covered by a particular surface with the rest being liquid water. Trees are shown as unfilled triangles (complete coverage) and squares as reference to other VRE studies. The blue data point represents present-day Earth. Region I defines the area of extreme Earth surfaces; region II includes surface vegetation for non-extreme forms of life.

The VRE, indicated by the albedo of trees here, does not group with the *Synechococcus*-bearing bacterial mats and lichens, even though all three undergo photosynthesis and contain chlorophyll pigments. One explanation is that the bacterial mat used here is covered with a thin layer of water; therefore, the reflection spectrum has strong water absorption features longward of 0.70 μm. Lichens, on the other hand, are composite organisms composed of a fungus with a photosynthetic partner, usually either a green alga or a cyanobacterium. Therefore, properties of lichens are very different from those of isolated fungus or alga in culture (Kranner et al., 2005). Hence, the VRE signature in lichens is observed to be weak or sloping (Kiang et al., 2007a).

The albedo and therefore the position in a color-color diagram of vegetation or any chlorophyll-bearing photosynthetic organism on an extrasolar rocky planet depend on the radiation received from the host star. For example, the chlorophyll signature for planets around hot stars may have a "blue-edge" that reflects some of the high-energy radiation and prevents the leaves from overheating (Kiang et al., 2007b). The chlorophyll signature for planets orbiting cooler stars may appear black due to the total absorption of energy in the entire visible waveband such that plants gain as much available light as possible for photosynthetic metabolism (O'Malley-James et al., 2012). Therefore, the positions of trees, microbial mats, and lichens in Fig. 2.2 are only valid for an Earth analog planet orbiting around a Sun-like star and should be taken as guides. The albedo of vegetation and chlorophyll-bearing organisms for non-Sun-like stars requires further study.

Radiation is a major factor when considering the habitability on extrasolar planets since it is capable of causing extensive damage to nucleic acids, proteins, and lipids in the UV regime (Rothschild, 2009). For the case of present-day Earth, the presence of an ozone layer in the atmosphere acts as an envelope by absorbing UV radiation and thereby shields surface life from high doses of UV light. Such an ozone layer was absent on early Earth until about 2.3 billion years ago (Kasting and Catling, 2003), but life still remained abundant. In addition, the young Sun emitted substantially more UV radiation than its current values (Canuto et al., 1982; Cockell, 2000), making the surface of Earth extremely hazardous to most current life-forms that evolved in a low-radiation environment. Subsurface or ocean life would not have been affected by such radiation. Therefore, although radiation extremophiles are not yet found on

Earth, we explore radiation as one of the physical extremes while looking for potential niches on extrasolar rocky planets.

Most of the extremophiles considered in this work are based on individual physical or geochemical extremes (e.g., temperature, pH). The strategy implemented in this work is also applicable to "polyextremophiles," that are, organisms thriving in multiple environmental extremes as well as organisms found in new niches once their characteristics become available.

The results presented here were obtained by using the standard Johnson-Cousins broadband filters. Varying the bandpass definitions by using custom filters does not improve the results significantly. For further in-depth characterization, the bandpass definitions could be optimized to distinguish specific surfaces; or narrow-band filters could be used, provided a high enough SNR is available.

2.7 Conclusions

For direct imaging of discovered exoplanets, information on habitability can be explored by using atmospheric and surface properties of the planet as seen through the observations of Earth from interplanetary spacecrafts (e.g., Sagan et al., 1993; Geissler et al., 1995) and from atmospheric modeling studies (see, e.g., Des Marais et al., 2002; Traub and Jucks, 2002; Segura et al., 2003, 2007; Selsis et al., 2007; Kaltenegger et al., 2010, for an in-depth discussion). The low SNRs that are presently achievable limit high-resolution spectroscopic measurements of rocky exoplanets.

This chapter shows how filter photometry can serve as a first step in the characterization of Earth analog exoplanets with different surfaces. We use a simple low-resolution color-color diagram to remotely characterize different types of rocky planet environments. We link those remotely detectable surface signatures to extreme forms of life that such environments could potentially support for aerobic as well as anaerobic atmospheres.

Our approach can be used to prioritize exoplanets for follow-up spectroscopy. An Earth-type rocky planet placed outside the contour region in Fig. 2.4 should receive lower priority for follow-up since the surface environment would not correspond to known environments on Earth supporting life based on our current knowledge. New discoveries of extreme life-forms could expand these

contours in the future. Our results also indicate that the priority of the target planet for follow-up characterization should increase towards the lower left corner in the color-color diagram due to a higher probability of liquid water being indicated on the surface.

Detailed spectroscopic studies will be needed to learn more as to the potential habitability of extrasolar rocky planets.

3

Surface biosignatures of exo-Earths: Remote detection of extraterrestrial life

---

From Hegde et al., (2014): *Proceedings of the National Academy of Sciences of the United States of America (PNAS), In Review*

3.1 Abstract

Exoplanet discovery has made remarkable progress with the first rocky planets having been detected in the central star's liquid water habitable zone. The remote sensing techniques used to characterize such planets for potential habitability and life rely solely on our understanding of life on Earth. The Vegetation Red Edge (VRE) from terrestrial land plants is often used as a direct signature of life but it occupies only a small niche in the environmental parameter space that binds life on present-day Earth, and has been widespread for only about 460 million years. To more fully exploit the diversity of the one example of life known, we measured the spectral characteristics of 137 microorganisms containing a range of pigments, including ones isolated from Earth's most extreme environments. Our database covers the visible and near infrared (VNIR) to the short wavelength infrared (SWIR) (0.35-2.5 μm) portions of the electromagnetic spectrum.

Our results show how the reflectance properties are dominated by the absorption of light by pigments in the visible portion, and by strong absorptions by the cellular water of hydration in the infrared (up to 2.5 μm) portion of the spectrum. Our spectral library provides a broader and more realistic guide based on Earth life for the search for surface features of extraterrestrial life. The library when used as inputs for modeling disk-integrated spectra of exoplanets, in preparation for the next generation of space- and ground-based instruments, will increase the chances of detecting life.

3.2 Introduction

In the last decade, the field of exoplanet research has transitioned rapidly from detection to detection and characterization with the first rocky exoplanets detected in the central star's liquid water habitable zone. Much of the excitement of this research in both the astrobiology community and the general public is motivated by the quest to discover a second genesis of life. The great distances that separate us from even the most nearby stars dictate that all measurements of the exoplanet must be made through remote sensing techniques for the foreseeable future. Thus it is critical for us to determine the types of biosignatures that we should be looking for when designing the next generation of ground- and space-based instruments that will observe these planets at high spectral and possibly spatial resolutions.

Since the mid 1960s, a primary life-searching strategy has been to look for a specific combination of an oxidizing and a reducing gas in the exoplanetary atmosphere, such as the O_2 and CH_4 in our atmosphere as this is a thermodynamically unstable situation suggesting that an active agent such as life is responsible for the chemical disequilibrium (Lederberg, 1965; Lovelock, 1965). Of particular interest, both from an observational and modeling perspective, is to complement those indirect life detection studies with surface features that are direct properties of the organisms themselves (Hegde and Kaltenegger, 2013).

While there is a considerable knowledge base of the spectral properties of land plants (Clark et al., 2007; Baldridge et al., 2009), very little information is present in the literature on the reflectance properties of microorganisms. Land plants are widespread on present-day Earth and are easily detected from high-resolution spacecraft observations (Sagan et al., 1993). However, they occupy only a small niche in the environmental parameter space that brackets known terrestrial life. Additionally, land plants have been widespread on Earth for only about 460 million years (Carroll, 2001), while much of the history of life has been dominated by single-celled microbial life. Within the prokaryotic and eukaryotic microbes there is a far greater diversity of pigmentation than in land plants. For this reason, any hypotheses about extraterrestrial life based solely on land plants ignore much of the diversity of known life. In order to develop a more representative library of terrestrial spectra, we produced a digital spectral library that provides high-resolution hemispherical reflectance measurements for

137 phylogenetically diverse microorganisms from the visible and near infrared (VNIR, 0.35-1.0 µm) to the short wavelength infrared (SWIR, 1.0-2.5 µm) regions of the electromagnetic spectrum. The library is made available in the *Appendix*.

One approach when searching for life on exoplanets is to explore the range of pigmentation types that have evolved on this Earth. In order to examine the widest possible environmental range for life on Earth to inform our search, we have chosen to include a diversity of extremophiles, organisms that live and thrive under conditions that make it challenging for a carbon-based organism using water as a solvent to survive (Rothschild and Mancinelli, 2001). At the same time, we are cognizant of the fact that extremophiles are phylogenetically diverse and are unlikely to show spectral signatures not found among other pigmented organisms. Thus we present reflectance spectra of organisms possessing a wide range of pigmentation but also complement this with the reflectance properties of various microorganisms that are isolated from some of Earth's most extreme environments.

The differences in the spectral characteristics between microorganisms is observed to be a result of the wavelength dependent absorption by the pigmentation making up the organism and is independent of the functionality and hardiness that are often associated with extremophiles (Dalton et al., 2003). While pigments play an active role in screening UV radiation, oxidative damage prevention, and photosynthesis, they are often a result of secondary metabolic processes and are not primarily responsible for the hardiness of organisms to extreme environments (Schroeder and Johnson, 1993; Singaravelan et al., 2008).

The data presented in this chapter can be used as a reference for future disk-integrated observations of rocky exoplanets and serve as surface albedo input parameters to atmospheric radiative transfer models. Albedo is the directional-integration of diffuse reflectance over all viewing angles and is therefore strongly dependent on the bi-directional reflectance distribution function (BRDF) of the sample material. For materials with large BRDF anisotropy, bi-directional reflectance measurements at a single viewing angle can often result in a poor approximation of the albedo. In addition, aside from the geometry differences, confounding effects of the atmosphere, stray light, multiple scattering due to the surroundings, and sample biomass, have to be often accounted for in a bi-directional configuration, thereby creating several

layers of complexities and uncertainties in the sample spectrum. We therefore focus on hemispherical reflectance measurements for all our sample organisms. The added advantage of this, besides severely reducing the confounding effects, is that one can approximate the surface to be Lambertian as is commonly the case in exoplanetary atmospheric and climate models.

3.3 Materials and Methods

Of the 137 microorganisms selected for spectroscopic analysis in this work, 107 pure cultures were isolated from various source locations and grown at NASA Ames Research Center. The remaining samples were obtained from the Culture Collection of Algae at the University of Texas, Austin (21 samples) and from the University of California, Santa Cruz (9 samples) in 10 ml test tubes at late log phases and were stored under ambient laboratory conditions. Detailed information on the source location and donor is provided in the *Appendix*. All hemispherical reflectance measurements were performed at the Center for Spatial Technologies and Remote Sensing (CSTARS) at the University of California, Davis.

3.3.1 Sample preparation

Cryostocks in 20% glycerol of pure heterotrophic isolates were stored in a minus 78 $^{\circ}$C freezer to preserve the viability of cells. Reagents for the culture media were purchased (Blue-Green medium (BG-11): Sigma-Aldrich; Lysogeny Broth (LB): Sigma-Aldrich; Reasoner's 2A Broth (R2A): Teknova; Marine Broth (MB): Becton, Dickinson and Company) and prepared as liquid media. Heterotrophic cultures were grown aerobically in an incubator at 30 $^{\circ}$C (180 rpm) up to stationary phase, with the exception of *Ectothiorhodospira* sp. str. BSL-9, which was grown anaerobically. Phototrophic cultures were incubated at room temperature under 12 hour light/dark cycles. Depending on the isolate, the time required for growth varied from about 24 hours to 1 week for heterotrophic cultures, and up to 6 months for phototrophic cultures. Care was taken to preserve axenic samples throughout the culturing process and all inoculations were carried out in a laminar flow hood.

3.3.2 Spectrometer system

Hemispherical reflectance measurements were acquired using an Analytical Spectral Devices FieldSpec 4 Hi-Res Spectroradiometer that was interfaced with a LI-COR 1800-12 integrating sphere. This spectroradiometer operates in the 0.35-2.5 µm spectral range utilizing three detectors: a 512-element silicon photodiode array in the VNIR portion (up to 1.0 µm) having a spectral resolution of 3 nm, and two identical thermoelectrically cooled, graded index indium-gallium-arsenide (InGaAs) photodiodes having a spectral resolution of 8 nm in the SWIR 1 (1.0-1.8 µm) and SWIR 2 (1.8-2.5 µm) portions of the electromagnetic spectrum. The spectroradiometer thus operates in an array mode in the VNIR region and in a scanning mode in the SWIR region of the spectral range. The scanning time reported is 100 milliseconds per scan with a wavelength reproducibility of 0.1 nm. Wavelength and radiometric calibrations for the spectroradiometer were carried out by the manufacturer before and after the spectral measurements in this chapter were performed, and were found to be stable. The spectroradiometer was linked to the observation port of the integrating sphere using a bare fiber optic cable that comprised of 57 fibers and a 25-degree field of view.

The LI-COR 1800-12 is an external integrating sphere. The sample is placed outside of the sphere and a portion of the sample makes up the sphere wall. The sample port is 1.45 cm in diameter and is illuminated using a 6 Volt, 10 Watt glass-halogen lamp (Welch Allen Type 787) having a color temperature of 3215 K and a luminous flux of 207.34 lumens. The spot diameter of the illuminator is 1.14 cm with stray light amounting to $< 0.5\%$. The integrating sphere has 3 entrance ports, one each for reference, reflectance and transmittance measurements. The reference sample disk uses pressed barium sulfate powder as a standard, and the interior of the sphere uses a barium sulfate coating making it a uniform diffuse reflector. The fiber optic sensor from the spectroradiometer does not observe the sample directly but rather a fixed section of the internal sphere wall throughout all reference, dark and sample measurements. Sample measurements made are of total reflectance (specular + diffuse) since there is no mechanism provided in the sphere to distinguish between the two components.

3.3.3 Sample measurements

Pure sample cultures growing as cell suspension in liquid media were deposited on a plain white filter (Millipore, HAWP02500) using a 10 ml syringe and a filtration system. The filter is made of biologically inert membranes of mixed cellulose esters and has a diameter of 2.5 cm with a thickness, pore size and porosity of 150 µm, 0.45 µm, and 79%, respectively. Fig. 3.1 shows Scanning Electron Microscope (SEM) images of homogeneously layered microbial cells deposited onto the filter substrate. The substantially larger cell size (1-10 µm) of the samples to the pore size of the filter allowed for a clear filtrate to pass through the filter. In addition, the filtration system also ensured that only a fixed amount of cells, depending on the cell size and morphology, be deposited onto the filter. This was due to an increase in pressure gradient inside the filtration system that resulted from the continuous deposition of cells thereby causing the cells to clog the filter pores after reaching a certain cell amount. Any additional cell deposition caused the filter to crack apart and break open. This thus set the threshold pressure and the limiting amount of sample cells that could be deposited onto the filter substrate. The saturation limit was reached at about 3 ml $\pm$ 0.2 ml of cell suspension volume for most bacterial cultures and about 10 ml $\pm$ 1 ml for algal cultures. The sample was then used to acquire high-resolution hemispherical reflectance measurements using the spectrometer system described before.

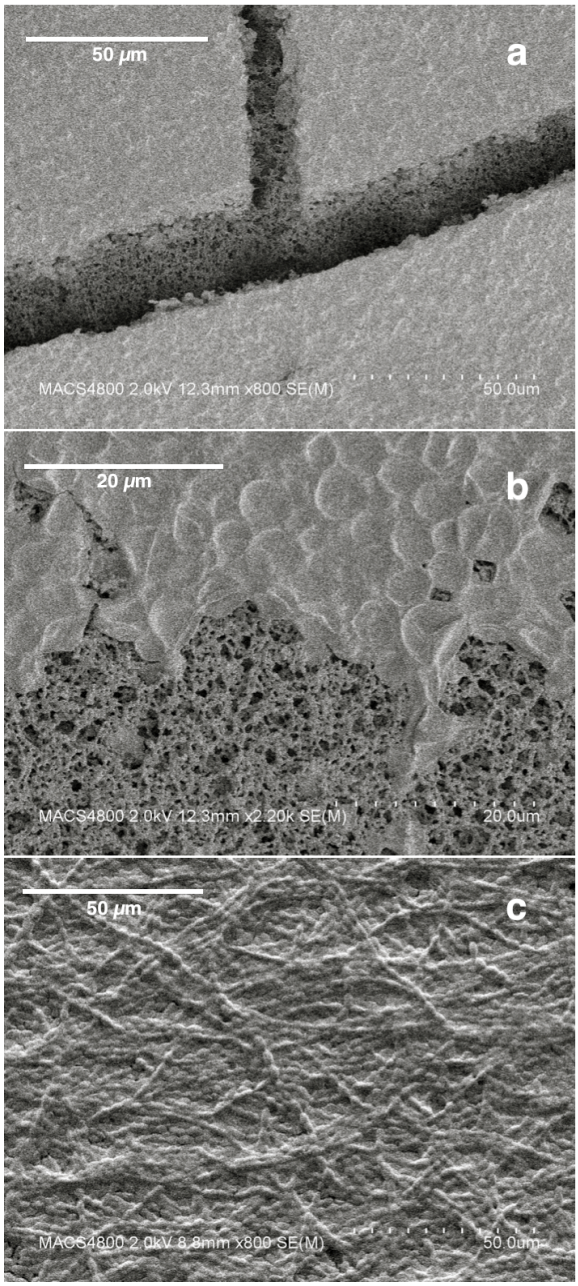

FIG. 3.1: Scanning Electron Microscope (SEM) images of sample cells deposited on a filter substrate.

Homogeneous layers of cells were deposited until the filter substrate reached a saturation limit. (A) Cell layers of *Chlorella* sp. over the filter showing an approximate thickness of sample layering in a crack caused during sample manipulation. The thickness varied from 10-50 µm depending on the sample cell size and morphology. The porous feature of the filter is shown beneath the cell layering. (B) Image at the filter edge showing a colony of *Cyanidium caldarium* cells covering its pores. (C) Filamentous structure of *Anabaena* sp. as observed on the filter substrate. Due to the optically rough surface feature of the samples, as seen in the images, the reflected light is predominantly diffuse. All SEM images were obtained using a Hitachi S4800 Field Emission Scanning Electron Microscope at NASA Ames Research Center, CA, USA.

The Analytical Spectral Devices FieldSpec 4 Hi-Res Spectroradiometer was programmed to take 100 readings averaged to one spectrum each for reference, dark and sample measurements. Readings were taken at equal intervals of 1 nm for the entire spectral range. All measurements were taken in radiance mode using the instrument-specific calibration files provided by the manufacturer. This allowed for dark current and stray light correction during post-processing. Stray light from outside the sphere was avoided by placing the sample in the sample port using the support of a pair of rubber gaskets that acted as a sample holder. The rubber gaskets had an inner diameter of the same size as the filter substrate (2.5 cm) and were held tightly together by metal clips to prevent any light from entering or leaving the sample port of the integrating sphere. Fig. 3.2 shows the spectrometer system design. The spectroradiometer was warmed-up prior to each measurement session for a minimum of 45 minutes to achieve stability from the inherent variations in detector sensitivity arising due to system temperature differences. Furthermore, the system was optimized once per hour to account for any minor fluctuations in the illuminator lamp irradiance between measurements. Two sets of readings for each sample were carried out, one with a light trap, and the other with a calibrated Analytical Spectral Devices spectralon panel (99% hemispherical reflectance), placed behind the sample holder, in order to remove the spectral contamination of the filter from the overall measured reflectance of the sample-substrate system. For a few sample measurements, the cells did not cover the entire filter or were inhomogeneous in their distribution. In such cases, due to a limited supply of sample culture, the problem was overcome by positioning the sample in a way as to have a homogeneous layering of cells spread over the light exposed portion of the filter. All radiance measurements were checked for temperature sensitive channels and corrected for, by utilizing standard parabolic correction procedures using Analytical Spectral Devices ViewSpec Pro spectroradiometer software.

3.3.4 Microscopy

The micrographs of samples were obtained by analyzing fresh aliquots of 10 µl from cell suspension of isolates through a Canon EOS Rebel T3i (18-55 mm IS II lens) attached to a Zeiss Axio Imager Z1 PH/DIC/Fluorescence compound microscope. Micrographs of cells were taken under bright field (BF) at 400x magnification with phase-contrast (PH) microscopy for most samples. For algal

cultures, the cell micrographs are those using a differential-interference contrast (DIC) microscopy.

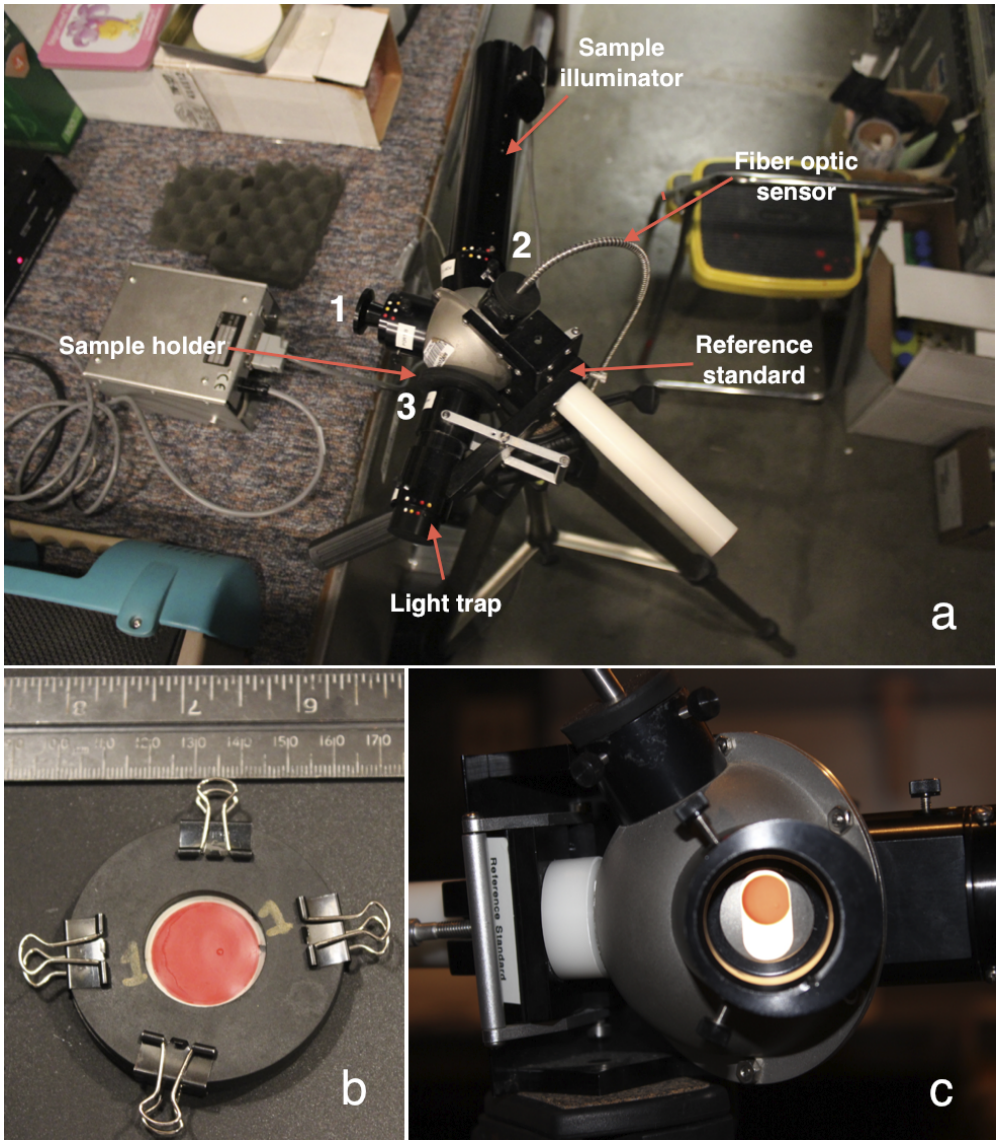

FIG. 3.2: Spectrometer system used in hemispherical reflectance measurements.

The LI-COR 1800-12 integrating sphere (shown) was interfaced to the Analytical Spectral Devices spectroradiometer using a fiber optic sensor. (A) The integrating sphere has three entrance ports, with one each for (1) reference, (2) reflectance, and (3) transmittance mode. Two sets of reflectance measurements were acquired for each sample, one with a light trap, and the other with a spectralon panel, placed behind the sample holder. Dark current and stray light measurements were obtained using a light trap in the reflectance mode configuration with no sample in the sample holder. (B) The sample holder consisted of a pair of rubber gaskets held strongly by metal clips to prevent any light from entering or leaving the sphere. (C) Sample as seen through the illuminator port for reflectance measurements. The reference disk uses pressed barium sulfate powder as a standard.

3.4 Results

We present high-resolution hemispherical reflectance spectra for 137 microorganisms in this chapter. The radiance measurements are corrected for dark current and stray light and converted to absolute reflectance as

$$R_{sample,\lambda} = \frac{\left(J_{sample,\lambda} - J_{dark,\lambda}\right) R_{reference,\lambda}}{\left(J_{reference,\lambda} - J_{dark,\lambda}\right)} \tag{3.1}$$

where J_{sample} and $J_{reference}$ are measurements of the sample and reference standard, respectively, in $W/m^2/nm/sr$. J_{dark} is the dark current and stray light contribution and has the same radiance units. $R_{reference}$ is the calibrated reflectance factor of pressed barium sulfate powder.

Fig. 3.3 shows an example of the diversity in reflectance spectra for eight sample organisms for (A) the entire measured spectral range (0.35-2.5 µm), and (B) only the VNIR portion (0.35-1.0 µm) of the spectrum. Standard deviations are not calculated due to a limited supply of culture for most samples. However, sample sets of *Anabaena* sp. measurements showed consistent results and very high instrument stability.

In addition, every reflectance spectrum has a sample description page (see *Appendix*) as shown in Fig. 3.4. The individual sample fields are populated based on available data. For most samples, the organism has been classified only up to the genus level. Where available, we have also provided accession numbers for the 16S rRNA partial gene sequences that gives additional information on differentiating organisms belonging to the same genus. The sequences can be found by inserting the accession numbers on the National Center for Biotechnology Information (NCBI) website at http://www.ncbi.nlm.nih.gov/nuccore/.

FIG. 3.3: Diversity in reflectance spectra for eight sample organisms for (A) the entire measured spectral range (0.35-2.5 µm), and (B) only the VNIR portion (0.35-1.0 µm) of the spectrum.

Spectral characterizability between microorganisms is best observed in the VNIR portion of the spectrum where absorption is primary due to pigments. At longer wavelengths, the spectral features are from weak absorptions by biomolecular components and strong absorptions from water in its free and bound states. The features in the infrared look quite similar for all our sample microorganisms with variations seen only in the relative strengths and depths of individual absorption features, which may be due to differences in cell composition and constituent concentrations. Note that the reflectance characteristics for *Kocuria* sp. (isolated from Sonoran desert, AZ, USA) look quite similar to *Halorubrum* sp. (isolated from Evaporitic salt crystal, Baja California, Mexico) despite originating from very different environmental conditions, highlighting our aim to explore the spectra of a diverse range of pigmented organisms. The sample spectra have been modeled to remove the spectral contamination of the filter in our reduction scheme (see Model description).

(A)

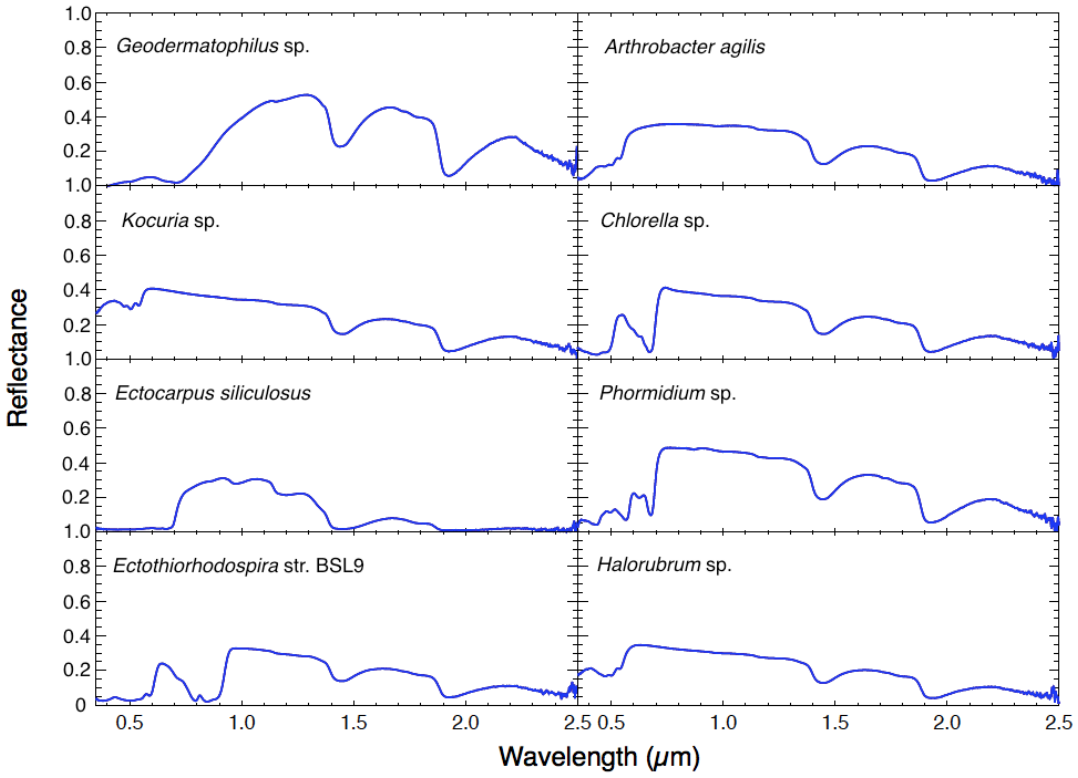

(B)

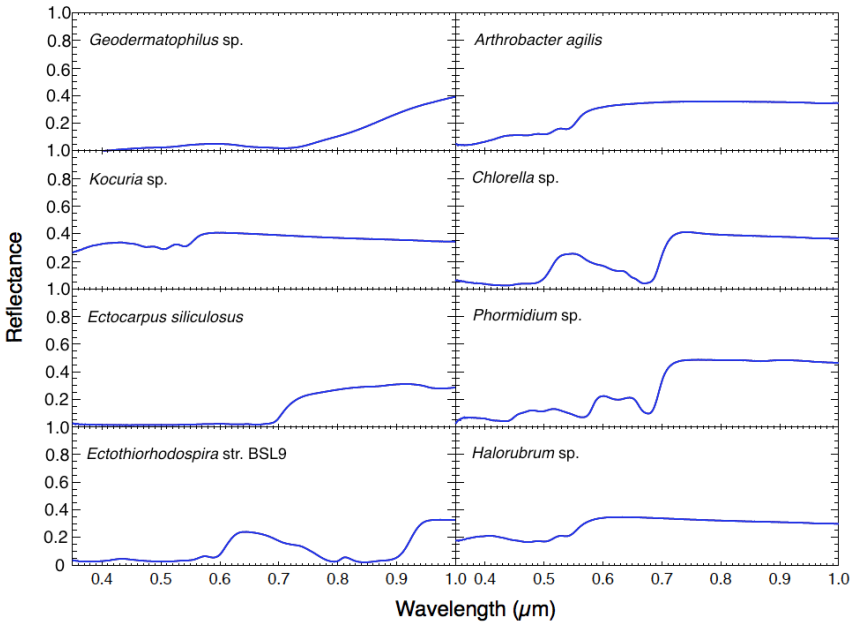

***Halorubrum chaoviator* str. Halo-G^{*T}_ AM048786**

Sample name: *Halorubrum chaoviator* str. Halo-G^{*T}

Accession number for 16S rRNA partial gene sequence: AM048786

Classification: Archaea; Euryarchaeota; Halobacteria; Halobacteriales; Halobacteriaceae; Halorubrum

Origin: Evaporitic salt crystal, Baja California, Mexico

Isolation: Rocco Mancinelli (BAER Institute at NASA Ames, CA, USA)

Sample concentration: 8.19 × 10^7 cells/ml

Sample count on filter pad: 2.46 ± 0.16 × 10^8 cells

Laboratory growth conditions: 37 °C, 180 rpm, 1 week

Culture medium: CASEIN medium ATCC#876

Sample Photograph:

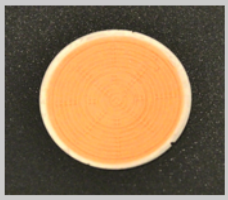

Sample Micrograph:

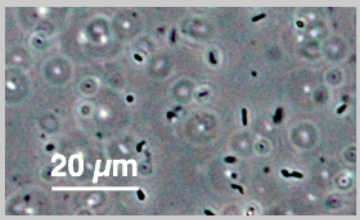

FIG. 3.4: Template of the sample description page showing the information provided (when available).

The micrographs of cells were obtained using a Zeiss Axio Imager Z1 PH/DIC/Fluorescence compound scope at NASA Ames Research Center, CA, USA. The micrographic images of cells provided for most samples are those using a phase-contrast (PH) microscopy. For algal cultures, the cell micrographs are those using a differential-interference contrast (DIC) microscopy.

3.5 Discussion

Detection of microbial life on extrasolar planets is based on remote sensing of any signatures that are indicative of such life forms. In this work, we expand the knowledge base by building a spectral database of 137 microorganisms from 0.35-2.5 µm (currently data for 3 such organisms is available in the literature, see Clark et al., 2007). There are several advantages of choosing this wavelength range. An Earth-like atmosphere is relatively transparent in the visible when compared to the far infrared portion of the electromagnetic spectrum, which is strongly absorbing due to the water vapor in the atmosphere. At wavelengths longward of 2.5 µm, strong thermal emission is expected from planets having masses similar to that of Earth thereby causing a considerable amount of spectral contamination in the surface signatures. Toward lower wavelengths, radiation in the ultra-violet regime is capable of causing extensive damage to nucleic acids, proteins, and lipids of any carbon-based life forms that dwell on the planetary surface (Rothschild, 2009). In addition, recent studies show that planet characterizability (Hegde and Kaltenegger, 2013; Traub, 2003b) is usually excellent in the visible waveband, which is useful in distinguishing different surface features. Finally, reflection spectra of microbes in the near infrared (up to 2.5 µm) portion are thought to have absorption features unique to life due to their water of hydration and biomolecular components (Dalton et al., 2003).

As seen in Fig. 3.3, spectral characterizability between microorganisms is best observed in the VNIR portion of the spectrum where the absorption is primary due to pigmentation. This is not surprising given the relative transparency of the atmosphere and water in these regions on Earth, allowing for a substantial amount of solar radiation to reach the surface. This excess energy causes the development of pigments that the organism uses for screening UV radiation, photosynthesis, and oxidative damage prevention. In the SWIR region of the spectrum, the spectral features are from weak absorptions by functional groups present in cellular proteins, nucleic acids, lipids, and carbohydrates; and strong absorptions from water in its free and bound states (water of hydration)(Dalton et al., 2009). The absorption features of microorganisms due to their water of hydration are seen to occur near 0.95, 1.15, 1.45 and 1.92 µm. These features in the infrared look quite similar throughout our spectral library with minor variations seen only in the relative

strengths and depths of individual absorption features, which may be due to differences in cell composition and constituent concentrations. Our results agree with Dalton et al. (Dalton et al., 2003), who based on their research on the spectral characteristics of *Escherichia coli* and *Deinococcus radiodurans*, suggest that all carbon-based organisms irrespective of their functionality or hardiness will look quite similar in the infrared portion of the reflectance spectrum. This feature in the infrared up to 2.5 µm may be a unique biosignature of life on potentially habitable planets. Beyond 2.5 µm, reflectance values of less than 5% are expected due to strong atmospheric and water absorptions (Roy, 1989).

Since the spectra are dependent on the pigment composition of the organism in the visible waveband, there is no general consensus observed that correlates the spectra with the phylogeny of the microorganisms. This is particularly true for heterotrophic bacteria, where pigmentation is a product of the secondary metabolism, which is regulated essentially by environmental conditions, such as availability of nutrients (Demain, 1998). For instance, spectra of heterotrophic bacteria belonging to the Phylum Firmicutes showed very few differences in spectral patterns between organisms belonging to this taxon, whereas for phototrophic bacteria like the Phylum Cyanobacteria, major variations in the spectral patterns between organisms of this taxon are observed. Also, as seen in Fig. 3.3, while *Kocuria* sp. and *Halorubrum* sp. have reflectance characteristics that look quite similar despite their classification in different domains (Bacteria and Archaea, respectively), a great diversity is observed even for the lowest taxonomic level depending on the growth phase. Cultures from the same strain of a particular isolate, identified as *Geodermatophilus* sp., start as white then appear orange, then dark green and finally black, and this is a common aspect for representatives of the family Geodermatophilaceae (Normand, 2006; Montero-Calasanz, 2014). Spectral features of similar molecules can also change depending on the environment. For example, chlorophyll a has an absorption peak at 663 nm when diluted in acetone and in monomeric state (Björn (ed.), 2008). This peak is red-shifted in vivo to 680 nm and in some cases to even longer wavelengths, as high as 720 nm (Halldal, 1968).

Our reflectance measurements of the sample microorganisms were carried out on top of a filter substrate. It is therefore likely that there is some spectral contamination due to the reflectance characteristics of the filter itself. This

problem is often encountered in the dye and paper industry and is generally resolved using the Kubelka-Munk two-flux transport theory (Kubelka and Munk, 1931; Saunderson, 1942). We tried using a similar approach initially in our work but encountered limitations in the sample abundances that are needed for the accurate determination of the absorption and scattering coefficients required by the model for an optically thick sample layer. In addition, our sample filtering methodology described before would only allow for a fixed amount of cell layers to be deposited on the substrate thereby limiting the application of the Kubelka-Munk theory. To remove the spectral contribution of the substrate, we have instead used a one-dimensional two-stream radiative transfer model that takes into account all light interactions and multiple scattering between the sample layer and the filter substrate (see Section 3.6 below). For this reason, we have taken two sets of reflectance measurements for each sample, one using a light trap, and the other with a spectralon panel, placed behind the sample, which is useful in determining the transmittance properties of the sample that is required by our model.

Dehydration of cells is a major factor when measuring the reflectance characteristics of microbes. As seen in Fig. 3.5 for *Anabaena* sp., there is a significant change in both the absolute reflectance level and the spectral features especially at wavelengths greater than 0.7 µm. Prolonged exposure of cells to intense irradiation from the illuminator lamp causes the cells to desiccate and lose its water of hydration thereby severely damaging the cells. In this work, the microbial reflectance spectra were measured as soon as the sample cells were deposited on the filter substrate and all measurements are those of the sample in its vegetative state.

Our measurements were carried out at standard room temperature and pressure. The spectral characteristics may undergo minor changes for measurements made at different temperatures and pressures due to changes in the cellular constituent concentrations especially for the water content within the cell. Further work needs to be carried out in this regard, which may be useful, for instance, in the application of microbial spectral properties to search for potential life on icy planets and satellites.

The absolute reflectance value is a function of the thickness of the sample layering that is being measured. Most of our sample reflectance is for a cell count of 10^6-10^8 cells (or for a concentration of 10^2-10^5 cells/µl) corresponding

to a sample layering of 10-50 µm in thickness, depending on the cell morphology. A lower pigmentation biomass content results in a higher reflectance (and transmittance) value due to a lower absorption of radiation, and vice-versa (Roy, 1989; Sims and Gamon, 2002). Similar results may be expected due to variations in the thickness of the sample layering or for differing sample concentrations. Hence changes in sample biomass may affect the absolute reflectance level to a certain degree, but the overall spectral features may remain the same.

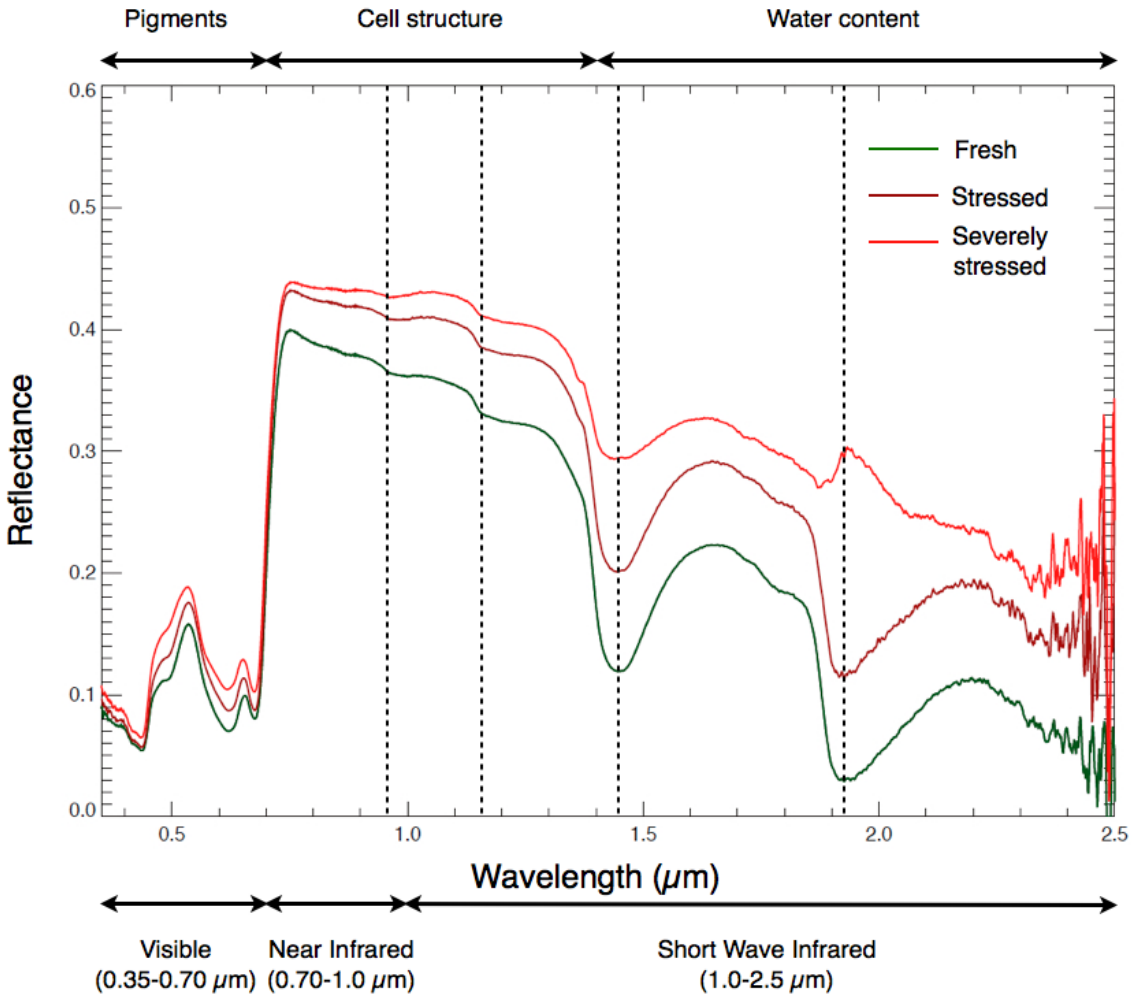

FIG. 3.5: Effect of cell dehydration on the reflectance spectrum.

Significant changes in both the absolute reflectance level and the spectral features are seen in *Anabaena* sp. due to prolonged desiccation of cells. Fresh cells were exposed to intense illuminator irradiation for 5 and 10 minutes, causing loss of water thereby severely damaging the cells. The upper panel denotes the dominating factors contributing to the microbial reflectance. The dotted lines indicate the absorption bands due to water of hydration of the cell.

3.6 Model description

We use a one-dimensional two-stream radiative transfer model to remove the spectral contribution of the filter substrate from the overall measured reflectance of the sample-substrate system. The filter is made of biologically inert membranes of mixed cellulose esters and has a diameter of 2.5 cm with a thickness, pore size and porosity of 150 µm, 0.45 µm, and 79%, respectively. The measured spectral characteristics of a dry and wet filter are shown in Fig. 3.6.

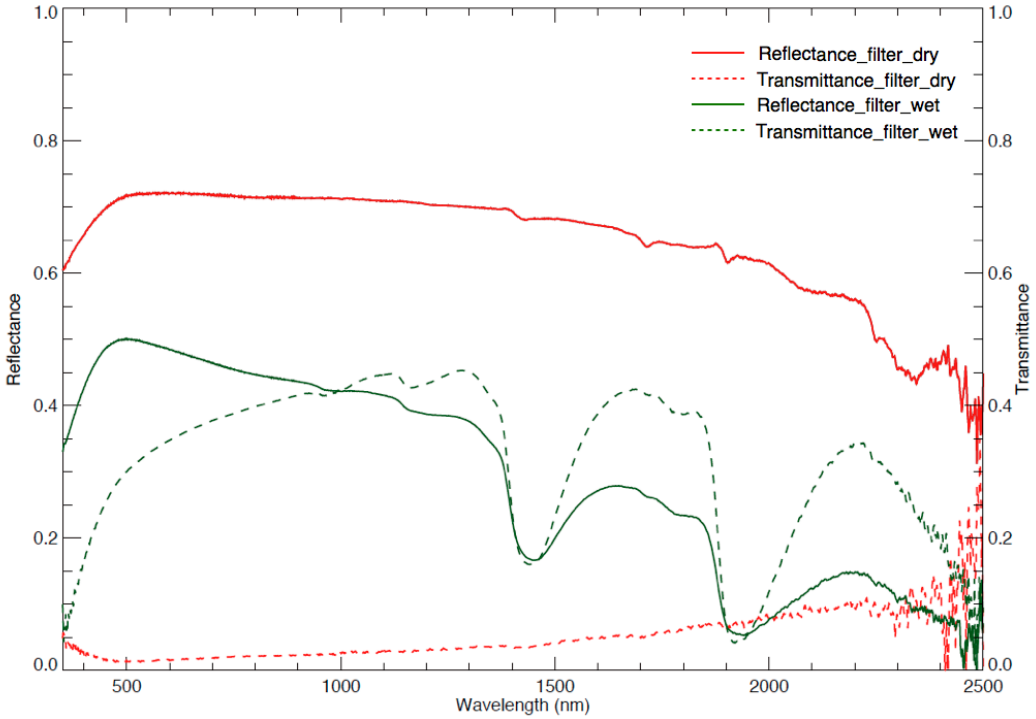

FIG. 3.6: Spectral characteristics of the filter substrate used (plain, white, Millipore, HAWP02500).

The reflectance and transmittance properties of the wet filter have been used in our reduction scheme.

The spectral features of a wet filter saturated with distilled water is seen to be markedly different from those in its dry state due to strong water absorptions. Also observed, is a substantial variation in the absolute reflectance and transmittance levels between the dry and wet filters. One explanation for

the change is the forward alignment of the membrane filter fibers when it is wet, thereby allowing for a higher percentage of the incident light to scatter in the forward direction through the filter pores, resulting in an increase in the transmittance values. Since all of our sample reflectance measurements were made using a wet filter, we use the spectral characteristics of a wet filter in our reduction scheme when removing the effect of the filter substrate from the measured reflectance of the sample-substrate system. Two sets of reflectance measurements were made for each sample, one using a light trap, and the other with a calibrated Analytical Spectral Devices spectralon panel (99% hemispherical reflectance), placed behind the sample holder. Derivations for the light interactions and multiple scattering between the sample layer and the filter substrate for the two cases are carried out below, allowing for the successful removal of the spectral contribution of the filter substrate from the overall measured reflectance of the sample-substrate system.

3.6.1 Simplifying assumptions

We make the following assumptions for the sample in our model:

1. The sample is modeled as a single plane layer of finite thickness, but having an infinite lateral extent, such that there are no boundary effects.

2. The sample is considered to be non-fluorescent and polarization effects are ignored such that the only interactions of light with the sample are scattering and absorption.

3. The sample is considered to be homogeneous and isotropic throughout the layer, with the reflectance values at the front and back surfaces of the sample layer assumed to be equal.

4. The incident, reflected and transmitted light are assumed to travel only in two directions, upwards and downwards, with variations in the light intensity taking place only along one axis.

3.6.2 Case 1: Sample-substrate system with a light trap back

A light trap was placed behind the sample-substrate system, which ensured that any light transmitted through the system was not scattered back in the opposite direction. Let R_f, T_f, and R_s, T_s, represent the reflectance and

transmittance factors as a function of wavelength for the filter substrate and the sample, respectively. The light interactions can then be illustrated as shown in Fig. 3.7.

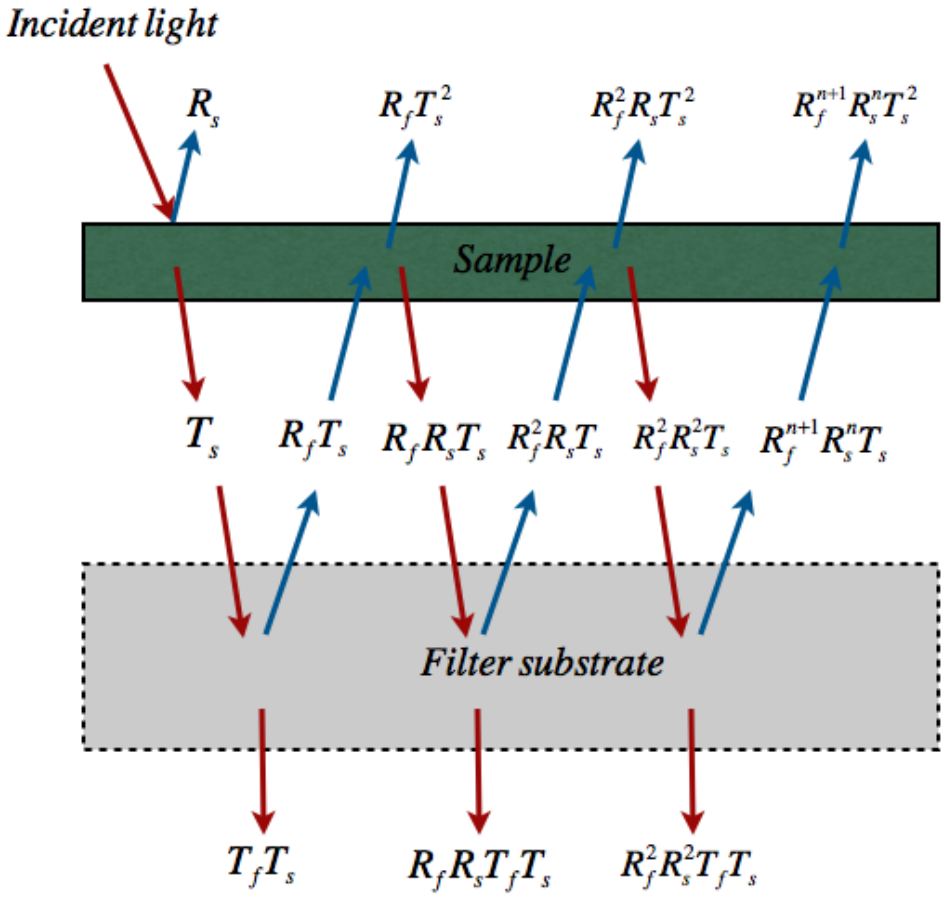

FIG. 3.7: Simplified illustration of the light interactions and multiple scattering between the sample layer and the filter substrate.

For a sample-substrate system placed in front of light trap, the light that is transmitted through the sample and the filter is lost. For a sample-substrate system with a spectralon panel back, this transmitted light is back scattered and undergoes multiple scattering between the spectralon panel, filter, and the sample.

The absolute reflectance for the filter (R_f) and sample-substrate system ($R_{system_light\text{-}trap}$) is calculated using the radiance measurements in the reflectance configuration of the medium (filter or sample-substrate system) and the reference standard (pressed barium sulfate powder) as:

$$R_f = \frac{\left(J_{filter} - J_{dark}\right)R_{reference}}{\left(J_{reference} - J_{dark}\right)} \tag{3.2}$$

$$R_{system_light-trap} = \frac{\left(J_{system_light-trap} - J_{dark}\right)R_{reference}}{\left(J_{reference} - J_{dark}\right)} \tag{3.3}$$

where J_{dark} is the dark current and stray light measurement and $R_{reference}$ is the calibrated reflectance factor of pressed barium sulfate powder as shown in Fig. 3.8.

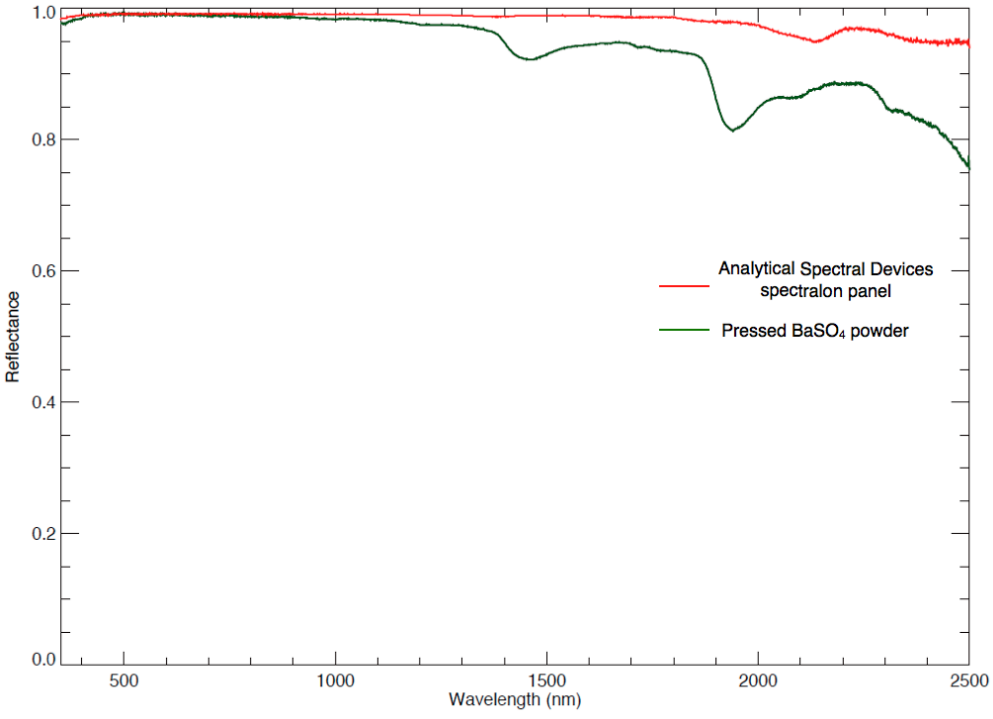

FIG. 3.8: Spectral characteristics of the pressed barium sulfate powder that was used as a reference standard inside of the LI-COR 1800-12 integrating sphere.

Also shown, is the reflectance factor of the Analytical Spectral Devices spectralon panel that was placed behind the sample-substrate system during part of our measurements.

From Fig. 3.7, the measured reflectance of the sample-substrate system with a light trap back can be interpreted by summing all the individual scattering components as:

$$\begin{aligned} R_{system_light-trap} &= R_s + R_f T_s^2 + R_f^2 R_s T_s^2 + R_f^3 R_s^2 T_s^2 + \ldots + R_f^{n+1} R_s^n T_s^2 \\ &= R_s + R_f T_s^2 \left(1 + R_f R_s + R_f^2 R_s^2 + \ldots + R_f^n R_s^n\right) \end{aligned} \tag{3.4}$$

Let, $R_f R_s = x$ (3.5)

Then, $R_{system_light-trap} = R_s + R_f T_s^2 \left(1 + x + x^2 + \ldots + x^n\right)$

The term $1 + x + x^2 + \ldots + x^n$ represents a geometric series having a solution:

$$1 + x + x^2 + \ldots + x^n = \frac{1 - x^{n+1}}{1 - x}$$

For $|x| < 1$, the above power series reduces to $\sum_0^\infty x^n = \frac{1}{1-x}$

Since, R_f and R_s are both positive numbers and have values between 0 and 1, Eq. (3.4) takes the form:

$$R_{system_light-trap} = R_s + R_f T_s^2 \left(\frac{1}{1 - R_f R_s}\right) \tag{3.6}$$

The measured reflectance of a sample-filter system placed in front of a light trap can be expressed as a summation of the two terms as shown in Eq. (3.6).

3.6.3 Case 2: Sample-substrate system with a spectralon panel back

A calibrated Analytical Spectral Devices spectralon panel was placed behind the sample-substrate system, ensuring that any light that was transmitted through the system was scattered back in the opposite direction. The reflectance factor (γ) of the spectralon panel is shown in Fig. 3.8. The absolute reflectance for the sample-substrate system with a spectralon panel back ($R_{system_spectralon\text{-}panel}$) is calculated using the radiance measurements as:

$$R_{system_spectralon-panel} = \frac{\left(J_{system_spectralon-panel} - J_{dark}\right)R_{reference}}{\left(J_{reference} - J_{dark}\right)} \tag{3.7}$$

where all terms have their definitions as described before and $J_{system_spectralon\text{-}panel}$ is the radiance measurement in the reflectance mode of the sample-substrate system when placed in front of a spectralon panel.

The transmitted light undergoes the following interactions after being scattered back from the spectralon panel:

1. Multiple scattering ($n \to \infty$) of light between the filter and the spectralon panel.

2. Multiple scattering ($n \to \infty$) of light between the sample layer and the filter substrate.

3. Multiple scattering of higher order light terms ($n \to \infty$) incorporating steps (1) and (2).

The overall measured reflectance ($R_{system_spectralon\text{-}panel}$) in this case, can be interpreted by taking into account all light interactions and multiple scattering between the sample, filter and spectralon panel:

Let, x' denote the total light contribution due to multiple scattering between the sample layer and the filter substrate:

$$x' = \sum_{0}^{\infty} R_f^n R_s^n = 1 + R_f R_s + R_f^2 R_s^2 + \ldots + R_f^n R_s^n \tag{3.8}$$

and y' denote the total contribution of light due to multiple scattering between the filter substrate and the Analytical Spectral Devices spectralon panel:

$$y' = \sum_{0}^{\infty} \gamma^n R_f^n = 1 + \gamma R_f + \gamma^2 R_f^2 + \ldots + \gamma^n R_f^n \tag{3.9}$$

Then, the reflectance of the sample-substrate system for a spectralon panel back can be derived as:

$$\begin{aligned}
&R_{system_spectralon-panel} = R_s + R_f T_s^2 x' + \\
&\left[\gamma T_f^2 T_s^2 y'x' + \gamma R_f R_s T_f^2 T_s^2 y'x' + \ldots + \gamma R_f^n R_s^n T_f^2 T_s^2 y'x'\right] + \\
&\left[\gamma^2 R_s T_f^4 T_s^2 y'^2 x'^2 + \gamma^2 R_f R_s^2 T_f^4 T_s^2 y'^2 x'^2 + \ldots + \gamma^2 R_f^n R_s^{n+1} T_f^4 T_s^2 y'^2 x'^2\right] + \\
&\left[\gamma^3 R_s^2 T_f^6 T_s^2 y'^3 x'^3 + \gamma^3 R_f R_s^3 T_f^6 T_s^2 y'^3 x'^3 + \ldots + \gamma^3 R_f^n R_s^{n+2} T_f^6 T_s^2 y'^3 x'^3\right] + \ldots + \\
&\left[\begin{array}{l}\gamma^{n+1} R_s^n T_f^{2(n+1)} T_s^2 y'^{n+1} x'^{n+1} + \gamma^{n+1} R_f R_s^{n+1} T_f^{2(n+1)} T_s^2 y'^{n+1} x'^{n+1} + \ldots + \\ \gamma^{n+1} R_f^n R_s^{2n} T_f^{2(n+1)} T_s^2 y'^{n+1} x'^{n+1}\end{array}\right]
\end{aligned} \tag{3.10}$$

Eq. (3.10) can be re-written in the form:

$$\begin{aligned}
&R_{system_spectralon-panel} = R_s + R_f T_s^2 x' + \gamma T_f^2 T_s^2 y'x'^2 + \gamma^2 R_s T_f^4 T_s^2 y'^2 x'^3 + \\
&\gamma^3 R_s^2 T_f^6 T_s^2 y'^3 x'^4 + \ldots + \gamma^{n+1} R_s^n T_f^{2(n+1)} T_s^2 y'^{n+1} x'^{n+2}
\end{aligned} \tag{3.11}$$

which can further be simplified as:

$$\begin{aligned}
&R_{system_spectralon-panel} = R_s + R_f T_s^2 x' + \\
&\gamma T_f^2 T_s^2 y'x'^2 \left[1 + \gamma R_s T_f^2 y'x' + \gamma^2 R_s^2 T_f^4 y'^2 x'^2 + \ldots + \gamma^n R_s^n T_f^{2n} y'^n x'^n\right]
\end{aligned} \tag{3.12}$$

Substituting back Eqs. (3.8) and (3.9) into Eq. (3.12) and solving for the power series gives the following expression:

$$R_{system_spectralon-panel} = R_s + R_f T_s^2 \left(\frac{1}{1-R_f R_s} \right) + \gamma T_f^2 T_s^2 \left(\frac{1}{1-\gamma R_f} \right) \left(\frac{1}{1-R_f R_s} \right)^2 \left(\frac{1}{1-\left(\gamma R_s T_f^2 \left(\frac{1}{1-\gamma R_f} \right) \left(\frac{1}{1-R_f R_s} \right) \right)} \right) \tag{3.13}$$

The measured reflectance of the sample-substrate system when placed in front of an Analytical Spectral Devices spectralon panel having a reflectance factor γ is expressed as the summation of terms as shown in Eq. (3.13). Note that the first two terms in Eq. (3.13) are the same as in Eq. (3.6).

3.6.4 Sample reflectance

We deduce the spectral characteristics for the sample layer by using expressions (3.6) and (3.13) for the two cases derived above:

$$T_s^2 \left(\frac{1}{1-R_f R_s} \right) = \frac{\left(R_{system_spectralon-panel} - R_{system_light-trap} \right)}{\gamma T_f^2 \left(\frac{1}{1-\gamma R_f} \right) \left(\frac{1}{1-R_f R_s} \right) \left(\frac{1}{1-\left(\gamma R_s T_f^2 \left(\frac{1}{1-\gamma R_f} \right) \left(\frac{1}{1-R_f R_s} \right) \right)} \right)} \tag{3.14}$$

The reflectance of the sample layer is obtained by substituting Eq. (3.14) in Eq. (3.6):

$$R_{sample} = R_{system_light-trap} - R_f \left[\frac{\left(R_{system_spectralon-panel} - R_{system_light-trap}\right)}{\gamma T_f^2 \left(\frac{1}{1-\gamma R_f}\right)\left(\frac{1}{1-R_f R_s}\right)\left(\frac{1}{1-\left(\gamma R_s T_f^2 \left(\frac{1}{1-\gamma R_f}\right)\left(\frac{1}{1-R_f R_s}\right)\right)}\right)} \right] \tag{3.15}$$

The reflectance of the sample can be obtained using Eq. (3.15). However, during our reduction process, we noticed that implementing the above expression alone gave unphysical values for the sample reflectance and transmittance factors. One likely explanation is the expansion of the filter pores due to an increase in pressure gradient inside the filtration system during the cell deposition process. Deposition of additional cells over the threshold limit caused the filter to crack apart and break open and hence it is very likely that the filter pores expanded until this breaking limit was reached. The increased expansion causes a percentage of the incident light to undergo forward scattering and should be taken into account in Eq. (3.15) when calculating the reflectance of the sample layer. The following term accounts for the forward scattering component in our model:

$$\sum_0^\infty \gamma^n R_s^n = 1 + \gamma R_s + \gamma^2 R_s^2 + \ldots + \gamma^n R_s^n \tag{3.16}$$

Eq. (3.16) represents the total amount of light that would undergo multiple scattering between the sample layer and the spectralon panel. This holds true for cases when the incident light is forward scattered due to the expansion of the filter pores that results from an increased pressure gradient during our sample filtering methodology.

Our calculations indicate that at least 20% of the filter would undergo pore expansion for forward scattering of light, in order to achieve physical results for sample reflectance when using Eq. (3.15). The porosity of the filter substrate used is 79% and therefore a maximum of 79% of the filter can undergo forward scattering. In our model, we set the value to 50% such that about 50% of the wet filter has spectral properties as shown in Fig. 3.6 and the remainder of the filter undergoes forward scattering due to increased pore expansion.

On incorporating Eq. (3.16) into Eq. (3.15), we get the expression for the sample reflectance as:

$$R_{sample} = R_{system_light-trap} - R_f \left[\frac{\left(R_{system_spectralon-panel} - R_{system_light-trap}\right)}{\gamma \left[0.5 \cdot T_f^2 \left(\frac{1}{1-\gamma R_f} \right) \left(\frac{1}{1-R_f R_s} \right) \left(\frac{1}{1-\left(\gamma R_s T_f^2 \left(\frac{1}{1-\gamma R_f} \right) \left(\frac{1}{1-R_f R_s} \right) \right)} \right) + 0.5 \cdot \left(\frac{1-R_f R_s}{1-\gamma R_s} \right) \right]} \right] \quad (3.17)$$

We use the above equation to remove the effect of the filter substrate from the overall reflectance of the sample-substrate system in our reduction scheme.

Fig. 3.9 shows the uncertainty in the sample reflectance with respect to the minimum and maximum fraction of filter substrate that can undergo forward scattering.

From Eq. (3.6), the sample reflectance (R_s) can take values between $0 \leq R_s \leq R_{system_light-trap}$. As a first-order approximation, we use the function $R_s = R_{system_light-trap}/2$ in Eq. (3.17), in order to simplify the expression. As seen in Fig. 3.10, this approximation of R_s for the higher-order terms in Eq. (3.17) has

little effect in the overall value for the sample reflectance, with minor uncertainties.

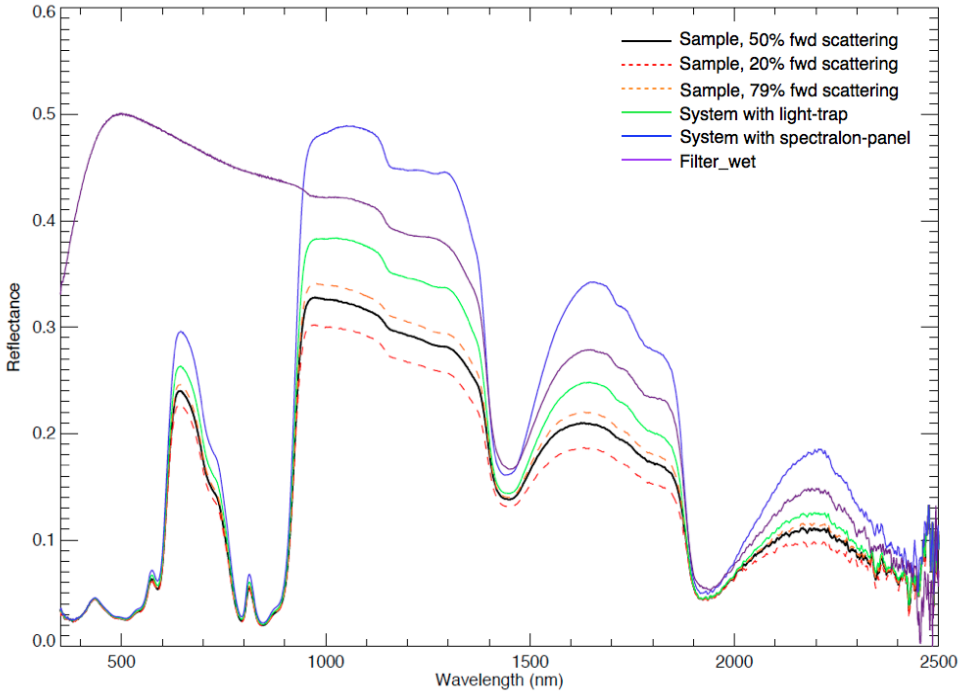

FIG. 3.9: Figure showing the uncertainty in the sample reflectance spectrum for a minimum (20%) and maximum (79%) fraction of filter substrate that can undergo forward scattering.

We have considered 50% of the filter to undergo forward scattering in our reduction model (see supporting text for more information). The characteristics of the sample-substrate system with a light trap and spectralon panel back, as well as the wet filter, are shown in the figure for comparison.

Results from our reduction process indicate that the spectral features observed from the sample-substrate system are primarily due to the overlaying sample coating itself with very little contribution from the filter substrate. This is especially true in the visible portion of the electromagnetic spectrum due to an optically thick layer of pigmented sample cells (10 – 50 µm) that are responsible for the spectral properties in this region. In the infrared portion, the spectral shape of both the sample and filter substrate is quite similar, with similar water absorption bands that vary in strength and depth. This is expected since the filter is made of mixed cellulose esters that also form similar bonds with water, like the sample organism, when wet. Based on the methodology used by us and

due to a dense layer of sample cells, the filter substrate is seen to have very little effect on the spectral features and is only observed to affect the absolute reflectance values when measured together with the sample. This has been corrected for during our reduction scheme, using the model described above.

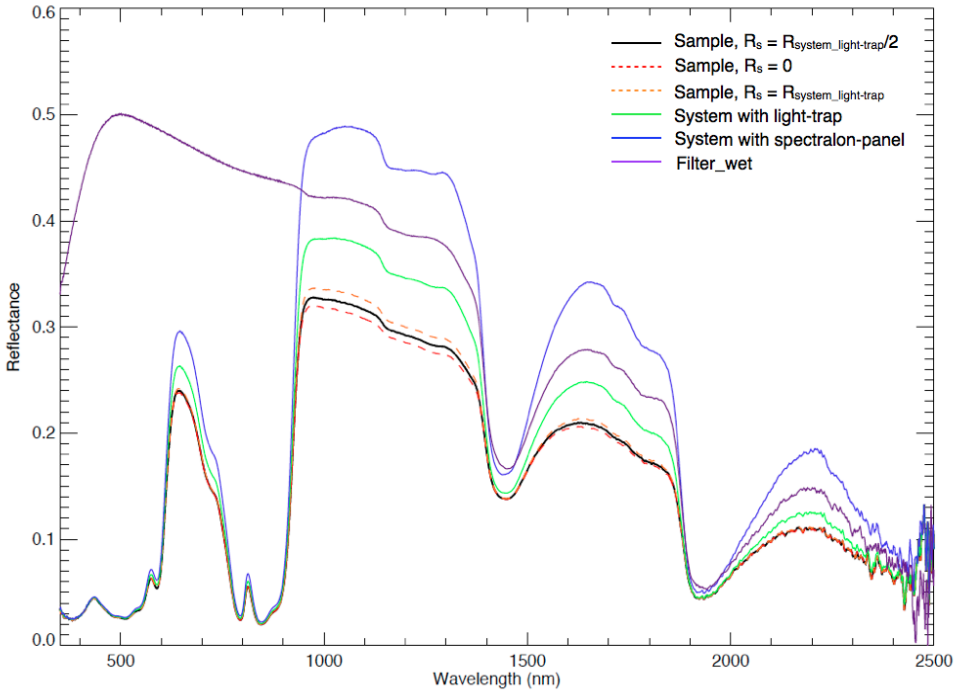

FIG. 3.10: Figure showing the uncertainty in the sample reflectance spectrum for the minimum and maximum values that can be used for the parameter R_s in Eq. (3.17).

We have considered the function $R_s = R_{system_light\text{-}trap}/2$ as the value for R_s in Eq. (3.17) of our reduction model (see supporting text for more information). The characteristics of the sample-substrate system with a light trap and spectralon panel back, as well as the wet filter, are shown in the figure for comparison.

3.7 Conclusions

We have assembled a digital spectral library containing of 137 microorganisms in the 0.35-2.5 µm spectral range (see *Appendix*). Such a detailed library is critical to capture the range of pigmentation patterns on Earth. The measurements made are those of hemispherical reflectance, covering a wide range of pigmented organisms, most of which are isolated from some of Earth's extreme environments.

This spectral database addresses the need for microbial reflectance spectra to support imaging photometric and spectroscopic studies for potential habitability of rocky extrasolar planets in the habitable zone of the central star (see Hegde and Kaltenegger, 2013). The spectra can be used to inform disk-integrated observations of rocky exoplanets as well as serve as surface albedo input parameters to atmospheric radiative transfer models (see, for example, Kaltenegger et al., 2007). This microbial spectral library complements existing spectral libraries that provide reflectance characteristics of other natural and man-made materials (Clark et al., 2007; Baldridge et al., 2009).

To facilitate comparison of our spectra with future observations of exoplanets, convolution of spectral resolution and bandpass can be performed, for example, by using a Gaussian convolution routine such as those made available in the SpecPr program (Clark, 1993).

Further additions to this library will be made in the near future, when more samples are made available, to help serve the growing need for microbial reflectance spectra to support future rocky exoplanet characterization studies. Our freely available database can be used as inputs to models of rocky exoplanets as well as help plan observational strategies to detect a variety of life on extrasolar planets.

4

Exploring colors of extreme exo-Earths: Prioritizing rocky exoplanets for potential habitability

4.1 Abstract

Over a thousand exoplanets have now been discovered and this number is expected to rise substantially over the coming years. Recent population studies suggest that the smaller planets are prevalent in our galaxy. The next generation of space- and ground-based instruments will provide the first opportunity to characterize rocky planets, but will have limited observation time available, and therefore it is critical to prioritize exoplanets for follow up characterization.

In this chapter, we use low-resolution broadband filter photometry in the visible to near infrared portions of the electromagnetic spectrum to explore how color-color diagrams can help in prioritizing potentially habitable planets for detailed follow up. This work builds upon our previous study by including a diverse range of 137 surface biota, a dataset that was recently added to the literature, in our analysis.

We show that color-color diagrams are a useful tool to differentiate types of planets as well as help prioritize exoplanets for spectroscopic characterization, and point out potential false positives based on the color of Solar System planets.

4.2 Introduction

OVER A THOUSAND EXOPLANETS have been detected by ground- and space-based telescopes, with several thousand planet candidates awaiting confirmation (see, for e.g., Batalha, 2014; Seager, 2013). Recent population study estimates reveal that small planets outnumber bigger ones (Fressin et al., 2013; Howard, 2013), a trend that is also seen in the radial velocity data based on planetary masses. The first estimates of Earth-sized planets in the habitable zone of their central stars (eta-Earth) range between 10 to 50%, depending on what limits for the habitable zone and what planetary radii/masses are used as cut-off (Traub, 2012, Dressing and Charbonneau, 2013; Kopparapu, 2013; Gaidos, 2013; Bonfils et al., 2013; Petigura et al., 2013). All sky survey missions like TESS (Ricker et al., 2014) and PLATO (Rauer et al., 2014) are expected to provide further data on the occurrence rate of small planets around close-by and bright stars.

Remote sensing of the planetary atmosphere and surface in the form of in-depth spectroscopic characterization can then explore the potential habitability of a planet and look for atmospheric biosignatures that are indicative of life. The next generation of space- (JWST) and ground-based telescopes (E-ELT, GMT, TMT) will provide the first opportunity to characterize rocky planets, but will have limited observation time available, and therefore it is critical to prioritize exoplanets for follow up characterization.

In this chapter, we explore how broadband filter photometry in the visible to near infrared portions of the electromagnetic spectrum can help prioritize exoplanet targets for follow up spectroscopic characterization (see also Hegde and Kaltenegger, 2013). For reflected light through direct imaging or secondary eclipse measurements, the color of a planet can give an initial approximation on its physical properties (Traub, 2003a, 2003b), and place constraints on the atmospheric composition (Crow et al., 2011).

For planets with clear atmospheres, the color of the surface environment can help build a link to the extreme life forms that may live in subsurface conditions (Hegde and Kaltenegger, 2013). In this chapter, we expand on that approach by adding a diverse range of 137 biota, a surface reflectivity dataset that was recently added to the literature (Hegde et al., 2014), in our analysis. Remote direct detection of surface life becomes possible when organisms live close to or on top of the surface environment and form large biological

structures. We explore the color signatures of planets dominated by such organisms by including a diverse range of surface reflectivity in our exo-Earth model that are properties of the organisms themselves. The diversity of exoplanets and planet candidates show a broad range in the physical and geochemical parameter space, suggesting that any environment on a planet is possible as long as they satisfy the laws of physics and chemistry. The stochastic nature of planet formation means that small changes in the initial conditions can have a major impact on the evolution of an exoplanet, which may lead to changes that allow for biota that is considered extreme on present-day Earth to be the dominant life form on a potentially habitable exoplanet. In this chapter, we explore the colors of surface dwelling organisms on a hypothetical exoplanet by considering the spectral signatures of a wide range of 137 phylogenetically diverse microorganisms.

Exploring surface features is only possible when no significant cloud cover exists on the planet or the signal-to-noise ratio (SNR) of each observation is sufficiently high such that the cloud contribution can be removed from the overall detected signal. To achieve such a SNR, several observations over one rotation period of the planet are required (see Pallé et al., 2008). To compare planets in our color-color diagram, we in addition assume a similar atmospheric composition as well as cloud coverage for the planet. We run our model for a modern Earth-like atmosphere to explore the effect of surfaces on the colors of such a planet (Fig. 4.1 and Fig. 4.2). The effect of atmospheric composition on the results is shown in the example of planets in our own Solar System in Fig. 4.3. Note that the radius of the planet does not influence the results because of the use of a color-color diagram.

Section 4.3 explains our model, filters, as well as the range of surface features used. Section 4.4 presents our results. Section 4.5 discusses the results, and we conclude our study in Section 4.6.

4.3 Surface reflection features of biota

Geological evidences suggest that single-celled microbes have dominated the history of life on Earth (Schopf, 1999). Microbes, particularly algae, are known to form large biological structures on Earth both in marine environments and

on landmasses (Knacke, 2003; Graham and Wilcox, 2000), which for Earth are easily detected using remote sensing techniques of Earth-orbiting satellites.

One approach when searching for life on exoplanets is to explore the environmental limits on Earth that support extreme forms of life – extremophiles – organisms that live and thrive under conditions that would otherwise make it challenging for a carbon-based life form that uses water as a solvent to survive (Rothschild and Mancinelli, 2001). Extremophiles cover a wide definition for life and provide us with the minimum known envelope of environmental limits. For extremophiles that form large structures close to or on top of the surface environment, remotely detectable surface reflectance can be a direct signature of life. Note that extremophiles are polyphyletic and hence other biota can show similar pigmentation that does not live under extreme conditions (see Hegde et al., 2014, for details). Thus, we explore the color signatures of a wide range of pigmentation types that have evolved on Earth by using the surface characteristics of 137 phylogenetically diverse microorganisms in this study, most of which were isolated from Earth's extreme environments. The data for these spectra are shown in the *Appendix* (from Hegde et al., 2014).

The Vegetation Red Edge (VRE) from terrestrial land plants, characterized by a strong increase in the reflectance at wavelengths longward of 0.75 μm, is often used as a direct signature of life (see, e.g., Arnold et al., 2002; Woolf et al., 2002). While such a reflection signature is easily detected for Earth from close by high-resolution spacecraft observations (Sagan et al., 1993), land plants only occupy a small niche in the environmental parameter space that binds known terrestrial life, and have been widespread on Earth for only about 460 million years (Carroll, 2001).

By considering the diverse range of pigmentation types, we include extreme as well as non-extreme forms of life in our model. The results obtained reflect the diversity of life on Earth, as guidelines to prioritizing exoplanets.

The broadband filters (B, V, and I) used in generating the color-color diagram are filters defined for the Johnson-Cousins system. We define the color of a planet, as:

$$C_{BV} = B - V = -2.5 \log_{10}\left(\frac{r_B}{r_V}\right) \tag{4.1}$$

$$\text{and } r_B = \frac{\int_B A_{B,\lambda} R_{B,\lambda}\, d\lambda}{\int_B R_{B,\lambda}\, d\lambda} \tag{4.2}$$

where A_B and R_B are surface albedos and filter responses for the Johnson B-band, respectively.

To compare our results with earlier work (Traub, 2003b) that uses a color-color diagram to distinguish the types of planets in our own Solar System, we also use custom filters as defined in Traub (Traub, 2003b) from 0.4-1.0 μm with 0.2 μm bandwidth per filter.

The planetary data used for comparison to the Solar System planets with atmospheres, is based on data for Venus from Irvine (1968b), Mars and Jupiter from Irvine (1968a), and Saturn, Titan, Uranus, and Neptune from Karkoschka (1998). The albedo for present-day Earth was modeled by assigning 70% of the planetary surface as ocean, 2% as coast, and 28% as land. The land fraction is made up of 60% vegetation, 9% granite, 9% basalt, 15% snow, and 7% sand (following Kaltenegger et al., 2007).

4.4 Results

Using the surface reflectance characteristics of 137 microorganisms from 0.36 – 0.90 μm, we generate a low-resolution characterization of Earth-like planets using a color-color diagram. Our model assumes detected reflected flux from the planet, and therefore suppression of the stellar light or secondary eclipse measurements, while making this comparison for similar planets that differs only in surface composition. Following our assumption that the initial conditions during planet formation can have a major impact on the evolution of a planet, we assume a particular surface feature to have full surface coverage in our exo-Earth model to prove the principle. The effect of adding water as a second surface in a color-color diagram was explored by Hegde and Kaltenegger (Hegde and Kaltenegger, 2013) and moves the points toward the lower left corner of the diagram along parallel lines to the limits of the zones. Fig. 4.1 shows the B-V versus the B-I color-color diagram of the 137 microorganisms for an Earth analog planet with a clear atmosphere whose surface is covered by one of these microorganisms. Squared triangles denote a planet completely covered by a microorganism. Plusses denote a planet covered by a particular surface

that can host extremophiles (green) and the four organisms (including land plants) where reflection spectra were available in the literature (blue) (see Hegde and Kaltenegger, 2013). Region I defines the area of extreme Earths; region II denotes a wider contour of habitable planets. Region I and II fall between the contours of a diagonal in the color-color diagram, that we propose to use as a first prioritization for rocky planets in the habitable zones of their host stars to follow up.

Note that the new data for the 137 measured microorganisms, re-defines the contours for region I and II compared to the initial contours proposed by Hegde and Kaltenegger (Hegde and Kaltenegger, 2013) (see Discussion). As in that paper, adding water as a second surface fraction of the planet moves the position of the planet in the color-color diagram along the diagonal towards the lower left.

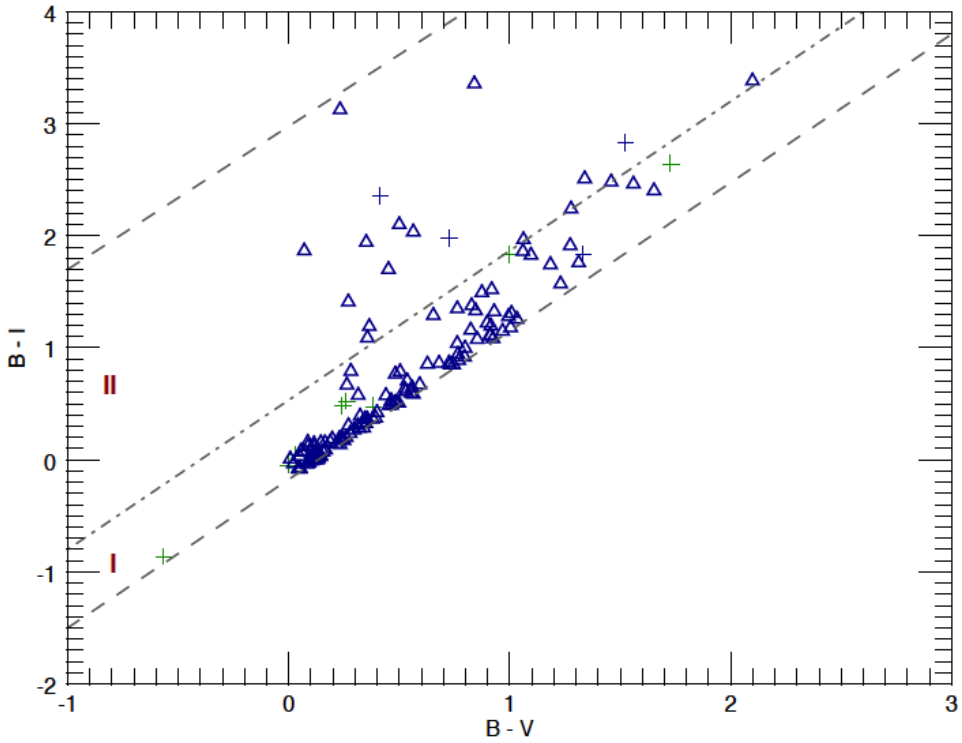

FIG. 4.1: Color-color diagram showing the position of remotely detectable surfaces features of life for 137 microorganisms.

Squared triangles denote a planet completely covered by one of these microorganisms. Plusses denote a planet covered by a particular surface that can host extremophiles (green) and the four organisms (includes land plants) where reflection spectra were available in the literature (blue) (see Hegde and Kaltenegger, 2013). Region I defines the area of extreme Earths; region II denotes a wider contour of habitable planets.

Fig. 4.2 shows the color-color diagram from Fig. 4.1 with the Solar System objects with atmospheres added, indicating that one can use color-color diagrams to differentiate a range of rocky planets and moons from gas giants, like the ones in our own Solar System. This was shown by Traub (Traub, 2003b) for the Solar System (Fig. 4.3a). Fig. 4.2 also shows that Saturn, Venus, and Titan fall within the contours of extreme life and are very similar to several of the measured biota. Saturn can be excluded as a habitable world due to initial radius or mass measurements but Venus will not be able to be separated from potentially habitable Earth-like planets and therefore is a false positive in the color-color diagram. Also, Titan falls within the contours of the extreme Earths and is a false positive because one cannot penetrate the cloud cover. Further work will be needed to distinguish different kind of planets in the color-color diagram proposed.

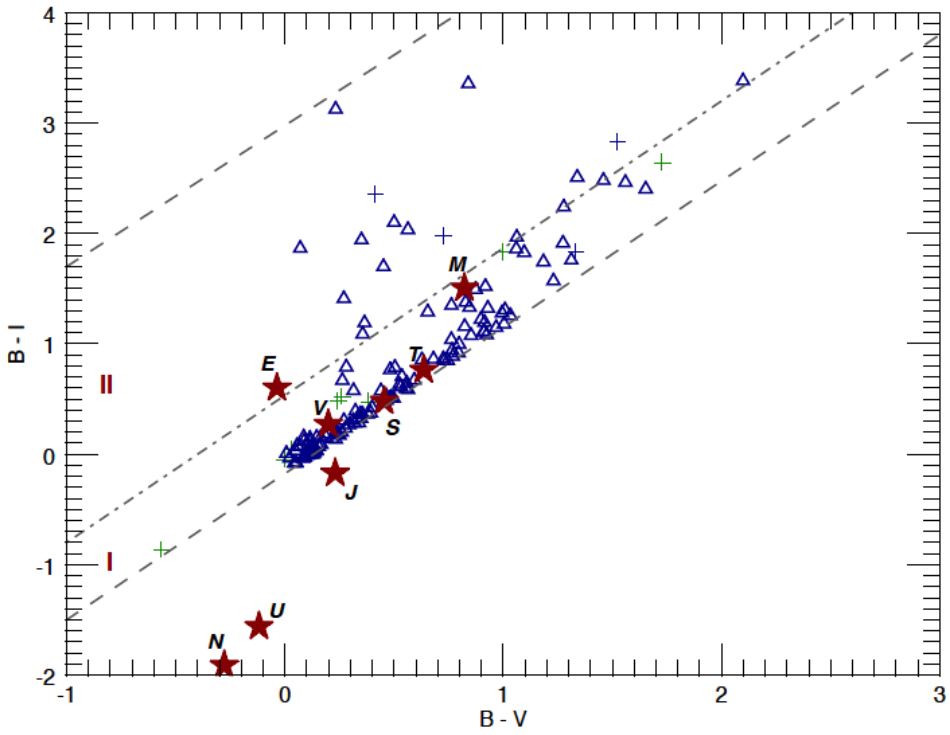

FIG. 4.2: Color-color diagram showing the position of hypothetical exo-Earths covered with one of 137 diverse microorganisms as well as the Solar System objects with an atmosphere.

The symbols have the same denotation as in Fig. 4.1.

4.5 Discussion

Remote sensing of surface characteristics of life can only be sampled directly when the organism is living close to or on top of the surface environment. For subsurface life, indirect connections can be drawn by linking the remotely detectable surface features to the extreme forms of life that such surfaces can support (see Hegde and Kaltenegger, 2013). However, any photosynthesizing organism on an exoplanet that uses chlorophyll or any light-gathering molecule will likely populate the surfaces of oceans and landmasses in order to utilize the energy from the central star.

The surface properties of organisms in the visible waveband are largely due to the pigmentation makeup, and independent of the hardiness and functionality that makes an extremophile (see Dalton et al., 2003; Hegde et al., 2014). For this reason, any hypotheses made about extraterrestrial surface life based on Earth life, should take into account the range of pigmentation types that have evolved on this Earth. Detection of surface signatures of life alone is not indicative of the organism being an extremophile. Hence, we have re-defined the contours in Fig. 4.1 and 4.2 by narrowing down the area for region I (extreme Earths) to include remotely detectable surface features that can be linked to extreme environments on Earth, and have expanded region II to include a wider contour of habitable planets that covers a broad range of surface life; both extreme and non-extreme.

Fig. 4.2 shows that gas giants like Neptune, Uranus, and Jupiter all fall outside the contours. Saturn falls at the boundary of region I possibly because of its icy rings that hide the methane and cloud colors. Planets with thick atmospheres like Venus and Titan fall in our extreme Earth region indicating where similar cloud covered planets may fall in our color-color diagram. Planets with clear atmospheres like Mars and Earth fall closer to region II defined as habitable planets. Note that detection of such surface features alone in a reflection spectrum is not indicative of potential habitability. The method presented here provides a first characterization for prioritization of rocky exoplanet targets to follow up using spectroscopic techniques. Our results indicate that higher priority should be given to any rocky planet that falls toward the lower left corner of region II indicating habitable environments as well as the presence of free surface liquid water.

A color-color diagram can be used to prioritize Earth-like exoplanets once they have been identified either from their physical properties (radius or mass measurements through transit or radial velocity or astroseismology methods). An alternative way is to use a color-color diagram with custom filters that distinguish the known planets in our own Solar System (Traub, 2003b) as shown in Fig. 4.3a. Fig. 4.3 illustrates where the different types of planets fall when using customized filter responses – instead of the generic Johnson-Cousins filters shown in Fig. 4.2 – as defined by Traub (Traub, 2003b) from 0.4-1.0 μm with 0.2 μm bandwidth per filter. We have added the microorganisms to the plot using the customized filters to show that this distinction gets harder to see when a wide range of surfaces and biota are considered (Fig. 4.3b).

(A)

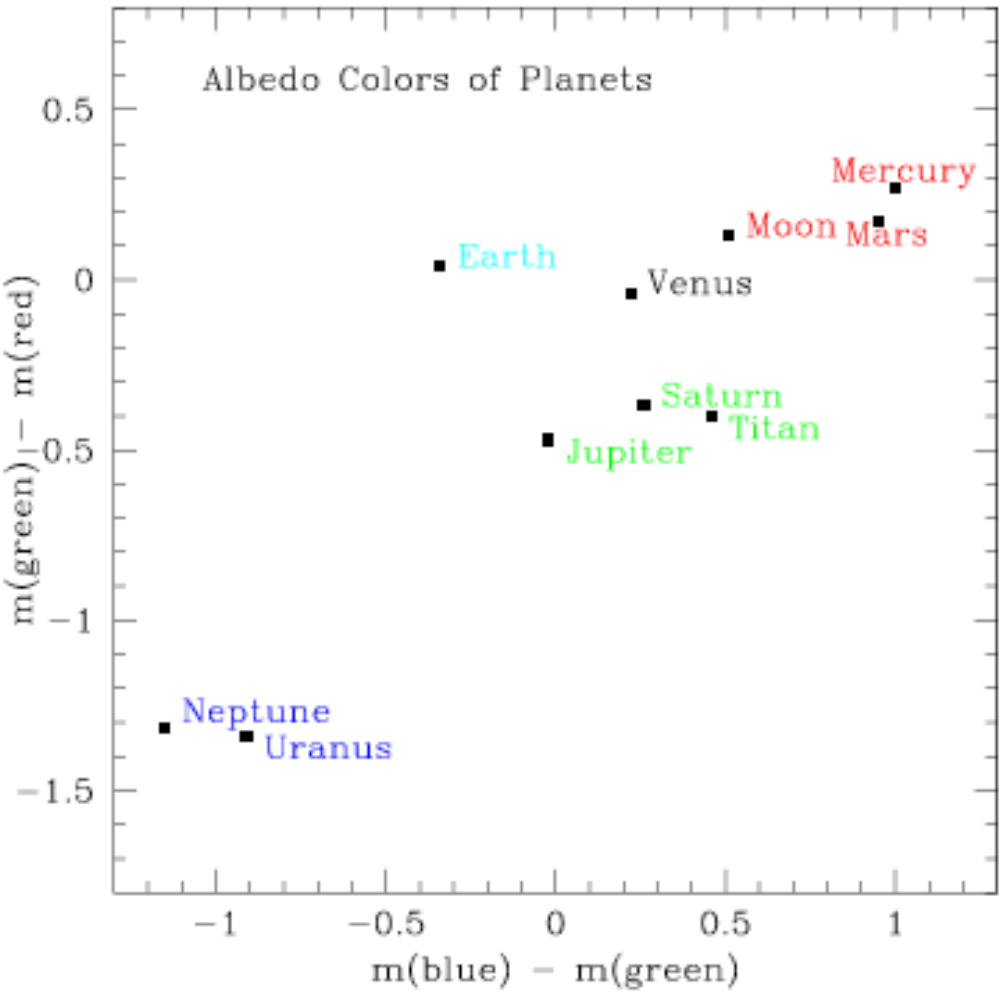

(B)

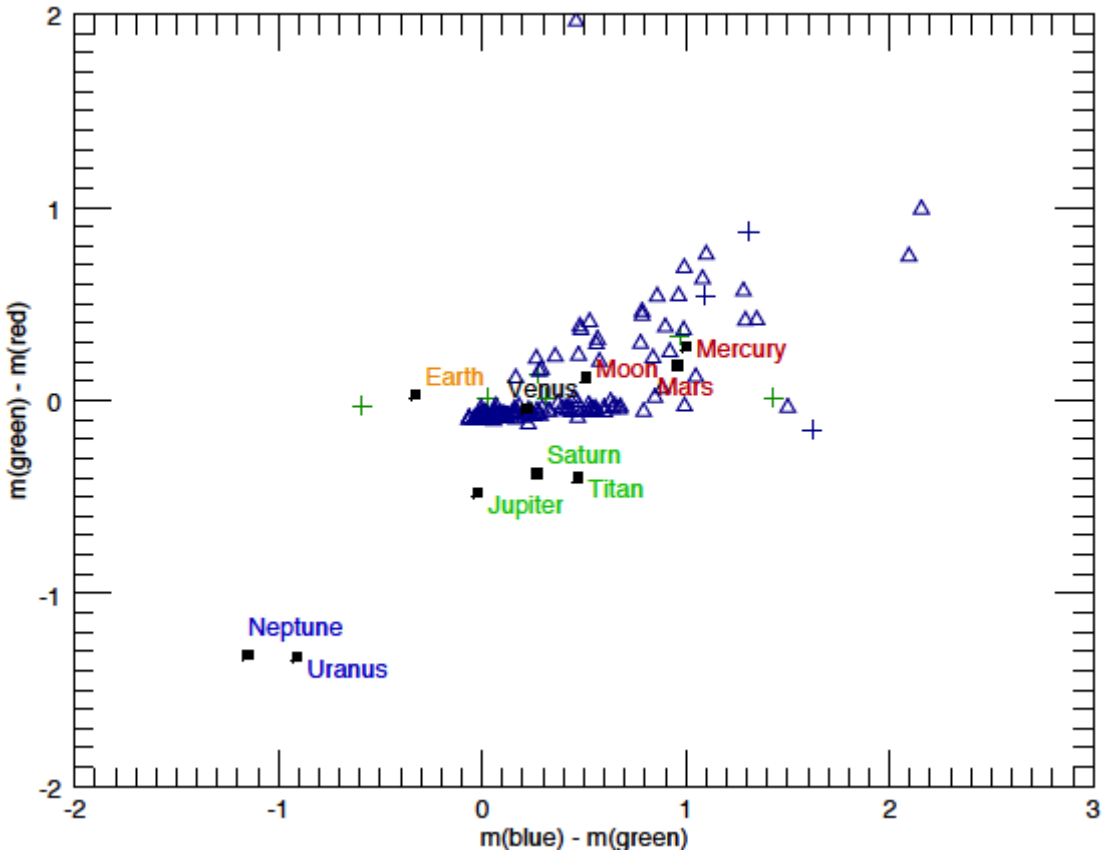

FIG. 4.3: Color-color diagram distinguishing the different classes of planets.

Unfilled triangles and plusses represent hypothetical exo-Earths having surface coverage as explored in Hegde and Kaltenegger (2013) and in this work. Fig. 4.3a as well as the data points for the Solar System objects were taken from Traub (Traub, 2003b).

Fig. 4.3a shows a better distinction for planetary characteristics – applied to our own Solar System – than Fig. 4.2. Gas giants (and Titan) fall in a different area of the diagram than the rocky planets in our Solar System. Like in Fig. 4.2, Venus falls within the boundary of the reflectivity seen by the microorganisms. Since Venus is very similar in radius and mass to the Earth, Venus will confuse the characterization of potentially habitable planets from a color-color diagram.

The inclusion of hypothetical exo-Earths with extreme environments and life in the diagram, seem to cluster together with the rocky planets, suggesting that customized filters can be useful in differentiating the types of planets.

The albedo and hence the color of surface life on extrasolar planets may depend on the local conditions that are prevalent there. For instance, any organism that uses a light-gathering molecule for photosynthesis may evolve such that the photosynthetic pigment has maximum absorption near the central star's spectral peak in order to utilize maximum energy from the star. The number of cooler and redder M-dwarf stars in our galaxy far outnumbers the Solar-type stars. Hence, the peak absorption may shift red-ward for organisms that inhabit planets around such stars. However, any such hypotheses made for life on potentially habitable planets should consider the strong atmospheric and water absorptions in the infrared portion of the electromagnetic spectrum. Therefore, the degree to which extraterrestrial life evolves its photosynthetic pigment remains an open question.

4.6 Conclusions

Over a thousand exoplanets have now been discovered with several thousands soon to be confirmed. Due to limited observation time on the next generation of telescopes, it becomes critical to prioritize the best exoplanet targets for spectroscopic follow up.

This chapter shows how broadband filter photometry can be a useful tool as a first step in prioritizing Earth-like planets for potential habitability and life. We explore the color signatures of hypothetical exo-Earths covered by life by making use of the surface biosignatures of 137 phylogenetically diverse microorganisms, most of which are isolated from extreme environments on Earth.

Our results show that an Earth-like planet placed outside the contour in Fig. 4.2 should receive lower priority for follow up since it does not correspond to any known environmental or surface biosignature on Earth. Our results also suggest that higher priority for follow up should be given to any planet that falls toward the lower left corner of region II in our color-color diagram indicating habitable environments and the presence of free surface liquid water. Venus is a false positive even in the color-color diagram with customized filters that cautions its exclusive use for prioritization. Additional data or new observations of surface features may move these contours in the future.

The method presented in this chapter is useful as a first characterization for prioritizing rocky extrasolar planets for follow up studies once they have been identified. Detailed spectroscopic analyses of the exoplanetary atmosphere and surface properties can then be carried out for further information on potential habitability and life.

5

Summary and Outlook

In this work, I show how broadband photometry is a useful tool with which to initially characterize rocky planets. I explore the color signatures of extreme environments and life in the visible and near infrared wavebands, and show that color-color diagrams can be used as a first step for differentiating the types of planets, and in getting an initial characterization on the potential habitability of Earth-like planets in the habitable zone of their central stars.

In Chapter 2, I have considered the various environments found on Earth that support the different classes of extremophiles. I have then built a link between these environments and the surface features that one would detect for remote observations. These surface features were then extrapolated to Earth-analogs and the colors obtained were useful in distinguishing the different types of potentially habitable planets. The effect of water as a second surface was also explored across the parameter space, which is useful in prioritizing rocky planets for follow up spectroscopy. The chapter provides a link between geomicrobiology and observational astronomy by exploring the low-resolution characterization of an Earth-like planet for various surface environments and the extreme forms of life that such environments support.

In Chapter 3, I provide a first spectral database of reflectance properties for a broad range of 137 pigmented organisms, including ones that were isolated from some of Earth's most extreme environments. The Vegetation Red Edge (VRE) from terrestrial land plants has long been used as a direct signature of life. But land plants occupy only a small niche in the environmental parameter space on Earth and have also been widespread for only about 460 million years. Our spectral database provides a broader and more realistic guide by exploiting the diversity of life known on Earth, and addresses the need for microbial reflectance spectra to support imaging photometric and spectroscopic studies for potential habitability of exoplanets.

In Chapter 4, I complement and build upon the work carried out in Chapter 2 by considering the color signatures of biota that live close to or on top of the surface environment, and form large biological structures, which can be detected remotely for direct signatures of life. I make use of the spectral database presented in Chapter 3 and model a plethora of exo-Earths that are dominated by one kind of biota. In this chapter, I explore both standard and customized filters. The results show that while customized filters like the ones used by Traub (2003b) are useful in differentiating the planet types, placing prioritization for rocky planets becomes challenging. Standard Johnson-Cousins filters give better results for prioritizing Earth-like planets in the habitable zone for follow up studies. It must be noted though that the method is prone to false-positives with Solar System objects like Venus and Titan showing similar colors to several biota. Further work needs to be carried out in this regard in terms of refining the filter definitions. Our results show that an Earth-like planet placed outside the contour in our color-color diagrams should receive lower priority for follow up since it does not correspond to any known environment or surface biosignature on Earth. Our results also show that higher priority for follow up should be given to any planet that falls toward the lower left corner of region II in our color-color diagram – indicating potentially habitable environments and the presence of free surface liquid water.

Exploring the surface signatures is only possible when no significant cloud cover exists on the planet or the signal-to-noise ratio of each observation is sufficiently high to remove the cloud contribution from the overall detected signal.

Finally, detection of surface features of environments or biota in a reflection spectrum alone is not a reliable detection of potential habitability or life. This diagnostic needs to be complemented with atmospheric properties. The work presented in this thesis provides a first characterization of rocky planets in the habitable zone, in order to prioritize exoplanet targets for in-depth spectroscopic analysis.

The thesis builds a strong interdisciplinary bridge between observational astronomy and geomicrobiology, and provides a first step toward characterizing a second Earth, in preparation for the next generation of space- and ground-based instruments that will look for potentially habitable planets and search for a wide variety of life.

Appendix

Description of samples used for measuring the surface biosignatures of exo-Earths.

The sample description pages that follow provide detailed information on the 137 samples used by us while carrying out our hemispherical reflectance measurements. Each page provides information on an individual sample as below:

Sample header: Sample name + _ + accession number (when available).

Sample name: Scientific name of the isolate.

Accession number for 16S rRNA partial gene sequence: Accession numbers (when available) that gives additional information on differentiating organisms belonging to the same genus. The sequences can be found by inserting the accession numbers on the National Center for Biotechnology Information (NCBI) website at http://www.ncbi.nlm.nih.gov/nuccore/.

Classification: Biological classification of the organism.

Metabolism: States whether the organism uses photosynthetic (with type) or non-photosynthetic metabolic processes.

Origin: Source location of the organism from where it was isolated.

Isolation/Collection: Information on the isolate donor.

Sample concentration: Quantitative estimate on the concentration of the pure sample culture growing as cell suspension in liquid media.

Sample count on filter substrate: Quantitative estimate on the total amount of cells that were deposited on the filter substrate before cell saturation was reached.

Laboratory growth conditions: Information on the growth conditions used by us while growing the sample from seed cultures.

Culture medium: The medium that was used to grow the culture.

Sample photograph: Photographic image of the sample on the filter substrate.

Sample micrograph: Microscopic image of the sample cells. The microscopic images of cells provided for most samples are those using a phase-contrast (PH) microscopy. For algal cultures, the cell micrographs are those using a differential-interference contrast (DIC) microscopy.

Sample reflectance spectrum: Hemispherical reflectance characteristics of the sample organism from 350 – 2500 nm.

Agrococcus sp._KM349956

Sample name: *Agrococcus* sp.

Accession number for 16S rRNA partial gene sequence: KM349956

Classification: Bacteria; Actinobacteria; Actinobacteridae; Actinomycetales; Micrococcineae; Microbacteriaceae; Agrococcus

Metabolism: Heterotrophic

Origin: Atacama desert, Chile

Isolation: Ivan P. Lima (NPP at NASA Ames, CA, USA)

Sample concentration: 1.63×10^8 cells/ml

Sample count on filter substrate: $4.90 \pm 0.33 \times 10^8$ cells

Laboratory growth conditions: 30 °C, 180 rpm, 24 h

Culture medium: Marine Broth (MB)

Sample photograph:

Sample micrograph:

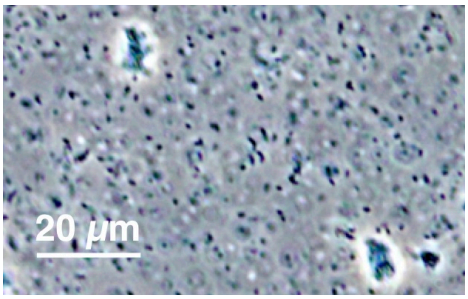

Sample reflectance spectrum:

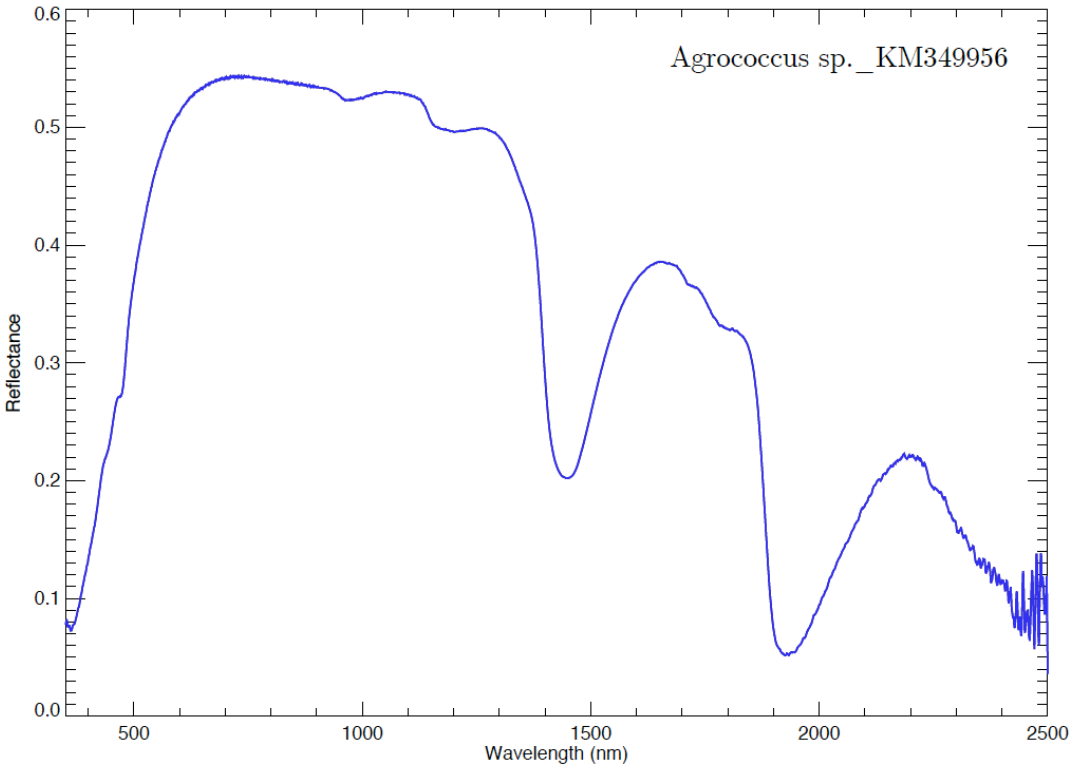

Alphaproteobacteria_KM349946

Sample name: Alphaproteobacteria

Accession number for 16S rRNA partial gene sequence: KM349946

Classification: Bacteria; Proteobacteria; Alphaproteobacteria

Metabolism: Heterotrophic

Origin: Atacama desert, Chile

Isolation: Ivan P. Lima (NPP at NASA Ames, CA, USA)

Sample concentration: 3.37 $\times$ 10^7 cells/ml

Sample count on filter substrate: 1.01 $\pm$ 0.07 $\times$ 10^8 cells

Laboratory growth conditions: 30 °C, 180 rpm, 24 h

Culture medium: Reasoner's 2A (R2A)

Sample photograph:

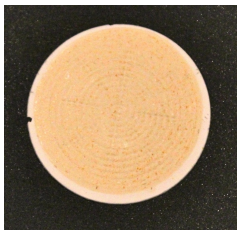

Sample micrograph:

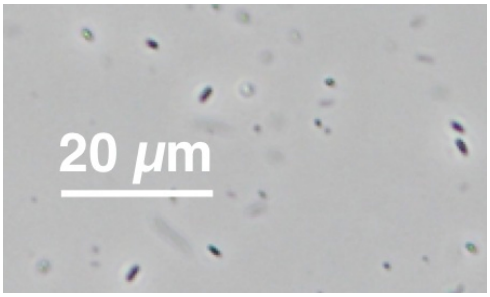

Sample reflectance spectrum:

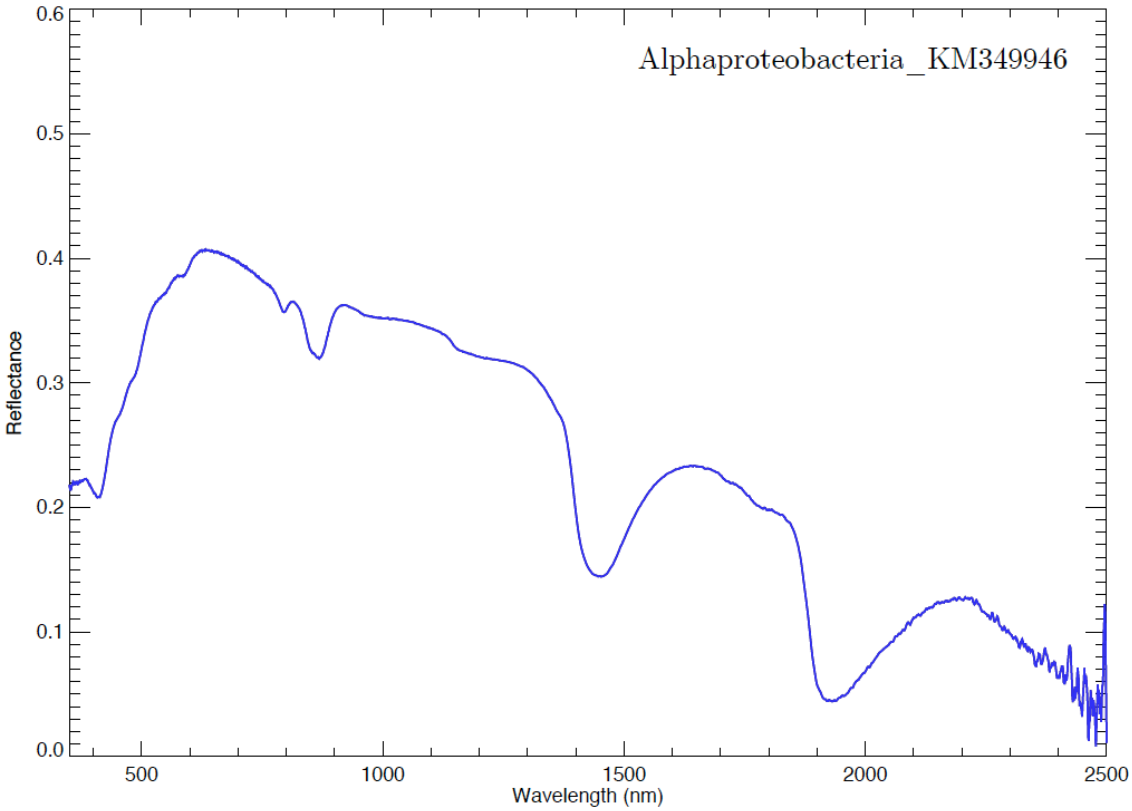

Amphidinium carterae

Sample name: *Amphidinium carterae*

Accession number for 16S rRNA partial gene sequence: Not available

Classification: Eukaryota; Dinophyta; Dinophyceae; Gymnodiniales; Gymnodiniaceae; Amphidinium

Metabolism: Autotrophic (oxygenic photosynthesis)

Origin: Found on the coasts of the Atlantic and Pacific oceans

Collection: Kudela laboratory (UCSC, CA, USA)

Sample concentration: 2.70×10^5 cells/ml

Sample count on filter substrate: $2.70 \pm 0.27 \times 10^6$ cells

Laboratory growth conditions: 25 °C, up to 6 months

Culture medium: Enriched Seawater medium (f/2)

Sample photograph:

Sample micrograph:

Sample reflectance spectrum:

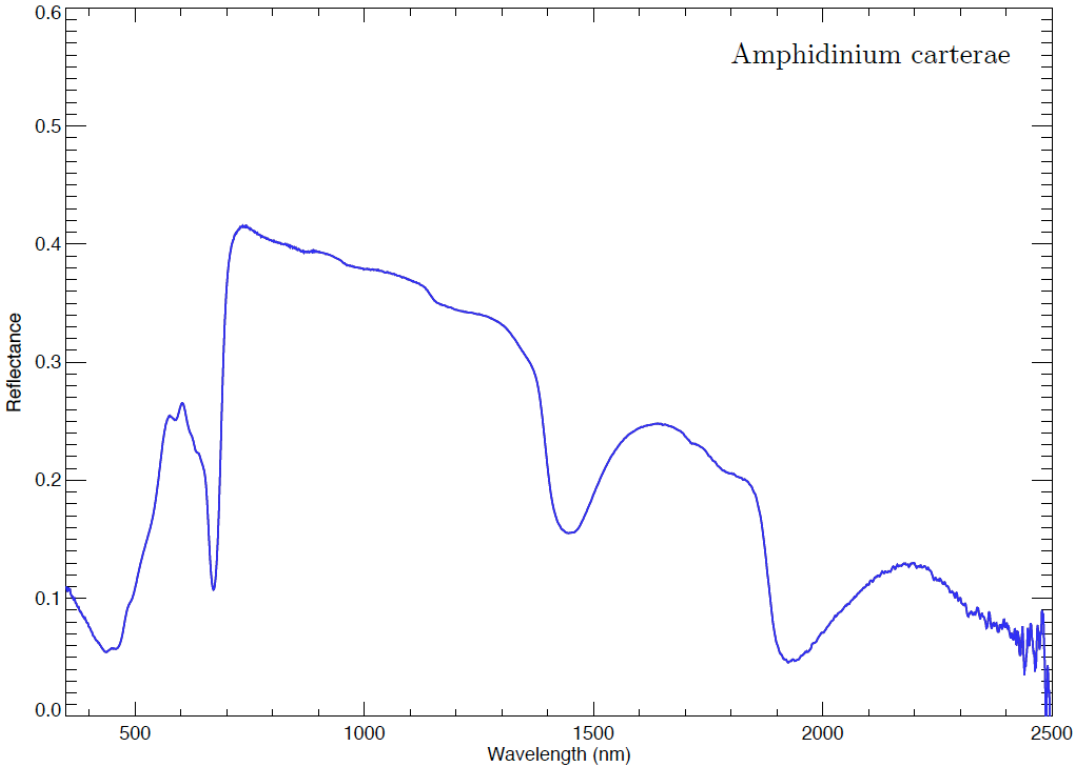

Anabaena sp. str. PCC 7120

Sample name: *Anabaena* sp. str. PCC 7120

Accession number for 16S rRNA partial gene sequence: Not available

Classification: Bacteria; Cyanobacteria; Cyanophyceae; Nostocales; Nostocaceae; Anabaena

Metabolism: Autotrophic (oxygenic photosynthesis)

Origin: Stagnant Freshwater

Collection: Rothschild laboratory (NASA Ames, CA, USA)

Sample concentration: 1.26×10^7 cells/ml

Sample count on filter substrate: $3.79 \pm 0.25 \times 10^7$ cells

Laboratory growth conditions: 25 °C, up to 6 months

Culture medium: Blue-Green medium (BG-11)

Sample photograph:

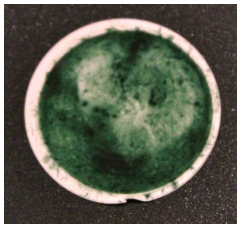

Sample micrograph:

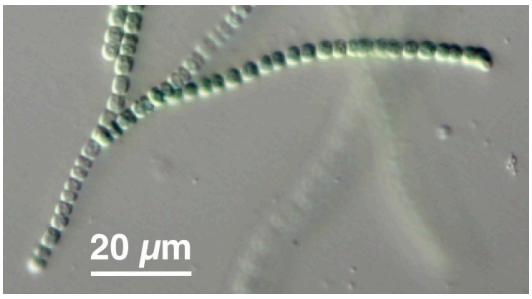

Sample reflectance spectrum:

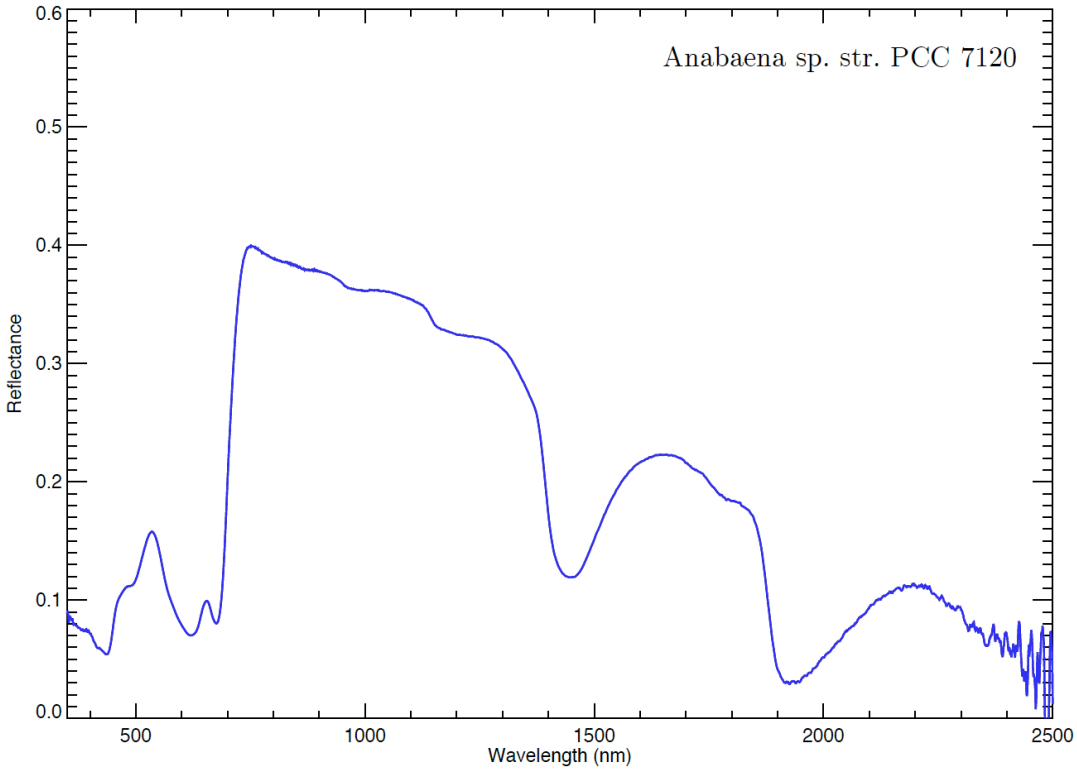

Anabaena sp. str. PCC 7120 with green fluorescent protein

Sample name: *Anabaena* sp. str. PCC 7120 with green fluorescent protein

Accession number for 16S rRNA partial gene sequence: Not available

Classification: Bacteria; Cyanobacteria; Cyanophyceae; Nostocales; Nostocaceae; Anabaena

Metabolism: Autotrophic (oxygenic photosynthesis)

Origin: Stagnant Freshwater

Collection: Rothschild laboratory (NASA Ames, CA, USA)

Sample concentration: 1.26×10^7 cells/ml

Sample count on filter substrate: $3.79 \pm 0.25 \times 10^7$ cells

Laboratory growth conditions: 25 °C, up to 6 months

Culture medium: Blue-Green medium (BG-11)

Sample photograph:

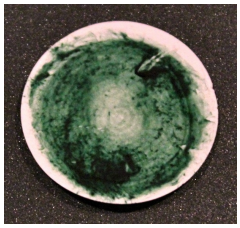

Sample micrograph:

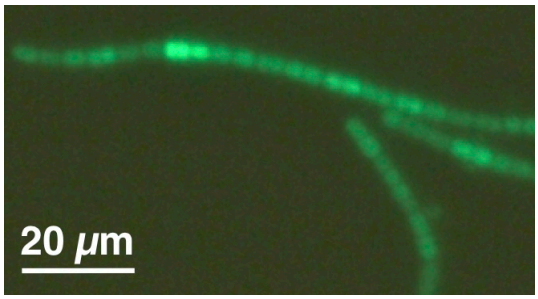

Sample reflectance spectrum:

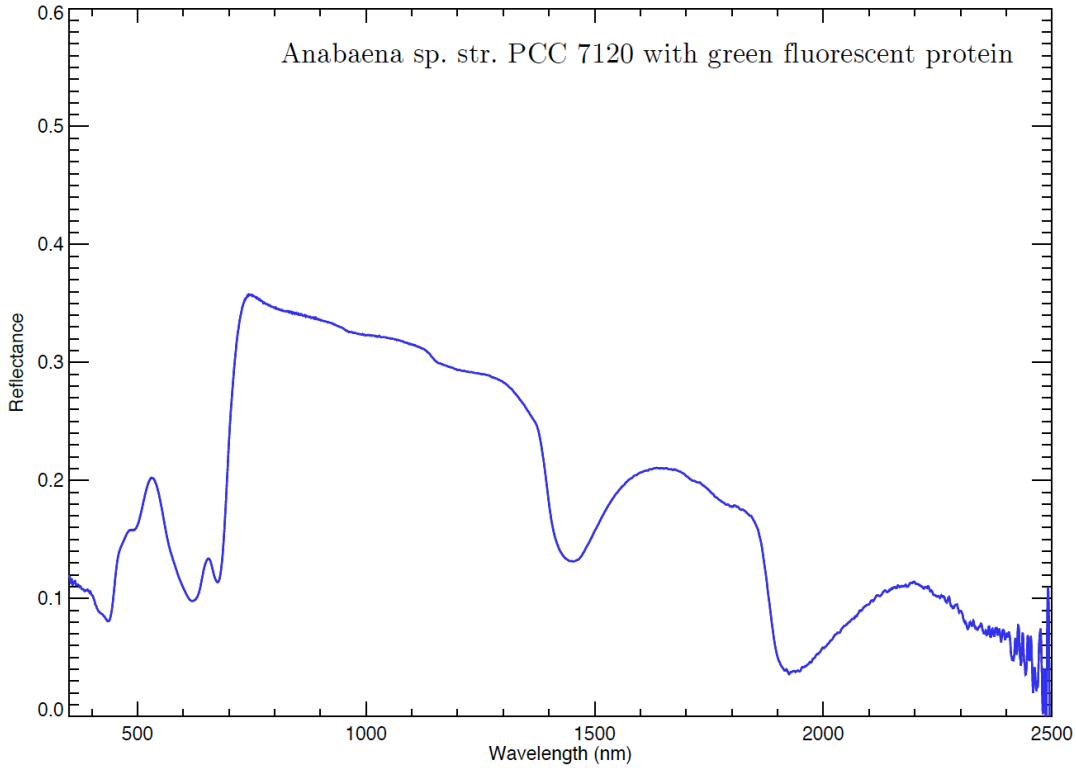

Arthrobacter sp._KM349883

Sample name: *Arthrobacter* sp.

Accession number for 16S rRNA partial gene sequence: KM349883

Classification: Bacteria; Actinobacteria; Actinobacteridae; Actinomycetales; Micrococcineae; Micrococcaceae; Arthrobacter

Metabolism: Heterotrophic

Origin: Atacama desert, Chile

Isolation: Ivan P. Lima (NPP at NASA Ames, CA, USA)

Sample concentration: 6.39×10^7 cells/ml

Sample count on filter substrate: $1.92 \pm 0.13 \times 10^8$ cells

Laboratory growth conditions: 30 °C, 180 rpm, 24 h

Culture medium: Marine Broth (MB)

Sample photograph:

Sample micrograph:

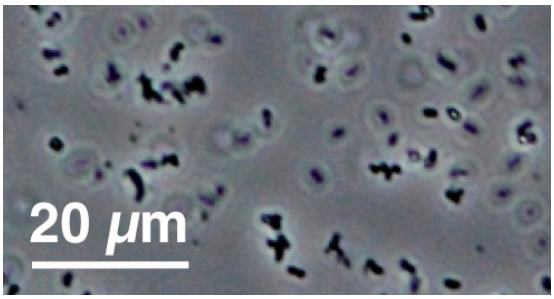

Sample reflectance spectrum:

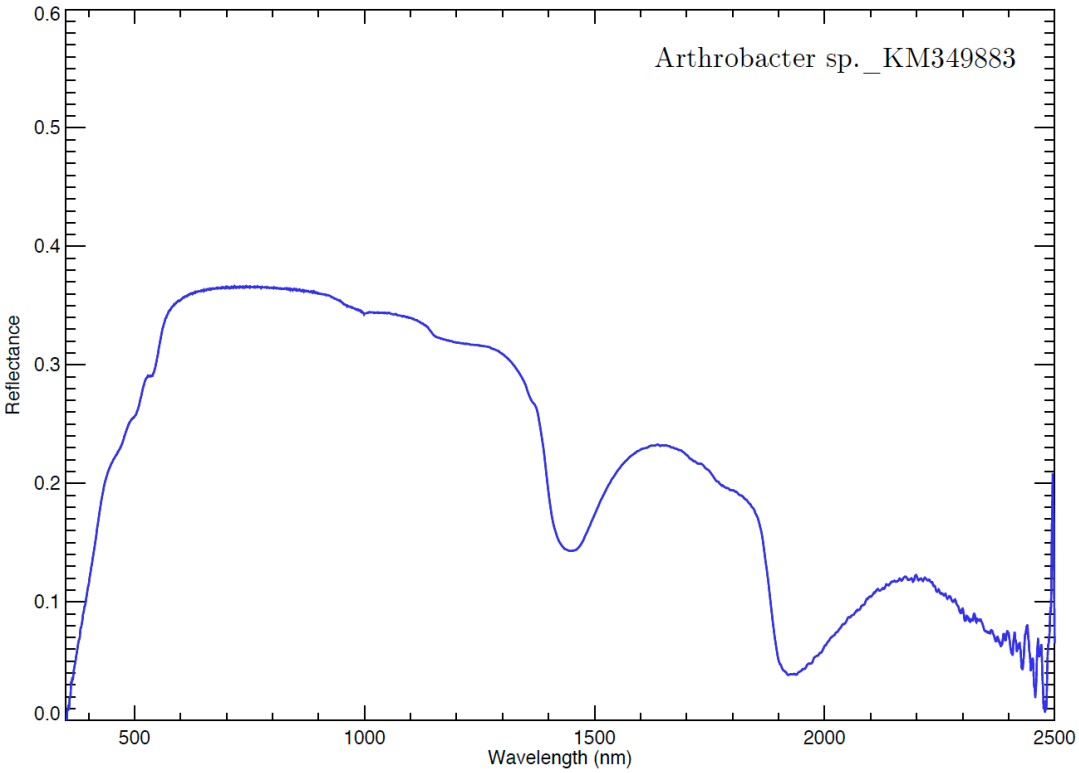

Arthrobacter sp._KM349893

Sample name: *Arthrobacter* sp.

Accession number for 16S rRNA partial gene sequence: KM349893

Classification: Bacteria; Actinobacteria; Actinobacteridae; Actinomycetales; Micrococcineae; Micrococcaceae; Arthrobacter

Metabolism: Heterotrophic

Origin: Atacama desert, Chile

Isolation: Ivan P. Lima (NPP at NASA Ames, CA, USA)

Sample concentration: 4.35×10^7 cells/ml

Sample count on filter substrate: $1.30 \pm 0.09 \times 10^8$ cells

Laboratory growth conditions: 30 °C, 180 rpm, 24 h

Culture medium: Lysogeny Broth (LB)

Sample photograph:

Sample micrograph:

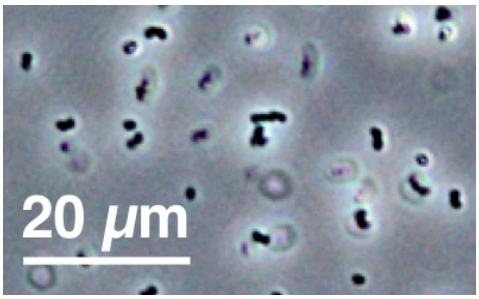

Sample reflectance spectrum:

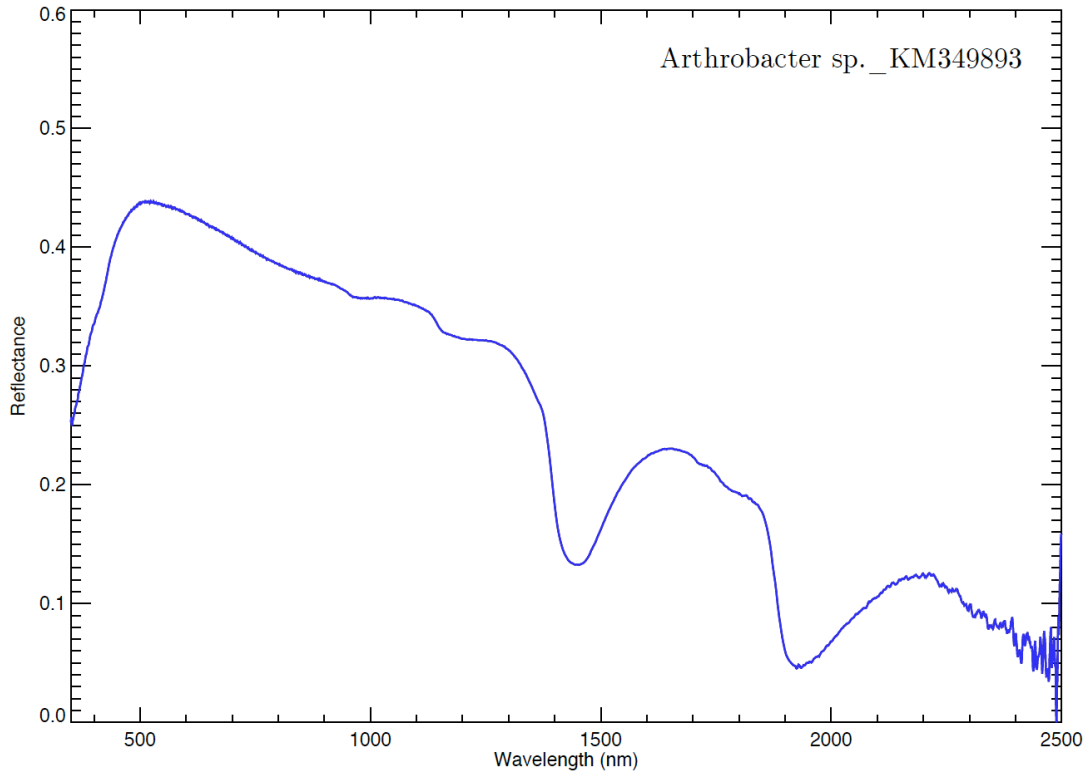

Arthrobacter sp._KM349898

Sample name: *Arthrobacter* sp.

Accession number for 16S rRNA partial gene sequence: KM349898

Classification: Bacteria; Actinobacteria; Actinobacteridae; Actinomycetales; Micrococcineae; Micrococcaceae; Arthrobacter

Metabolism: Heterotrophic

Origin: Atacama desert, Chile

Isolation: Ivan P. Lima (NPP at NASA Ames, CA, USA)

Sample concentration: 1.97×10^7 cells/ml

Sample count on filter substrate: $5.90 \pm 0.39 \times 10^7$ cells

Laboratory growth conditions: 30 °C, 180 rpm, 24 h

Culture medium: Marine Broth (MB)

Sample photograph:

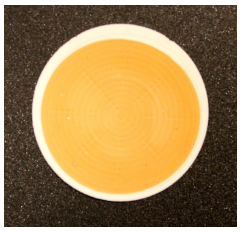

Sample micrograph:

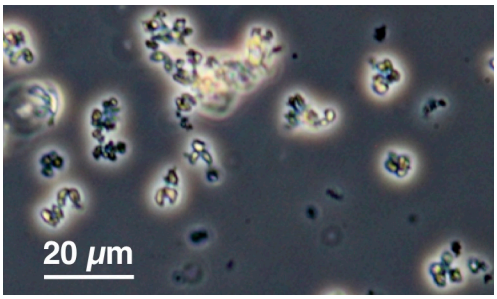

Sample reflectance spectrum:

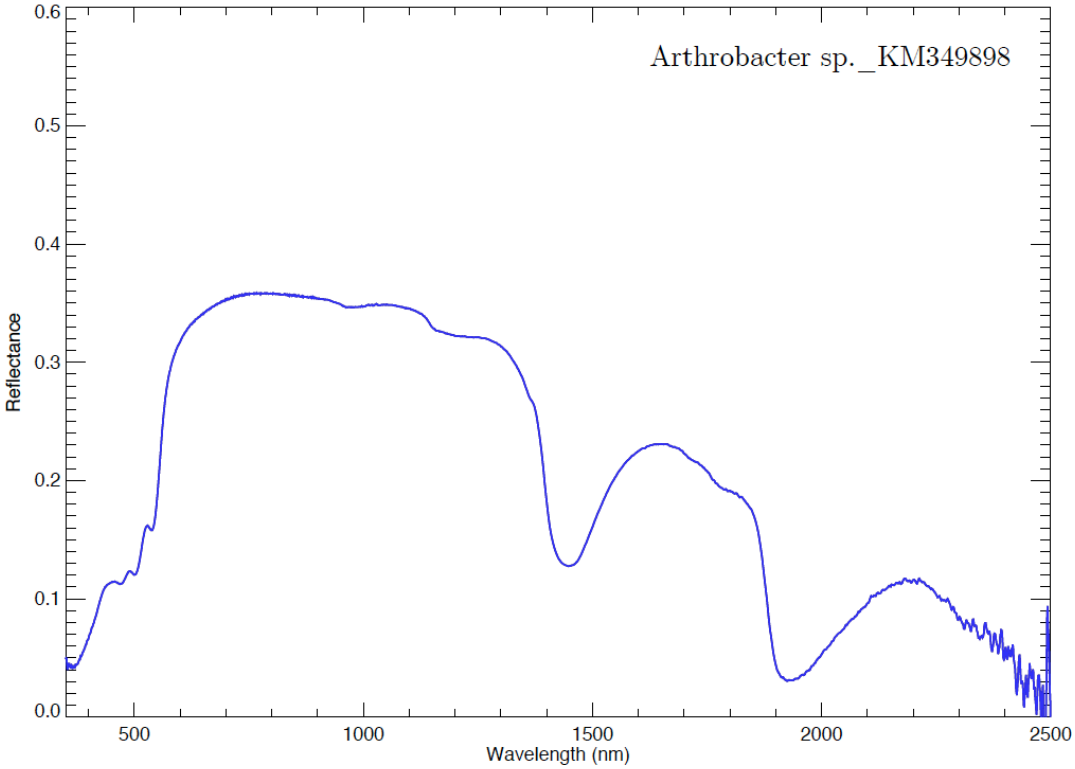

Arthrobacter sp._KM349916

Sample name: *Arthrobacter* sp.

Accession number for 16S rRNA partial gene sequence: KM349916

Classification: Bacteria; Actinobacteria; Actinobacteridae; Actinomycetales; Micrococcineae; Micrococcaceae; Arthrobacter

Metabolism: Heterotrophic

Origin: Sonoran desert, AZ, USA

Isolation: Ivan P. Lima (NPP at NASA Ames, CA, USA)

Sample concentration: 2.78×10^7 cells/ml

Sample count on filter substrate: $8.34 \pm 0.56 \times 10^7$ cells

Laboratory growth conditions: 30 °C, 180 rpm, 24 h

Culture medium: Marine Broth (MB)

Sample photograph:

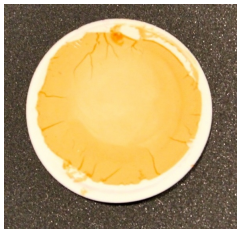

Sample micrograph:

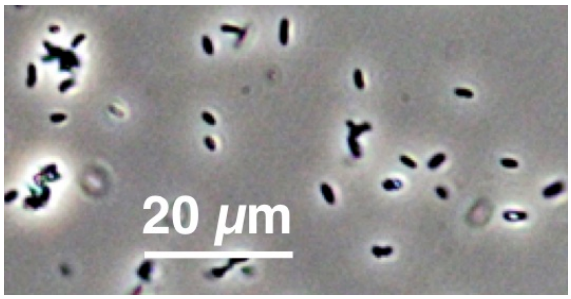

Sample reflectance spectrum:

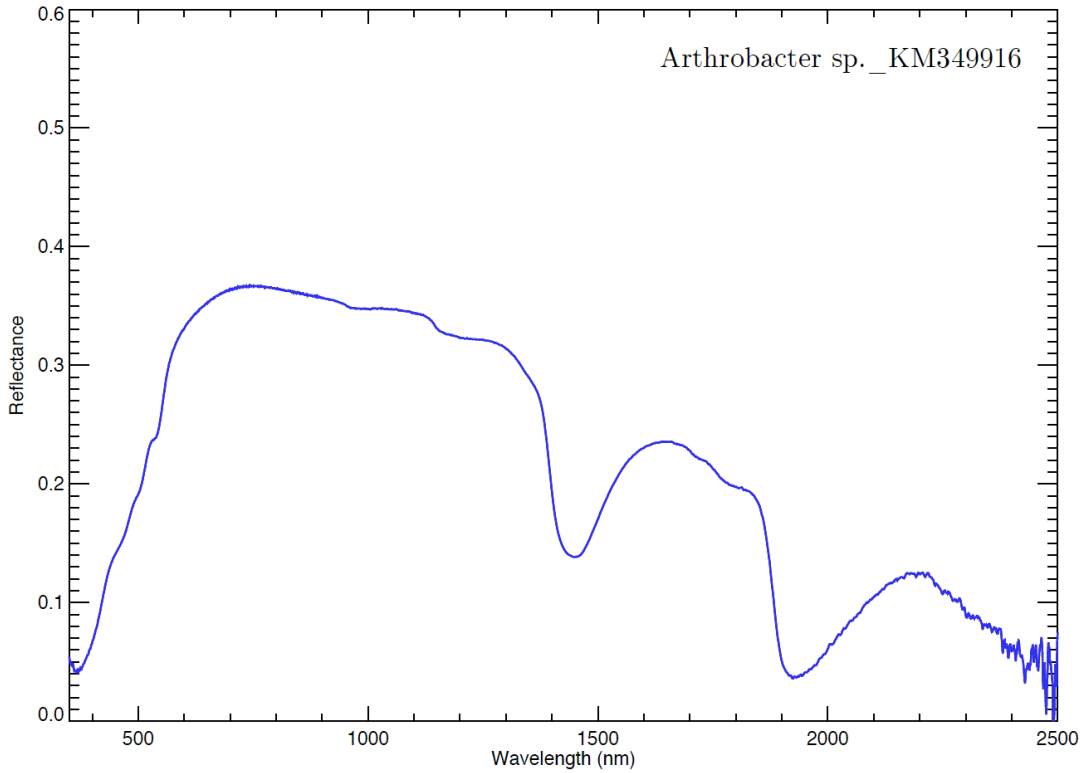

Arthrobacter sp._KM349918

Sample name: *Arthrobacter* sp.

Accession number for 16S rRNA partial gene sequence: KM349918

Classification: Bacteria; Actinobacteria; Actinobacteridae; Actinomycetales; Micrococcineae; Micrococcaceae; Arthrobacter

Metabolism: Heterotrophic

Origin: Sonoran desert, AZ, USA

Isolation: Ivan P. Lima (NPP at NASA Ames, CA, USA)

Sample concentration: 1.33 $\times$ 10^8 cells/ml

Sample count on filter substrate: 3.99 $\pm$ 0.27 $\times$ 10^8 cells

Laboratory growth conditions: 30 °C, 180 rpm, 24 h

Culture medium: Marine Broth (MB)

Sample photograph:

Sample micrograph:

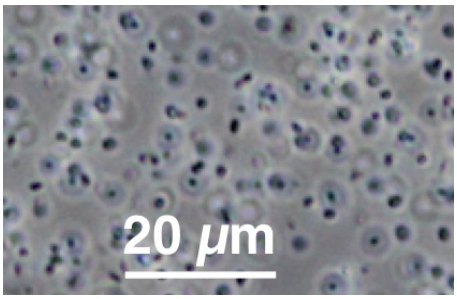

Sample reflectance spectrum:

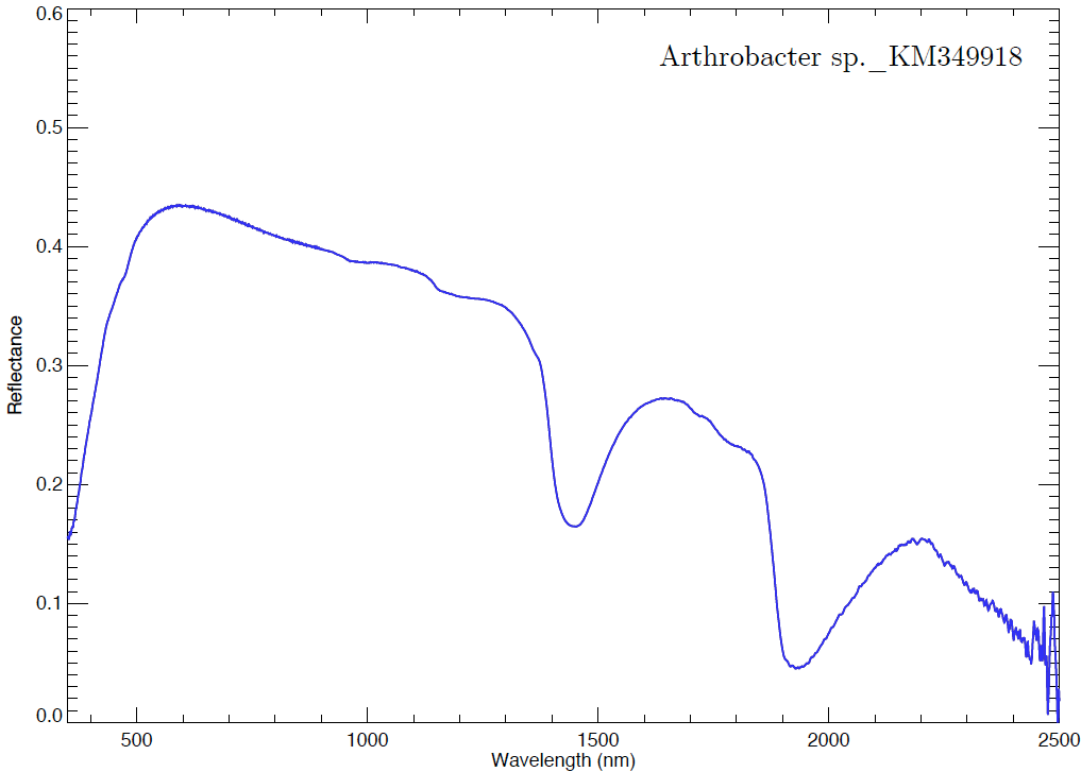

Arthrobacter sp._KM349919

Sample name: *Arthrobacter* sp.

Accession number for 16S rRNA partial gene sequence: KM349919

Classification: Bacteria; Actinobacteria; Actinobacteridae; Actinomycetales; Micrococcineae; Micrococcaceae; Arthrobacter

Metabolism: Heterotrophic

Origin: Sonoran desert, AZ, USA

Isolation: Ivan P. Lima (NPP at NASA Ames, CA, USA)

Sample concentration: 1.27×10^8 cells/ml

Sample count on filter substrate: $3.82 \pm 0.26 \times 10^8$ cells

Laboratory growth conditions: 30 °C, 180 rpm, 24 h

Culture medium: Marine Broth (MB)

Sample photograph:

Sample micrograph:

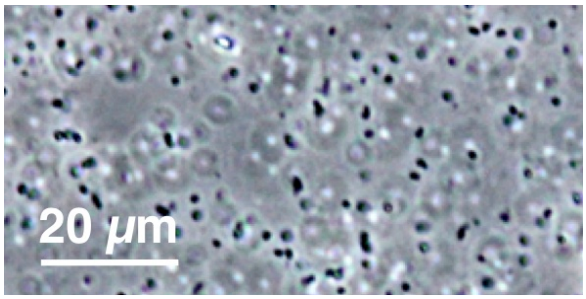

Sample reflectance spectrum:

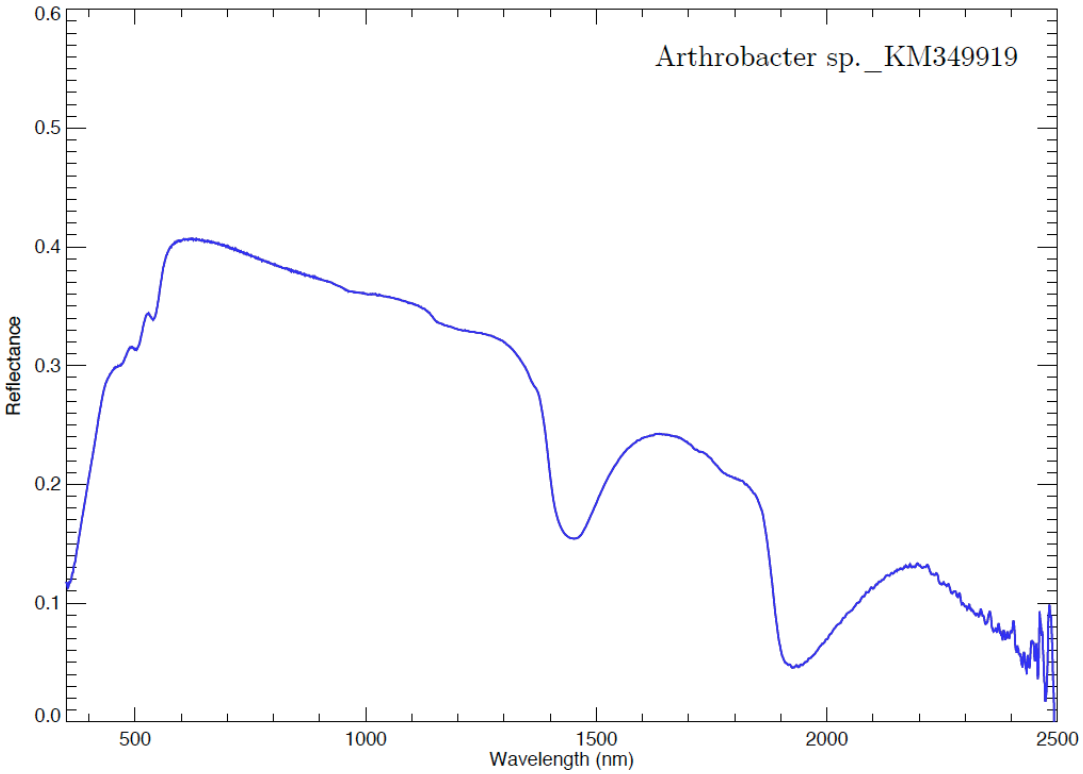

Arthrobacter sp._KM349921

Sample name: *Arthrobacter* sp.

Accession number for 16S rRNA partial gene sequence: KM349921

Classification: Bacteria; Actinobacteria; Actinobacteridae; Actinomycetales; Micrococcineae; Micrococcaceae; Arthrobacter

Metabolism: Heterotrophic

Origin: Sonoran desert, AZ, USA

Isolation: Ivan P. Lima (NPP at NASA Ames, CA, USA)

Sample concentration: 1.50×10^7 cells/ml

Sample count on filter substrate: $4.50 \pm 0.30 \times 10^7$ cells

Laboratory growth conditions: 30 °C, 180 rpm, 24 h

Culture medium: Reasoner's 2A (R2A)

Sample photograph:

Sample micrograph:

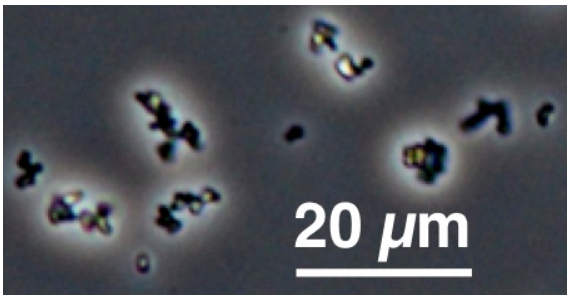

Sample reflectance spectrum:

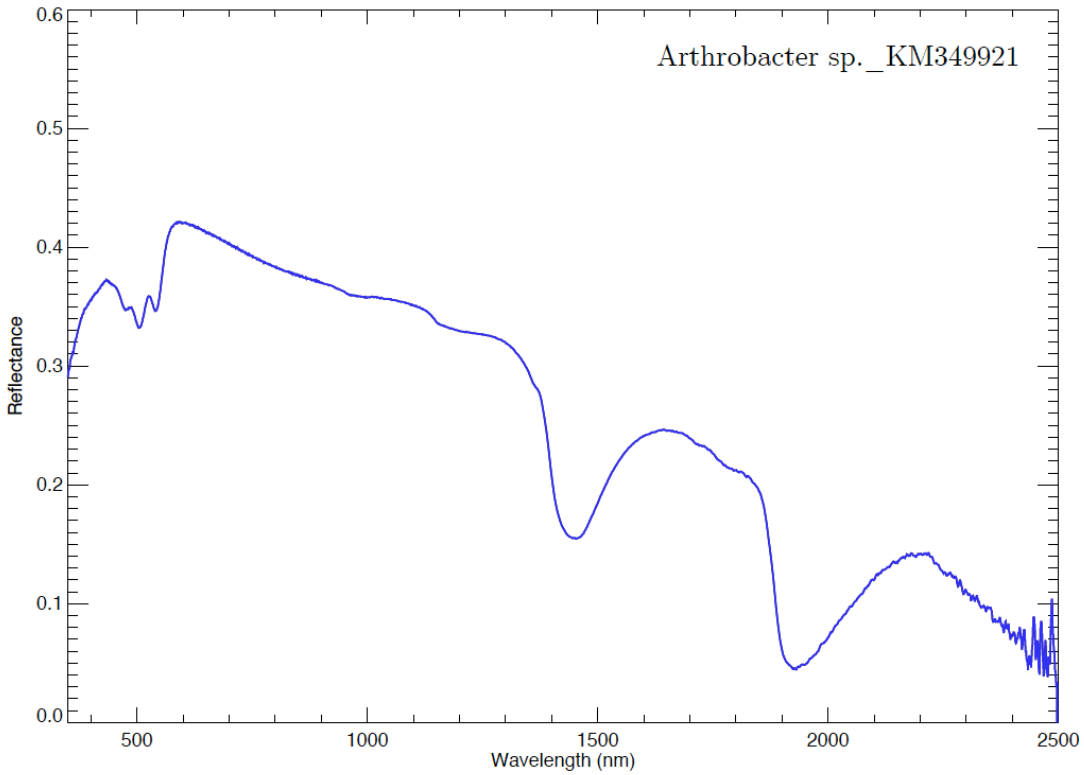

Arthrobacter sp._KM349924

Sample name: *Arthrobacter* sp.

Accession number for 16S rRNA partial gene sequence: KM349924

Classification: Bacteria; Actinobacteria; Actinobacteridae; Actinomycetales; Micrococcineae; Micrococcaceae; Arthrobacter

Metabolism: Heterotrophic

Origin: Sonoran desert, AZ, USA

Isolation: Ivan P. Lima (NPP at NASA Ames, CA, USA)

Sample concentration: 1.32×10^7 cells/ml

Sample count on filter substrate: $3.95 \pm 0.26 \times 10^7$ cells

Laboratory growth conditions: 30 °C, 180 rpm, 24 h

Culture medium: Marine Broth (MB)

Sample photograph:

Sample micrograph:

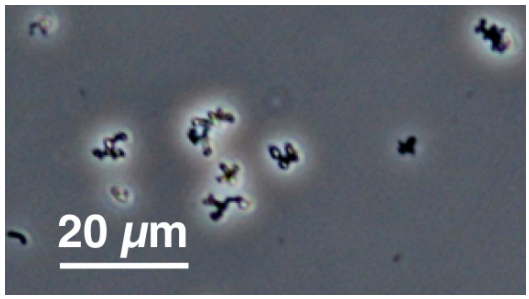

Sample reflectance spectrum:

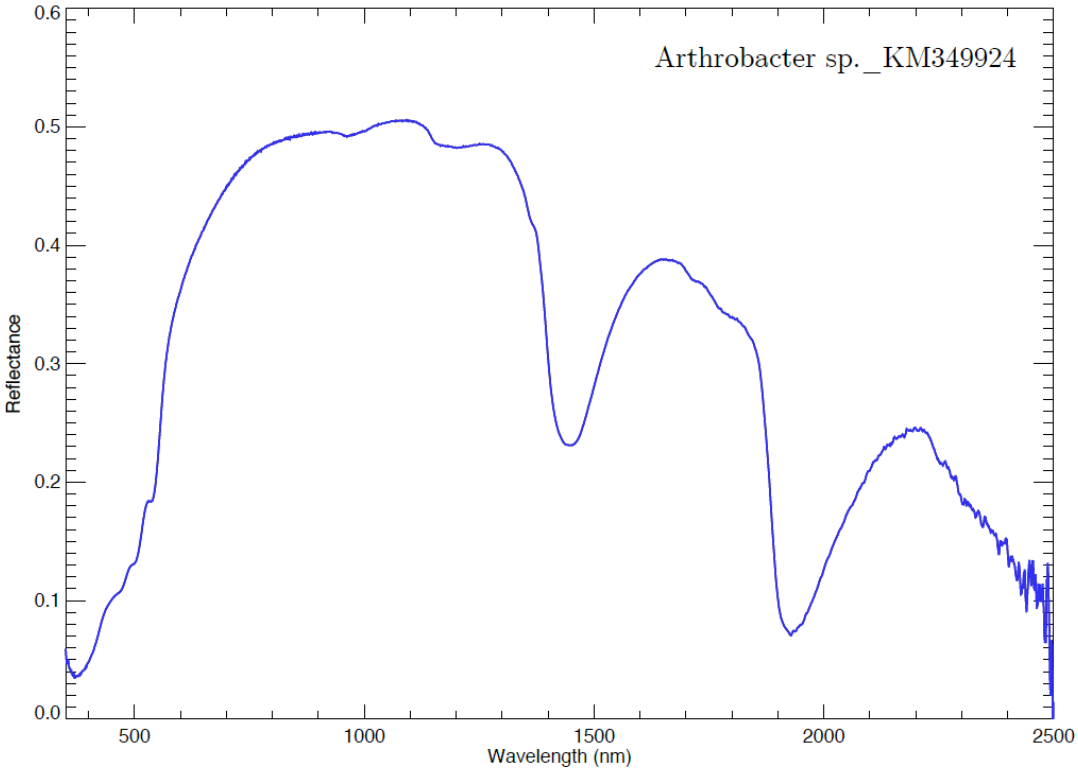

Arthrobacter sp._KM349938

Sample name: *Arthrobacter* sp.

Accession number for 16S rRNA partial gene sequence: KM349938

Classification: Bacteria; Actinobacteria; Actinobacteridae; Actinomycetales; Micrococcineae; Micrococcaceae; Arthrobacter

Metabolism: Heterotrophic

Origin: Atacama desert, Chile

Isolation: Ivan P. Lima (NPP at NASA Ames, CA, USA)

Sample concentration: 6.97×10^7 cells/ml

Sample count on filter substrate: $2.09 \pm 0.14 \times 10^8$ cells

Laboratory growth conditions: 30 °C, 180 rpm, 24 h

Culture medium: Lysogeny Broth (LB)

Sample photograph:

Sample micrograph:

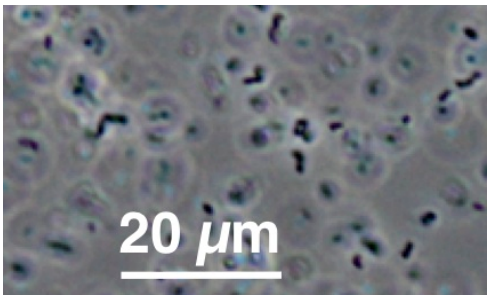

Sample reflectance spectrum:

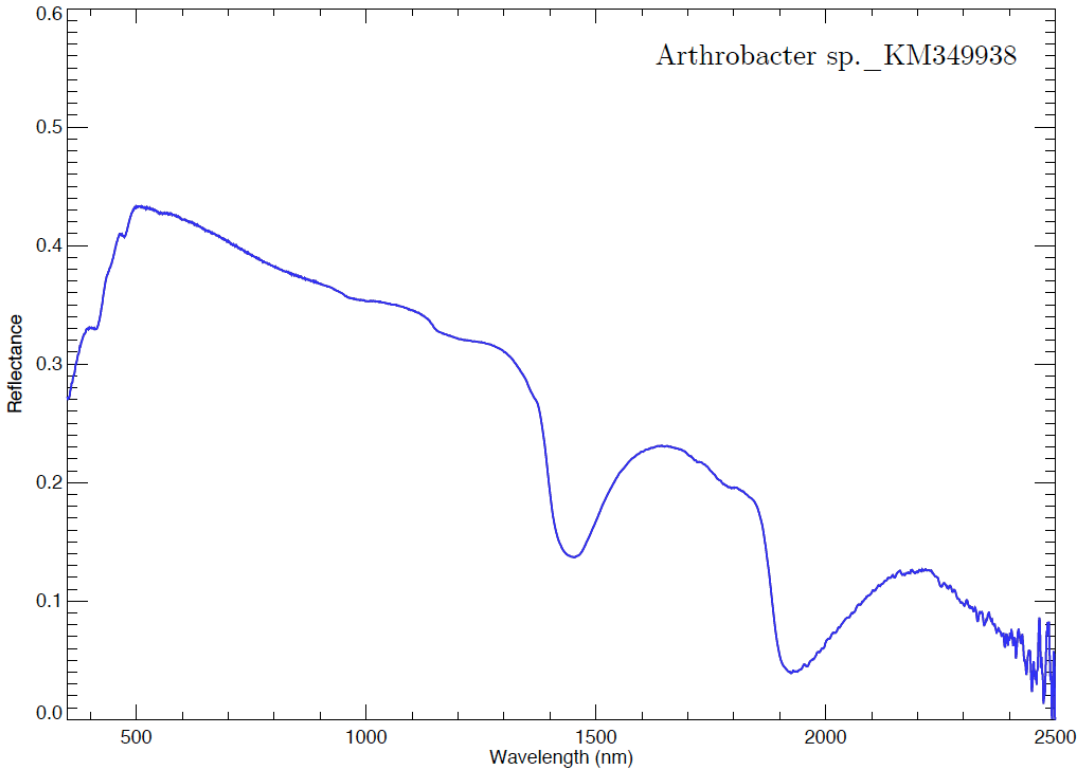

Arthrobacter sp._KM349939

Sample name: *Arthrobacter* sp.

Accession number for 16S rRNA partial gene sequence: KM349939

Classification: Bacteria; Actinobacteria; Actinobacteridae; Actinomycetales; Micrococcineae; Micrococcaceae; Arthrobacter

Metabolism: Heterotrophic

Origin: Atacama desert, Chile

Isolation: Ivan P. Lima (NPP at NASA Ames, CA, USA)

Sample concentration: 1.06×10^7 cells/ml

Sample count on filter substrate: $3.18 \pm 0.21 \times 10^7$ cells

Laboratory growth conditions: 30 °C, 180 rpm, 24 h

Culture medium: Marine Broth (MB)

Sample photograph:

Sample micrograph:

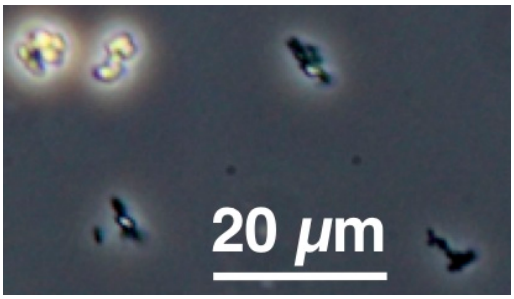

Sample reflectance spectrum:

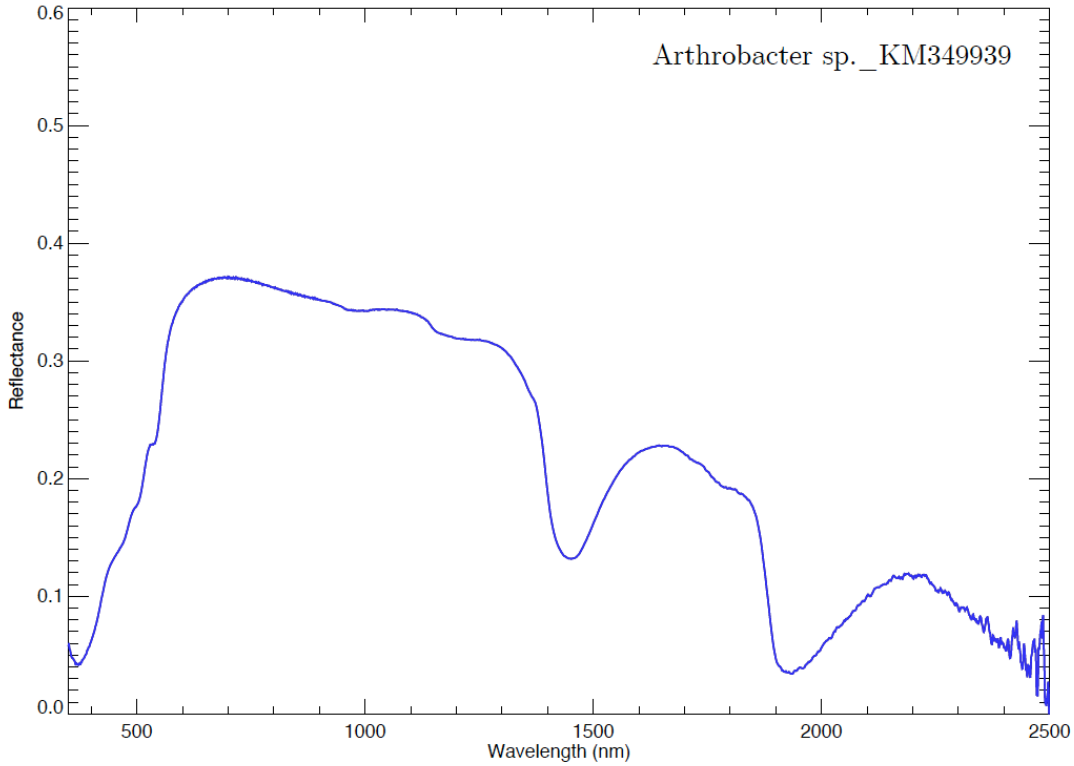

Arthrobacter sp._KM349943

Sample name: *Arthrobacter* sp.

Accession number for 16S rRNA partial gene sequence: KM349943

Classification: Bacteria; Actinobacteria; Actinobacteridae; Actinomycetales; Micrococcineae; Micrococcaceae; Arthrobacter

Metabolism: Heterotrophic

Origin: Atacama desert, Chile

Isolation: Ivan P. Lima (NPP at NASA Ames, CA, USA)

Sample concentration: 1.42×10^8 cells/ml

Sample count on filter substrate: $4.26 \pm 0.28 \times 10^8$ cells

Laboratory growth conditions: 30 °C, 180 rpm, 24 h

Culture medium: Marine Broth (MB)

Sample photograph:

Sample micrograph:

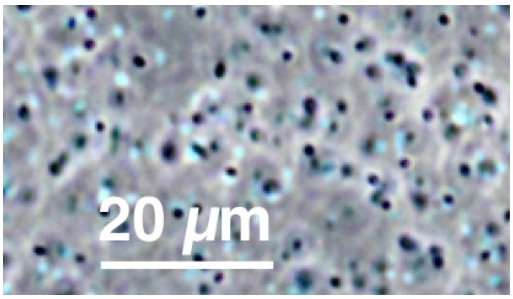

Sample reflectance spectrum:

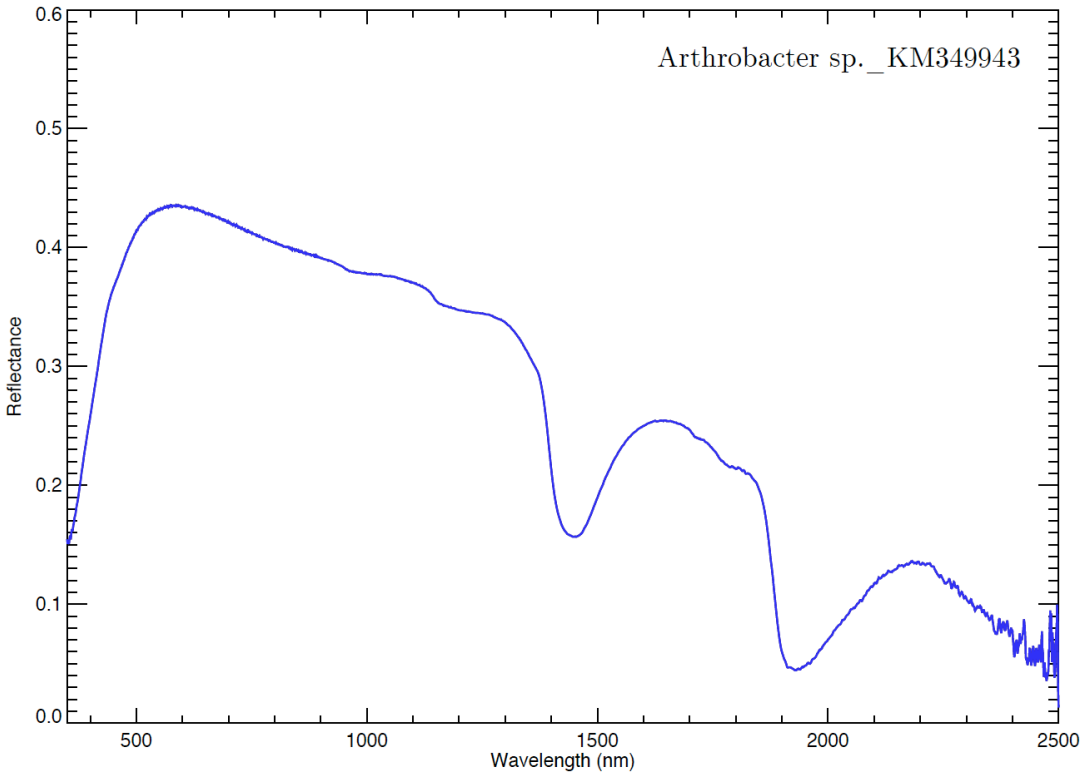

Arthrobacter sp._KM349958

Sample name: *Arthrobacter* sp.

Accession number for 16S rRNA partial gene sequence: KM349958

Classification: Bacteria; Actinobacteria; Actinobacteridae; Actinomycetales; Micrococcineae; Micrococcaceae; Arthrobacter

Metabolism: Heterotrophic

Origin: Atacama desert, Chile

Isolation: Ivan P. Lima (NPP at NASA Ames, CA, USA)

Sample concentration: 1.40×10^8 cells/ml

Sample count on filter substrate: $4.20 \pm 0.28 \times 10^8$ cells

Laboratory growth conditions: 30 °C, 180 rpm, 24 h

Culture medium: Reasoner's 2A (R2A)

Sample photograph:

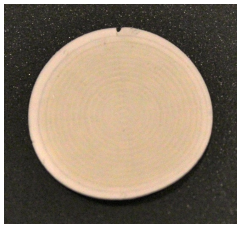

Sample micrograph:

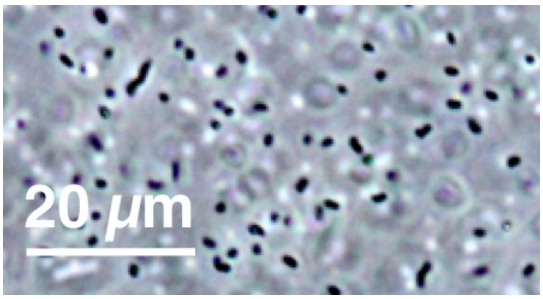

Sample reflectance spectrum:

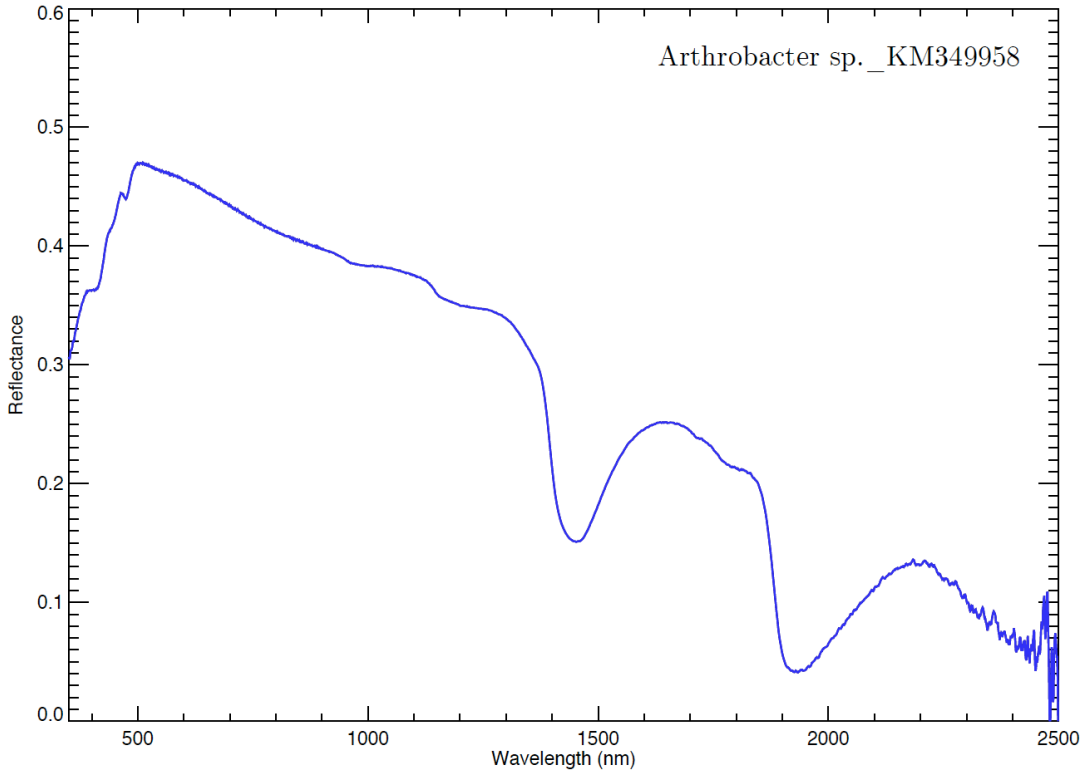

Azospirillum sp._KM349895

Sample name: *Azospirillum* sp.

Accession number for 16S rRNA partial gene sequence: KM349895

Classification: Bacteria; Proteobacteria; Alphaproteobacteria; Rhodospirillales; Rhodospirillaceae; Azospirillum

Metabolism: Heterotrophic

Origin: Atacama desert, Chile

Isolation: Ivan P. Lima (NPP at NASA Ames, CA, USA)

Sample concentration: 3.58×10^7 cells/ml

Sample count on filter substrate: $1.07 \pm 0.07 \times 10^8$ cells

Laboratory growth conditions: 30 °C, 180 rpm, 48 h

Culture medium: Lysogeny Broth (LB)

Sample photograph:

Sample micrograph:

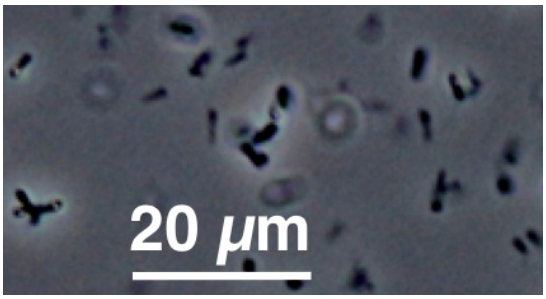

Sample reflectance spectrum:

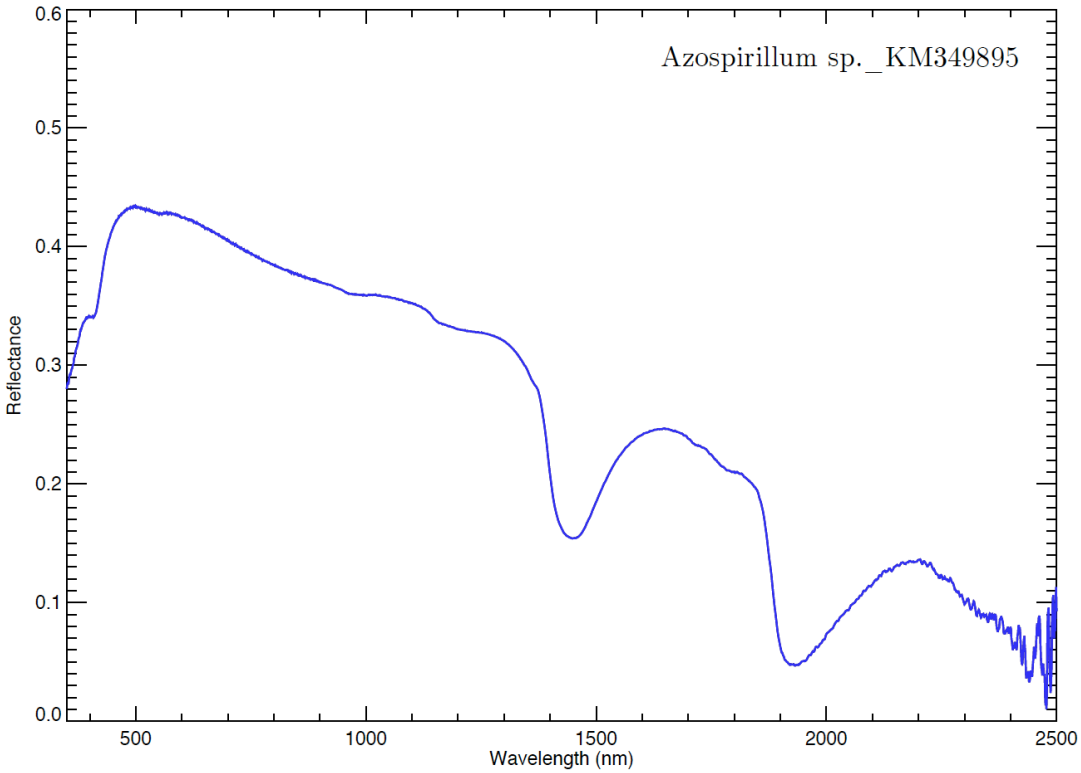

Bacillales_KM349901

Sample name: Bacillales

Accession number for 16S rRNA partial gene sequence: KM349901

Classification: Bacteria; Firmicutes; Bacilli; Bacillales

Metabolism: Heterotrophic

Origin: Moffett Field, CA, USA

Isolation: Ivan P. Lima (NPP at NASA Ames, CA, USA)

Sample concentration: 6.94 $\times$ 10^7 cells/ml

Sample count on filter substrate: 2.08 $\pm$ 0.14 $\times$ 10^8 cells

Laboratory growth conditions: 30 °C, 180 rpm, 24 h

Culture medium: Marine Broth (MB)

Sample photograph:

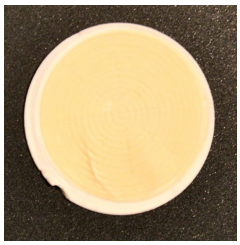

Sample micrograph:

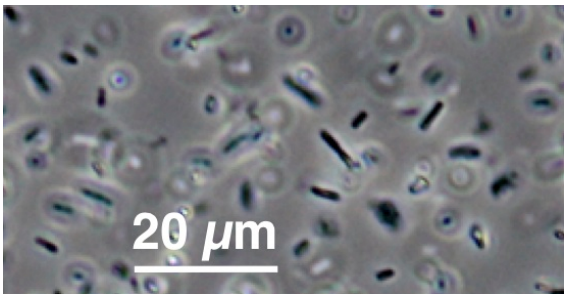

Sample reflectance spectrum:

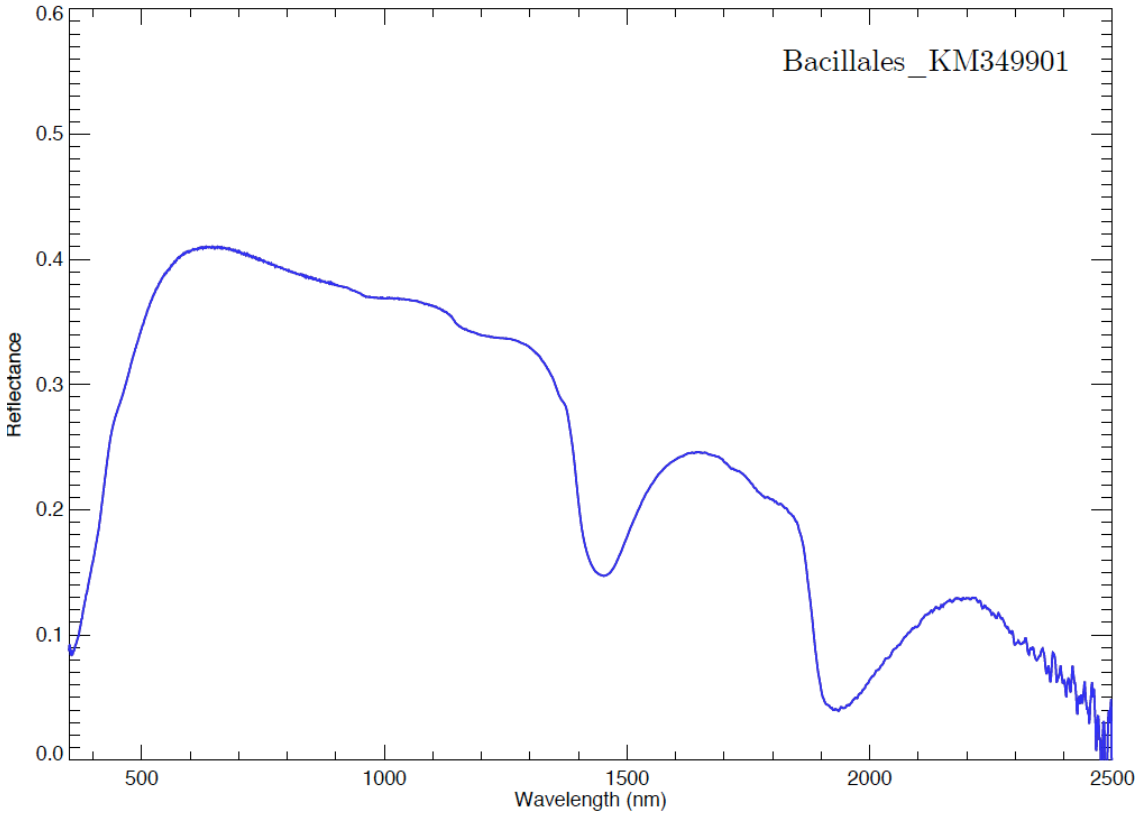

Bacillales_KM349923

Sample name: Bacillales

Accession number for 16S rRNA partial gene sequence: KM349923

Classification: Bacteria; Firmicutes; Bacilli; Bacillales

Metabolism: Heterotrophic

Origin: Sonoran desert, AZ, USA

Isolation: Ivan P. Lima (NPP at NASA Ames, CA, USA)

Sample concentration: 1.89 $\times$ 10^8 cells/ml

Sample count on filter substrate: 5.68 $\pm$ 0.38 $\times$ 10^8 cells

Laboratory growth conditions: 30 °C, 180 rpm, 24 h

Culture medium: Marine Broth (MB)

Sample photograph:

Sample micrograph:

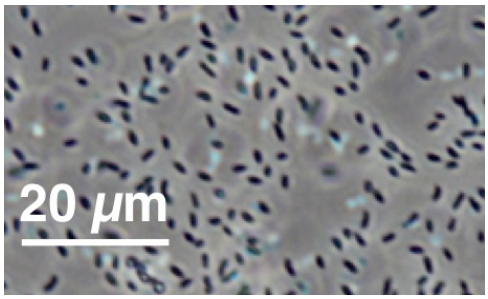

Sample reflectance spectrum:

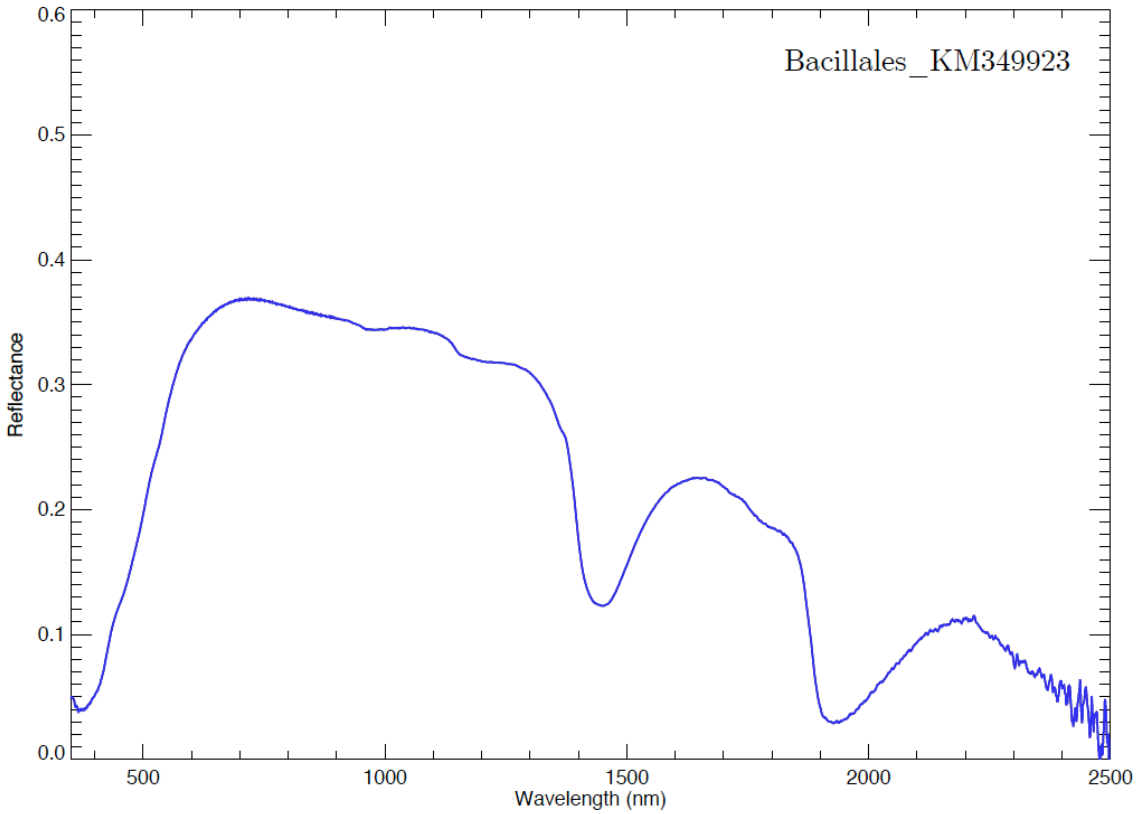

Bacillales_KM349934

Sample name: Bacillales

Accession number for 16S rRNA partial gene sequence: KM349934

Classification: Bacteria; Firmicutes; Bacilli; Bacillales

Metabolism: Heterotrophic

Origin: Atacama desert, Chile

Isolation: Ivan P. Lima (NPP at NASA Ames, CA, USA)

Sample concentration: 6.96 $\times$ 10^7 cells/ml

Sample count on filter substrate: 2.09 $\pm$ 0.14 $\times$ 10^8 cells

Laboratory growth conditions: 30 °C, 180 rpm, 24 h

Culture medium: Marine Broth (MB)

Sample photograph:

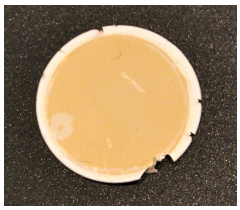

Sample micrograph:

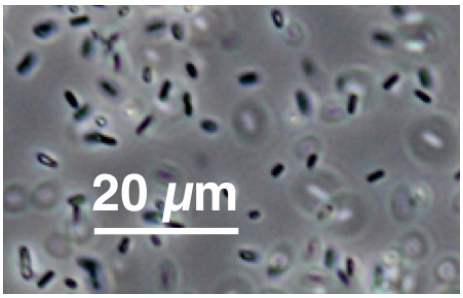

Sample reflectance spectrum:

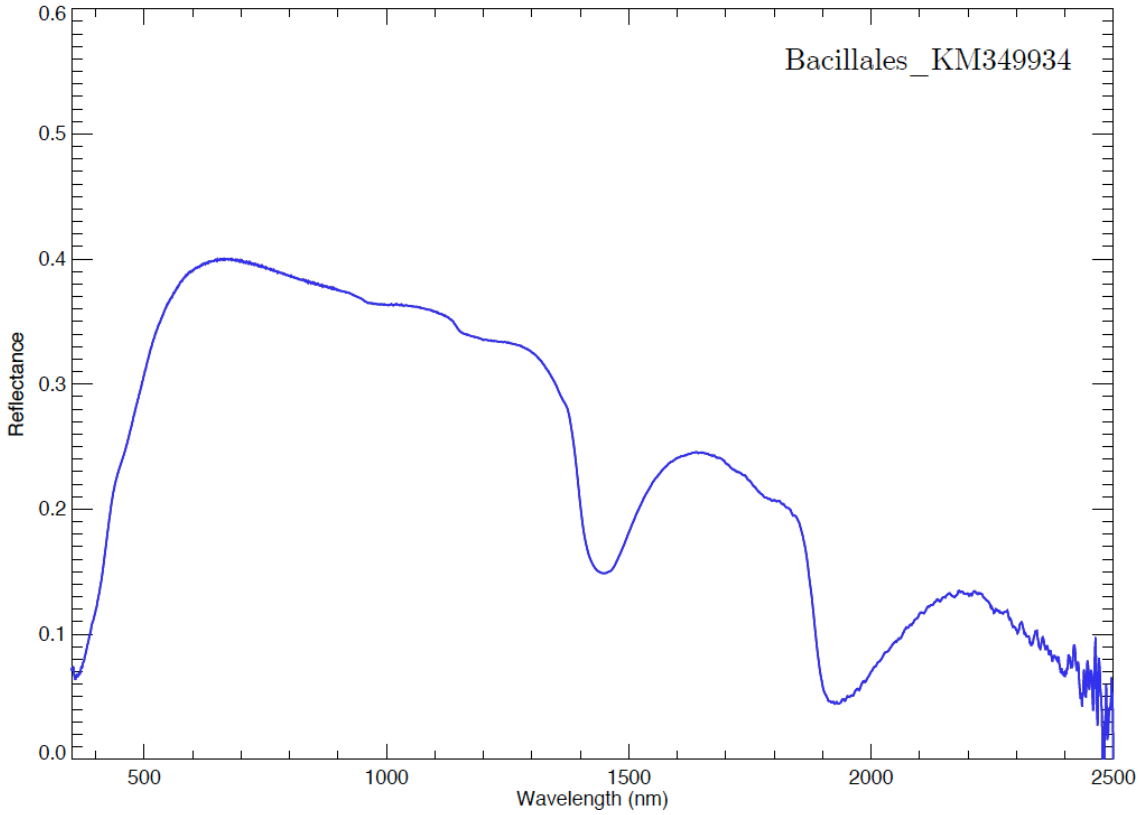

Bacillales_KM349937

Sample name: Bacillales

Accession number for 16S rRNA partial gene sequence: KM349937

Classification: Bacteria; Firmicutes; Bacilli; Bacillales

Metabolism: Heterotrophic

Origin: Atacama desert, Chile

Isolation: Ivan P. Lima (NPP at NASA Ames, CA, USA)

Sample concentration: 7.11 $\times$ 10^7 cells/ml

Sample count on filter substrate: 2.13 $\pm$ 0.14 $\times$ 10^8 cells

Laboratory growth conditions: 30 °C, 180 rpm, 24 h

Culture medium: Lysogeny Broth (LB)

Sample photograph:

Sample micrograph:

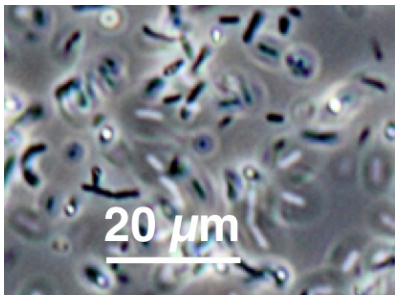

Sample reflectance spectrum:

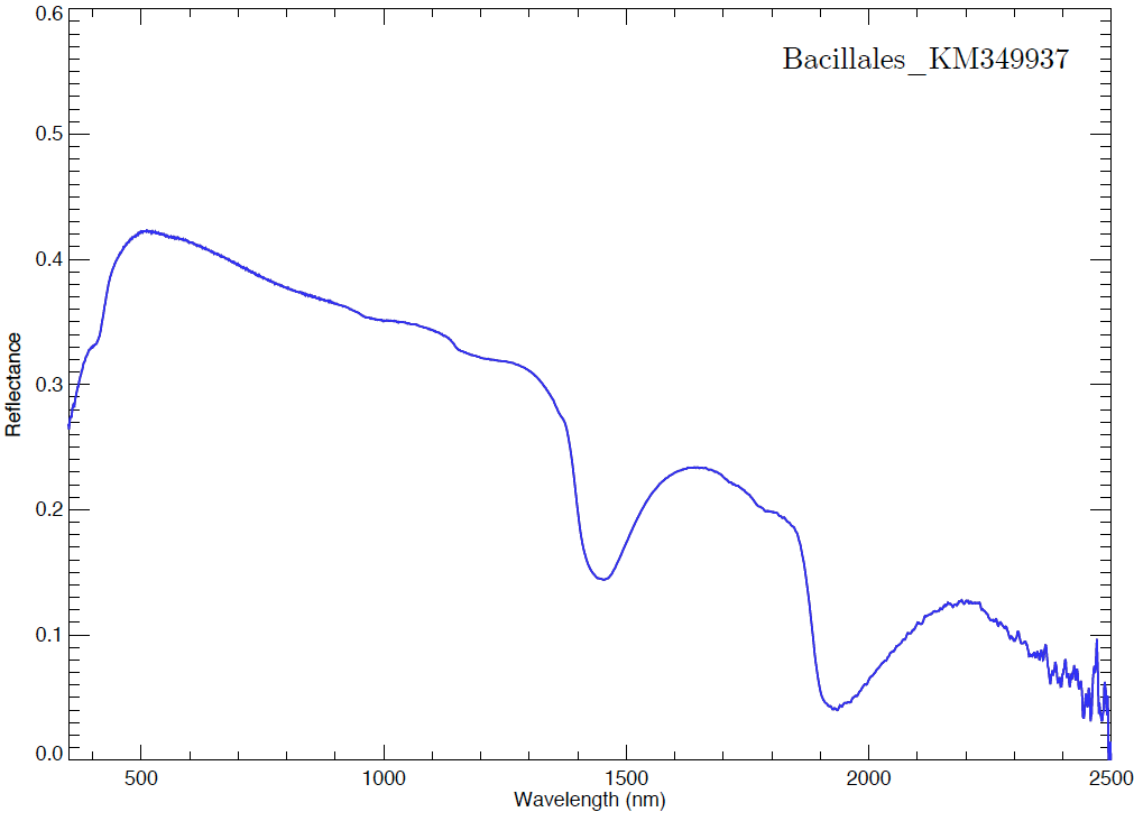

Bacillales_KM349940

Sample name: Bacillales

Accession number for 16S rRNA partial gene sequence: KM349940

Classification: Bacteria; Firmicutes; Bacilli; Bacillales

Metabolism: Heterotrophic

Origin: Atacama desert, Chile

Isolation: Ivan P. Lima (NPP at NASA Ames, CA, USA)

Sample concentration: 6.43 $\times$ 10^7 cells/ml

Sample count on filter substrate: 1.93 $\pm$ 0.13 $\times$ 10^8 cells

Laboratory growth conditions: 30 °C, 180 rpm, 24 h

Culture medium: Marine Broth (MB)

Sample photograph:

Sample micrograph:

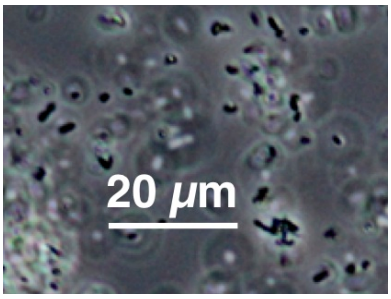

Sample reflectance spectrum:

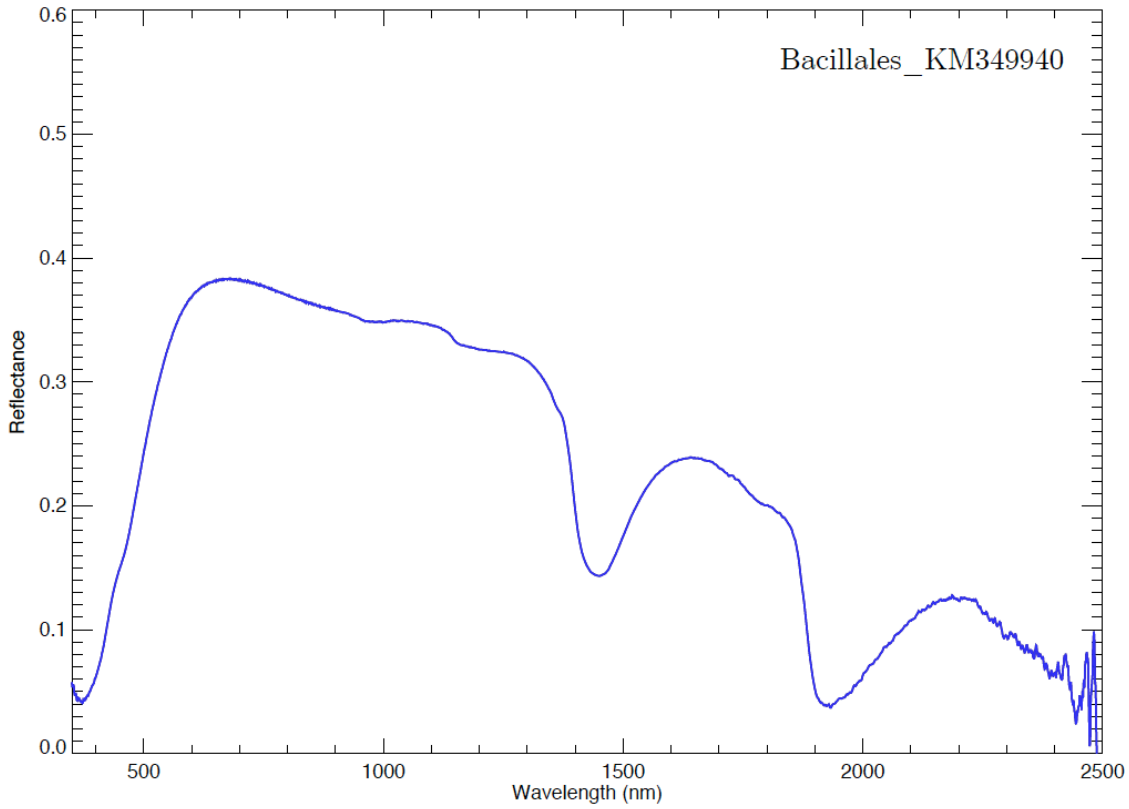

Bacillus sp._KM349861

Sample name: *Bacillus* sp.

Accession number for 16S rRNA partial gene sequence: KM349861

Classification: Bacteria; Firmicutes; Bacilli; Bacillales; Bacillaceae; Bacillus

Metabolism: Heterotrophic

Origin: Sonoran desert, AZ, USA

Isolation: Ivan P. Lima (NPP at NASA Ames, CA, USA)

Sample concentration: 3.47 $\times$ 10^7 cells/ml

Sample count on filter substrate: 1.04 $\pm$ 0.07 $\times$ 10^8 cells

Laboratory growth conditions: 30 °C, 180 rpm, 24 h

Culture medium: Marine Broth (MB)

Sample photograph:

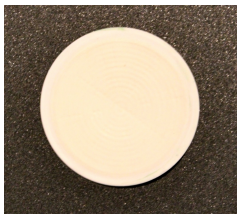

Sample micrograph:

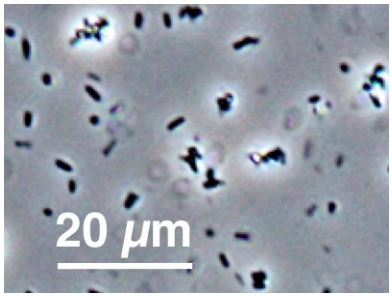

Sample reflectance spectrum:

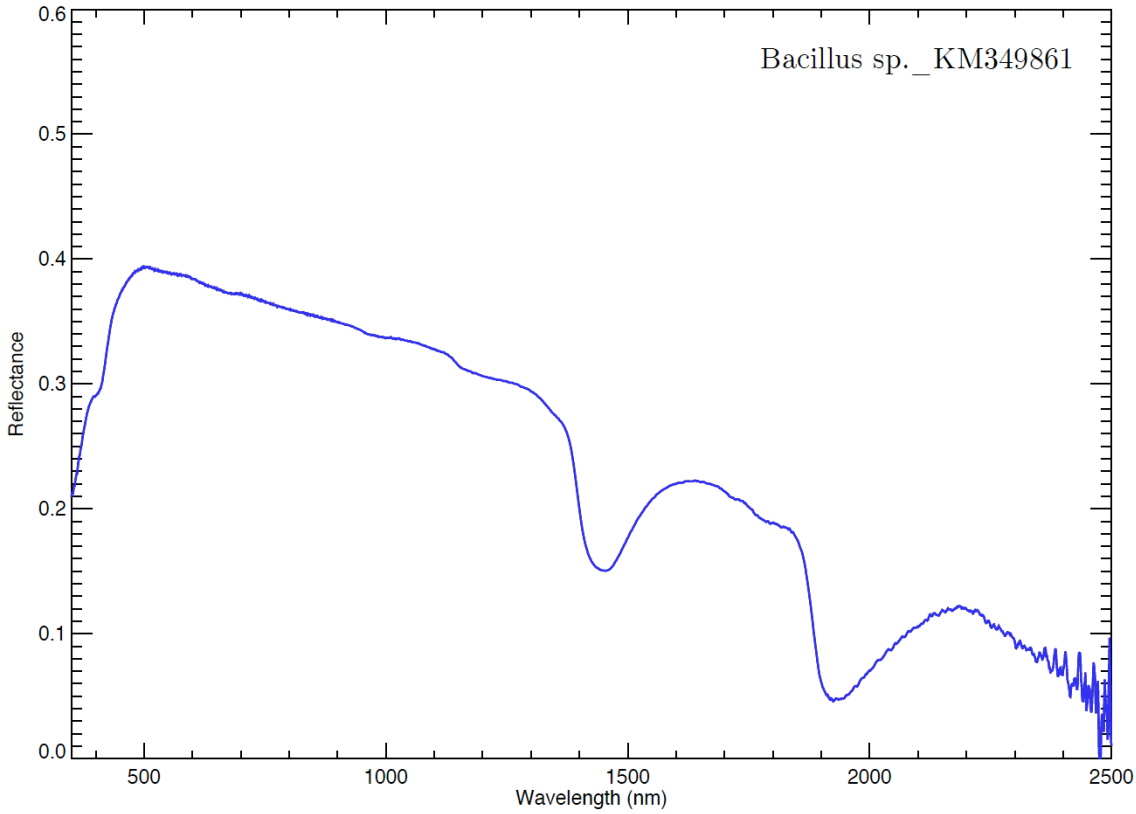

Bacillus sp._KM349863

Sample name: *Bacillus* sp.

Accession number for 16S rRNA partial gene sequence: KM349863

Classification: Bacteria; Firmicutes; Bacilli; Bacillales; Bacillaceae; Bacillus

Metabolism: Heterotrophic

Origin: Sonoran desert, AZ, USA

Isolation: Ivan P. Lima (NPP at NASA Ames, CA, USA)

Sample concentration: 4.42 $\times$ 10^7 cells/ml

Sample count on filter substrate: 1.33 $\pm$ 0.09 $\times$ 10^8 cells

Laboratory growth conditions: 30 °C, 180 rpm, 24 h

Culture medium: Marine Broth (MB)

Sample photograph:

Sample micrograph:

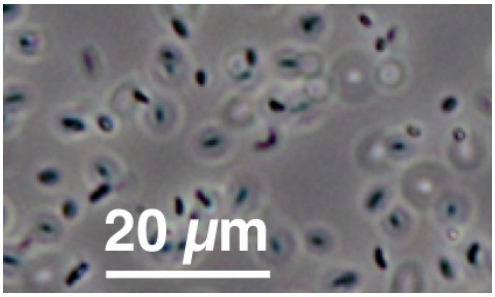

Sample reflectance spectrum:

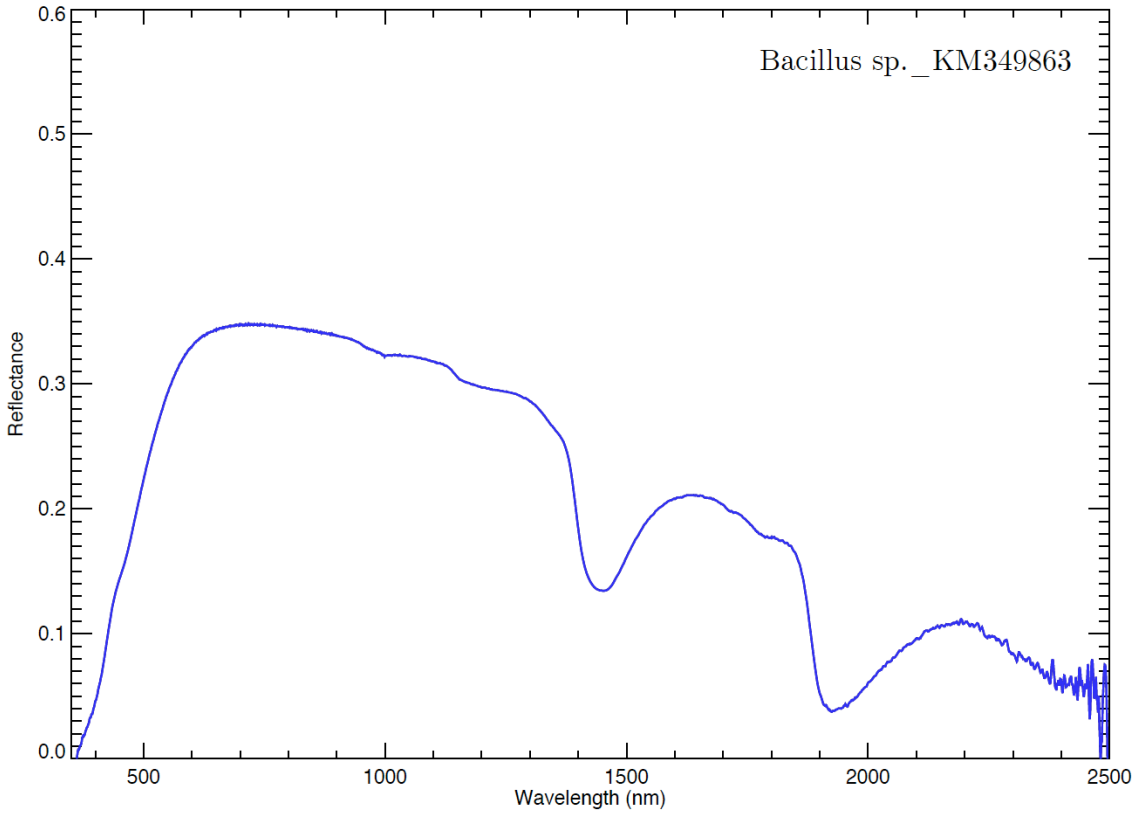

Bacillus sp._KM349864

Sample name: *Bacillus* sp.

Accession number for 16S rRNA partial gene sequence: KM349864

Classification: Bacteria; Firmicutes; Bacilli; Bacillales; Bacillaceae; Bacillus

Metabolism: Heterotrophic

Origin: Sonoran desert, AZ, USA

Isolation: Ivan P. Lima (NPP at NASA Ames, CA, USA)

Sample concentration: 3.73 $\times$ 10^7 cells/ml

Sample count on filter substrate: 1.12 $\pm$ 0.07 $\times$ 10^8 cells

Laboratory growth conditions: 30 °C, 180 rpm, 24 h

Culture medium: Marine Broth (MB)

Sample photograph:

Sample micrograph:

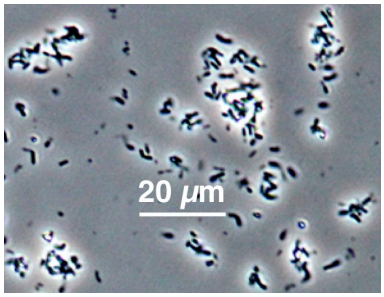

Sample reflectance spectrum:

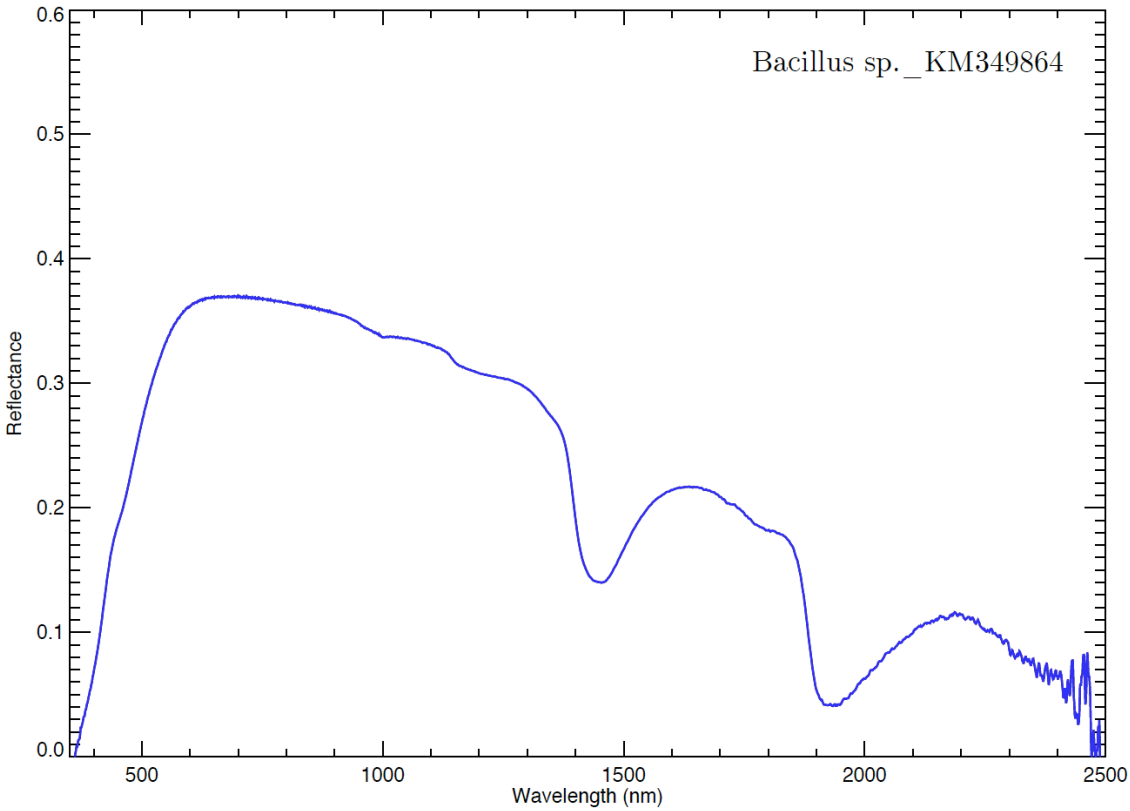

Bacillus sp._KM349865

Sample name: *Bacillus* sp.

Accession number for 16S rRNA partial gene sequence: KM349865

Classification: Bacteria; Firmicutes; Bacilli; Bacillales; Bacillaceae; Bacillus

Metabolism: Heterotrophic

Origin: Sonoran desert, AZ, USA

Isolation: Ivan P. Lima (NPP at NASA Ames, CA, USA)

Sample concentration: 4.33×10^7 cells/ml

Sample count on filter substrate: $1.30 \pm 0.09 \times 10^8$ cells

Laboratory growth conditions: 30 °C, 180 rpm, 24 h

Culture medium: Marine Broth (MB)

Sample photograph:

Sample micrograph:

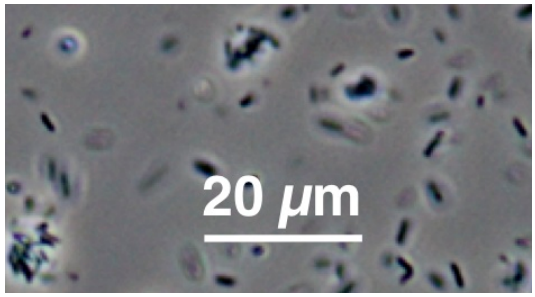

Sample reflectance spectrum:

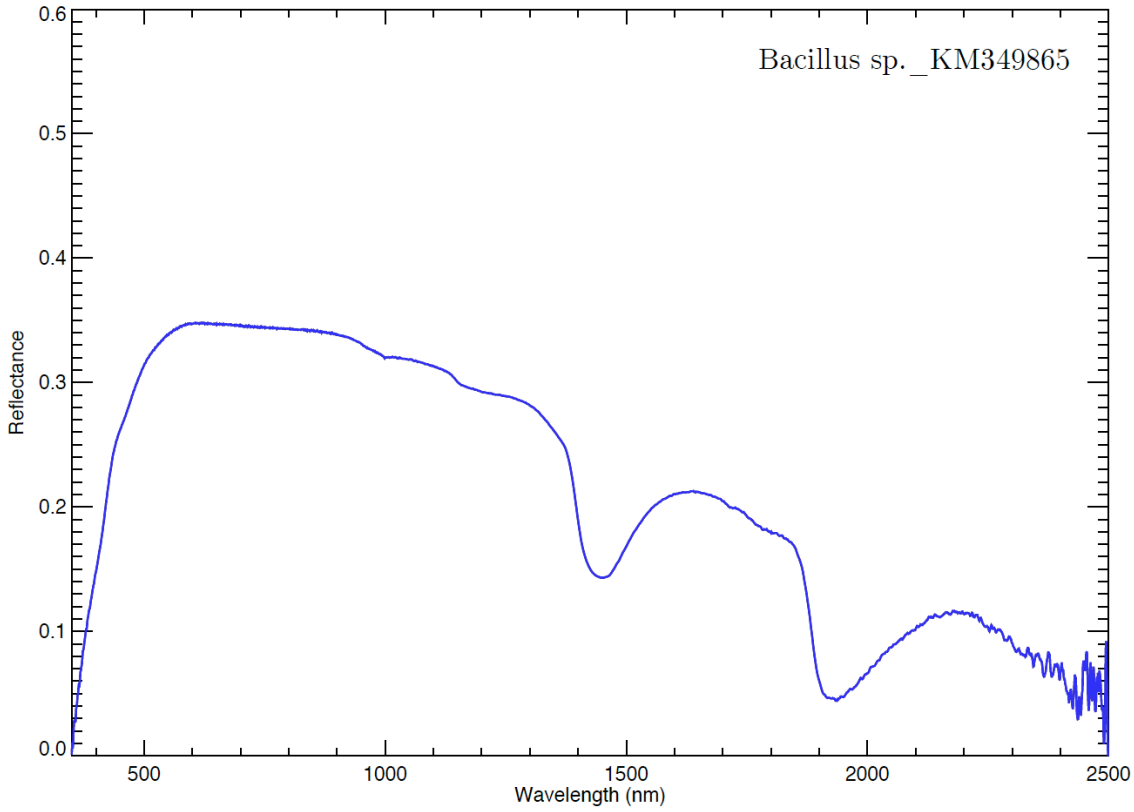

Bacillus sp._KM349866

Sample name: *Bacillus* sp.

Accession number for 16S rRNA partial gene sequence: KM349866

Classification: Bacteria; Firmicutes; Bacilli; Bacillales; Bacillaceae; Bacillus

Metabolism: Heterotrophic

Origin: Sonoran desert, AZ, USA

Isolation: Ivan P. Lima (NPP at NASA Ames, CA, USA)

Sample concentration: 6.71 $\times$ 10^7 cells/ml

Sample count on filter substrate: 2.01 $\pm$ 0.13 $\times$ 10^8 cells

Laboratory growth conditions: 30 °C, 180 rpm, 24 h

Culture medium: Marine Broth (MB)

Sample photograph:

Sample micrograph:

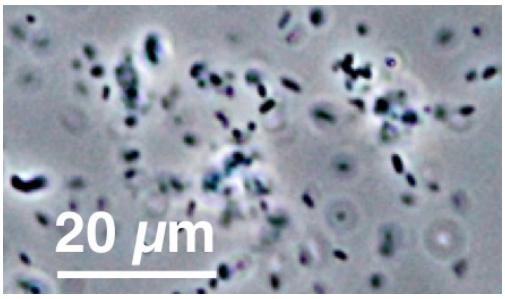

Sample reflectance spectrum:

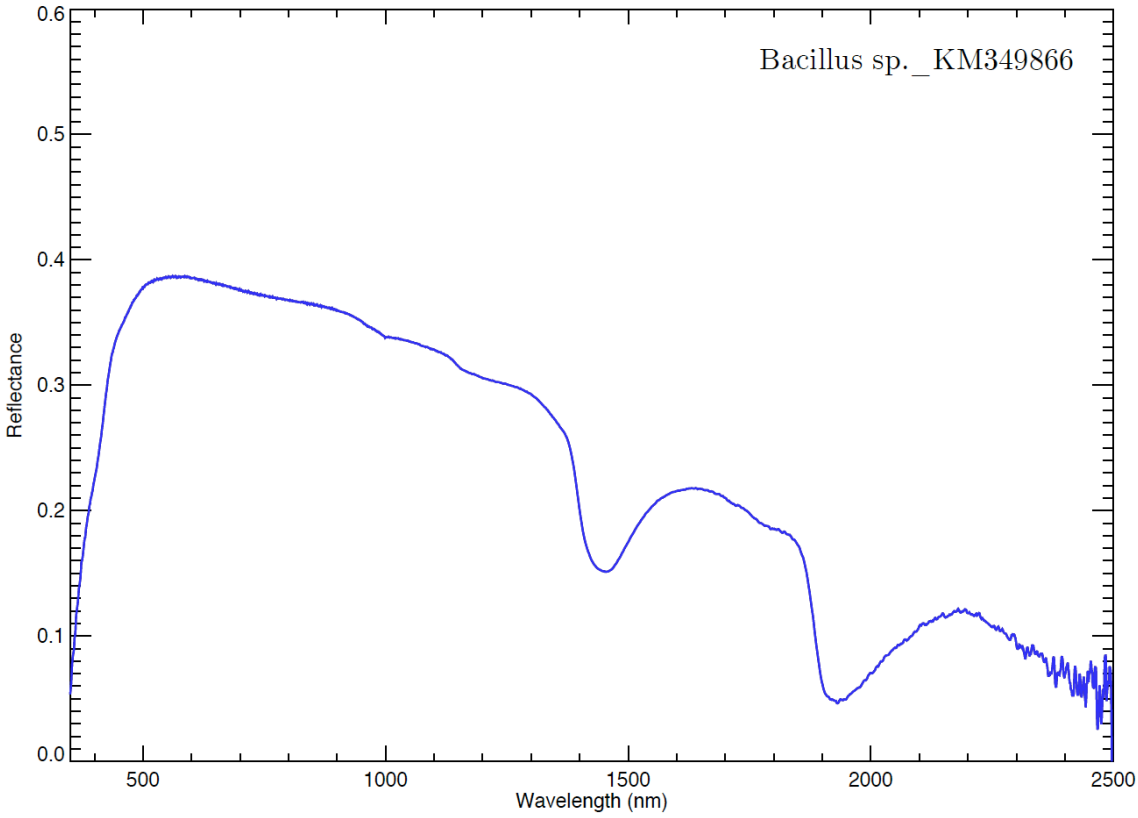

Bacillus sp._KM349867

Sample name: *Bacillus* sp.

Accession number for 16S rRNA partial gene sequence: KM349867

Classification: Bacteria; Firmicutes; Bacilli; Bacillales; Bacillaceae; Bacillus

Metabolism: Heterotrophic

Origin: Sonoran desert, AZ, USA

Isolation: Ivan P. Lima (NPP at NASA Ames, CA, USA)

Sample concentration: 3.00 $\times$ 10^7 cells/ml

Sample count on filter substrate: 9.00 $\pm$ 0.60 $\times$ 10^7 cells

Laboratory growth conditions: 30 °C, 180 rpm, 24 h

Culture medium: Marine Broth (MB)

Sample photograph:

Sample micrograph:

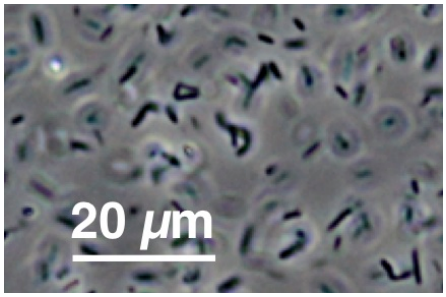

Sample reflectance spectrum:

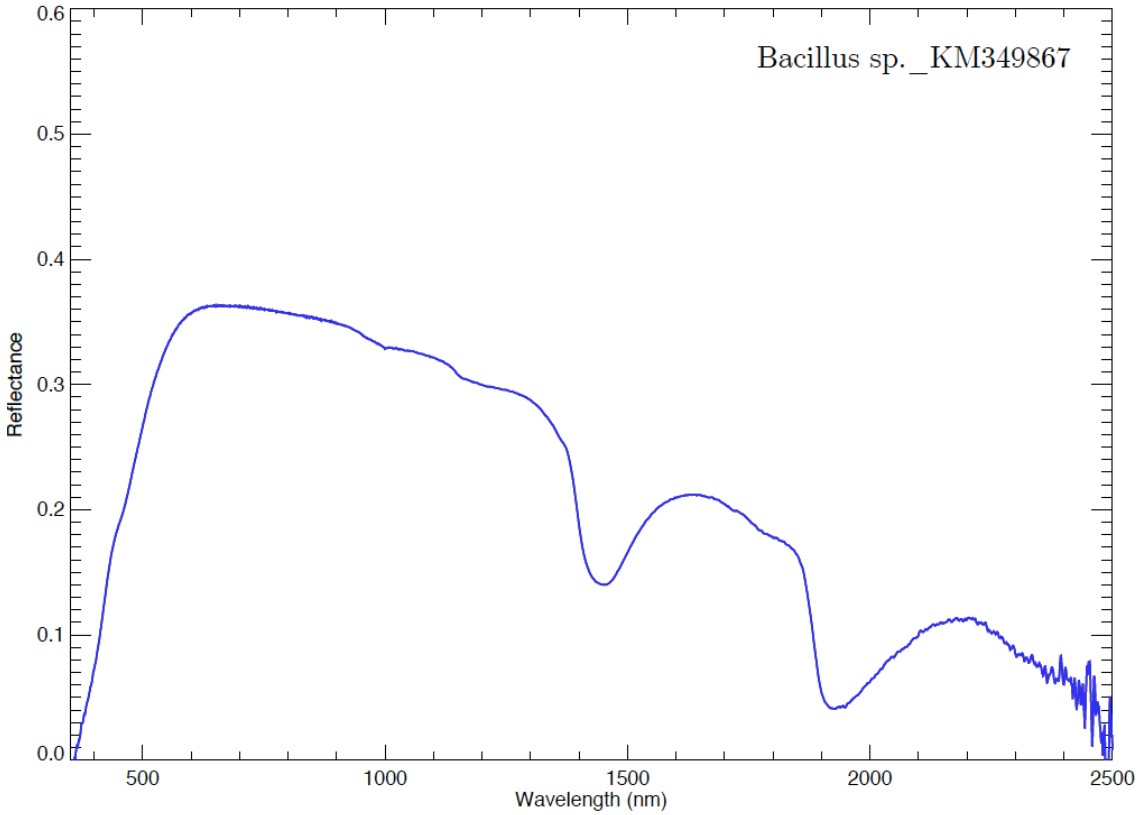

Bacillus sp._KM349868

Sample name: *Bacillus* sp.

Accession number for 16S rRNA partial gene sequence: KM349868

Classification: Bacteria; Firmicutes; Bacilli; Bacillales; Bacillaceae; Bacillus

Metabolism: Heterotrophic

Origin: Sonoran desert, AZ, USA

Isolation: Ivan P. Lima (NPP at NASA Ames, CA, USA)

Sample concentration: 7.80 $\times$ 10^7 cells/ml

Sample count on filter substrate: 2.34 $\pm$ 0.16 $\times$ 10^8 cells

Laboratory growth conditions: 30 °C, 180 rpm, 24 h

Culture medium: Marine Broth (MB)

Sample photograph:

Sample micrograph:

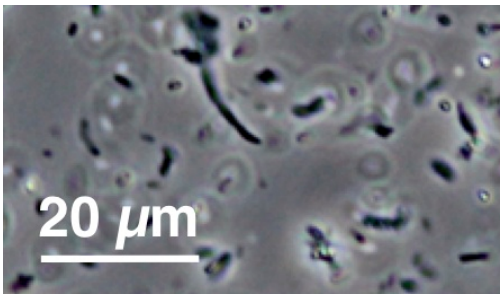

Sample reflectance spectrum:

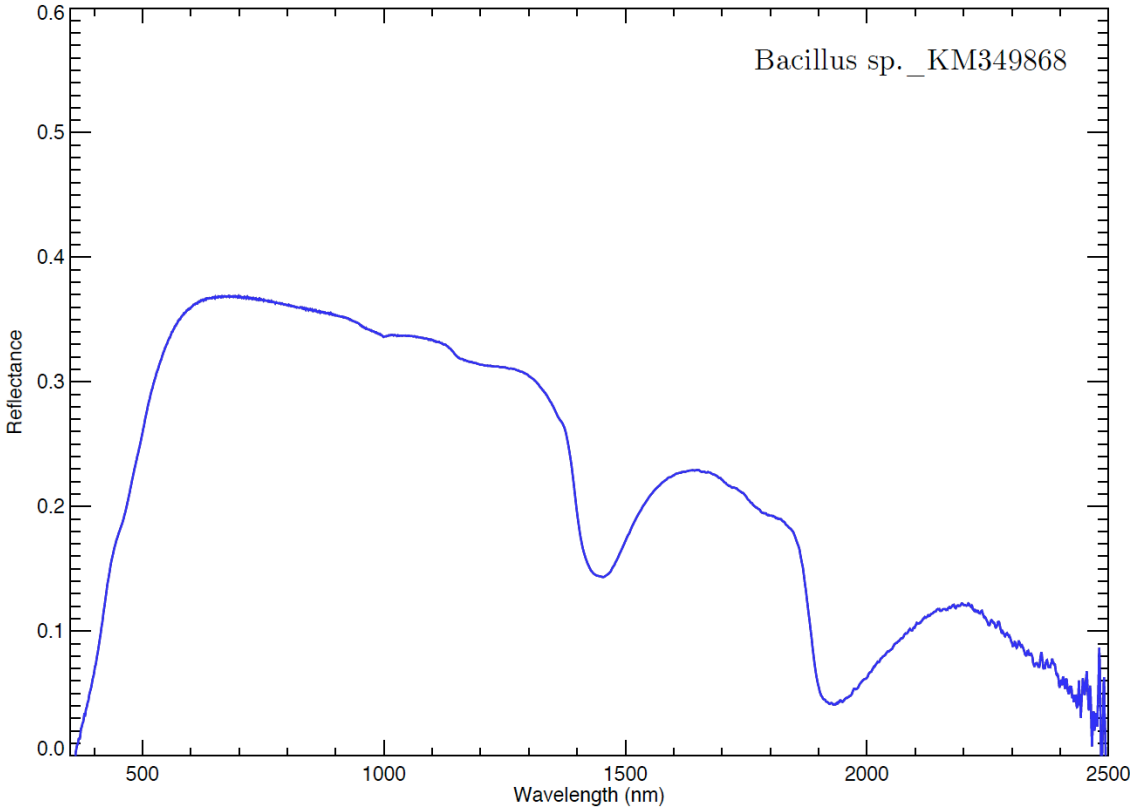

Bacillus sp._KM349869

Sample name: *Bacillus* sp.

Accession number for 16S rRNA partial gene sequence: KM349869

Classification: Bacteria; Firmicutes; Bacilli; Bacillales; Bacillaceae; Bacillus

Metabolism: Heterotrophic

Origin: Sonoran desert, AZ, USA

Isolation: Ivan P. Lima (NPP at NASA Ames, CA, USA)

Sample concentration: 4.48 $\times$ 10^7 cells/ml

Sample count on filter substrate: 1.34 $\pm$ 0.09 $\times$ 10^8 cells

Laboratory growth conditions: 30 °C, 180 rpm, 24 h

Culture medium: Marine Broth (MB)

Sample photograph:

Sample micrograph:

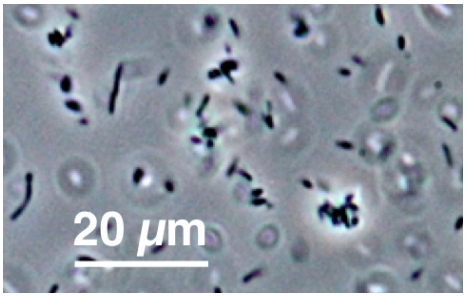

Sample reflectance spectrum:

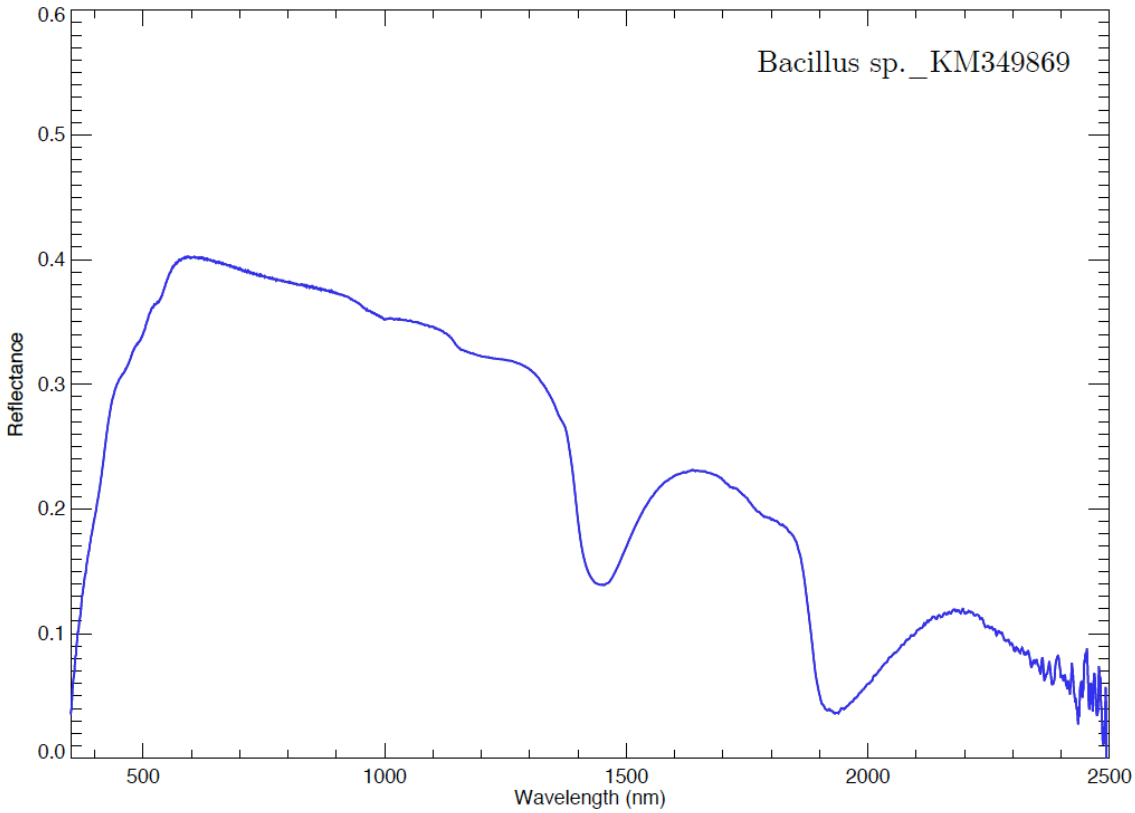

Bacillus sp._KM349870

Sample name: *Bacillus* sp.

Accession number for 16S rRNA partial gene sequence: KM349870

Classification: Bacteria; Firmicutes; Bacilli; Bacillales; Bacillaceae; Bacillus

Metabolism: Heterotrophic

Origin: Sonoran desert, AZ, USA

Isolation: Ivan P. Lima (NPP at NASA Ames, CA, USA)

Sample concentration: 3.04×10^7 cells/ml

Sample count on filter substrate: $9.11 \pm 0.61 \times 10^7$ cells

Laboratory growth conditions: 30 °C, 180 rpm, 24 h

Culture medium: Marine Broth (MB)

Sample photograph:

Sample micrograph:

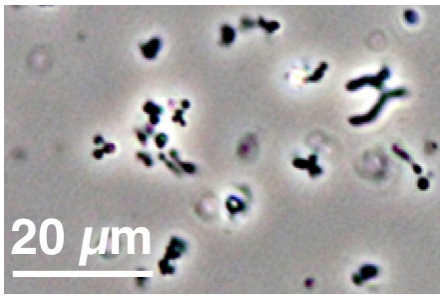

Sample reflectance spectrum:

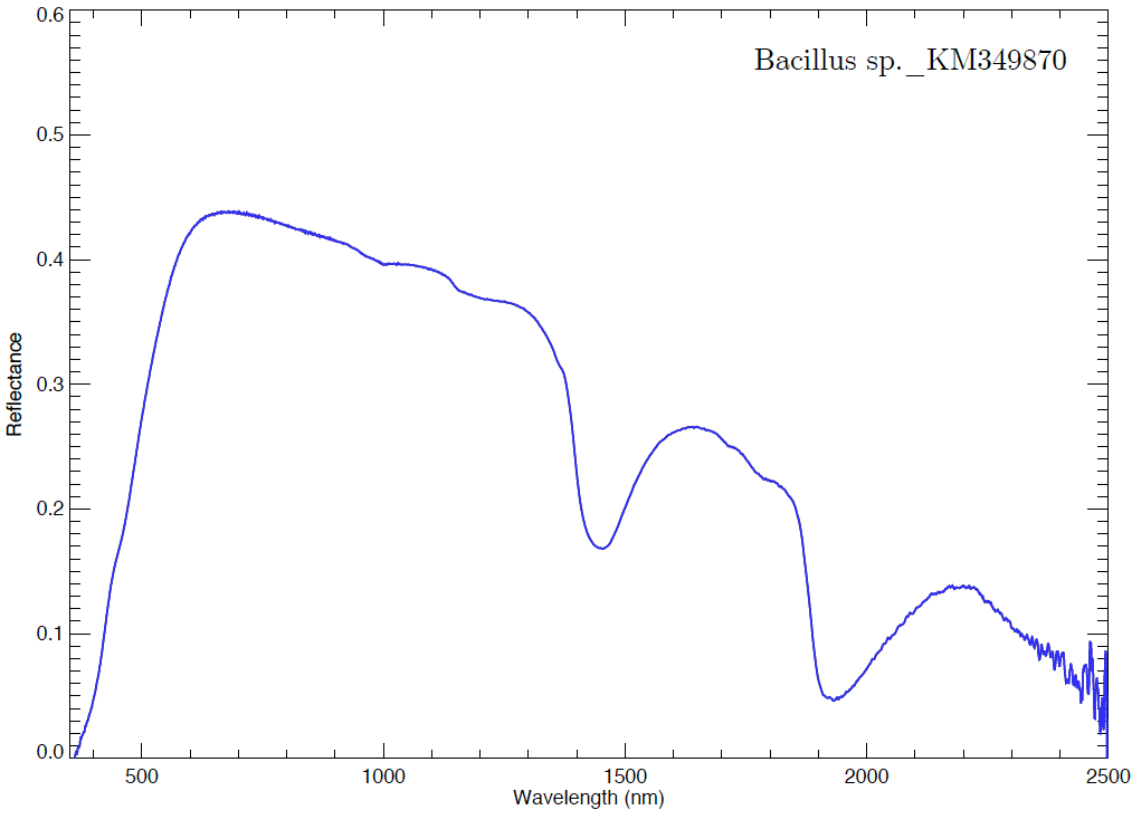

Bacillus sp._KM349871

Sample name: *Bacillus* sp.

Accession number for 16S rRNA partial gene sequence: KM349871

Classification: Bacteria; Firmicutes; Bacilli; Bacillales; Bacillaceae; Bacillus

Metabolism: Heterotrophic

Origin: Sonoran desert, AZ, USA

Isolation: Ivan P. Lima (NPP at NASA Ames, CA, USA)

Sample concentration: 2.62×10^7 cells/ml

Sample count on filter substrate: $7.85 \pm 0.52 \times 10^7$ cells

Laboratory growth conditions: 30 °C, 180 rpm, 24 h

Culture medium: Marine Broth (MB)

Sample photograph:

Sample micrograph:

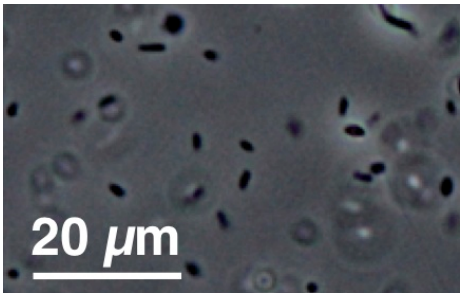

Sample reflectance spectrum:

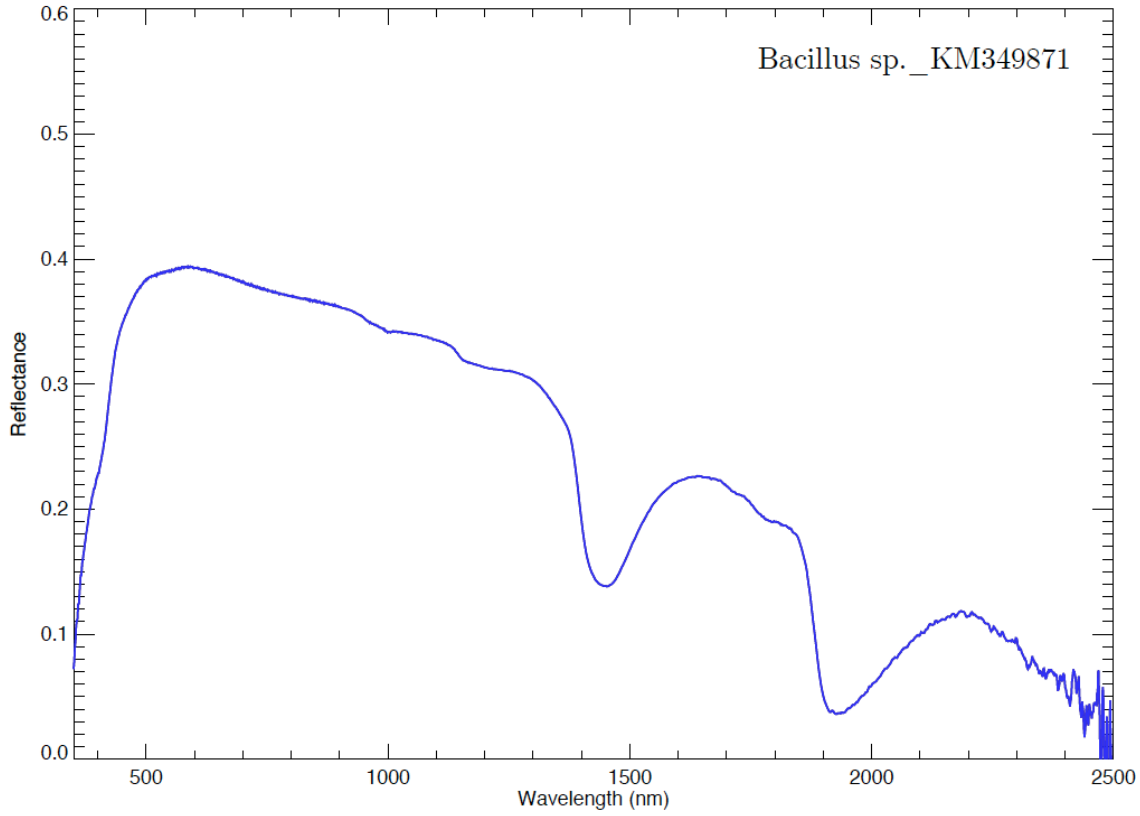

Bacillus sp._KM349872

Sample name: *Bacillus* sp.

Accession number for 16S rRNA partial gene sequence: KM349872

Classification: Bacteria; Firmicutes; Bacilli; Bacillales; Bacillaceae; Bacillus

Metabolism: Heterotrophic

Origin: Sonoran desert, AZ, USA

Isolation: Ivan P. Lima (NPP at NASA Ames, CA, USA)

Sample concentration: 2.28 $\times$ 10^7 cells/ml

Sample count on filter substrate: 6.85 $\pm$ 0.46 $\times$ 10^7 cells

Laboratory growth conditions: 30 °C, 180 rpm, 24 h

Culture medium: Marine Broth (MB)

Sample photograph:

Sample micrograph:

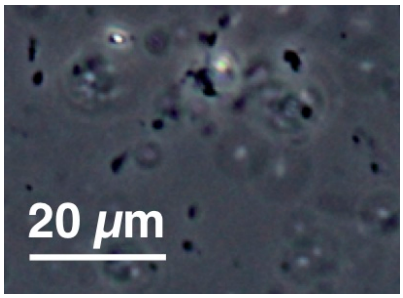

Sample reflectance spectrum:

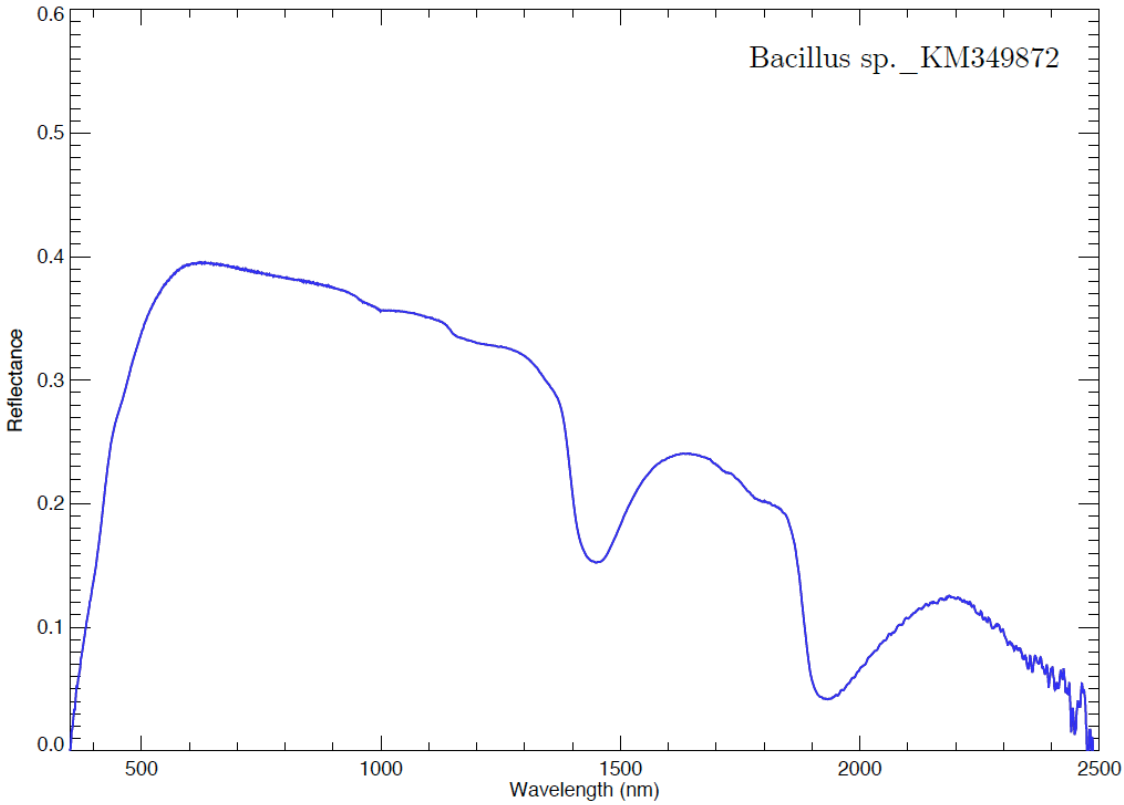

Bacillus sp._KM349873

Sample name: *Bacillus* sp.

Accession number for 16S rRNA partial gene sequence: KM349873

Classification: Bacteria; Firmicutes; Bacilli; Bacillales; Bacillaceae; Bacillus

Metabolism: Heterotrophic

Origin: Sonoran desert, AZ, USA

Isolation: Ivan P. Lima (NPP at NASA Ames, CA, USA)

Sample concentration: 3.48×10^7 cells/ml

Sample count on filter substrate: $1.04 \pm 0.07 \times 10^8$ cells

Laboratory growth conditions: 30 °C, 180 rpm, 24 h

Culture medium: Marine Broth (MB)

Sample photograph:

Sample micrograph:

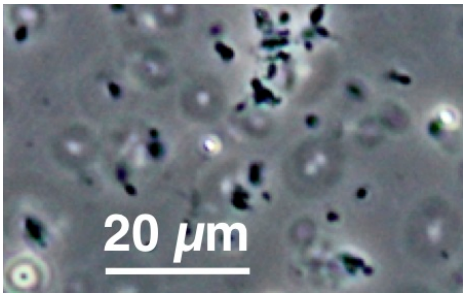

Sample reflectance spectrum:

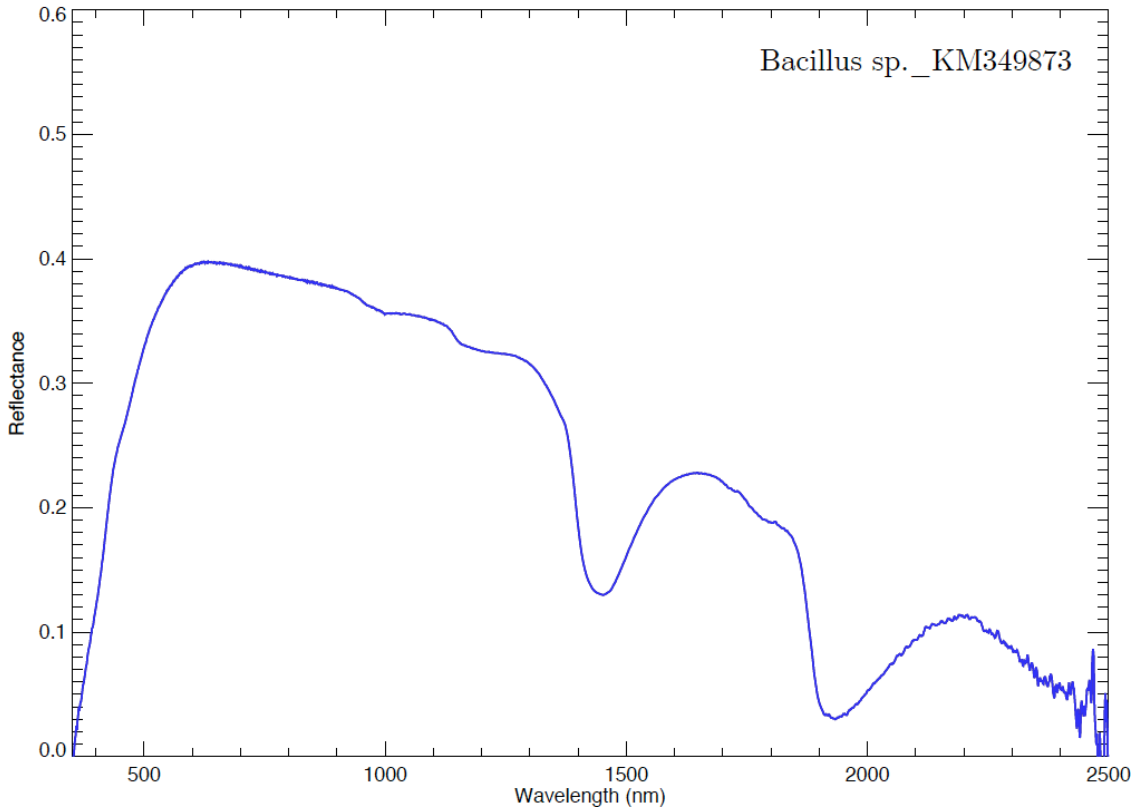

Bacillus sp._KM349874

Sample name: *Bacillus* sp.

Accession number for 16S rRNA partial gene sequence: KM349874

Classification: Bacteria; Firmicutes; Bacilli; Bacillales; Bacillaceae; Bacillus

Metabolism: Heterotrophic

Origin: Sonoran desert, AZ, USA

Isolation: Ivan P. Lima (NPP at NASA Ames, CA, USA)

Sample concentration: 2.60 $\times$ 10^7 cells/ml

Sample count on filter substrate: 7.81 $\pm$ 0.52 $\times$ 10^7 cells

Laboratory growth conditions: 30 °C, 180 rpm, 24 h

Culture medium: Marine Broth (MB)

Sample photograph:

Sample micrograph:

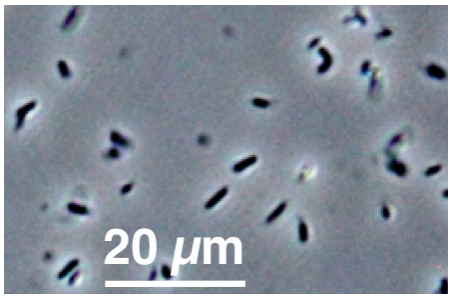

Sample reflectance spectrum:

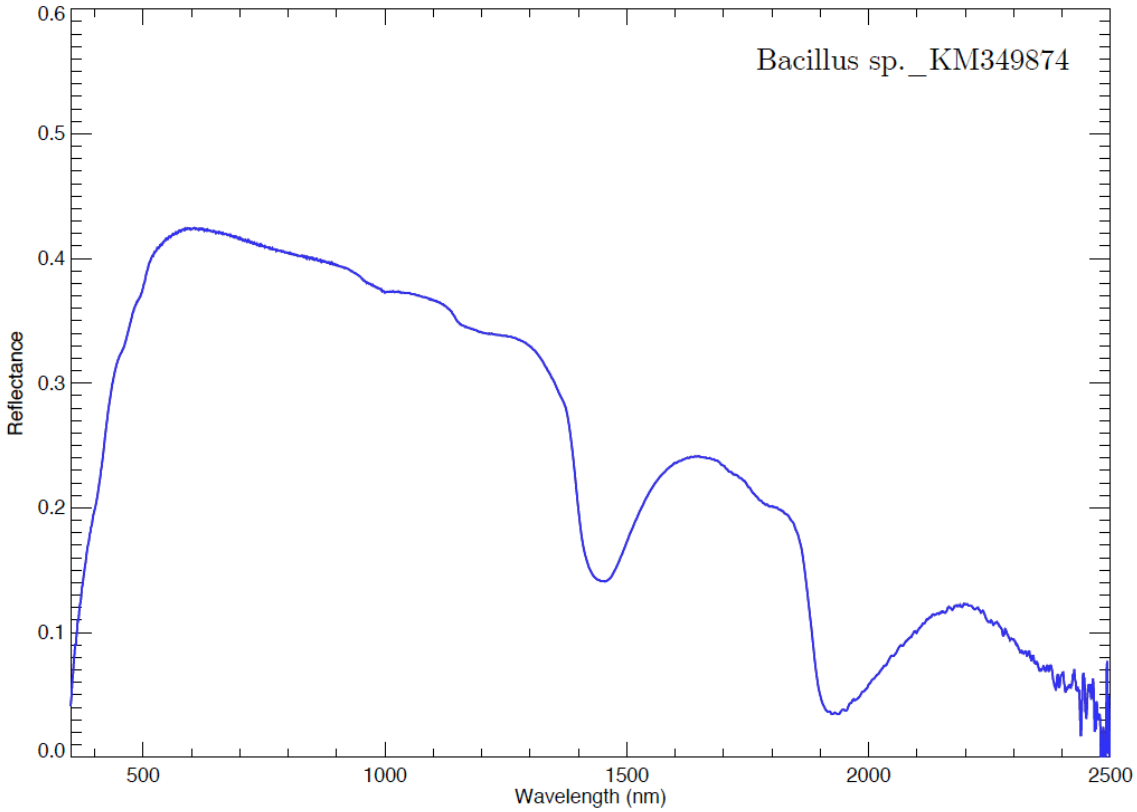

Bacillus sp._KM349875

Sample name: *Bacillus* sp.

Accession number for 16S rRNA partial gene sequence: KM349875

Classification: Bacteria; Firmicutes; Bacilli; Bacillales; Bacillaceae; Bacillus

Metabolism: Heterotrophic

Origin: Sonoran desert, AZ, USA

Isolation: Ivan P. Lima (NPP at NASA Ames, CA, USA)

Sample concentration: 1.16 $\times$ 10^7 cells/ml

Sample count on filter substrate: 3.47 $\pm$ 0.23 $\times$ 10^7 cells

Laboratory growth conditions: 30 °C, 180 rpm, 24 h

Culture medium: Marine Broth (MB)

Sample photograph:

Sample micrograph:

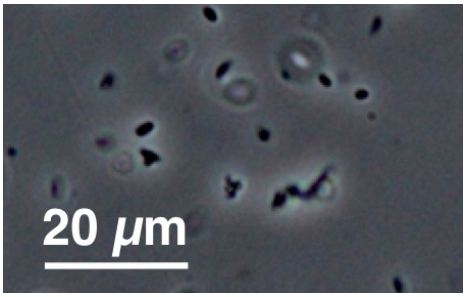

Sample reflectance spectrum:

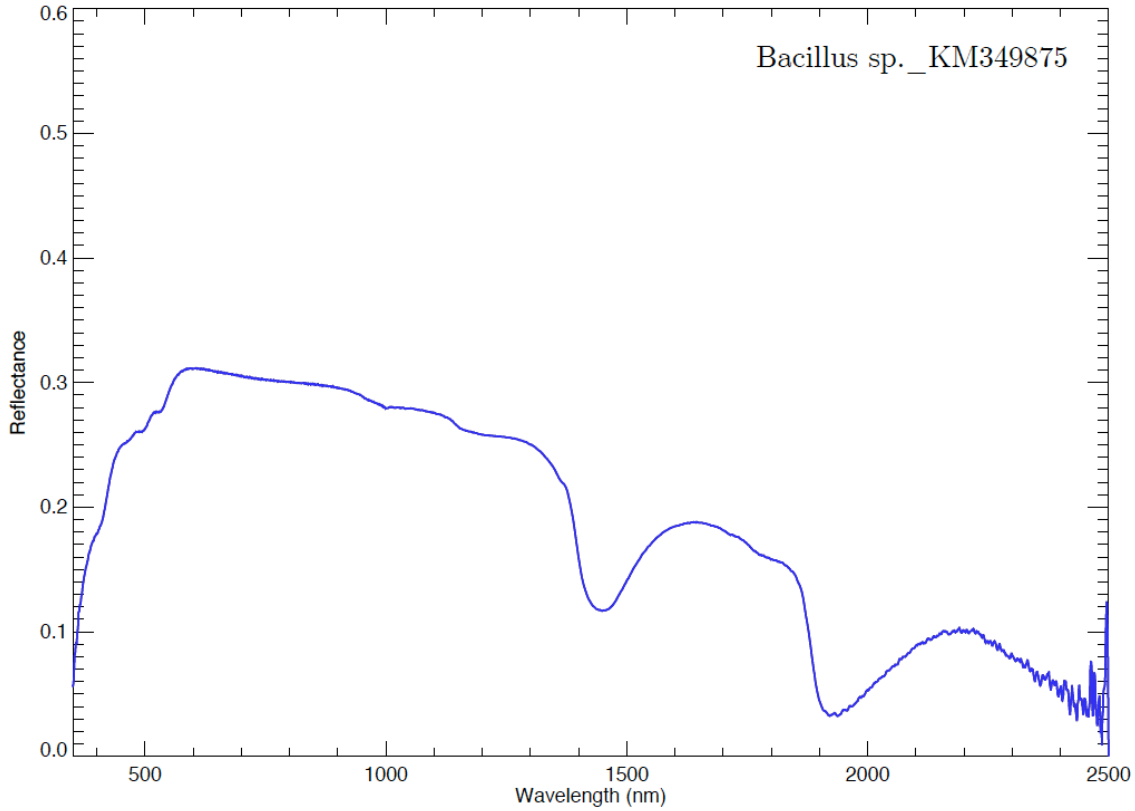

Bacillus sp._KM349876

Sample name: *Bacillus* sp.

Accession number for 16S rRNA partial gene sequence: KM349876

Classification: Bacteria; Firmicutes; Bacilli; Bacillales; Bacillaceae; Bacillus

Metabolism: Heterotrophic

Origin: Sonoran desert, AZ, USA

Isolation: Ivan P. Lima (NPP at NASA Ames, CA, USA)

Sample concentration: 4.73 $\times$ 10^7 cells/ml

Sample count on filter substrate: 1.42 $\pm$ 0.09 $\times$ 10^8 cells

Laboratory growth conditions: 30 °C, 180 rpm, 24 h

Culture medium: Marine Broth (MB)

Sample photograph:

Sample micrograph:

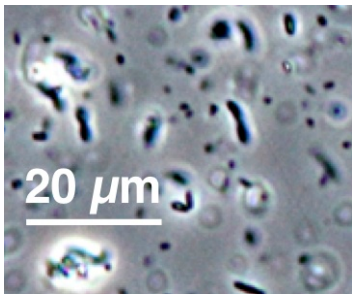

Sample reflectance spectrum:

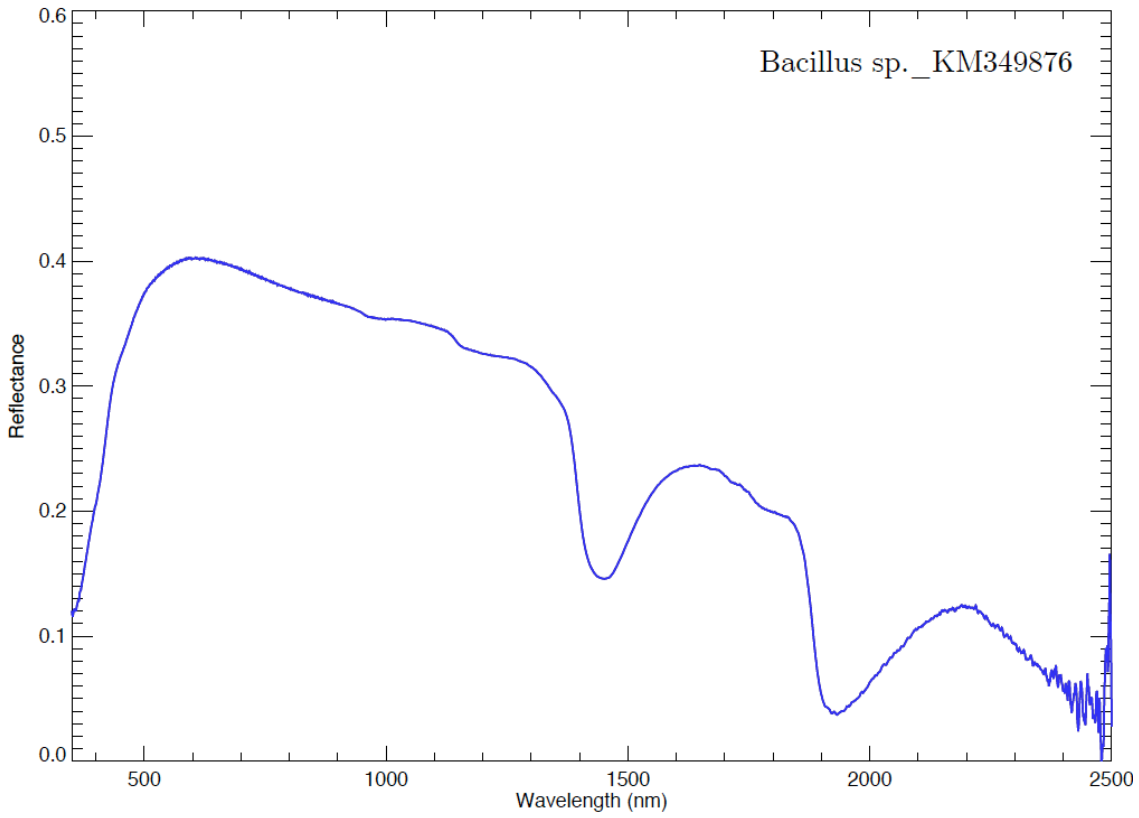

Bacillus sp._KM349877

Sample name: *Bacillus* sp.

Accession number for 16S rRNA partial gene sequence: KM349877

Classification: Bacteria; Firmicutes; Bacilli; Bacillales; Bacillaceae; Bacillus

Metabolism: Heterotrophic

Origin: Sonoran desert, AZ, USA

Isolation: Ivan P. Lima (NPP at NASA Ames, CA, USA)

Sample concentration: 1.08 $\times$ 10^7 cells/ml

Sample count on filter substrate: 3.24 $\pm$ 0.22 $\times$ 10^7 cells

Laboratory growth conditions: 30 °C, 180 rpm, 24 h

Culture medium: Marine Broth (MB)

Sample photograph:

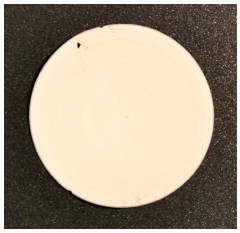

Sample micrograph:

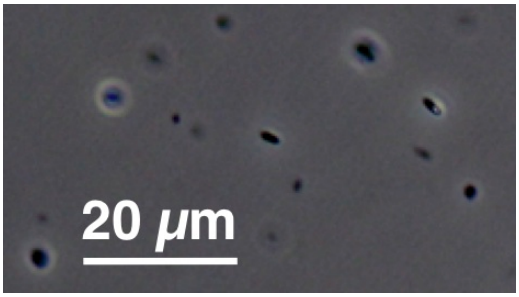

Sample reflectance spectrum:

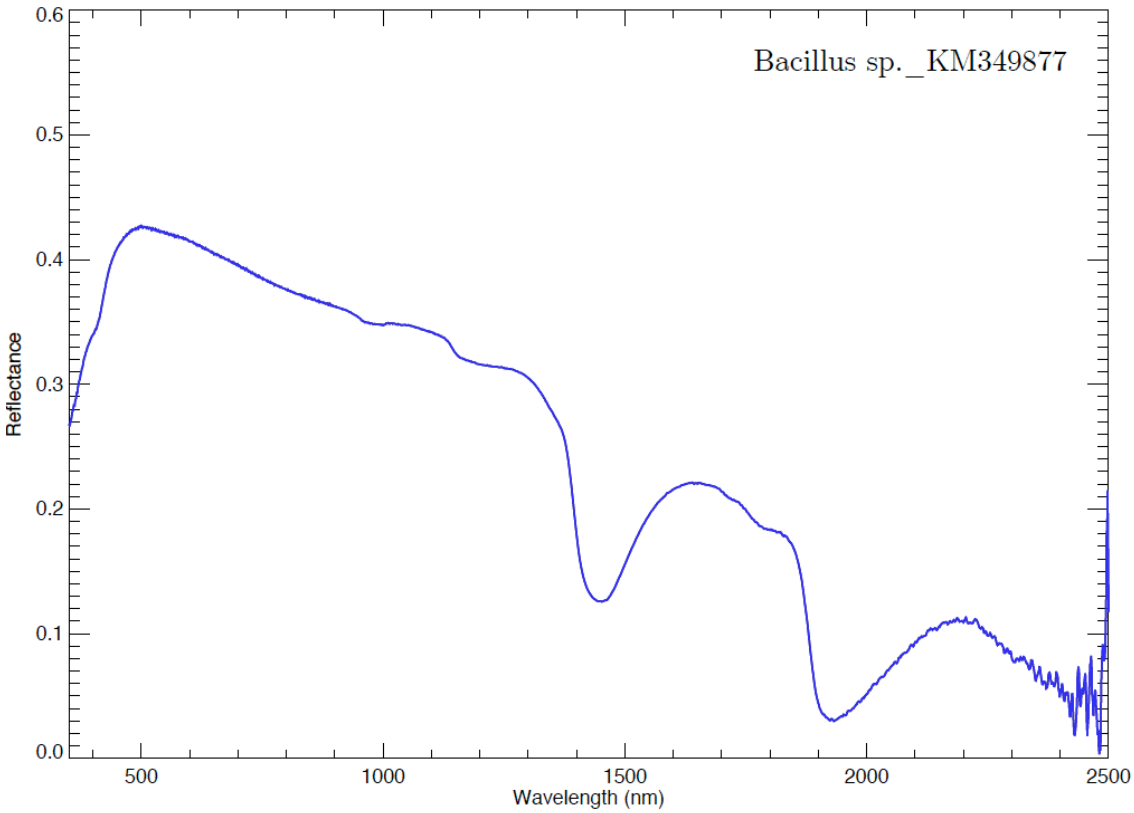

Bacillus sp._KM349878

Sample name: *Bacillus* sp.

Accession number for 16S rRNA partial gene sequence: KM349878

Classification: Bacteria; Firmicutes; Bacilli; Bacillales; Bacillaceae; Bacillus

Metabolism: Heterotrophic

Origin: Sonoran desert, AZ, USA

Isolation: Ivan P. Lima (NPP at NASA Ames, CA, USA)

Sample concentration: 4.61 $\times$ 10^7 cells/ml

Sample count on filter substrate: 1.38 $\pm$ 0.09 $\times$ 10^8 cells

Laboratory growth conditions: 30 °C, 180 rpm, 24 h

Culture medium: Marine Broth (MB)

Sample photograph:

Sample micrograph:

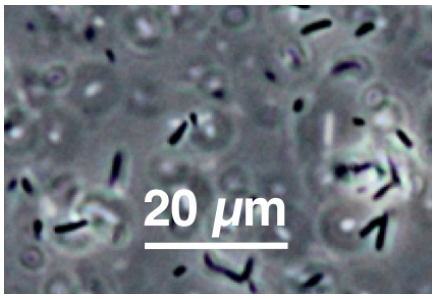

Sample reflectance spectrum:

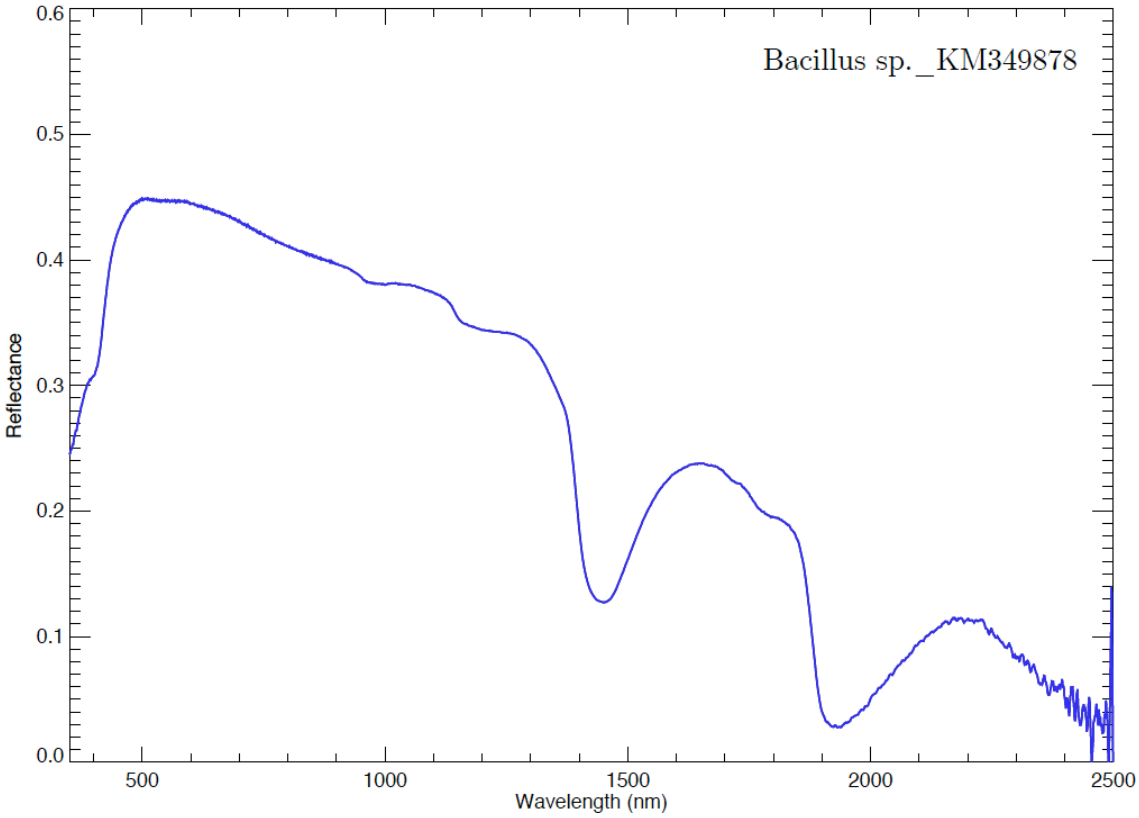

Bacillus sp._KM349887

Sample name: *Bacillus* sp.

Accession number for 16S rRNA partial gene sequence: KM349887

Classification: Bacteria; Firmicutes; Bacilli; Bacillales; Bacillaceae; Bacillus

Metabolism: Heterotrophic

Origin: Atacama desert, Chile

Isolation: Ivan P. Lima (NPP at NASA Ames, CA, USA)

Sample concentration: 5.89 $\times$ 10^7 cells/ml

Sample count on filter substrate: 1.77 $\pm$ 0.12 $\times$ 10^8 cells

Laboratory growth conditions: 30 °C, 180 rpm, 24 h

Culture medium: Marine Broth (MB)

Sample photograph:

Sample micrograph:

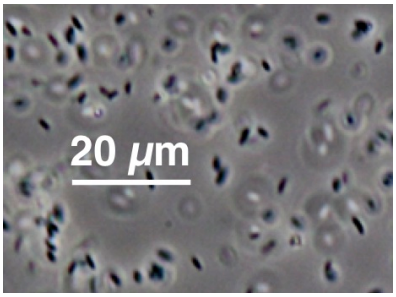

Sample reflectance spectrum:

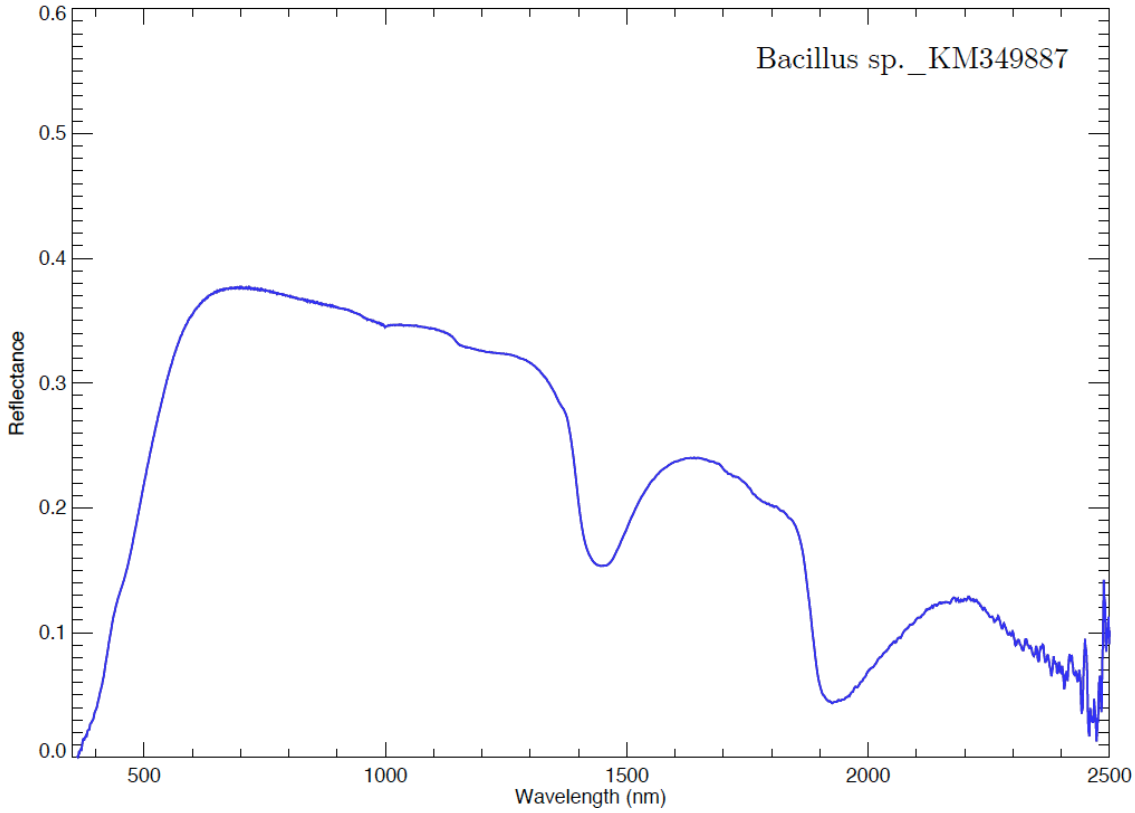

Bacillus sp._KM349899

Sample name: *Bacillus* sp.

Accession number for 16S rRNA partial gene sequence: KM349899

Classification: Bacteria; Firmicutes; Bacilli; Bacillales; Bacillaceae; Bacillus

Metabolism: Heterotrophic

Origin: Atacama desert, Chile

Isolation: Ivan P. Lima (NPP at NASA Ames, CA, USA)

Sample concentration: 3.17 $\times$ 10^7 cells/ml

Sample count on filter substrate: 9.51 $\pm$ 0.63 $\times$ 10^7 cells

Laboratory growth conditions: 30 °C, 180 rpm, 24 h

Culture medium: Marine Broth (MB)

Sample photograph:

Sample micrograph:

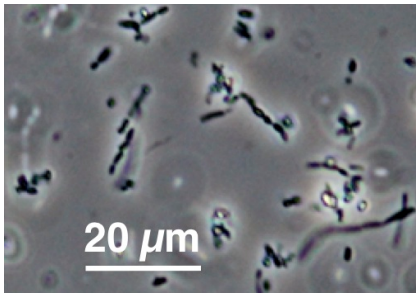

Sample reflectance spectrum:

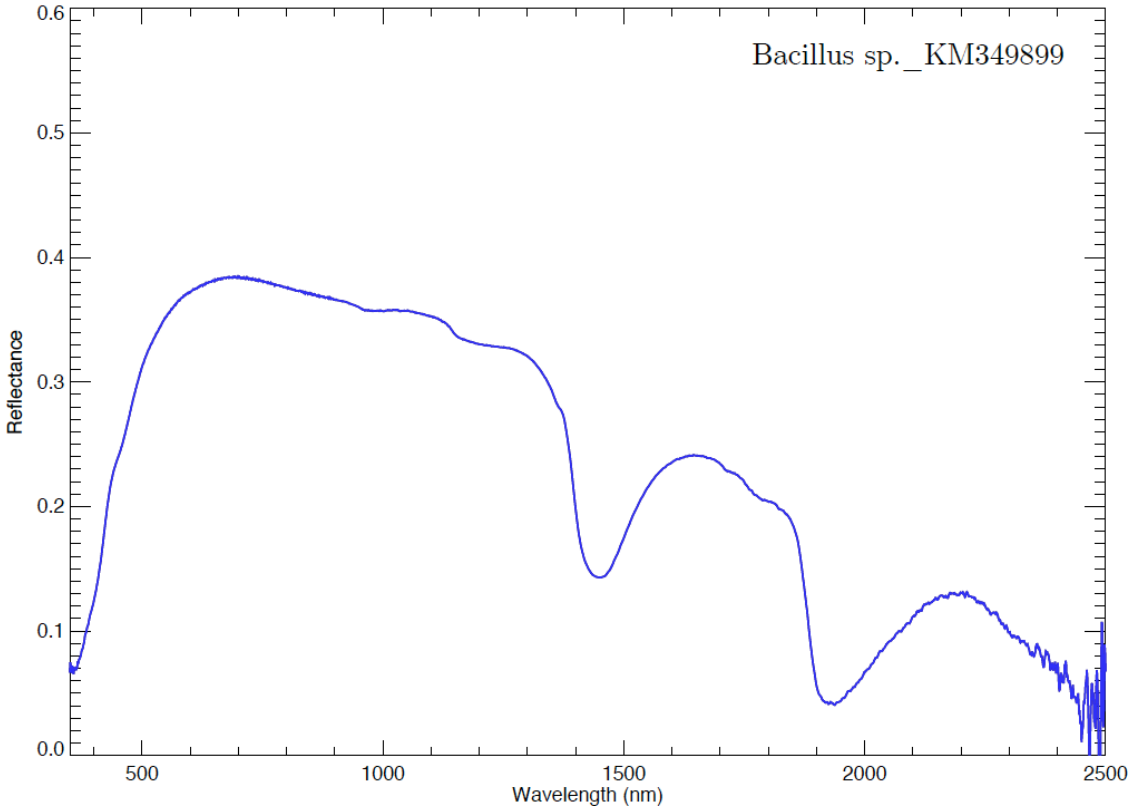

Bacillus sp._KM349902

Sample name: *Bacillus* sp.

Accession number for 16S rRNA partial gene sequence: KM349902

Classification: Bacteria; Firmicutes; Bacilli; Bacillales; Bacillaceae; Bacillus

Metabolism: Heterotrophic

Origin: Moffett Field, CA, USA

Isolation: Ivan P. Lima (NPP at NASA Ames, CA, USA)

Sample concentration: 1.37 $\times$ 10^7 cells/ml

Sample count on filter substrate: 4.12 $\pm$ 0.27 $\times$ 10^7 cells

Laboratory growth conditions: 30 °C, 180 rpm, 24 h

Culture medium: Marine Broth (MB)

Sample photograph:

Sample micrograph:

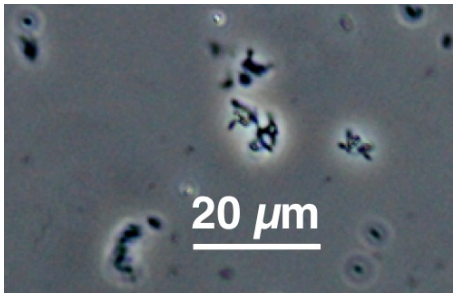

Sample reflectance spectrum:

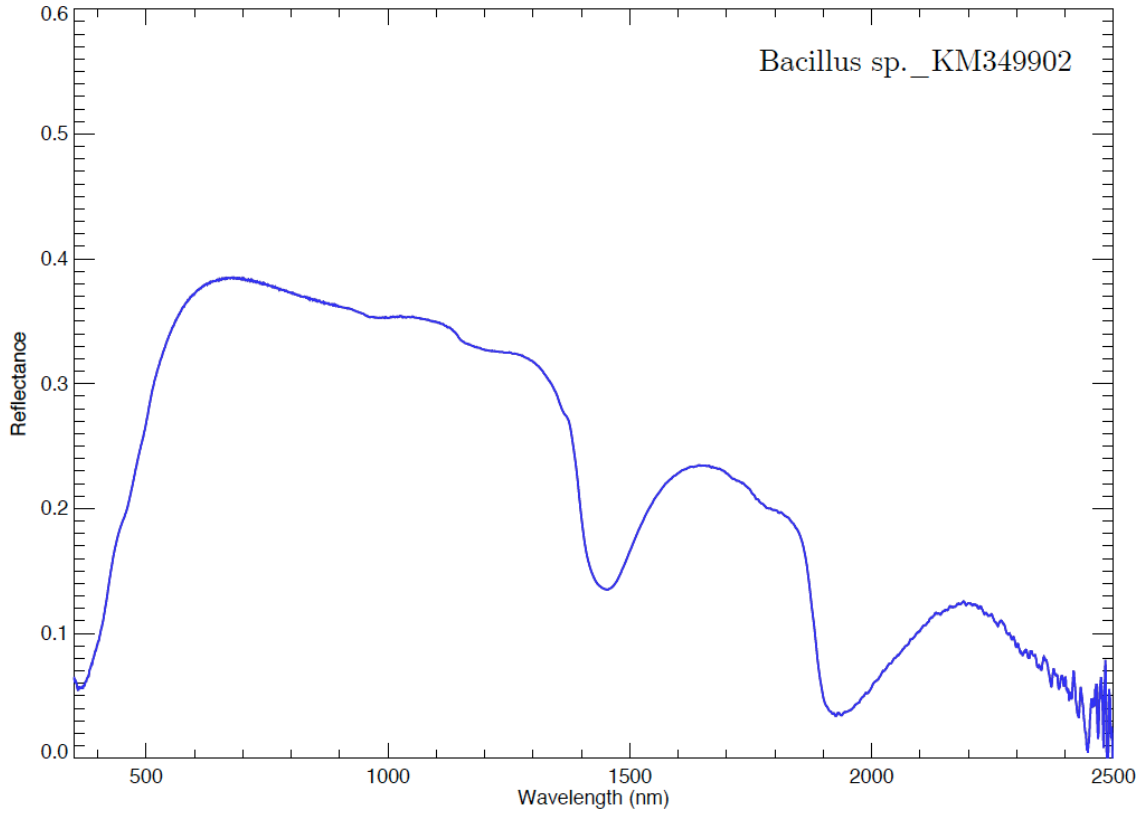

Bacillus sp._KM349906

Sample name: *Bacillus* sp.

Accession number for 16S rRNA partial gene sequence: KM349906

Classification: Bacteria; Firmicutes; Bacilli; Bacillales; Bacillaceae; Bacillus

Metabolism: Heterotrophic

Origin: Sonoran desert, AZ, USA

Isolation: Ivan P. Lima (NPP at NASA Ames, CA, USA)

Sample concentration: 1.13 $\times$ 10^8 cells/ml

Sample count on filter substrate: 3.40 $\pm$ 0.23 $\times$ 10^8 cells

Laboratory growth conditions: 30 °C, 180 rpm, 24 h

Culture medium: Lysogeny Broth (LB)

Sample photograph:

Sample micrograph:

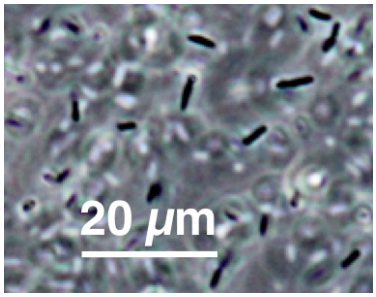

Sample reflectance spectrum:

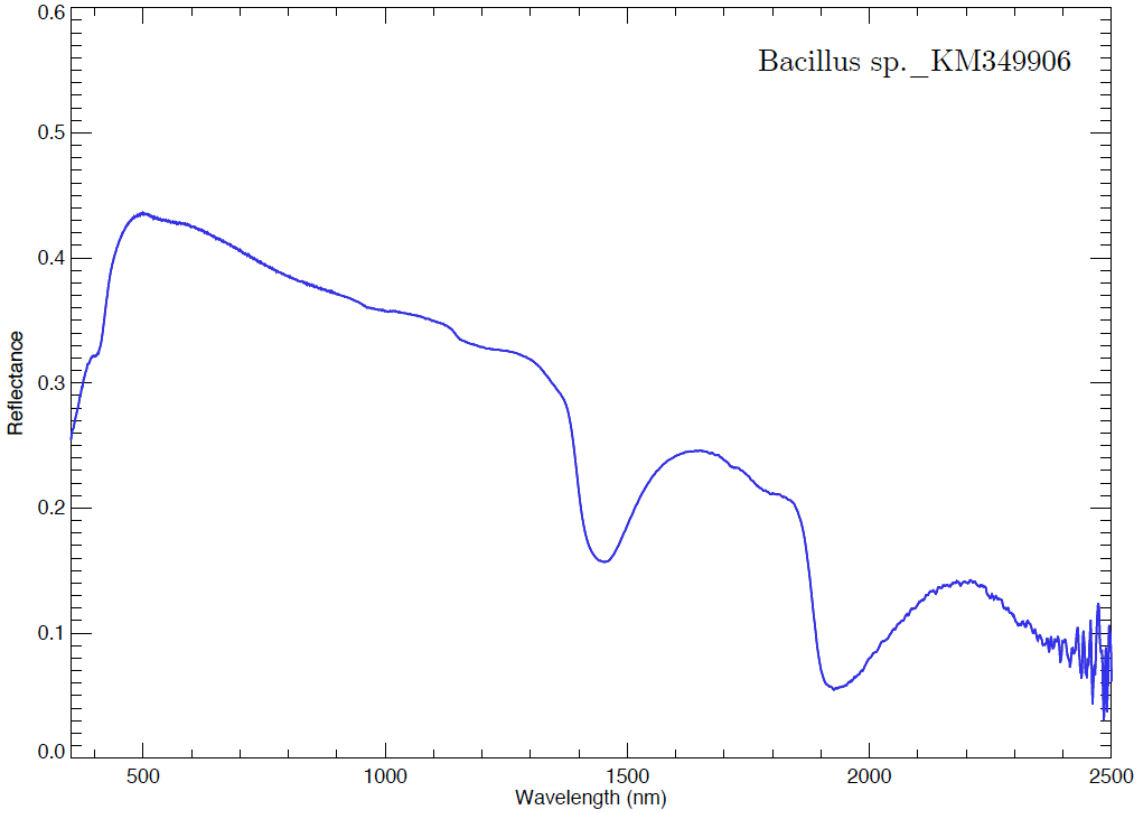

Bacillus sp._KM349911

Sample name: *Bacillus* sp.

Accession number for 16S rRNA partial gene sequence: KM349911

Classification: Bacteria; Firmicutes; Bacilli; Bacillales; Bacillaceae; Bacillus

Metabolism: Heterotrophic

Origin: Sonoran desert, AZ, USA

Isolation: Ivan P. Lima (NPP at NASA Ames, CA, USA)

Sample concentration: 2.87 $\times$ 10^7 cells/ml

Sample count on filter substrate: 8.60 $\pm$ 0.57 $\times$ 10^7 cells

Laboratory growth conditions: 30 °C, 180 rpm, 24 h

Culture medium: Marine Broth (MB)

Sample photograph:

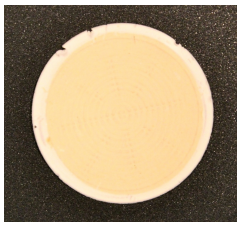

Sample micrograph:

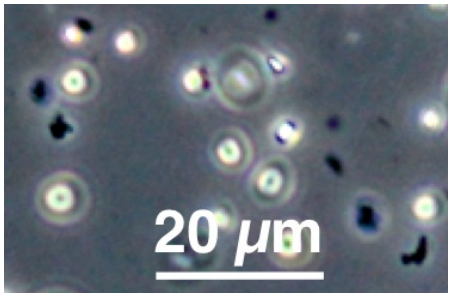

Sample reflectance spectrum:

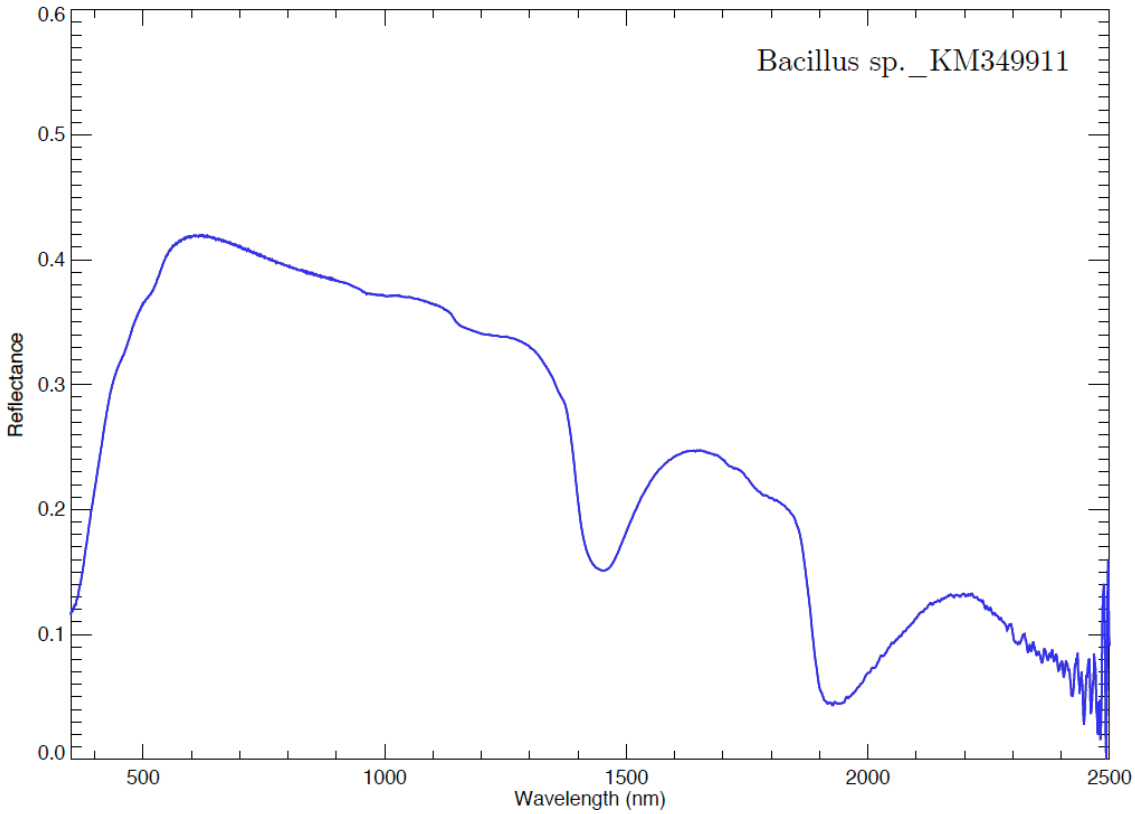

Bacillus sp._KM349913

Sample name: *Bacillus* sp.

Accession number for 16S rRNA partial gene sequence: KM349913

Classification: Bacteria; Firmicutes; Bacilli; Bacillales; Bacillaceae; Bacillus

Metabolism: Heterotrophic

Origin: Sonoran desert, AZ, USA

Isolation: Ivan P. Lima (NPP at NASA Ames, CA, USA)

Sample concentration: 2.44 $\times$ 10^7 cells/ml

Sample count on filter substrate: 7.32 $\pm$ 0.49 $\times$ 10^7 cells

Laboratory growth conditions: 30 °C, 180 rpm, 24 h

Culture medium: Marine Broth (MB)

Sample photograph:

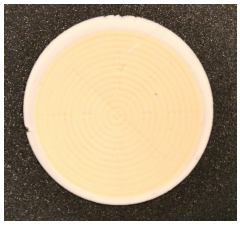

Sample micrograph:

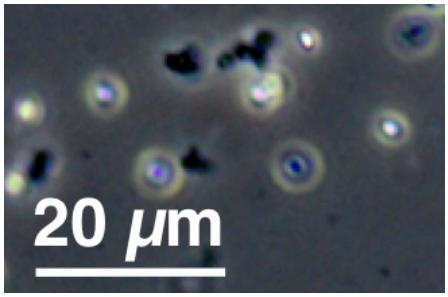

Sample reflectance spectrum:

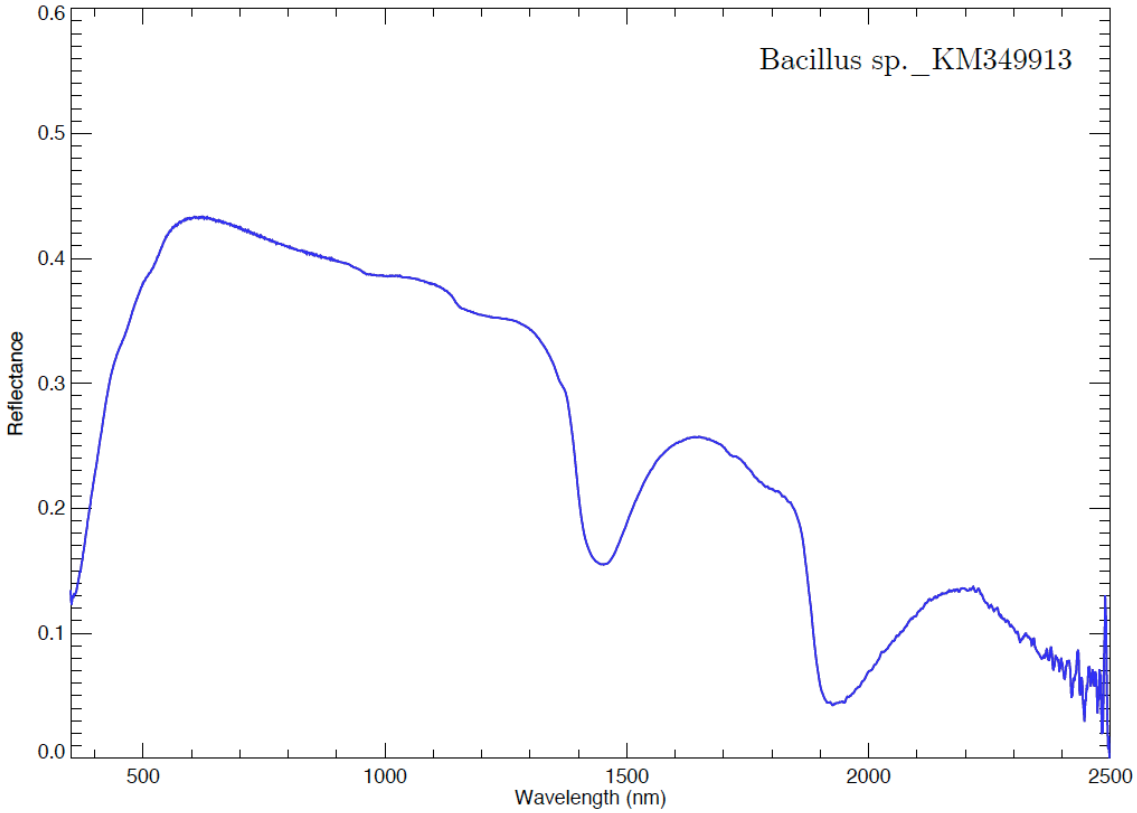

Bacillus sp._KM349915

Sample name: *Bacillus* sp.

Accession number for 16S rRNA partial gene sequence: KM349915

Classification: Bacteria; Firmicutes; Bacilli; Bacillales; Bacillaceae; Bacillus

Metabolism: Heterotrophic

Origin: Sonoran desert, AZ, USA

Isolation: Ivan P. Lima (NPP at NASA Ames, CA, USA)

Sample concentration: 1.88 $\times$ 10^7 cells/ml

Sample count on filter substrate: 5.64 $\pm$ 0.38 $\times$ 10^7 cells

Laboratory growth conditions: 30 °C, 180 rpm, 24 h

Culture medium: Marine Broth (MB)

Sample photograph:

Sample micrograph:

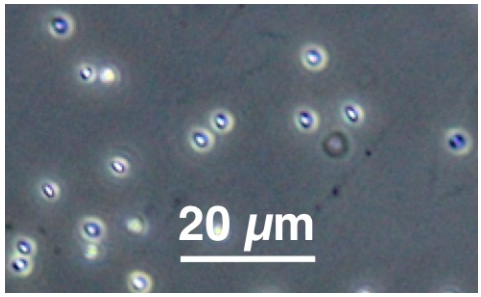

Sample reflectance spectrum:

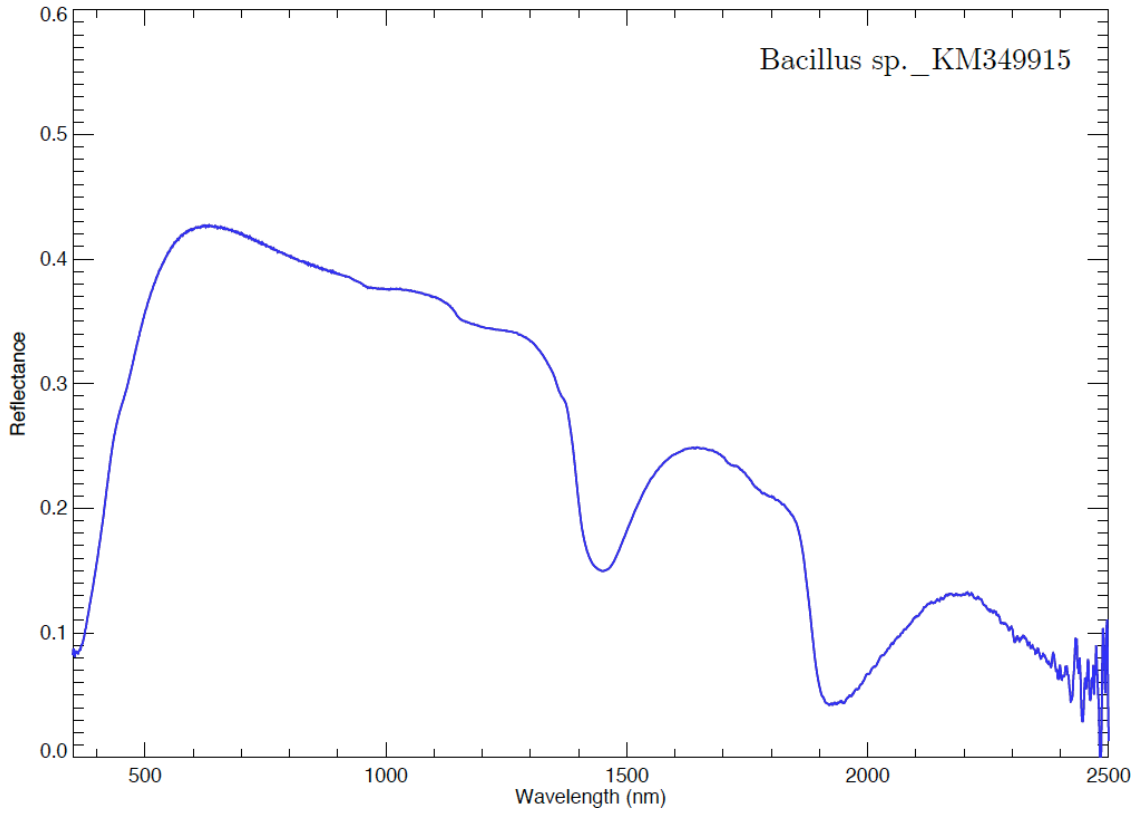

Bacillus sp._KM349927

Sample name: *Bacillus* sp.

Accession number for 16S rRNA partial gene sequence: KM349927

Classification: Bacteria; Firmicutes; Bacilli; Bacillales; Bacillaceae; Bacillus

Metabolism: Heterotrophic

Origin: Sonoran desert, AZ, USA

Isolation: Ivan P. Lima (NPP at NASA Ames, CA, USA)

Sample concentration: 2.22 $\times$ 10^7 cells/ml

Sample count on filter substrate: 6.65 $\pm$ 0.44 $\times$ 10^7 cells

Laboratory growth conditions: 30 °C, 180 rpm, 24 h

Culture medium: Lysogeny Broth (LB)

Sample photograph:

Sample micrograph:

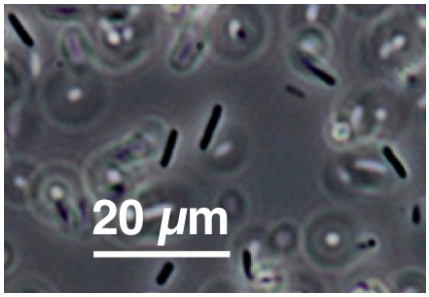

Sample reflectance spectrum:

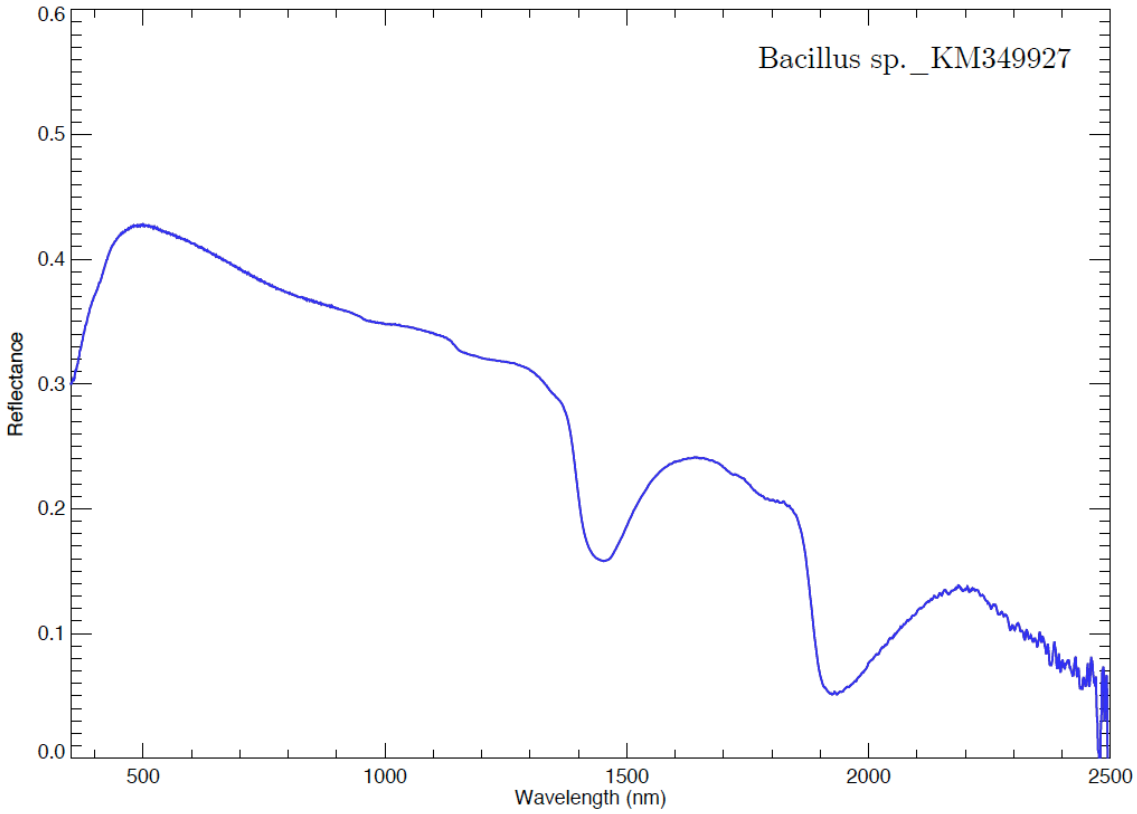

Bacillus sp._KM349928

Sample name: *Bacillus* sp.

Accession number for 16S rRNA partial gene sequence: KM349928

Classification: Bacteria; Firmicutes; Bacilli; Bacillales; Bacillaceae; Bacillus

Metabolism: Heterotrophic

Origin: Sonoran desert, AZ, USA

Isolation: Ivan P. Lima (NPP at NASA Ames, CA, USA)

Sample concentration: 4.62×10^7 cells/ml

Sample count on filter substrate: $1.39 \pm 0.09 \times 10^8$ cells

Laboratory growth conditions: 30 °C, 180 rpm, 24 h

Culture medium: Lysogeny Broth (LB)

Sample photograph:

Sample micrograph:

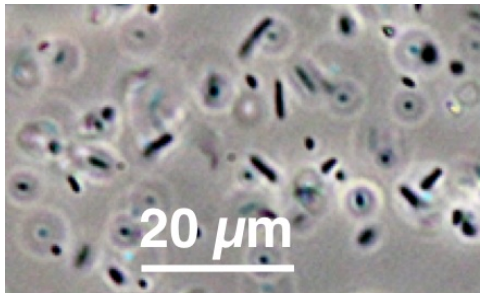

Sample reflectance spectrum:

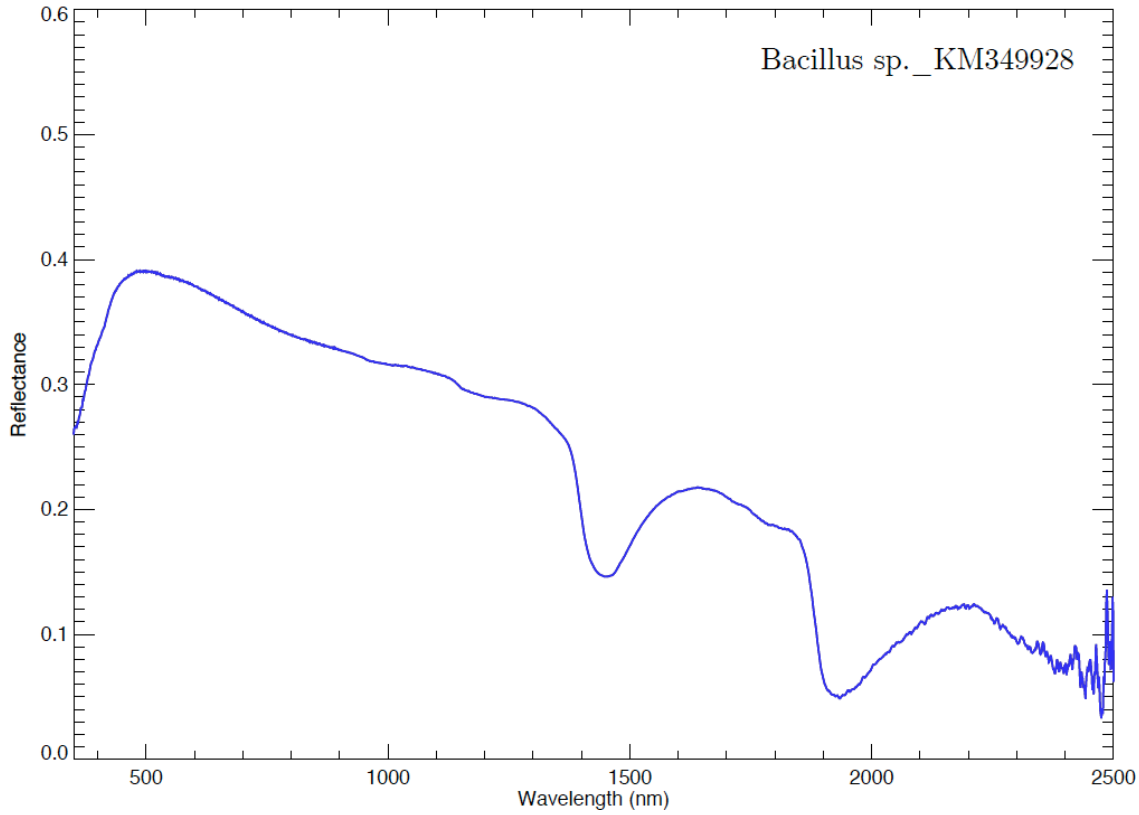

Bacillus sp._KM349929

Sample name: *Bacillus* sp.

Accession number for 16S rRNA partial gene sequence: KM349929

Classification: Bacteria; Firmicutes; Bacilli; Bacillales; Bacillaceae; Bacillus

Metabolism: Heterotrophic

Origin: Sonoran desert, AZ, USA

Isolation: Ivan P. Lima (NPP at NASA Ames, CA, USA)

Sample concentration: 6.60 $\times$ 10^7 cells/ml

Sample count on filter substrate: 1.98 $\pm$ 0.13 $\times$ 10^8 cells

Laboratory growth conditions: 30 °C, 180 rpm, 24 h

Culture medium: Lysogeny Broth (LB)

Sample photograph:

Sample micrograph:

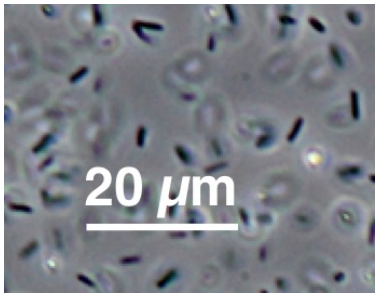

Sample reflectance spectrum:

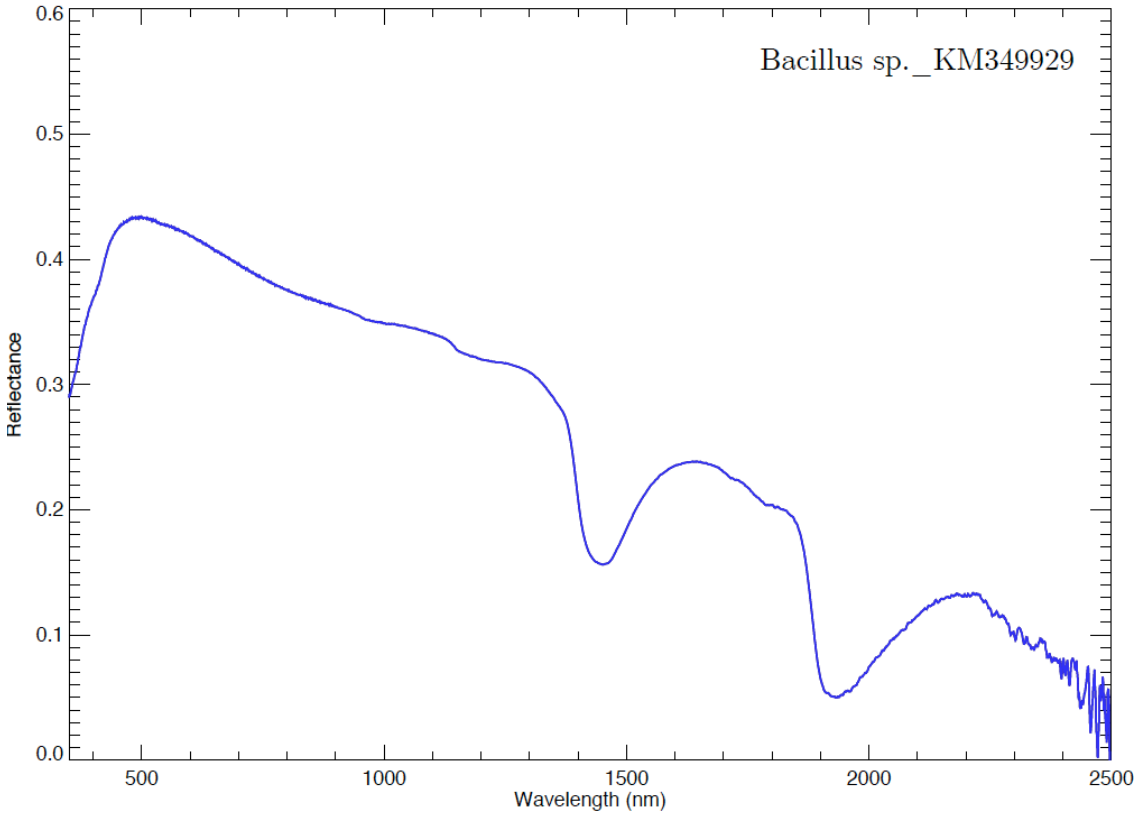

Bacillus sp._KM349930

Sample name: *Bacillus* sp.

Accession number for 16S rRNA partial gene sequence: KM349930

Classification: Bacteria; Firmicutes; Bacilli; Bacillales; Bacillaceae; Bacillus

Metabolism: Heterotrophic

Origin: Sonoran desert, AZ, USA

Isolation: Ivan P. Lima (NPP at NASA Ames, CA, USA)

Sample concentration: 2.22 $\times$ 10^7 cells/ml

Sample count on filter substrate: 6.65 $\pm$ 0.44 $\times$ 10^7 cells

Laboratory growth conditions: 30 °C, 180 rpm, 24 h

Culture medium: Marine Broth (MB)

Sample photograph:

Sample micrograph:

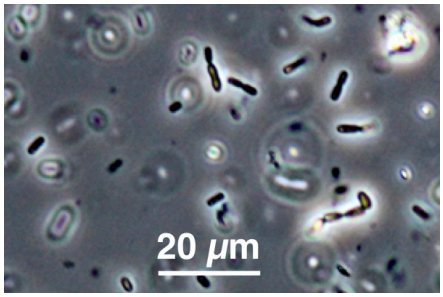

Sample reflectance spectrum:

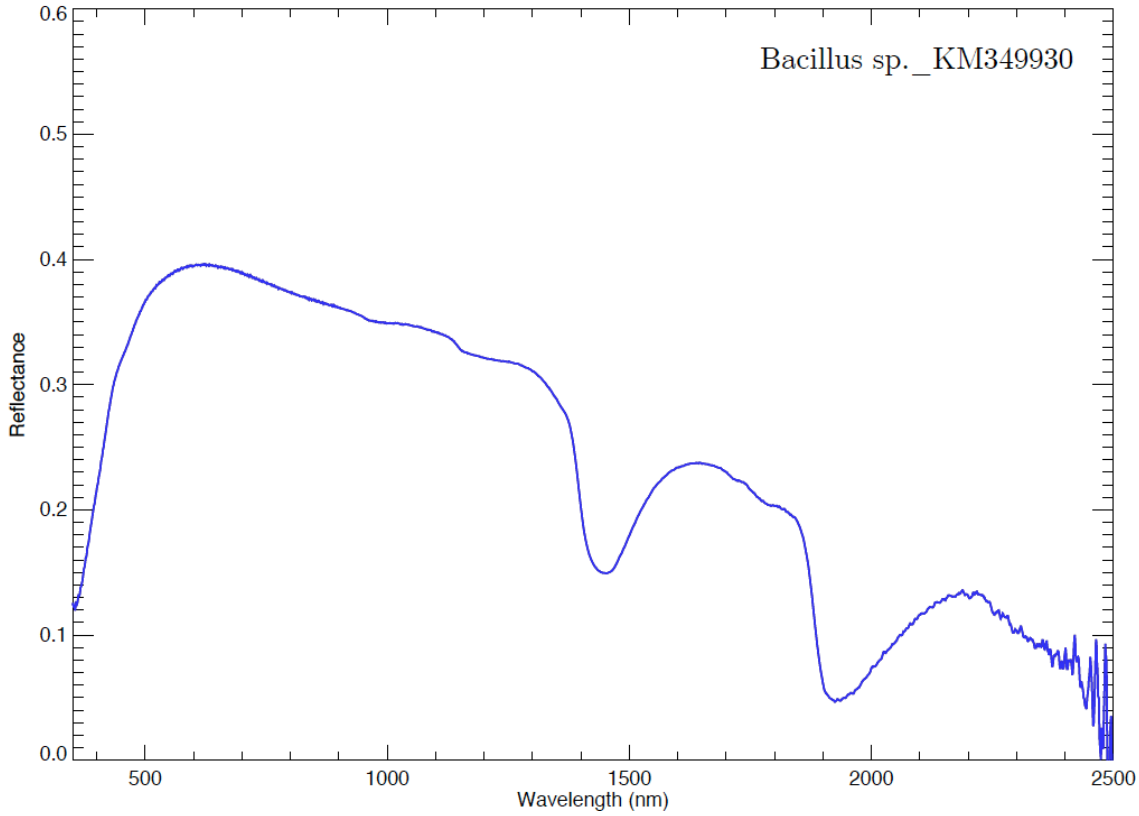

Bacillus sp._KM349931

Sample name: *Bacillus* sp.

Accession number for 16S rRNA partial gene sequence: KM349931

Classification: Bacteria; Firmicutes; Bacilli; Bacillales; Bacillaceae; Bacillus

Metabolism: Heterotrophic

Origin: Sonoran desert, AZ, USA

Isolation: Ivan P. Lima (NPP at NASA Ames, CA, USA)

Sample concentration: 7.76 $\times$ 10^7 cells/ml

Sample count on filter substrate: 2.33 $\pm$ 0.16 $\times$ 10^8 cells

Laboratory growth conditions: 30 °C, 180 rpm, 24 h

Culture medium: Marine Broth (MB)

Sample photograph:

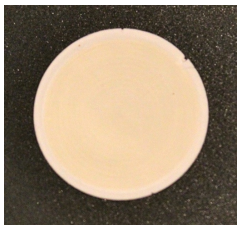

Sample micrograph:

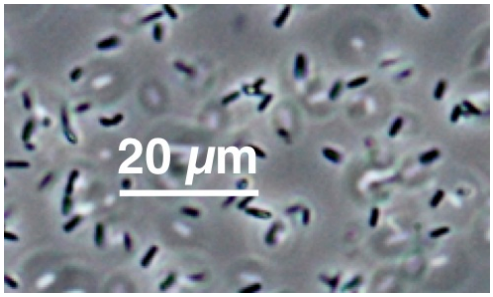

Sample reflectance spectrum:

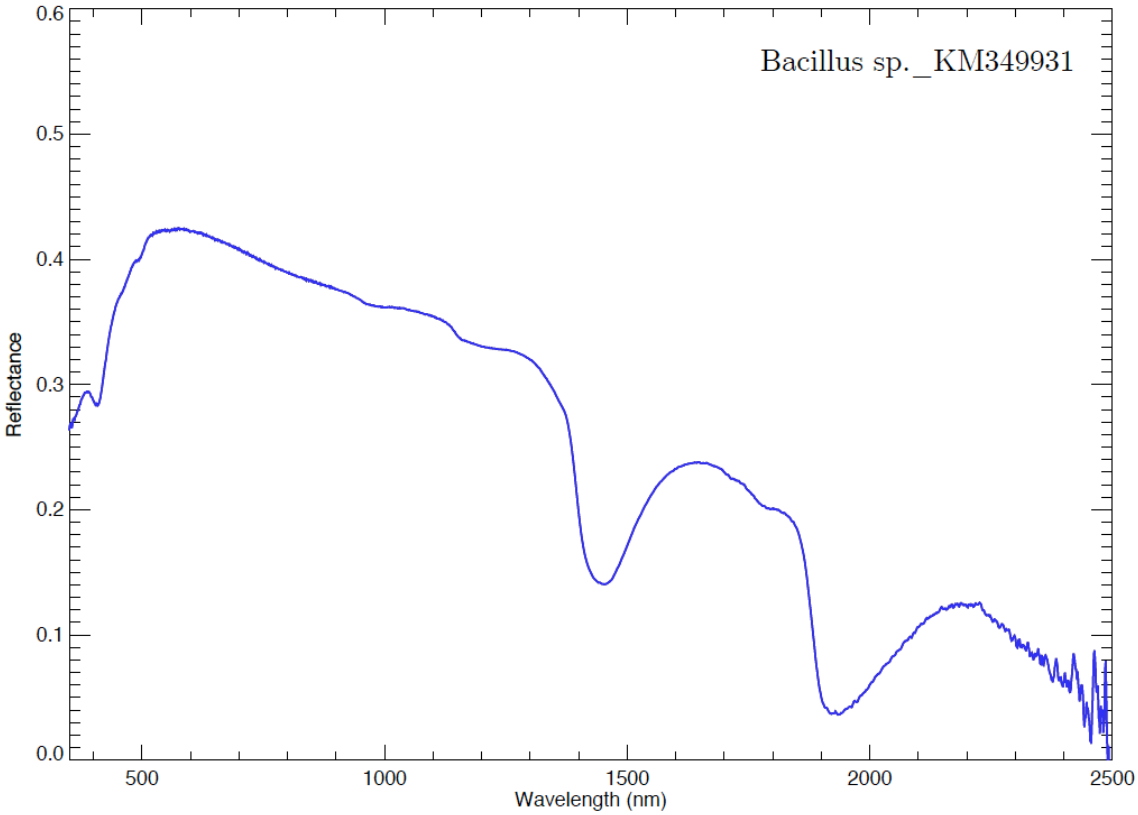

Bacillus sp._KM349941

Sample name: *Bacillus* sp.

Accession number for 16S rRNA partial gene sequence: KM349941

Classification: Bacteria; Firmicutes; Bacilli; Bacillales; Bacillaceae; Bacillus

Metabolism: Heterotrophic

Origin: Atacama desert, Chile

Isolation: Ivan P. Lima (NPP at NASA Ames, CA, USA)

Sample concentration: 5.56×10^7 cells/ml

Sample count on filter substrate: $1.67 \pm 0.11 \times 10^8$ cells

Laboratory growth conditions: 30 °C, 180 rpm, 24 h

Culture medium: Marine Broth (MB)

Sample photograph:

Sample micrograph:

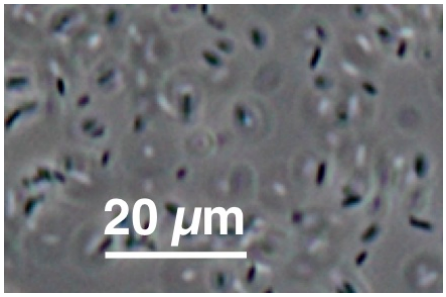

Sample reflectance spectrum:

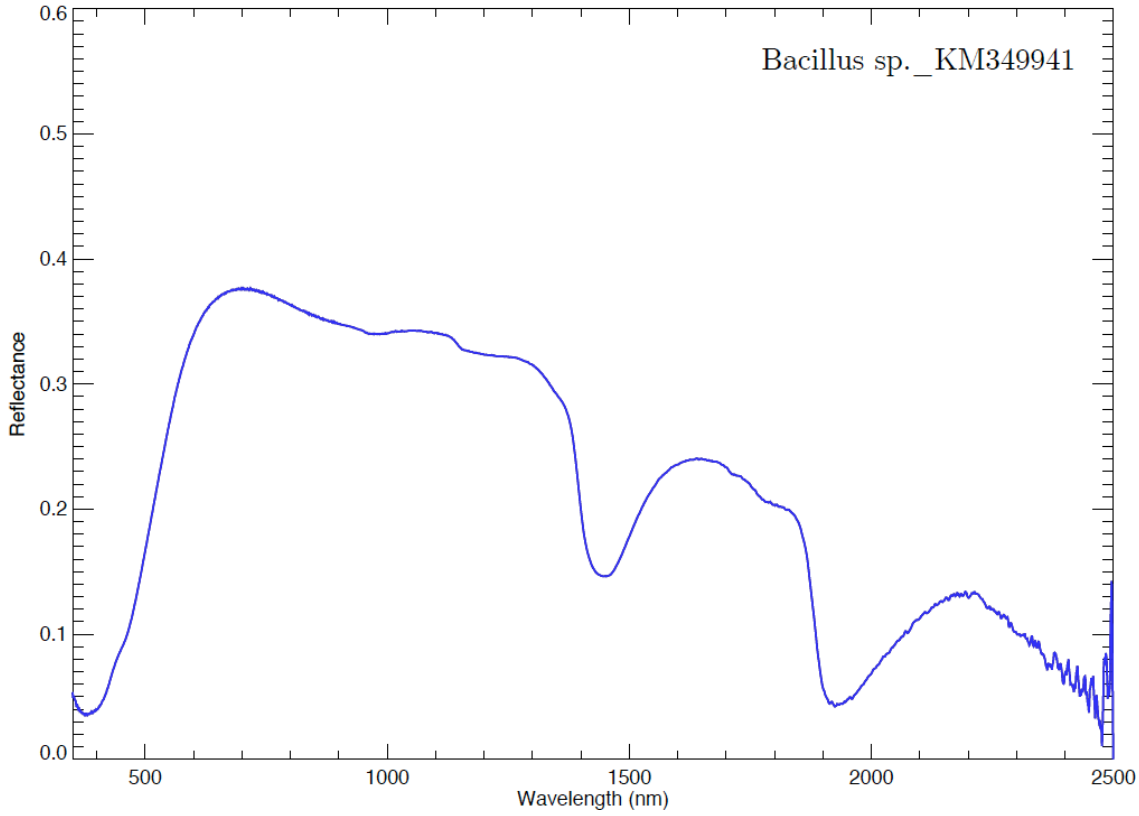

Bacillus subtilis 168 plus chromogenic protein

Sample name: *Bacillus subtilis* 168 plus chromogenic protein

Accession number for 16S rRNA partial gene sequence: Not available

Classification: Bacteria; Firmicutes; Bacilli; Bacillales; Bacillaceae; Bacillus

Metabolism: Heterotrophic

Origin: Laboratory strain most often found in soil samples

Collection: Rothschild laboratory (NASA Ames, CA, USA)

Sample concentration: 3.52×10^7 cells/ml

Sample count on filter substrate: $1.05 \pm 0.07 \times 10^8$ cells

Laboratory growth conditions: 30 °C, 180 rpm, 24 h

Culture medium: Lysogeny Broth (LB)

Sample photograph:

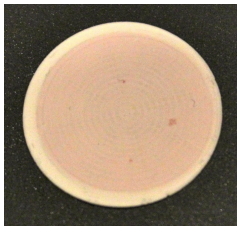

Sample micrograph:

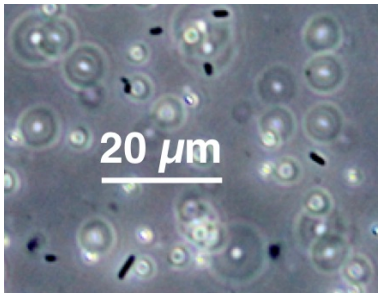

Sample reflectance spectrum:

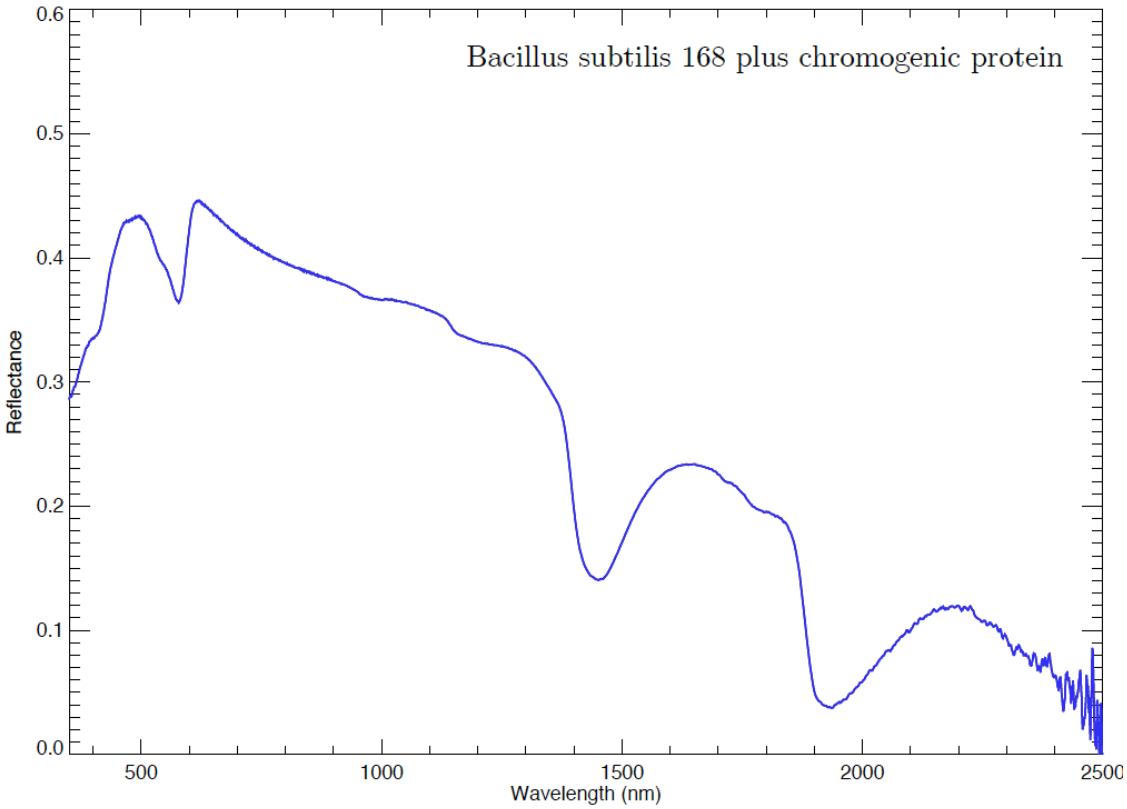

bacterium <AT06-05>_KM349936

Sample name: bacterium <AT06-05>

Accession number for 16S rRNA partial gene sequence: KM349936

Classification: Bacteria

Metabolism: Heterotrophic

Origin: Atacama desert, Chile

Isolation: Ivan P. Lima (NPP at NASA Ames, CA, USA)

Sample concentration: 2.32 × 10^7 cells/ml

Sample count on filter substrate: 6.96 ± 0.46 × 10^7 cells

Laboratory growth conditions: 30 °C, 180 rpm, 24 h

Culture medium: Lysogeny Broth (LB)

Sample photograph:

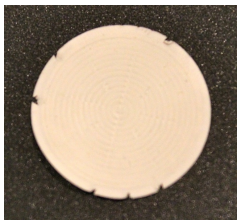

Sample micrograph:

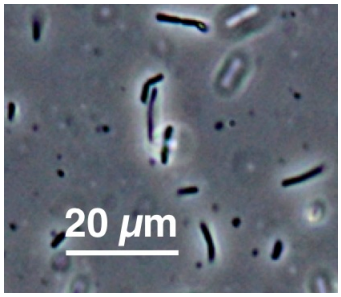

Sample reflectance spectrum:

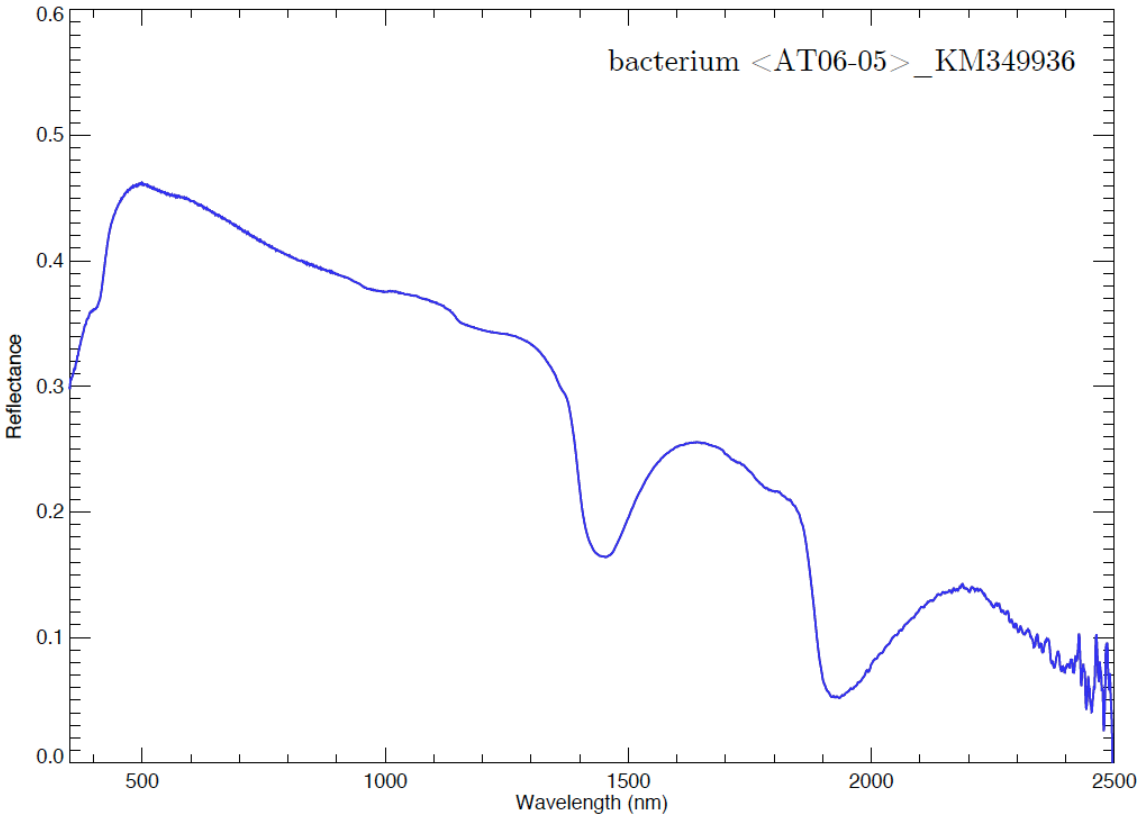

bacterium <AT09-02>_KM349950

Sample name: bacterium <AT09-02>

Accession number for 16S rRNA partial gene sequence: KM349950

Classification: Bacteria

Metabolism: Heterotrophic

Origin: Atacama desert, Chile

Isolation: Ivan P. Lima (NPP at NASA Ames, CA, USA)

Sample concentration: 6.39 $\times$ 10^7 cells/ml

Sample count on filter substrate: 1.92 $\pm$ 0.13 $\times$ 10^8 cells

Laboratory growth conditions: 30 °C, 180 rpm, 24 h

Culture medium: Lysogeny Broth (LB)

Sample photograph:

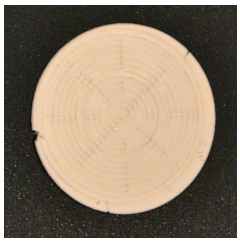

Sample micrograph:

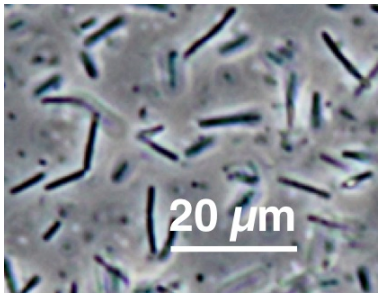

Sample reflectance spectrum:

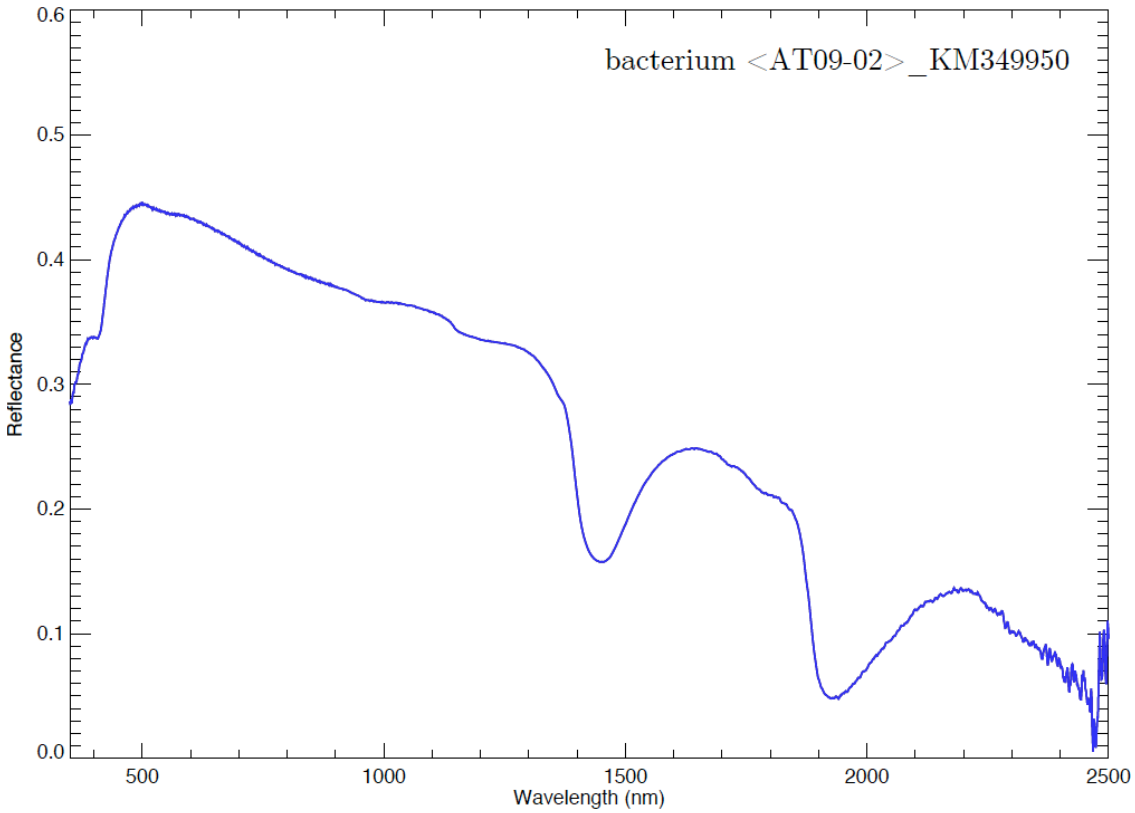

Basidiomycota_KM349879

Sample name: Basidiomycota

Accession number for 16S rRNA partial gene sequence: KM349879

Classification: Eukaryota; Fungi; Dikarya; Basidiomycota

Metabolism: Heterotrophic

Origin: Moffett Field, CA, USA

Isolation: Ivan P. Lima (NPP at NASA Ames, CA, USA)

Sample concentration: 3.18 $\times$ 10^6 cells/ml

Sample count on filter substrate: 9.53 $\pm$ 0.64 $\times$ 10^6 cells

Laboratory growth conditions: 30 °C, 180 rpm, 48 h

Culture medium: Lysogeny Broth (LB)

Sample photograph:

Sample micrograph:

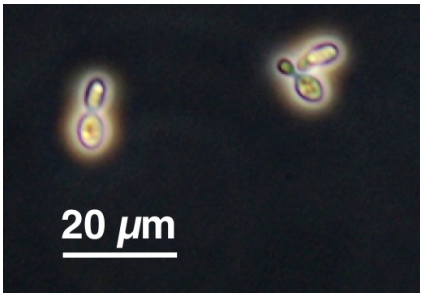

Sample reflectance spectrum:

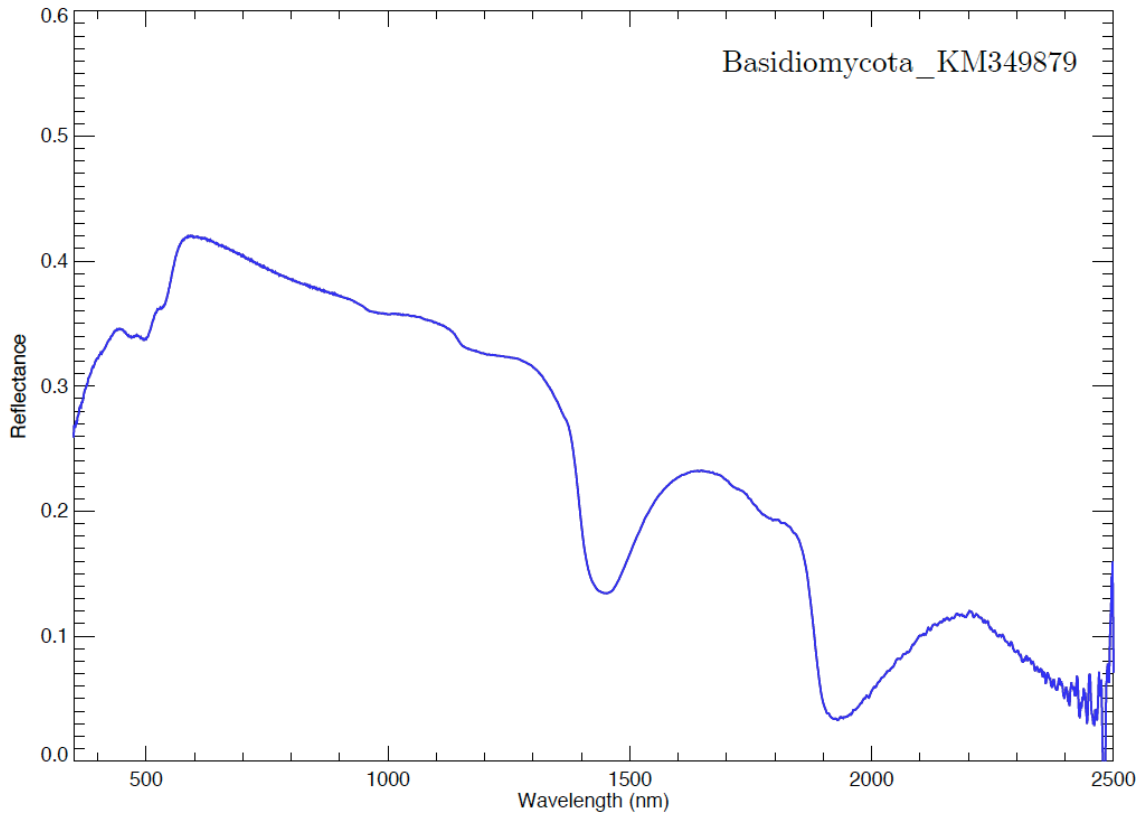

Betaproteobacteria_KM349948

Sample name: Betaproteobacteria

Accession number for 16S rRNA partial gene sequence: KM349948

Classification: Bacteria; Proteobacteria; Betaproteobacteria

Metabolism: Heterotrophic

Origin: Atacama desert, Chile

Isolation: Ivan P. Lima (NPP at NASA Ames, CA, USA)

Sample concentration: 3.86 $\times$ 10^8 cells/ml

Sample count on filter substrate: 1.16 $\pm$ 0.08 $\times$ 10^9 cells

Laboratory growth conditions: 30 °C, 180 rpm, 24 h

Culture medium: Reasoner's 2A (R2A)

Sample photograph:

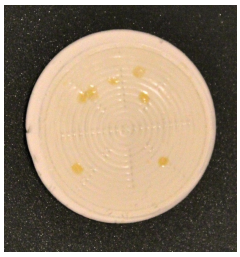

Sample micrograph:

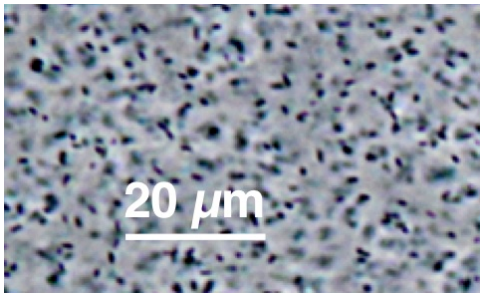

Sample reflectance spectrum:

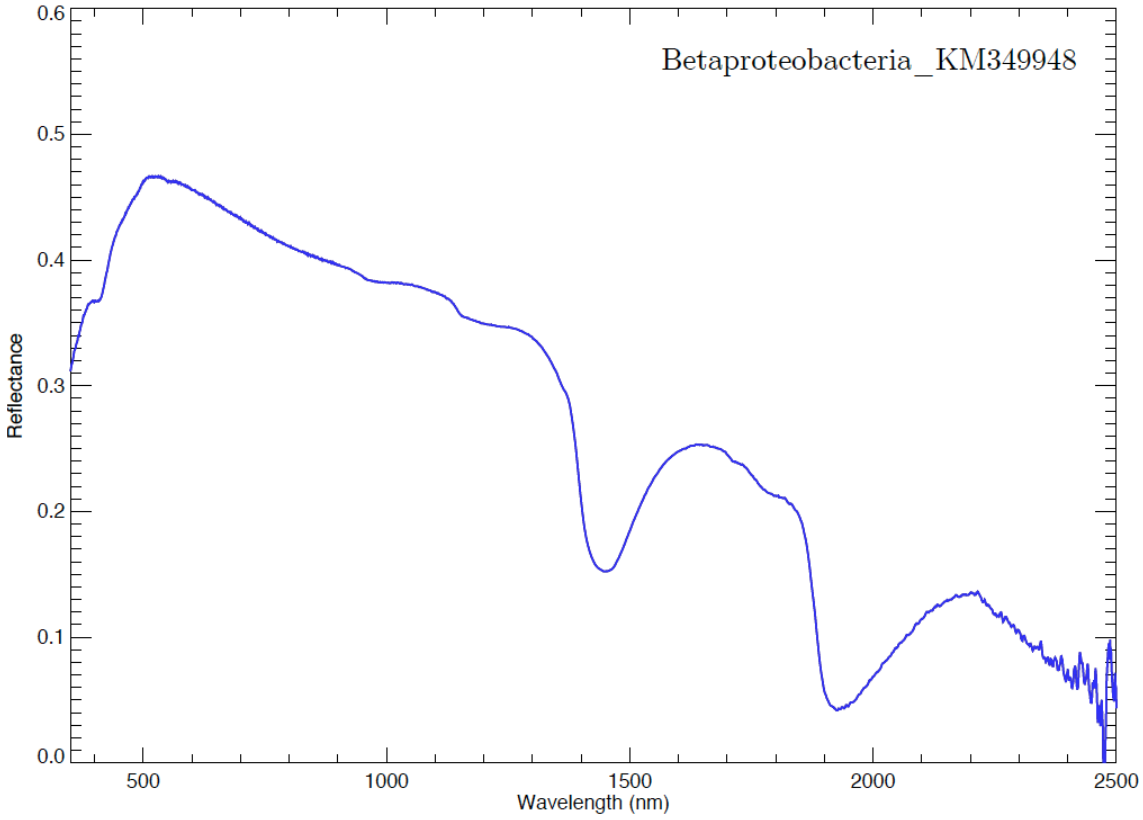

Calothrix parietina

Sample name: *Calothrix parietina*

Accession number for 16S rRNA partial gene sequence: Not available

Classification: Bacteria; Cyanobacteria; Cyanophyceae; Nostocales; Rivulariaceae; Calothrix

Metabolism: Autotrophic (oxygenic photosynthesis)

Origin: Swimming pool

Collection: UTEX (TX, USA)

Sample concentration: 3.04×10^6 cells/ml

Sample count on filter substrate: $3.04 \pm 0.30 \times 10^7$ cells

Laboratory growth conditions: 25 °C, up to 6 months

Culture medium: Modified Bold 3N medium

Sample photograph:

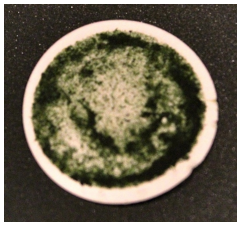

Sample micrograph:

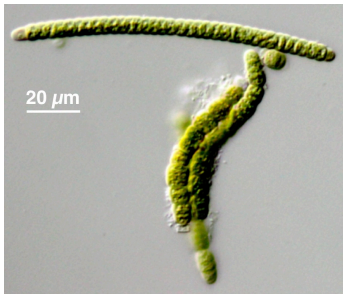

Sample reflectance spectrum:

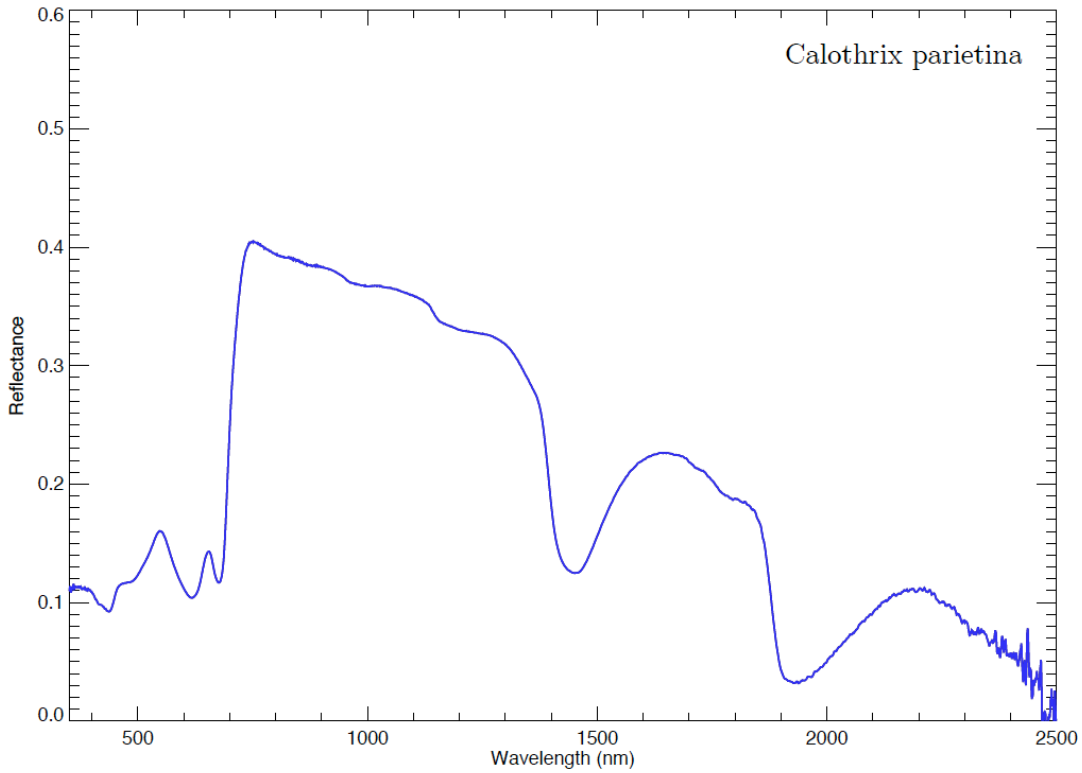

Cellulomonas sp._KM349959

Sample name: *Cellulomonas* sp.

Accession number for 16S rRNA partial gene sequence: KM349959

Classification: Bacteria; Actinobacteria; Actinobacteridae; Actinomycetales; Micrococcineae; Cellulomonadaceae; Cellulomonas

Metabolism: Heterotrophic

Origin: Atacama desert, Chile

Isolation: Ivan P. Lima (NPP at NASA Ames, CA, USA)

Sample concentration: 3.27 × 10^7 cells/ml

Sample count on filter substrate: 9.82 ± 0.65 × 10^7 cells

Laboratory growth conditions: 30 °C, 180 rpm, 24 h

Culture medium: Reasoner's 2A (R2A)

Sample photograph:

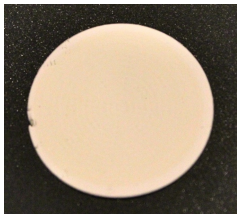

Sample micrograph:

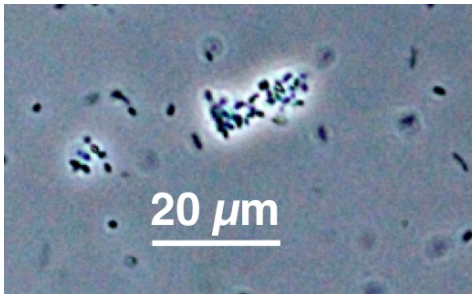

Sample reflectance spectrum:

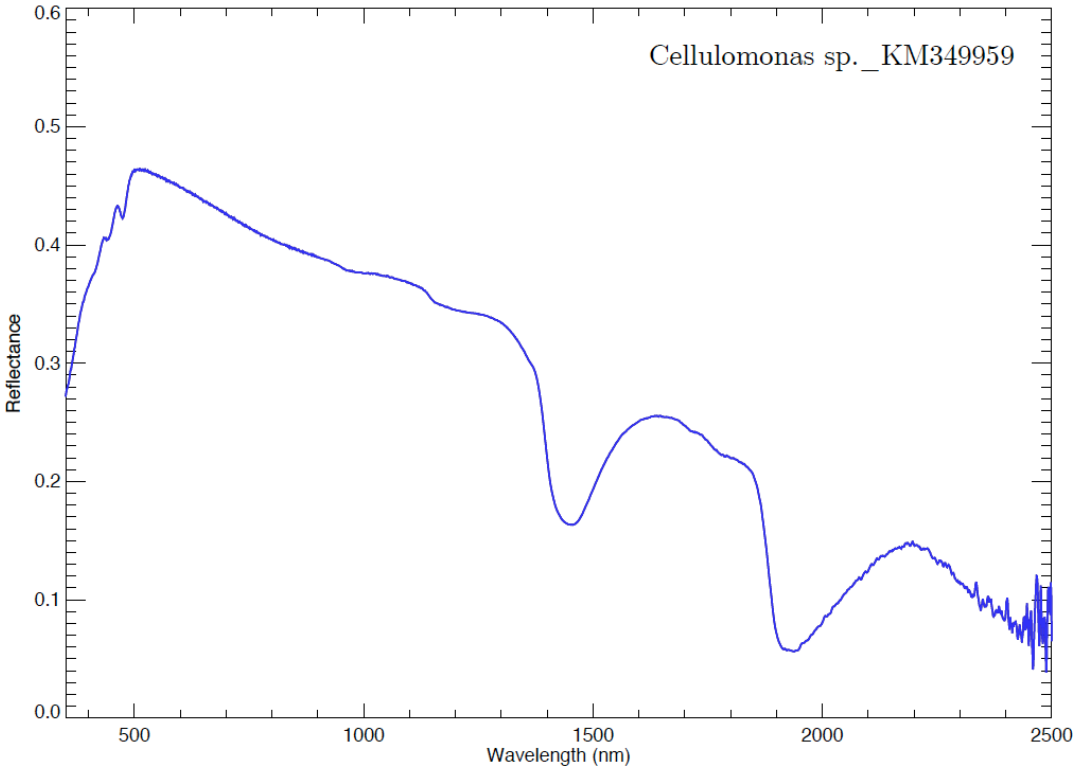

Chaetoceros gracilis

Sample name: *Chaetoceros gracilis*

Accession number for 16S rRNA partial gene sequence: Not available

Classification: Eukaryota; Ochrophyta; Bacillariophyceae; Chaetocerotales; Chaetocerotaceae; Chaetoceros

Metabolism: Autotrophic (oxygenic photosynthesis)

Origin: Marine sample, Hawaii, USA

Collection: UTEX (TX, USA)

Sample concentration: 8.11×10^5 cells/ml

Sample count on filter substrate: $8.11 \pm 0.81 \times 10^6$ cells

Laboratory growth conditions: 25 °C, up to 6 months

Culture medium: Erdschreiber's medium

Sample photograph:

Sample micrograph:

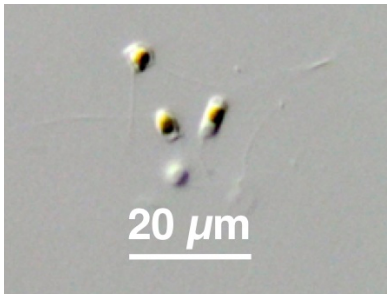

Sample reflectance spectrum:

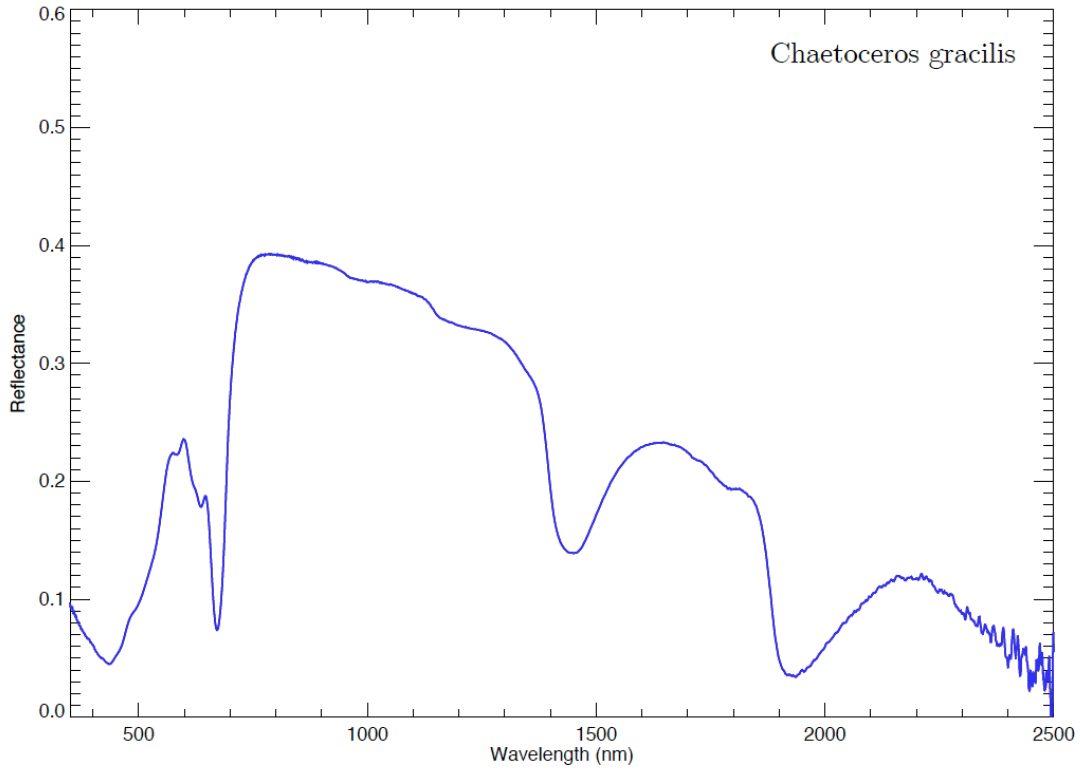

Chaetoceros sp.

Sample name: *Chaetoceros* sp.

Accession number for 16S rRNA partial gene sequence: Not available

Classification: Eukaryota; Ochrophyta; Bacillariophyceae; Chaetocerotales; Chaetocerotaceae; Chaetoceros

Metabolism: Autotrophic (oxygenic photosynthesis)

Origin: Monterey Bay, CA, USA

Collection: Kudela laboratory (UCSC, CA, USA)

Sample concentration: 4.06×10^5 cells/ml

Sample count on filter substrate: $4.06 \pm 0.41 \times 10^6$ cells

Laboratory growth conditions: 25 °C, up to 6 months

Culture medium: Enriched Seawater medium (f/2)

Sample photograph:

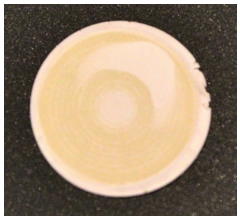

Sample micrograph:

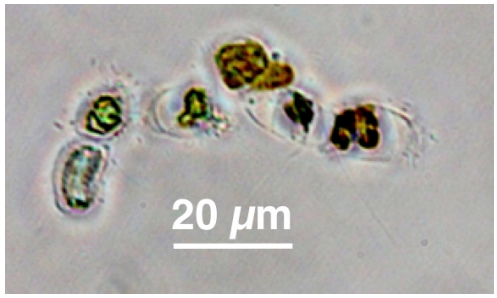

Sample reflectance spectrum:

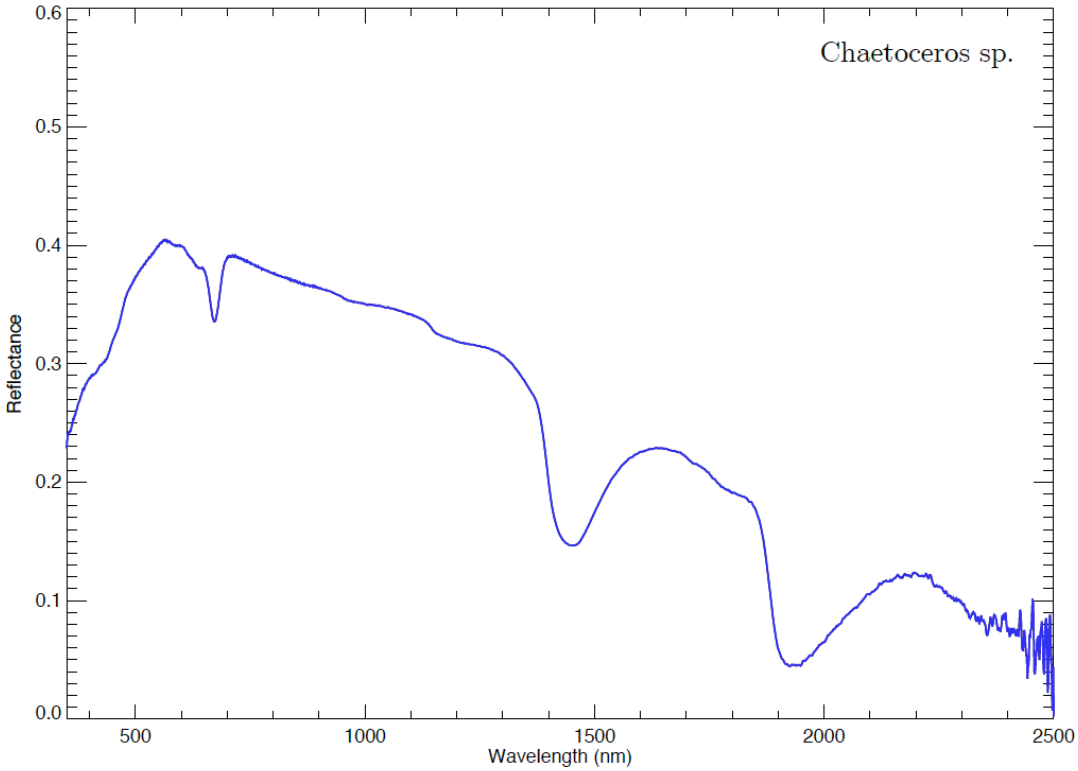

Chlorella protothecoides

Sample name: *Chlorella protothecoides*

Accession number for 16S rRNA partial gene sequence: Not available

Classification: Eukaryota; Chlorophyta; Trebouxiophyceae; Chlorellales; Chlorellaceae; Chlorella

Metabolism: Autotrophic (oxygenic photosynthesis)

Origin: Sap of wounded Populus alb

Collection: UTEX (TX, USA)

Sample concentration: 3.60×10^7 cells/ml

Sample count on filter substrate: $3.60 \pm 0.36 \times 10^8$ cells

Laboratory growth conditions: 25 °C, up to 6 months

Culture medium: Proteose medium

Sample photograph:

Sample micrograph:

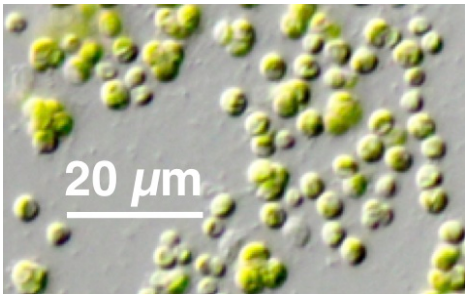

Sample reflectance spectrum:

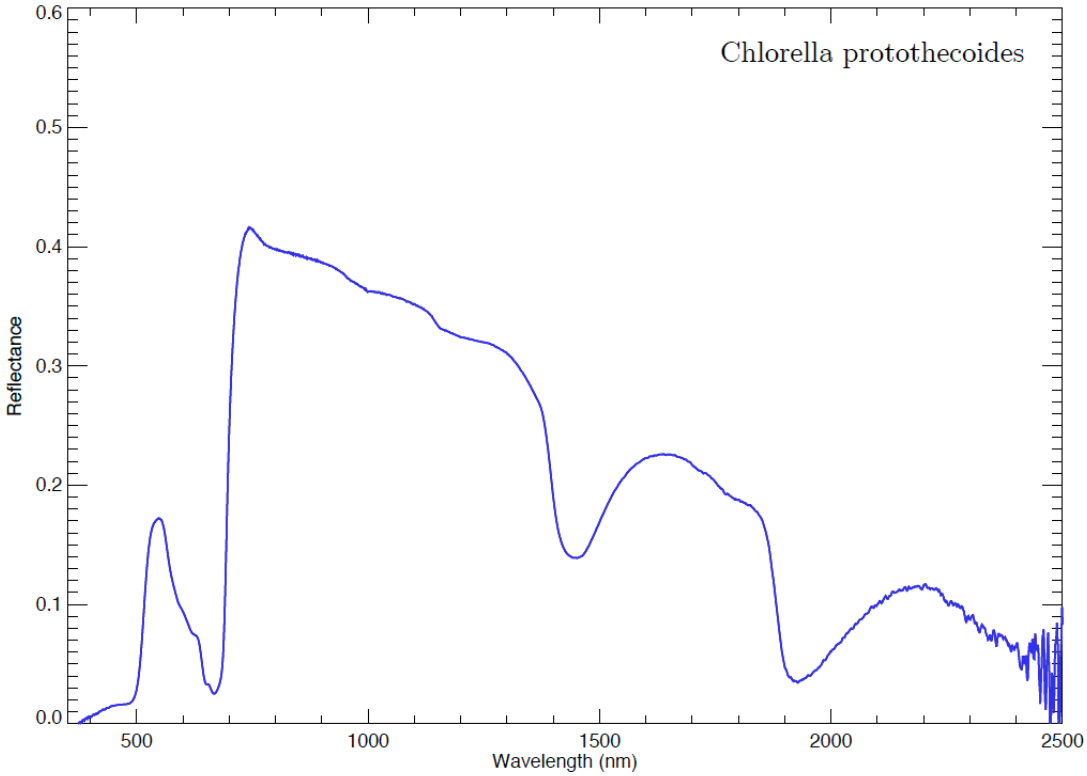

Chlorellaceae_KM349944

Sample name: Chlorellaceae

Accession number for 16S rRNA partial gene sequence: KM349944

Classification: Eukaryota; Viridiplantae; Chlorophyta; Trebouxiophyceae; Chlorellales; Chlorellaceae; unclassified Chlorellaceae

Metabolism: Autotrophic (oxygenic photosynthesis)

Origin: Atacama desert, Chile

Isolation: Ivan P. Lima (NPP at NASA Ames, CA, USA)

Sample concentration: 8.11 $\times$ 10^5 cells/ml

Sample count on filter substrate: 2.43 $\pm$ 0.16 $\times$ 10^6 cells

Laboratory growth conditions: 30 °C, 180 rpm, 96 h

Culture medium: Reasoner's 2A (R2A)

Sample photograph:

Sample micrograph:

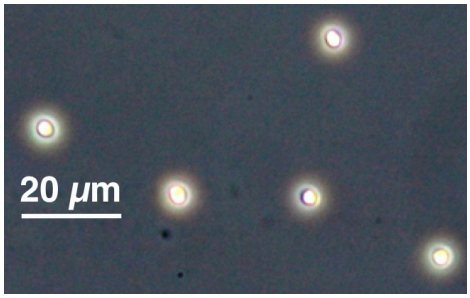

Sample reflectance spectrum:

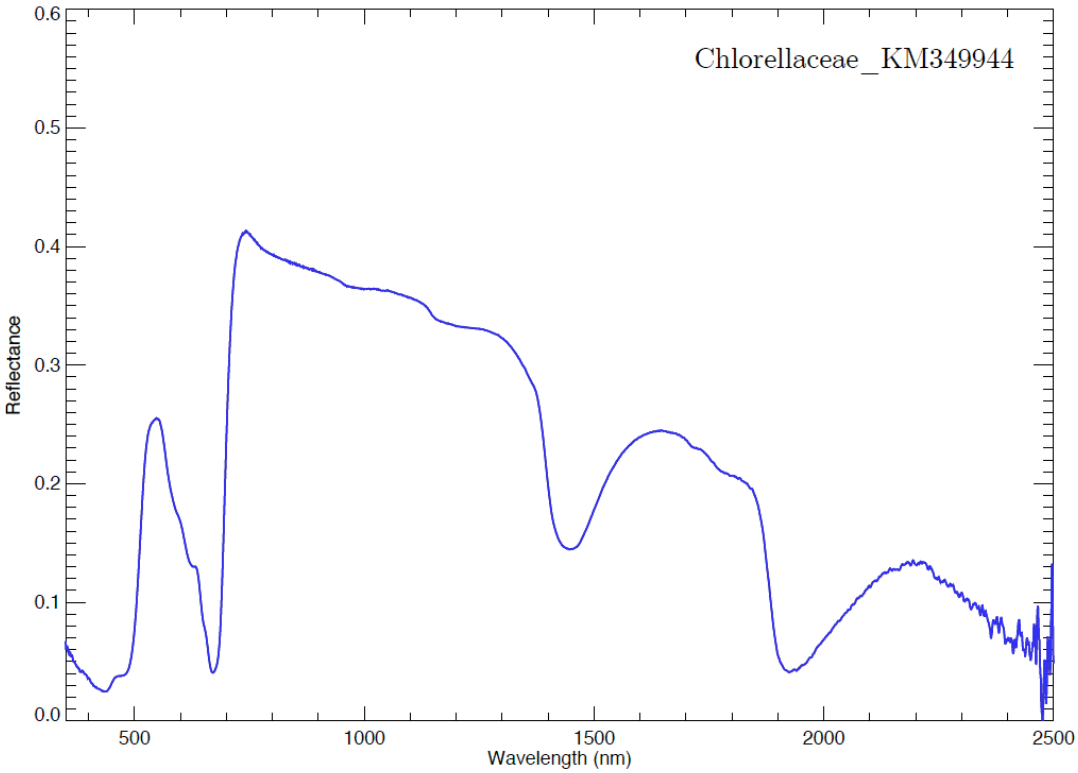

Chroococcidiopsis sp.

Sample name: *Chroococcidiopsis* sp.

Accession number for 16S rRNA partial gene sequence: Not available

Classification: Bacteria; Cyanobacteria; Cyanophyceae; Chroococcales; Xenococcaceae; Chroococcidiopsis

Metabolism: Autotrophic (oxygenic photosynthesis)

Origin: Thermal and mineral spring water

Collection: Rothschild laboratory (NASA Ames, CA, USA)

Sample concentration: 6.62×10^6 cells/ml

Sample count on filter substrate: $1.99 \pm 0.13 \times 10^7$ cells

Laboratory growth conditions: 25 °C, up to 6 months

Culture medium: Blue-Green medium (BG-11)

Sample photograph:

Sample micrograph:

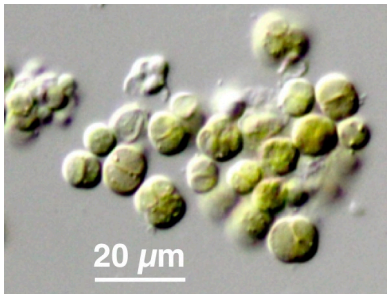

Sample reflectance spectrum:

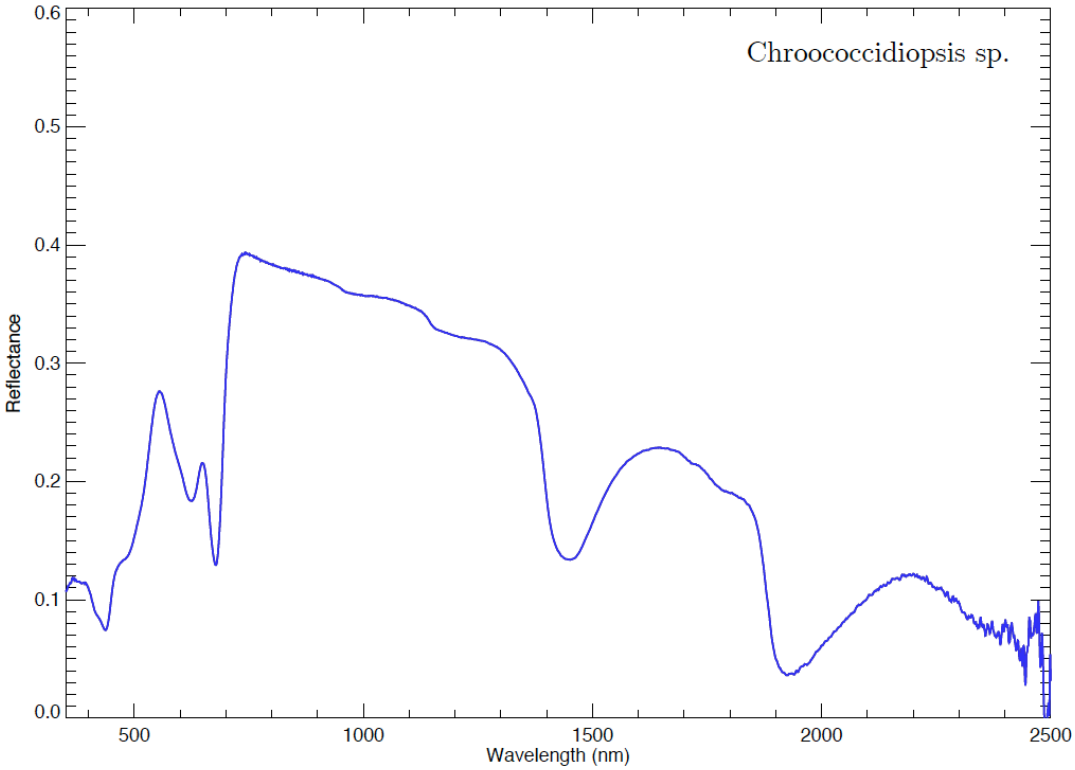

Cryptomonas ovata

Sample name: *Cryptomonas ovata*

Accession number for 16S rRNA partial gene sequence: Not available

Classification: Eukaryota; Cryptophyta; Cryptophyceae; Cryptomonadales; Cryptomonadaceae; Cryptomonas

Metabolism: Autotrophic (oxygenic photosynthesis)

Origin: Cowdrey Lake, near Crowdrey, Jackson Co., CO, USA

Collection: UTEX (TX, USA)

Sample concentration: 3.99×10^6 cells/ml

Sample count on filter substrate: $3.99 \pm 0.40 \times 10^7$ cells

Laboratory growth conditions: 25 °C, up to 6 months

Culture medium: Bold 1NV medium

Sample photograph:

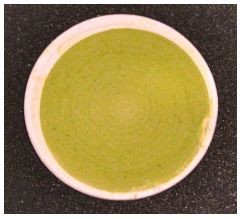

Sample micrograph:

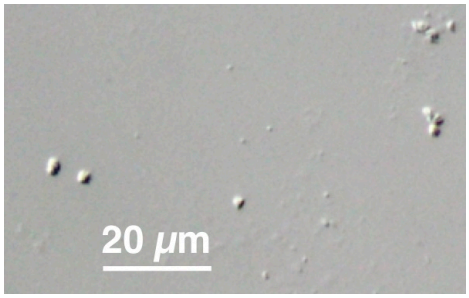

Sample reflectance spectrum:

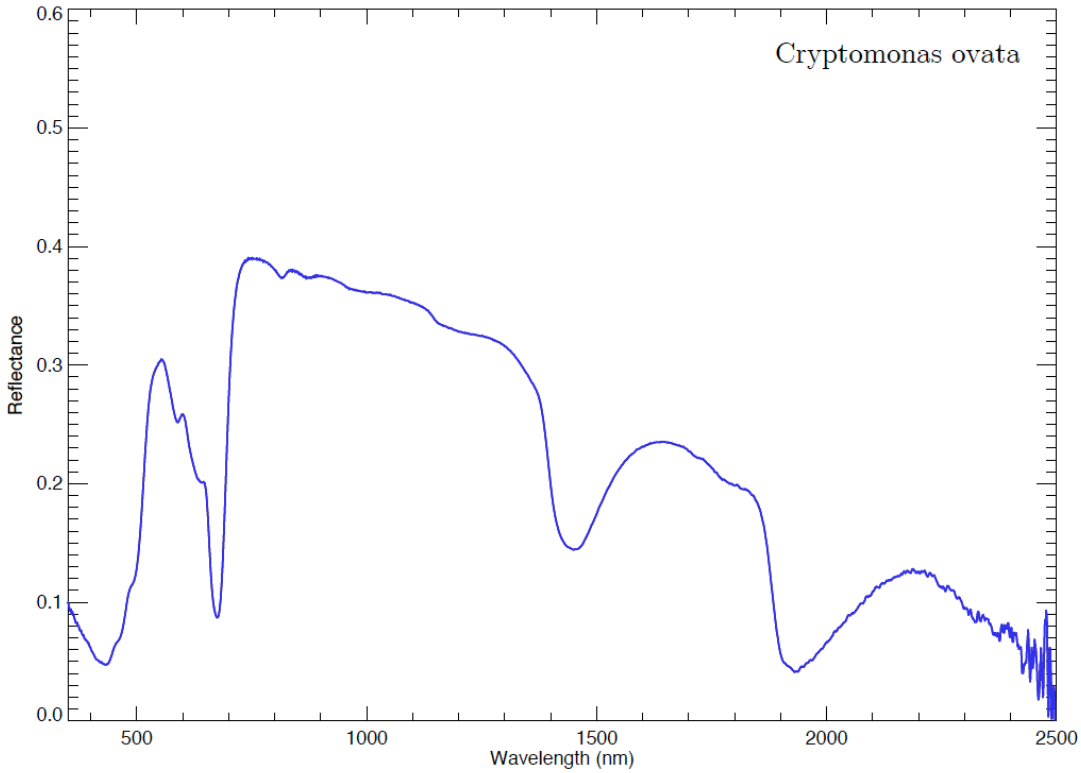

Cyanidium caldarium

Sample name: *Cyanidium caldarium*

Accession number for 16S rRNA partial gene sequence: Not available

Classification: Eukaryota; Rhodophyta; Cyanidiophyceae; Cyanidiales; Cyanidiaceae; Cyanidium

Metabolism: Autotrophic (oxygenic photosynthesis)

Origin: Freshwater, Acidic hot stream

Collection: UTEX (TX, USA)

Sample concentration: 1.96×10^6 cells/ml

Sample count on filter substrate: $1.96 \pm 0.20 \times 10^7$ cells

Laboratory growth conditions: 25 °C, up to 6 months

Culture medium: Cyanidium medium

Sample photograph:

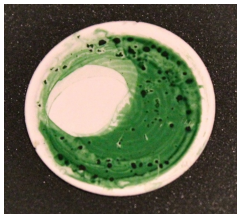

Sample micrograph:

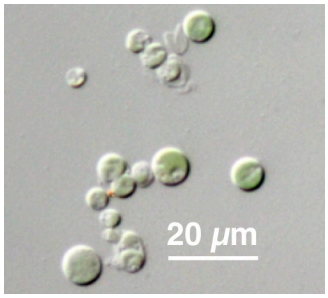

Sample reflectance spectrum:

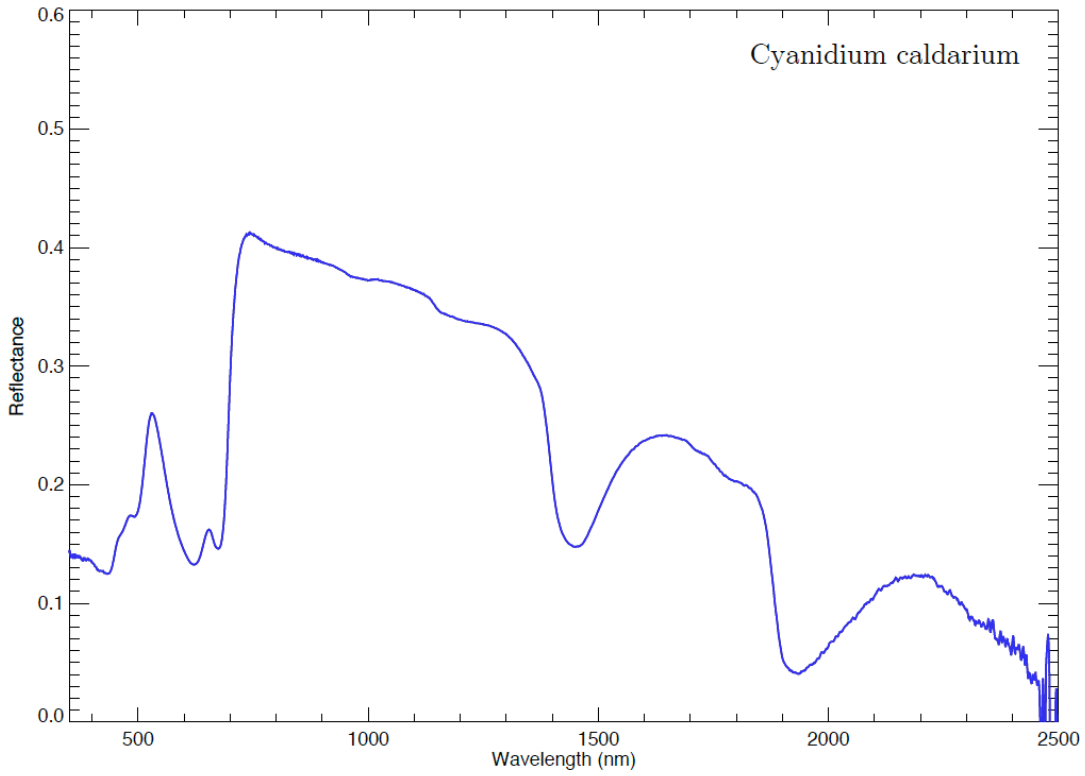

Cyanophora biloba

Sample name: *Cyanophora biloba*

Accession number for 16S rRNA partial gene sequence: Not available

Classification: Eukaryota; Glaucophyta; Glaucophyceae; Glaucocystales; Glaucocystaceae; Cyanophora

Metabolism: Autotrophic (oxygenic photosynthesis)

Origin: Ephemeral alpine pond; Roosevelt National Forest, CO, USA

Collection: UTEX (TX, USA)

Sample concentration: 6.76×10^4 cells/ml

Sample count on filter substrate: $6.76 \pm 0.68 \times 10^5$ cells

Laboratory growth conditions: 25 °C, up to 6 months

Culture medium: Bold 1NV medium

Sample photograph:

Sample micrograph:

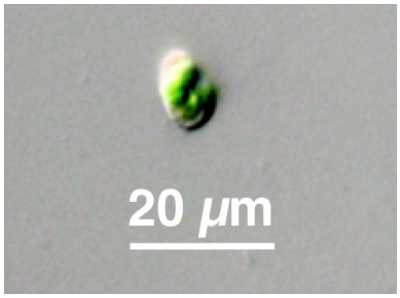

Sample reflectance spectrum:

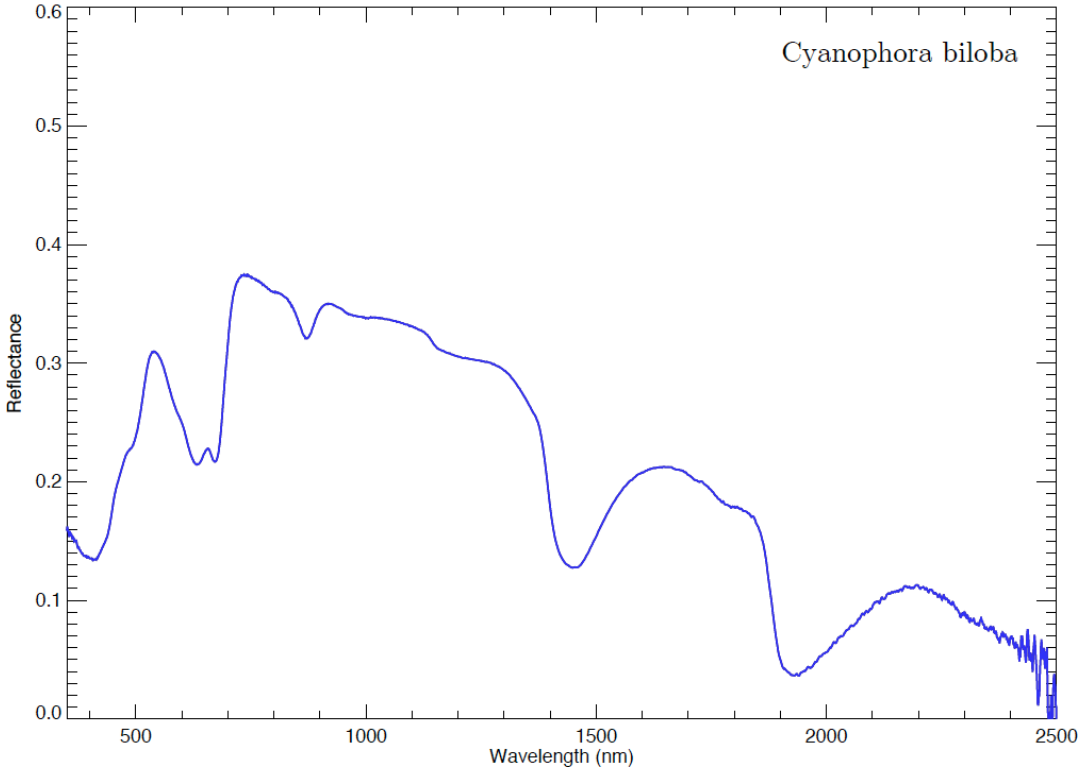

Cylindrotheca fusiformis

Sample name: *Cylindrotheca fusiformis*

Accession number for 16S rRNA partial gene sequence: Not available

Classification: Eukaryota; Ochrophyta; Bacillariophyceae; Bacillariales; Bacillariaceae; Cylindrotheca

Metabolism: Autotrophic (oxygenic photosynthesis)

Origin: Marine sample, Galveston, TX, USA

Collection: UTEX (TX, USA)

Sample concentration: 6.76×10^5 cells/ml

Sample count on filter substrate: $6.76 \pm 0.68 \times 10^6$ cells

Laboratory growth conditions: 25 °C, up to 6 months

Culture medium: Enriched Seawater medium (f/2)

Sample photograph:

Sample micrograph:

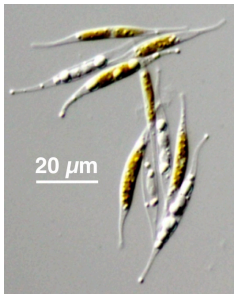

Sample reflectance spectrum:

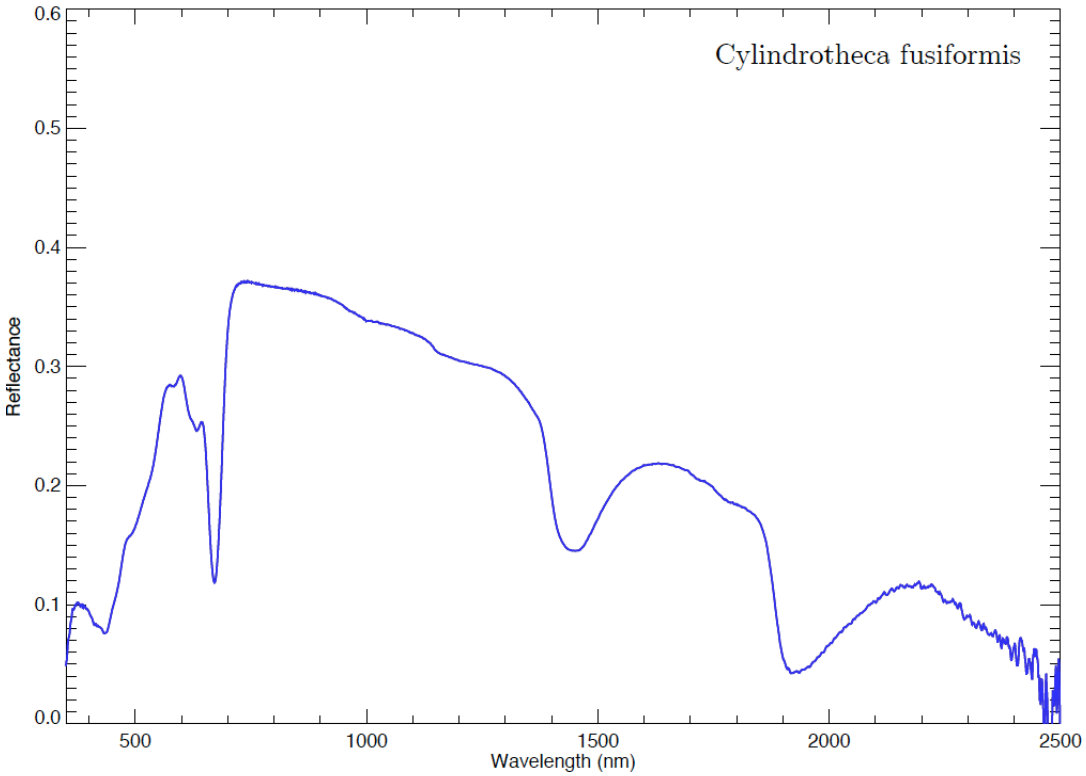

Cytophagaceae_KM349914

Sample name: Cytophagaceae

Accession number for 16S rRNA partial gene sequence: KM349914

Classification: Bacteria; Bacteroidetes; Cytophagia; Cytophagales; Cytophagaceae

Metabolism: Heterotrophic

Origin: Sonoran desert, AZ, USA

Isolation: Ivan P. Lima (NPP at NASA Ames, CA, USA)

Sample concentration: 1.22 $\times$ 10^7 cells/ml

Sample count on filter substrate: 3.65 $\pm$ 0.24 $\times$ 10^7 cells

Laboratory growth conditions: 30 °C, 180 rpm, 24 h

Culture medium: Marine Broth (MB)

Sample photograph:

Sample micrograph:

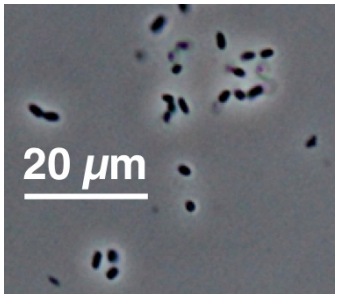

Sample reflectance spectrum:

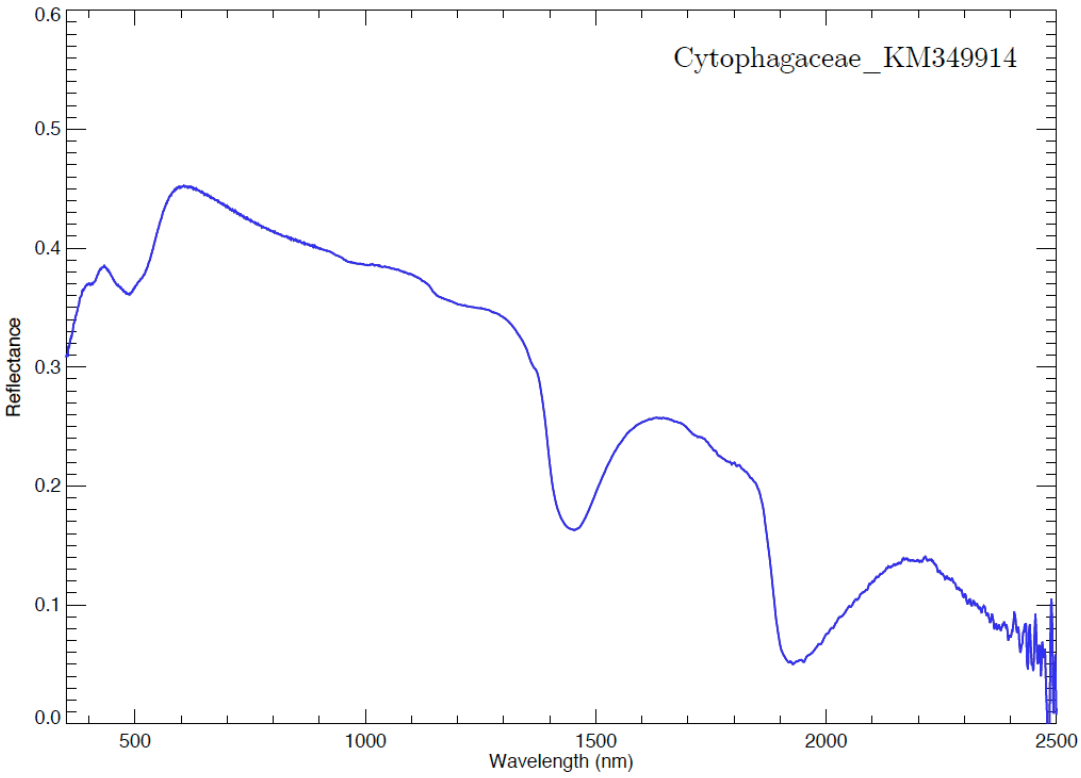

Deinococcus radiodurans

Sample name: *Deinococcus radiodurans*

Accession number for 16S rRNA partial gene sequence: Not available

Classification: Bacteria; Deinococcus-Thermus; Deinococci; Deinococcales; Deinococcaaceae; Deinococcus

Metabolism: Heterotrophic

Origin: Naturally found in a wide range of habitats inc. meat, clothing, deserts

Collection: Rothschild laboratory (NASA Ames, CA, USA)

Sample concentration: 3.16×10^7 cells/ml

Sample count on filter substrate: $9.47 \pm 0.63 \times 10^7$ cells

Laboratory growth conditions: 30 °C, 180 rpm, 48 h

Culture medium: Tryptone Glucose Yeast (TGY) medium

Sample photograph:

Sample micrograph:

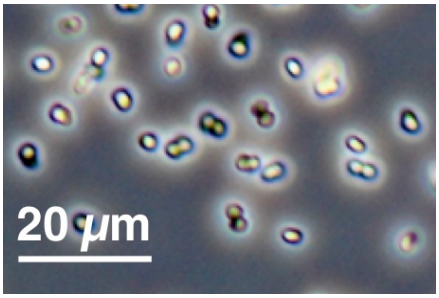

Sample reflectance spectrum:

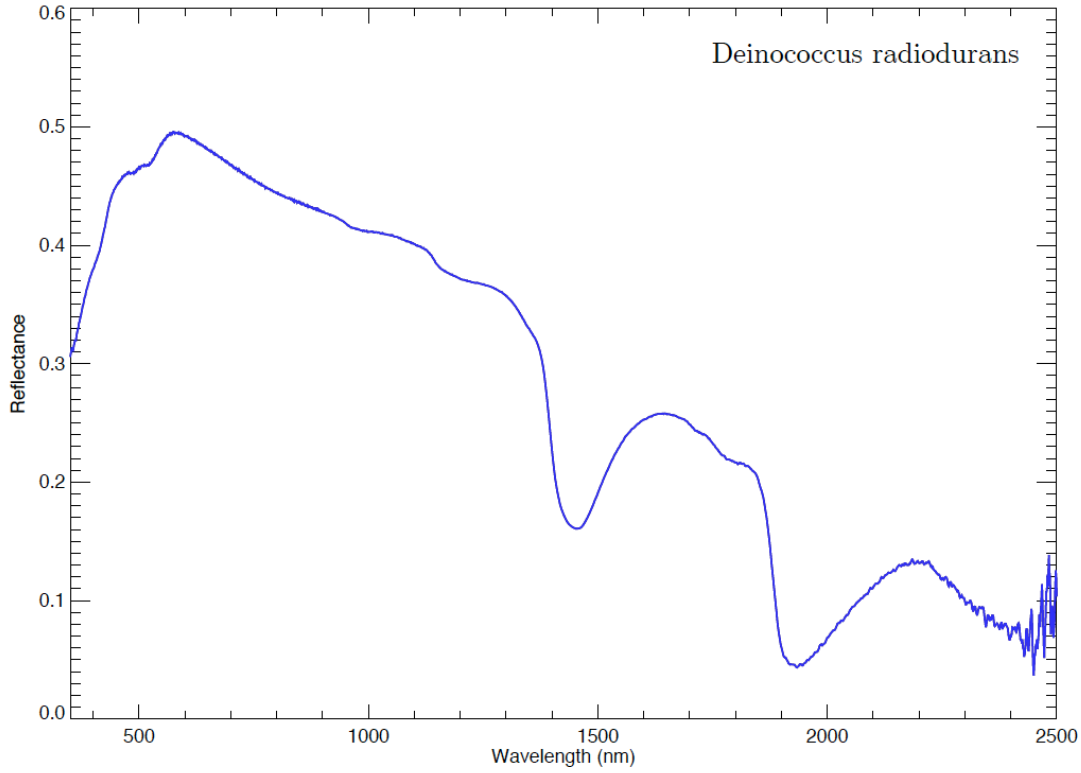

Dermocarpa violacea

Sample name: *Dermocarpa violacea*

Accession number for 16S rRNA partial gene sequence: Not available

Classification: Bacteria; Cyanobacteria; Cyanophyceae; Chroococcales; Dermocarpellaceae; Dermocarpa

Metabolism: Autotrophic (oxygenic photosynthesis)

Origin: Aquarium outflow, La Jolla, CA, USA

Collection: UTEX (TX, USA)

Sample concentration: 1.69×10^6 cells/ml

Sample count on filter substrate: $1.69 \pm 0.17 \times 10^7$ cells

Laboratory growth conditions: 25 °C, up to 6 months

Culture medium: Erdschreiber's medium

Sample photograph:

Sample micrograph:

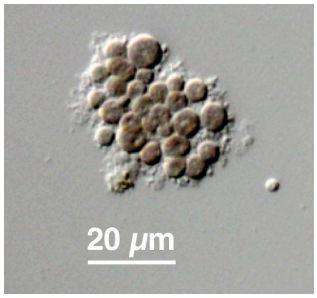

Sample reflectance spectrum:

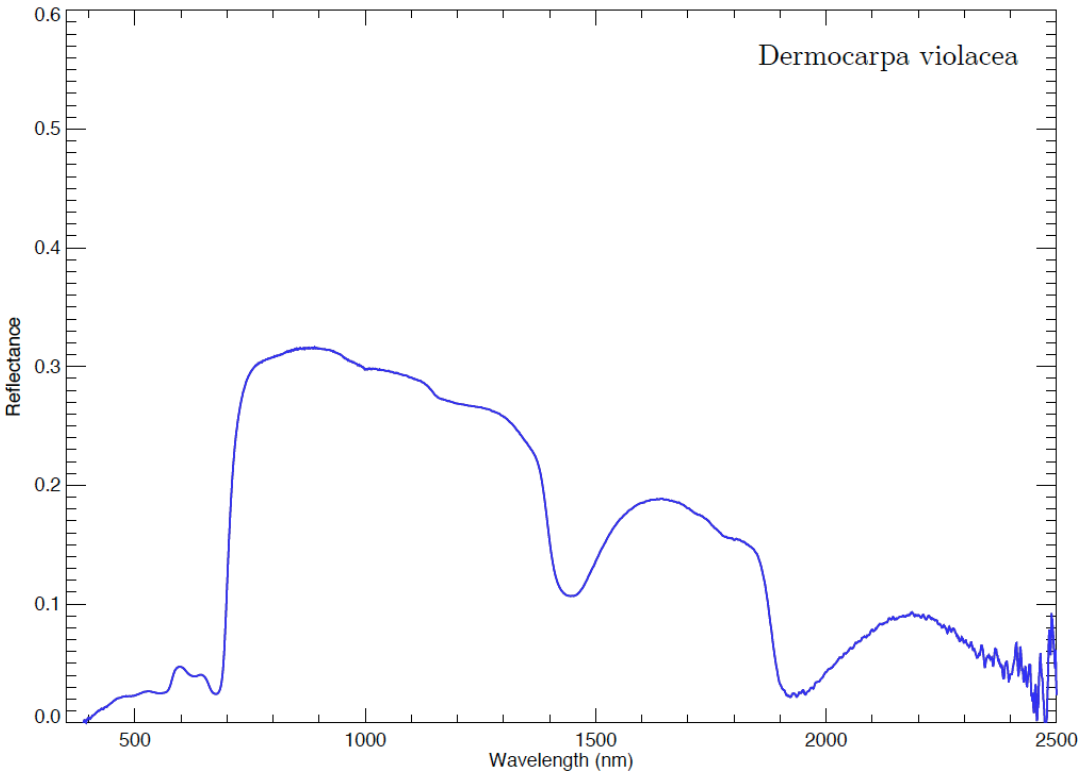

Dunaliella salina

Sample name: *Dunaliella salina*

Accession number for 16S rRNA partial gene sequence: Not available

Classification: Eukaryota; Chlorophyta; Chlorophyceae; Chlamydomonadales; Dunaliellaceae; Dunaliella

Metabolism: Autotrophic (oxygenic photosynthesis)

Origin: Salt lake, Russia

Collection: UTEX (TX, USA)

Sample concentration: 4.73×10^5 cells/ml

Sample count on filter substrate: $4.73 \pm 0.47 \times 10^6$ cells

Laboratory growth conditions: 25 °C, up to 6 months

Culture medium: 2X Erdschreiber's medium

Sample photograph:

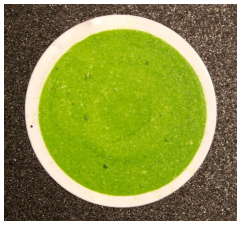

Sample micrograph:

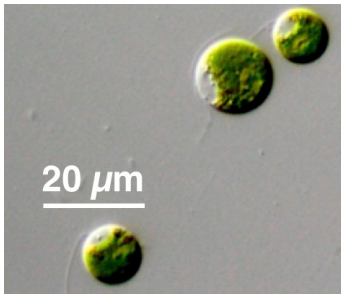

Sample reflectance spectrum:

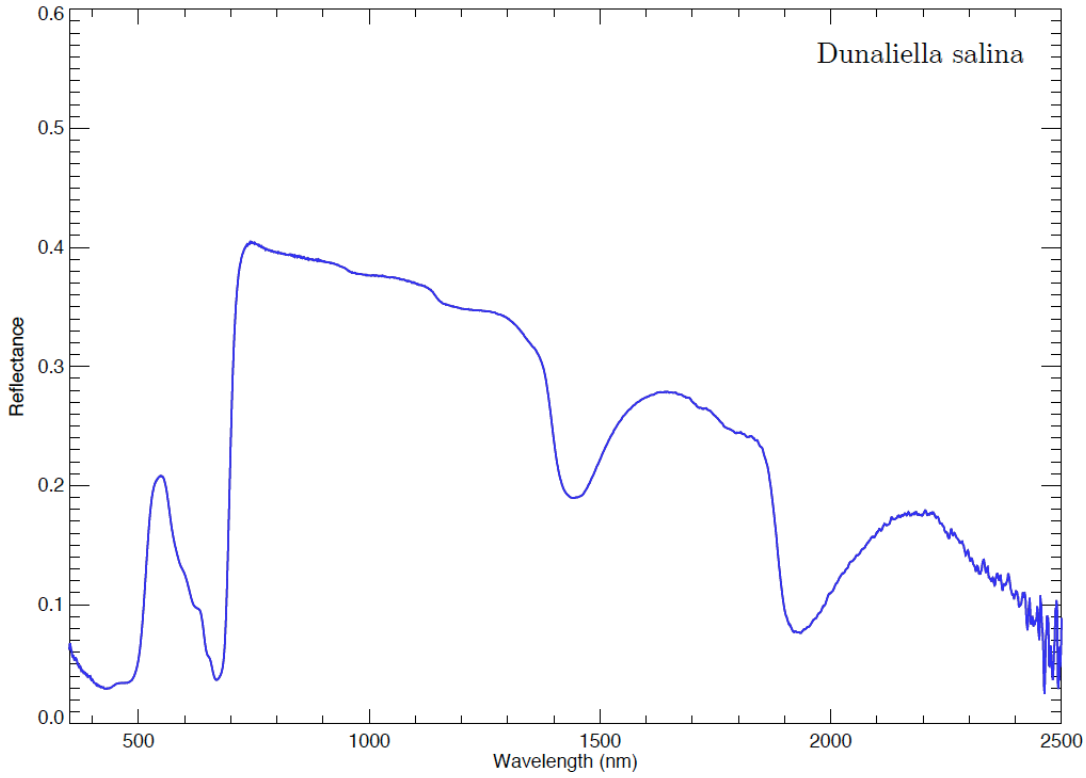

Dunaliella sp.

Sample name: *Dunaliella* sp.

Accession number for 16S rRNA partial gene sequence: Not available

Classification: Eukaryota; Chlorophyta; Chlorophyceae; Chlamydomonadales; Dunaliellaceae; Dunaliella

Metabolism: Autotrophic (oxygenic photosynthesis)

Origin: Solar saltworks, Yucatan Peninsula

Collection: Kudela laboratory (UCSC, CA, USA)

Sample concentration: 6.76×10^4 cells/ml

Sample count on filter substrate: $6.76 \pm 0.68 \times 10^5$ cells

Laboratory growth conditions: 25 °C, up to 6 months

Culture medium: Enriched Seawater medium (f/2)

Sample photograph:

Sample micrograph:

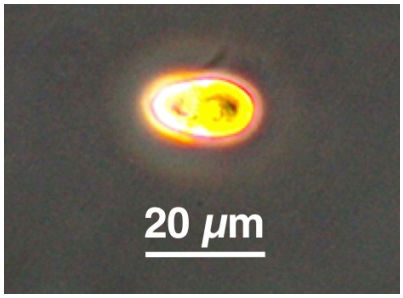

Sample reflectance spectrum:

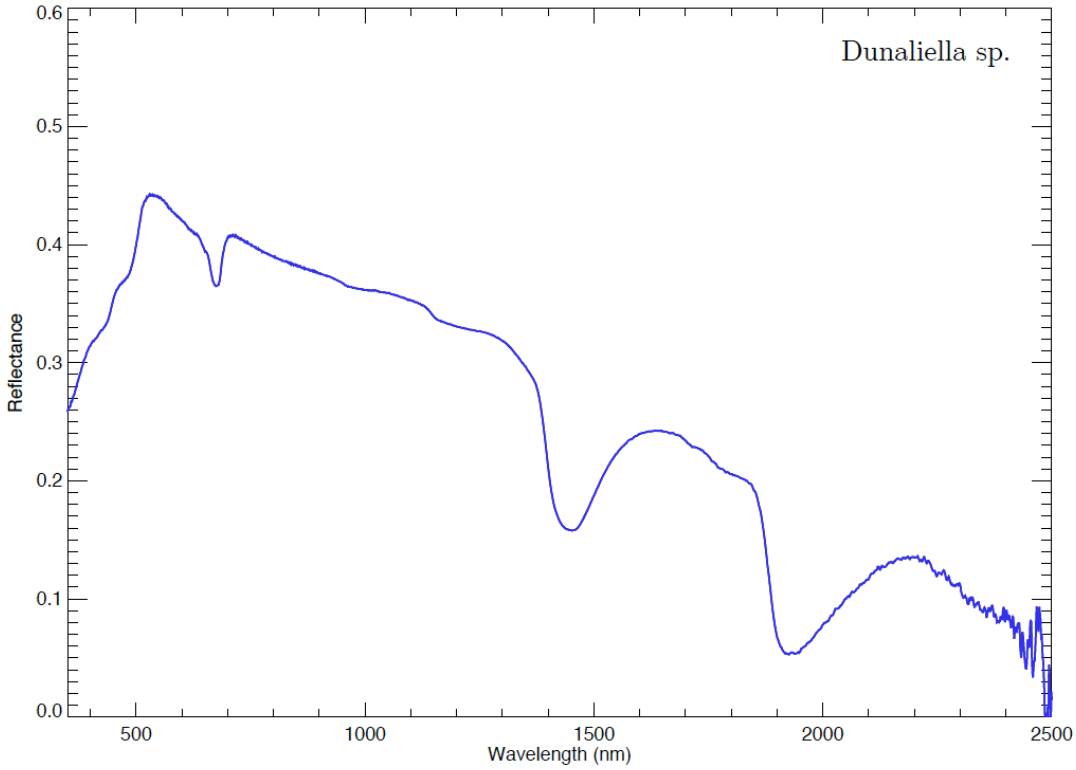

Ectocarpus siliculosus

Sample name: *Ectocarpus siliculosus*

Accession number for 16S rRNA partial gene sequence: Not available

Classification: Eukaryota; Ochrophyta; Phaeophyceae; Ectocarpales; Ectocarpaceae; Ectocarpus

Metabolism: Autotrophic (oxygenic photosynthesis)

Origin: Marine sample, Naples, Italy

Collection: UTEX (TX, USA)

Sample concentration: 2.03×10^5 cells/ml

Sample count on filter substrate: $2.03 \pm 0.20 \times 10^6$ cells

Laboratory growth conditions: 25 °C, up to 6 months

Culture medium: Erdschreiber's medium

Sample photograph:

Sample micrograph:

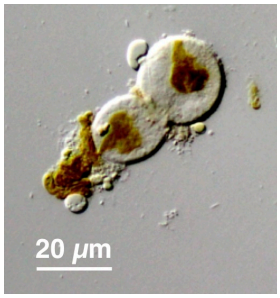

Sample reflectance spectrum:

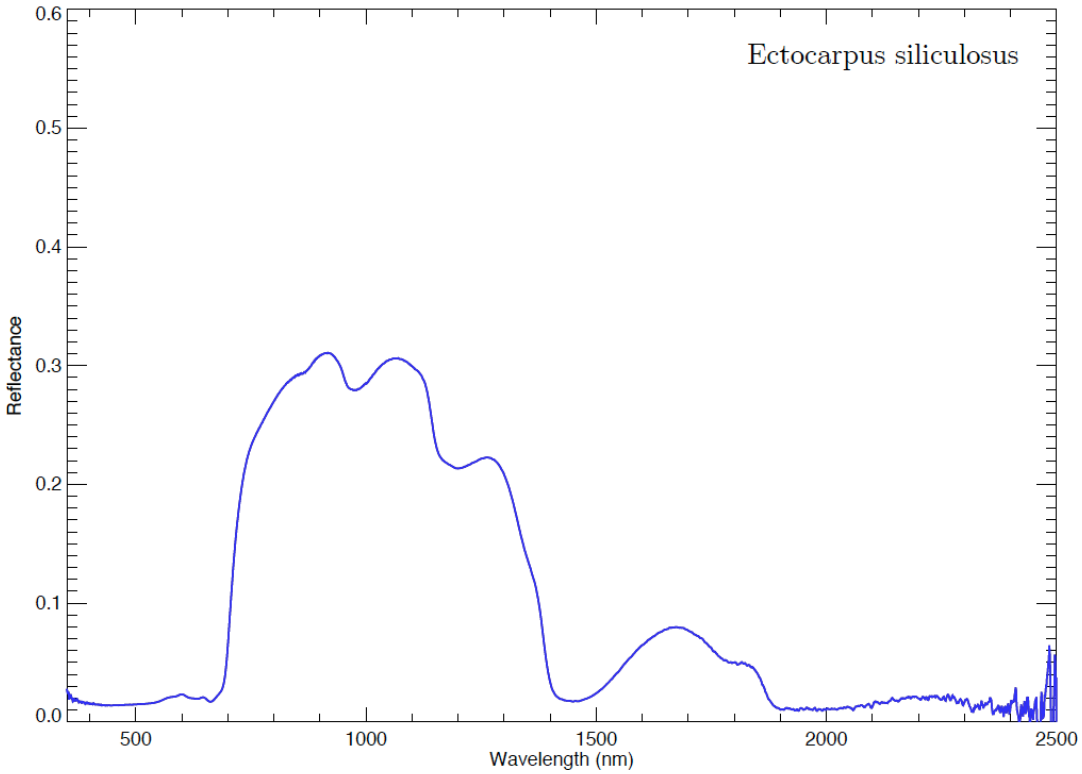

Ectothiorhodospira sp. str. BSL-9

Sample name: *Ectothiorhodospira* sp. str. BSL-9

Accession number for 16S rRNA partial gene sequence: Not available

Classification: Bacteria; Proteobacteria; Gamma Proteobacteria; Chromatiales; Ectothiorhodospiraceae; Ectothiorhodospira

Metabolism: Autotrophic (sulfur-based anoxygenic photosynthesis)

Origin: Big Soda Lake, NV, USA

Collection: Saltikov laboratory (UC Santa Cruz, CA, USA)

Sample concentration: 2.85×10^7 cells/ml

Sample count on filter substrate: $8.56 \pm 0.57 \times 10^7$ cells

Laboratory growth conditions: Anaerobically at 30 °C

Culture medium: Big Soda Minimal medium

Sample photograph:

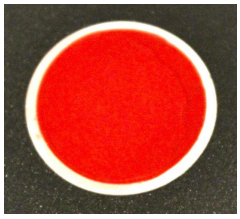

Sample micrograph:

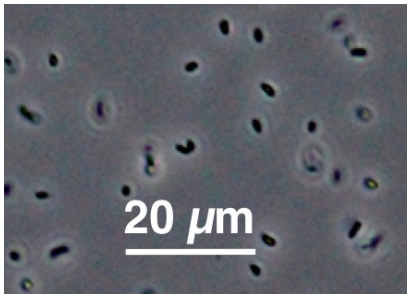

Sample reflectance spectrum:

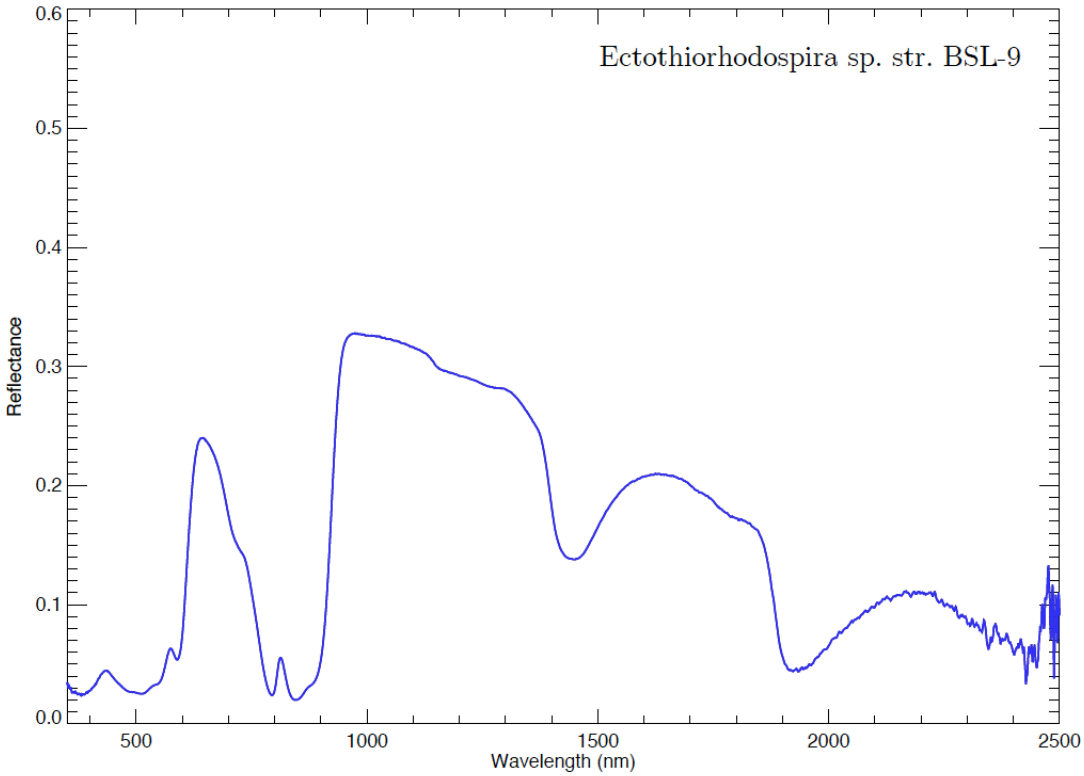

Escherichia coli

Sample name: *Escherichia coli*

Accession number for 16S rRNA partial gene sequence: Not available

Classification: Bacteria; Proteobacteria; Gamma Proteobacteria; Enterobacteriales; Enterobacteriaceae; Escherichia

Metabolism: Heterotrophic

Origin: Laboratory strain. Found in sand, soil,and sediments

Collection: Rothschild laboratory (NASA Ames, CA, USA)

Sample concentration: 8.60×10^7 cells/ml

Sample count on filter substrate: $2.58 \pm 0.17 \times 10^8$ cells

Laboratory growth conditions: 37 °C, 180 rpm, 16 h

Culture medium: Lysogeny Broth (LB)

Sample photograph:

Sample micrograph:

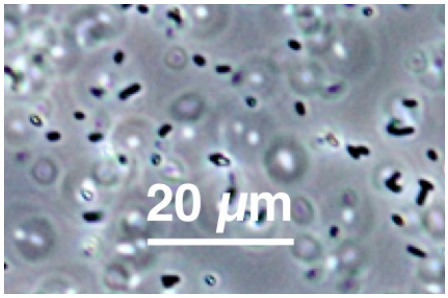

Sample reflectance spectrum:

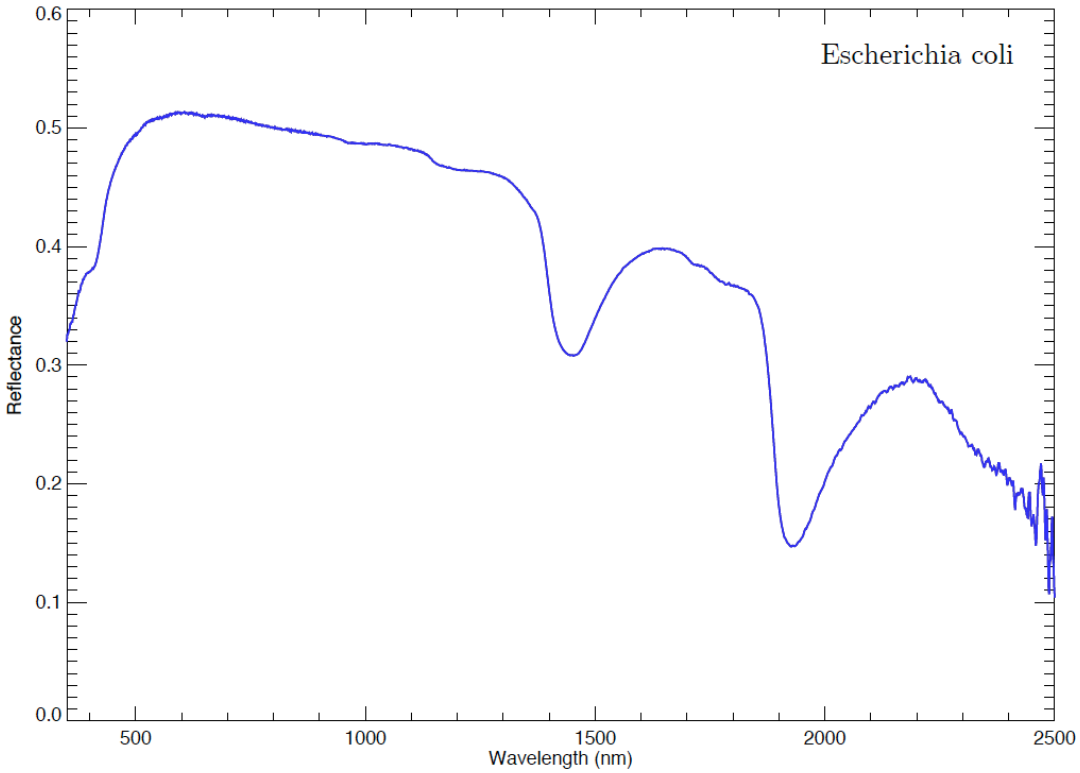

Euglena gracilis var. *saccharophila*

Sample name: *Euglena gracilis* var. *saccharophila*

Accession number for 16S rRNA partial gene sequence: Not available

Classification: Eukaryota; Euglenozoa; Euglenophyceae; Euglenales; Euglenaceae; Euglena

Metabolism: Autotrophic (oxygenic photosynthesis)

Origin: Pond water

Collection: UTEX (TX, USA)

Sample concentration: 7.77×10^6 cells/ml

Sample count on filter substrate: $7.77 \pm 0.78 \times 10^7$ cells

Laboratory growth conditions: 25 °C, up to 6 months

Culture medium: Euglena medium

Sample photograph:

Sample micrograph:

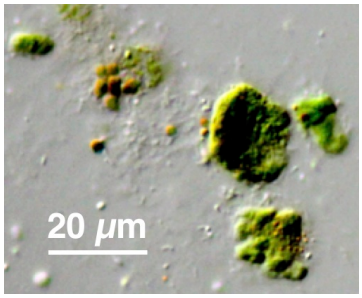

Sample reflectance spectrum:

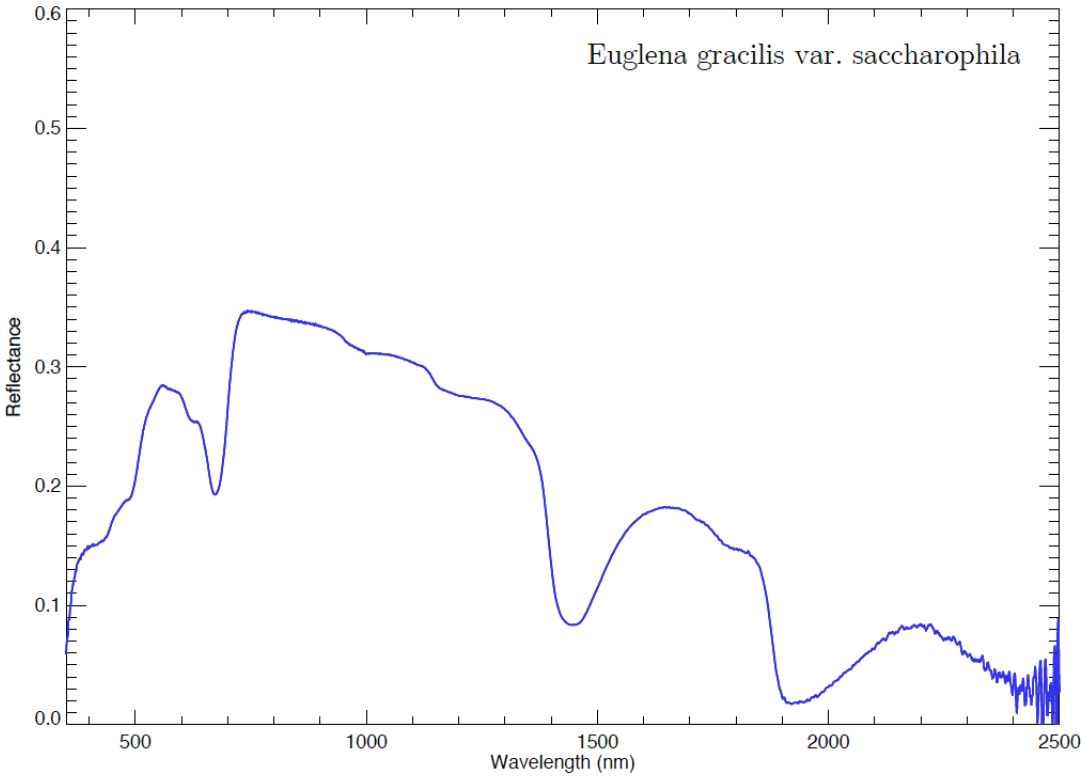

Firmicutes_KM349903

Sample name: Firmicutes

Accession number for 16S rRNA partial gene sequence: KM349903

Classification: Bacteria; Firmicutes; unclassified Firmicutes

Metabolism: Heterotrophic

Origin: Sonoran desert, AZ, USA

Isolation: Ivan P. Lima (NPP at NASA Ames, CA, USA)

Sample concentration: 4.93 $\times$ 10^7 cells/ml

Sample count on filter substrate: 1.48 $\pm$ 0.10 $\times$ 10^8 cells

Laboratory growth conditions: 30 °C, 180 rpm, 24 h

Culture medium: Marine Broth (MB)

Sample photograph:

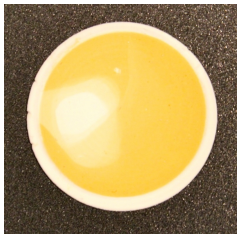

Sample micrograph:

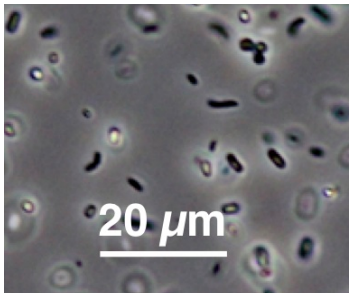

Sample reflectance spectrum:

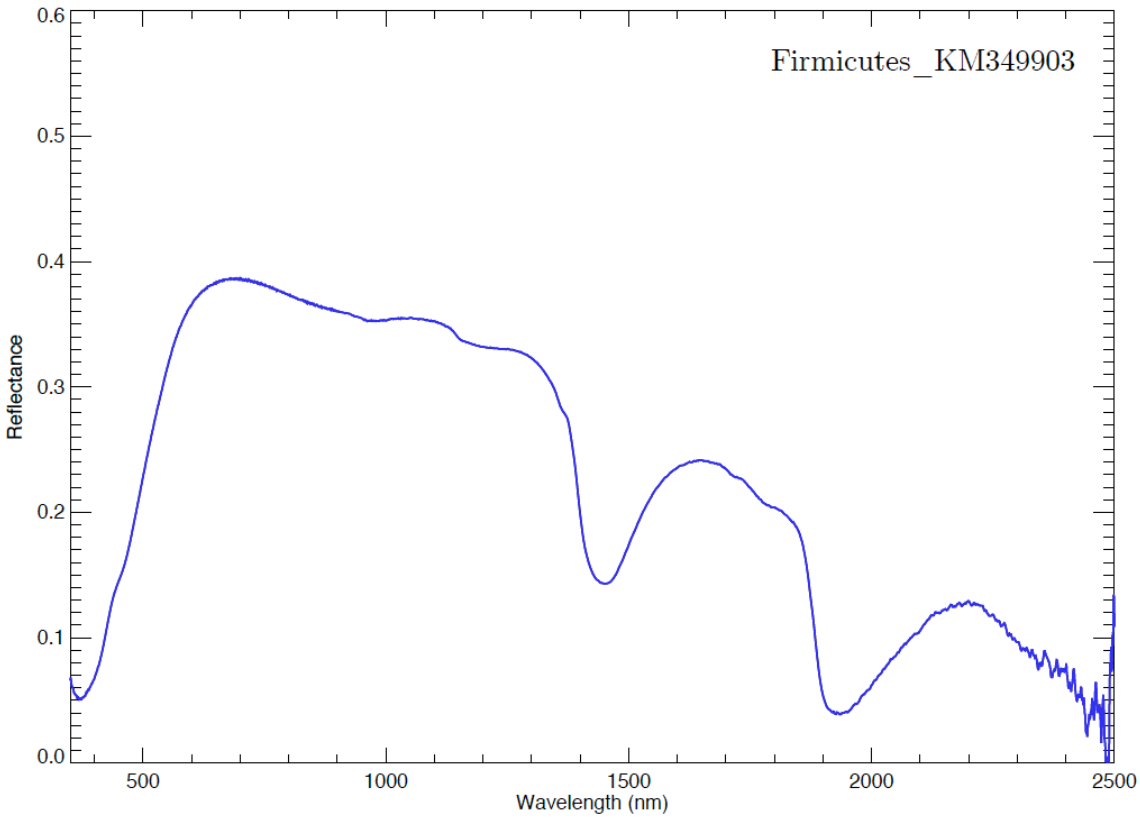

Flavobacterium sp._KM349957

Sample name: *Flavobacterium* sp.

Accession number for 16S rRNA partial gene sequence: KM349957

Classification: Bacteria; Bacteroidetes; Flavobacteriia; Flavobacteriales; Flavobacteriaceae; Flavobacterium

Metabolism: Heterotrophic

Origin: Atacama desert, Chile

Isolation: Ivan P. Lima (NPP at NASA Ames, CA, USA)

Sample concentration: 6.08×10^7 cells/ml

Sample count on filter substrate: $1.82 \pm 0.12 \times 10^8$ cells

Laboratory growth conditions: 30 °C, 180 rpm, 24 h

Culture medium: Reasoner's 2A (R2A)

Sample photograph:

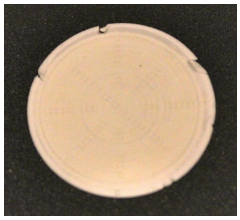

Sample micrograph:

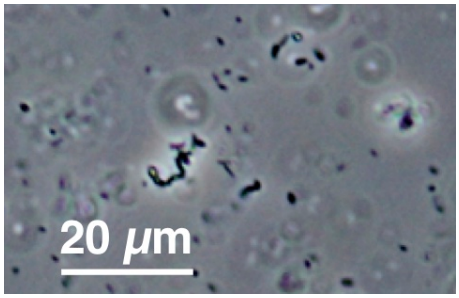

Sample reflectance spectrum:

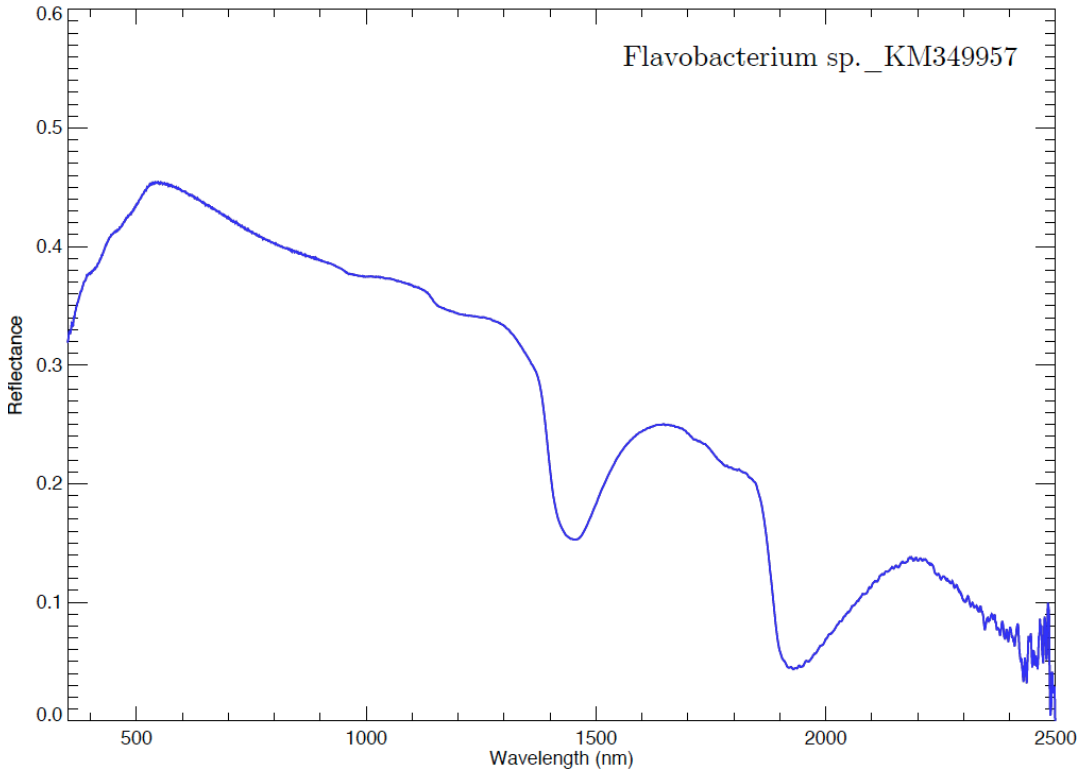

Geodermatophilaceae_KM349892

Sample name: Geodermatophilaceae

Accession number for 16S rRNA partial gene sequence: KM349892

Classification: Bacteria; Actinobacteria; Actinobacteridae; Actinomycetales; Frankineae; Geodermatophilaceae

Metabolism: Heterotrophic

Origin: Atacama desert, Chile

Isolation: Ivan P. Lima (NPP at NASA Ames, CA, USA)

Sample concentration: 1.39 $\times$ 10^7 cells/ml

Sample count on filter substrate: 4.18 $\pm$ 0.28 $\times$ 10^7 cells

Laboratory growth conditions: 30 °C, 180 rpm, 1 week

Culture medium: Reasoner's 2A (R2A)

Sample photograph:

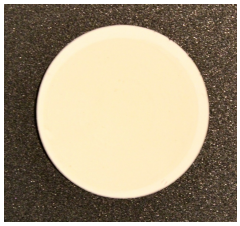

Sample micrograph:

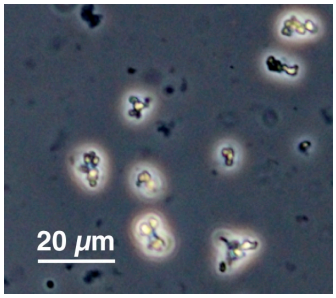

Sample reflectance spectrum:

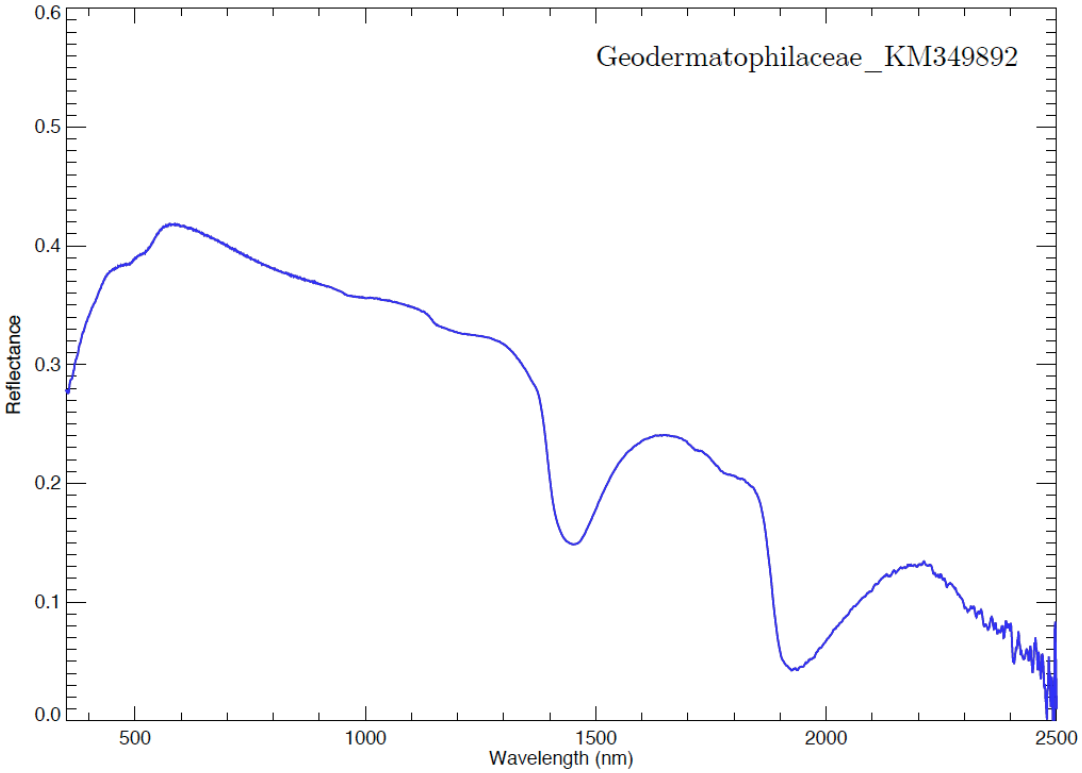

Geodermatophilus sp._KM349882

Sample name: *Geodermatophilus* sp.

Accession number for 16S rRNA partial gene sequence: KM349882

Classification: Bacteria; Actinobacteria; Actinobacteridae; Actinomycetales; Frankineae; Geodermatophilaceae; Geodermatophilus

Metabolism: Heterotrophic

Origin: Sonoran desert, AZ, USA

Isolation: Ivan P. Lima (NPP at NASA Ames, CA, USA)

Sample concentration: 6.02×10^6 cells/ml

Sample count on filter substrate: $1.80 \pm 0.12 \times 10^7$ cells

Laboratory growth conditions: 30 °C, 180 rpm, 1 week

Culture medium: Reasoner's 2A (R2A)

Sample photograph:

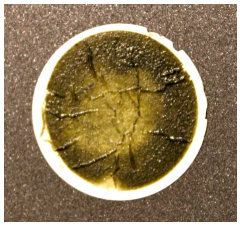

Sample micrograph:

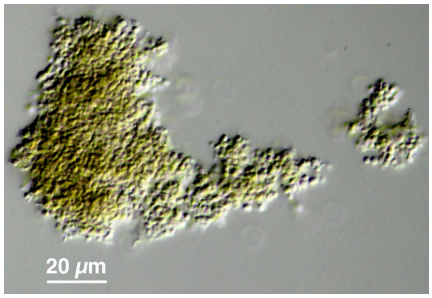

Sample reflectance spectrum:

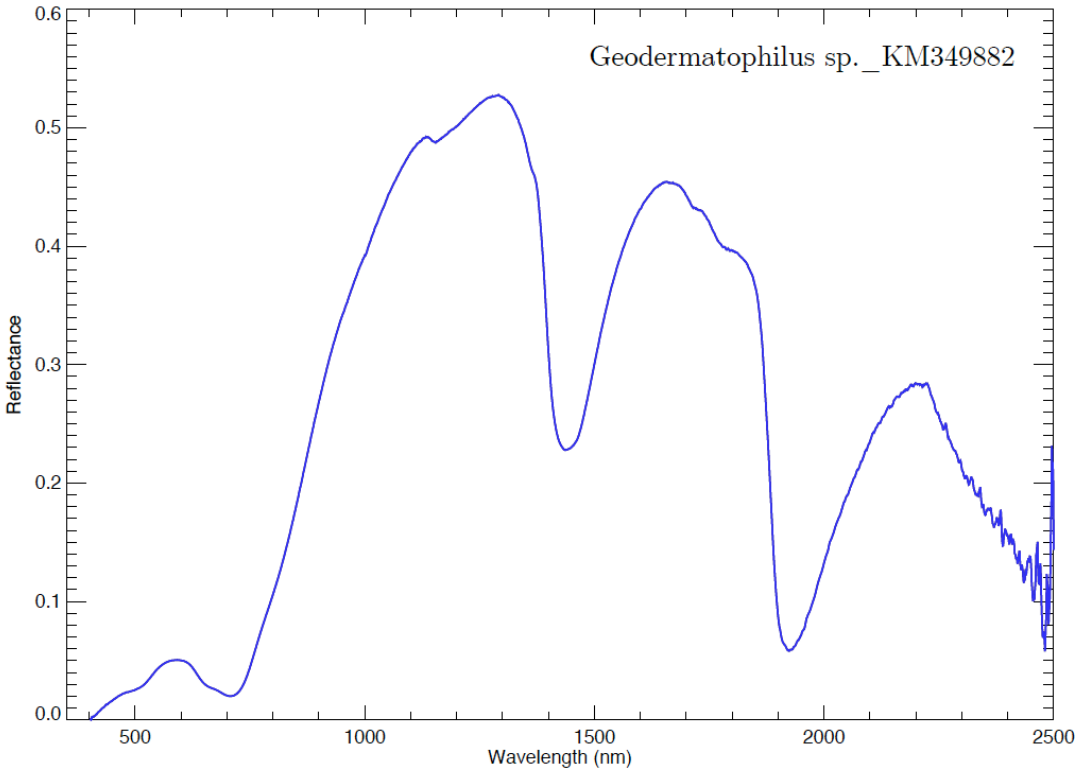

Gloeocapsa sp.

Sample name: *Gloeocapsa* sp.

Accession number for 16S rRNA partial gene sequence: Not available

Classification: Bacteria; Cyanobacteria; Cyanophyceae; Chroococcales; Microcystaceae; Gloeocapsa

Metabolism: Autotrophic (oxygenic photosynthesis)

Origin: Found in a wide range of habitats eg., limestone quarries, salt ponds

Collection: UTEX (TX, USA)

Sample concentration: 6.76×10^5 cells/ml

Sample count on filter substrate: $6.76 \pm 0.68 \times 10^6$ cells

Laboratory growth conditions: 25 °C, up to 6 months

Culture medium: Bold 3N medium

Sample photograph:

Sample micrograph:

Sample reflectance spectrum:

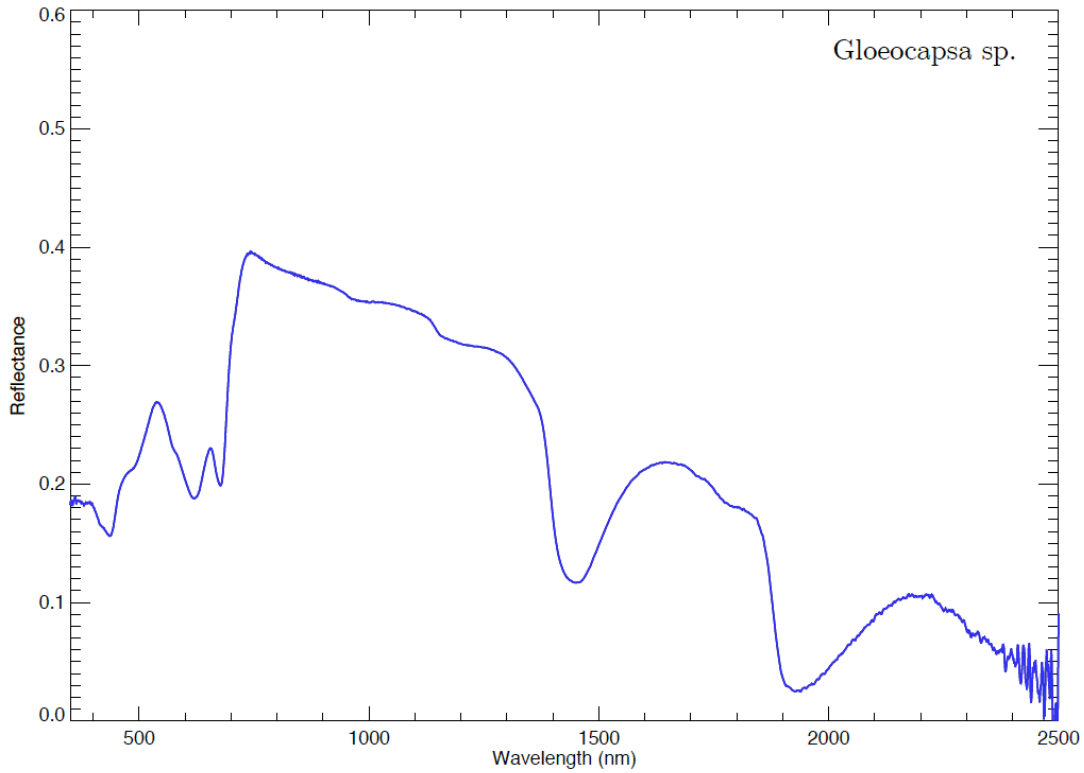

Haematococcus droebakensis

Sample name: *Haematococcus droebakensis*

Accession number for 16S rRNA partial gene sequence: Not available

Classification: Eukaryota; Chlorophyta; Chlorophyceae; Chlamydomonadales; Haematococcaceae; Haematococcus

Metabolism: Autotrophic (oxygenic photosynthesis)

Origin: Lake Erken, Sweden

Collection: UTEX (TX, USA)

Sample concentration: 2.03×10^5 cells/ml

Sample count on filter substrate: $2.03 \pm 0.20 \times 10^6$ cells

Laboratory growth conditions: 25 °C, up to 6 months

Culture medium: Modified Bold 3N medium

Sample photograph:

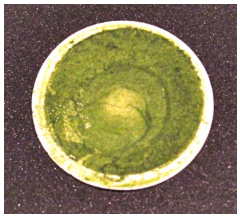

Sample micrograph:

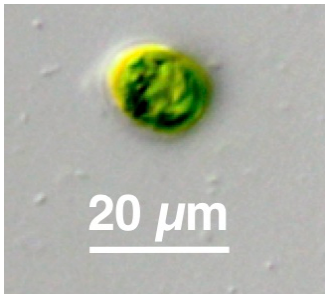

Sample reflectance spectrum:

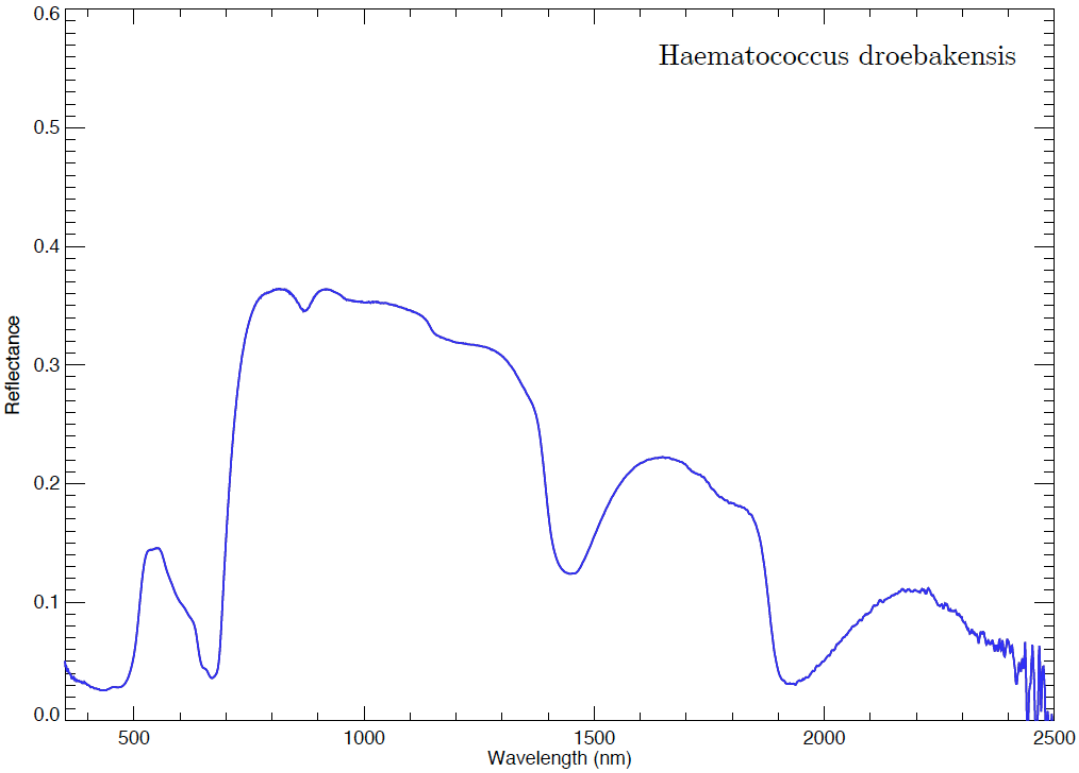

Halorubrum chaoviator str. Halo-G*^{T}_ AM048786

Sample name: *Halorubrum chaoviator* str. Halo-G*^{T}

Accession number for 16S rRNA partial gene sequence: AM048786

Classification: Archaea; Euryarchaeota; Halobacteria; Halobacteriales; Halobacteriaceae; Halorubrum

Metabolism: Heterotrophic

Origin: Evaporitic salt crystal, Baja California, Mexico

Isolation: Rocco Mancinelli (BAER Institute at NASA Ames, CA, USA)

Sample concentration: 8.19 $\times$ 10^{7} cells/ml

Sample count on filter substrate: 2.46 $\pm$ 0.16 $\times$ 10^{8} cells

Laboratory growth conditions: 37 °C, 180 rpm, 1 week

Culture medium: CASEIN medium ATCC#876

Sample photograph:

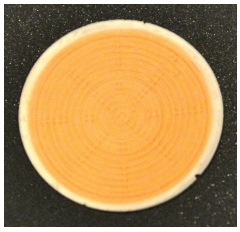

Sample micrograph:

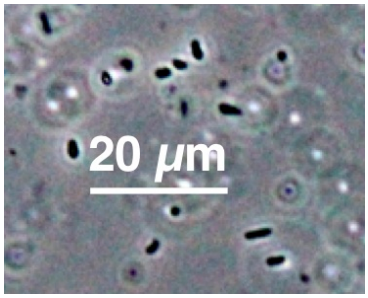

Sample reflectance spectrum:

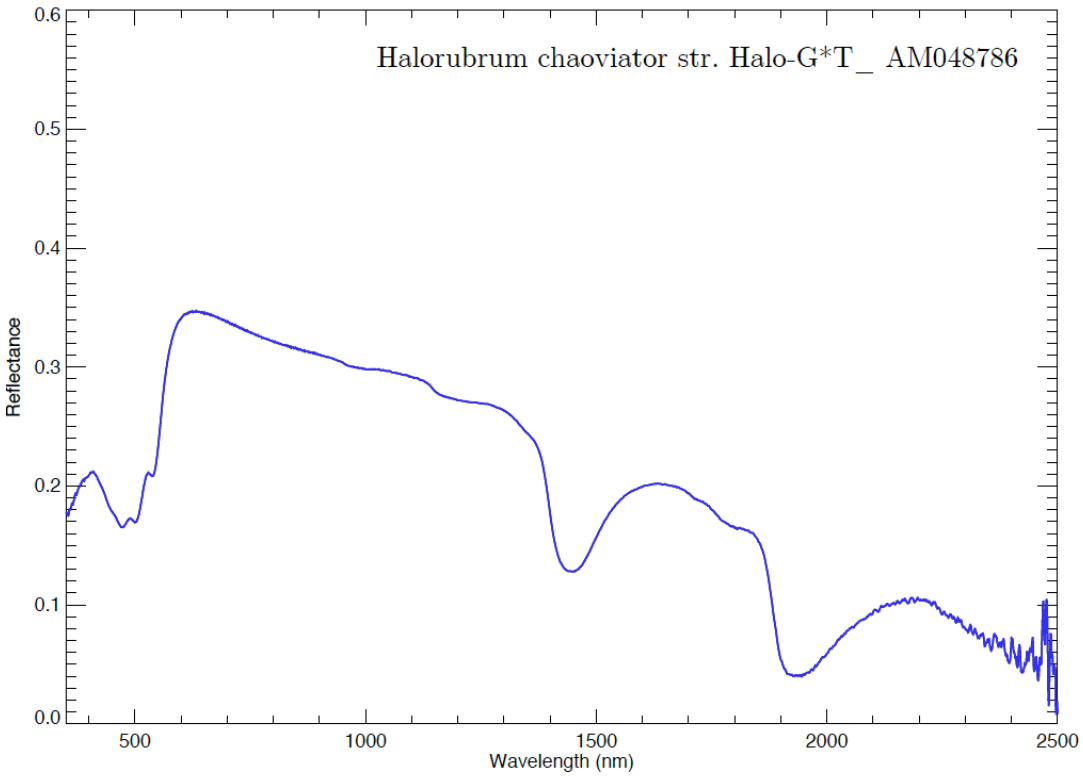

Hydrogenophaga sp._KM349947

Sample name: *Hydrogenophaga* sp.

Accession number for 16S rRNA partial gene sequence: KM349947

Classification: Bacteria; Proteobacteria; Betaproteobacteria; Burkholderiales; Comamonadaceae; Hydrogenophaga

Metabolism: Heterotrophic

Origin: Atacama desert, Chile

Isolation: Ivan P. Lima (NPP at NASA Ames, CA, USA)

Sample concentration: 3.71 $\times$ 10^7 cells/ml

Sample count on filter substrate: 1.11 $\pm$ 0.07 $\times$ 10^8 cells

Laboratory growth conditions: 30 °C, 180 rpm, 24 h

Culture medium: Reasoner's 2A (R2A)

Sample photograph:

Sample micrograph:

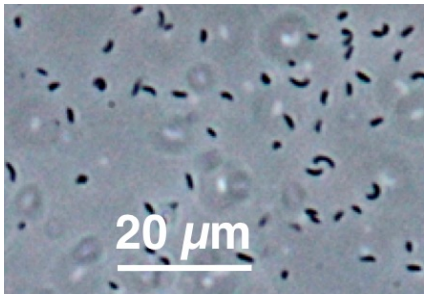

Sample reflectance spectrum:

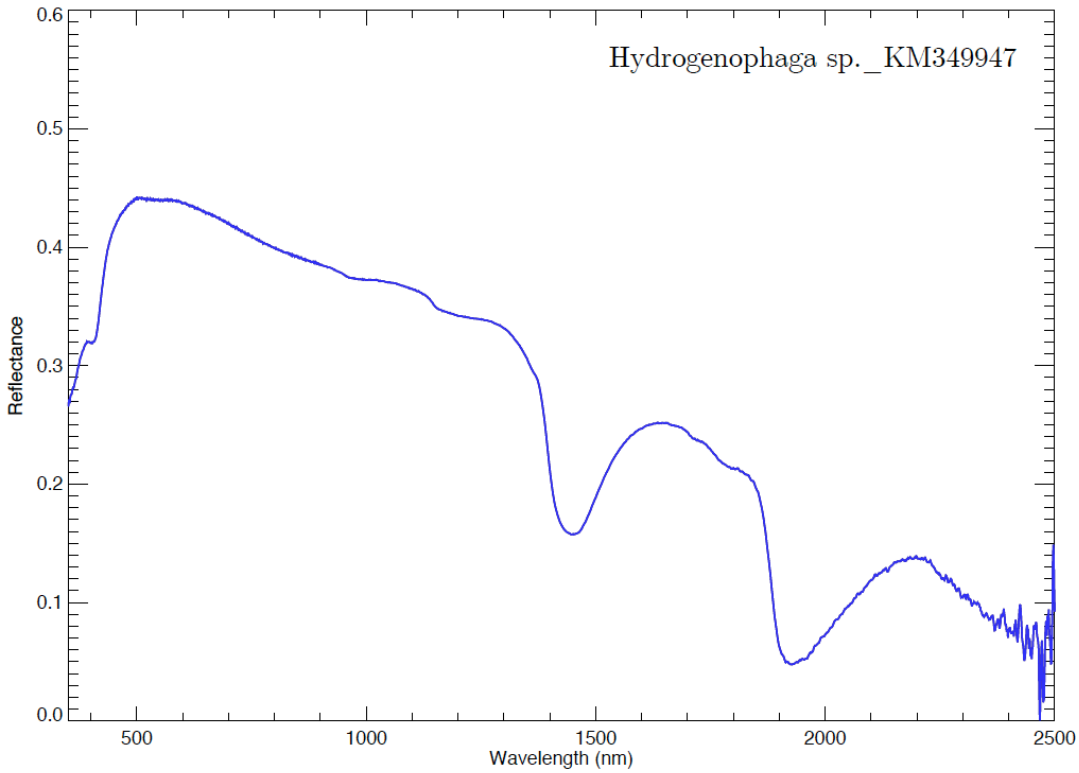

Hydrogenophaga sp._KM349962

Sample name: *Hydrogenophaga* sp.

Accession number for 16S rRNA partial gene sequence: KM349962

Classification: Bacteria; Proteobacteria; Betaproteobacteria; Burkholderiales; Comamonadaceae; Hydrogenophaga

Metabolism: Heterotrophic

Origin: Atacama desert, Chile

Isolation: Ivan P. Lima (NPP at NASA Ames, CA, USA)

Sample concentration: 6.65×10^7 cells/ml

Sample count on filter substrate: $1.99 \pm 0.13 \times 10^8$ cells

Laboratory growth conditions: 30 °C, 180 rpm, 24 h

Culture medium: Reasoner's 2A (R2A)

Sample photograph:

Sample micrograph:

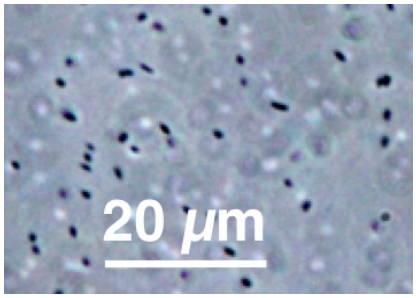

Sample reflectance spectrum:

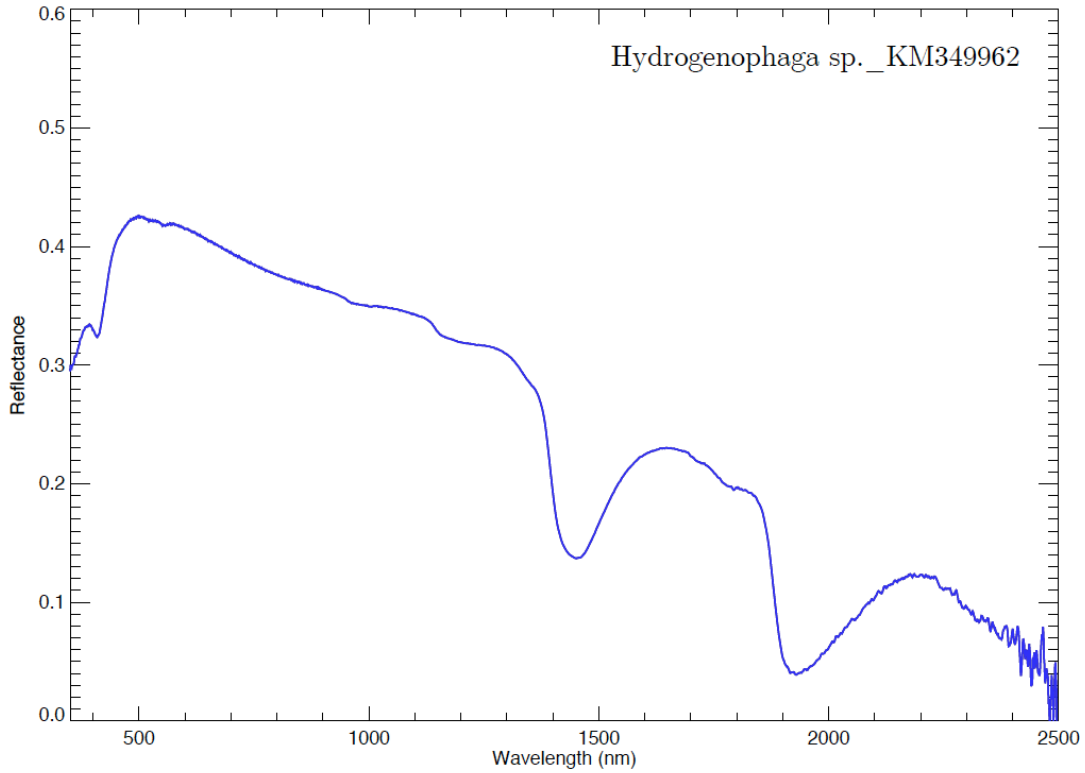

Hymenobacter sp._KM349884

Sample name: *Hymenobacter* sp.

Accession number for 16S rRNA partial gene sequence: KM349884

Classification: Bacteria; Bacteroidetes; Cytophagia; Cytophagales; Cytophagaceae; Hymenobacter

Metabolism: Heterotrophic

Origin: Atacama desert, Chile

Isolation: Ivan P. Lima (NPP at NASA Ames, CA, USA)

Sample concentration: 1.61 $\times$ 10^7 cells/ml

Sample count on filter substrate: 4.83 $\pm$ 0.32 $\times$ 10^7 cells

Laboratory growth conditions: 30 °C, 180 rpm, 48 h

Culture medium: Reasoner's 2A (R2A)

Sample photograph:

Sample micrograph:

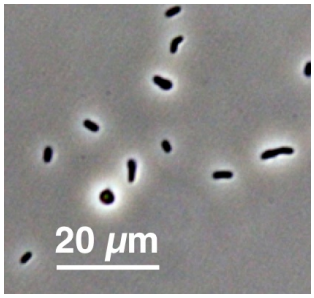

Sample reflectance spectrum:

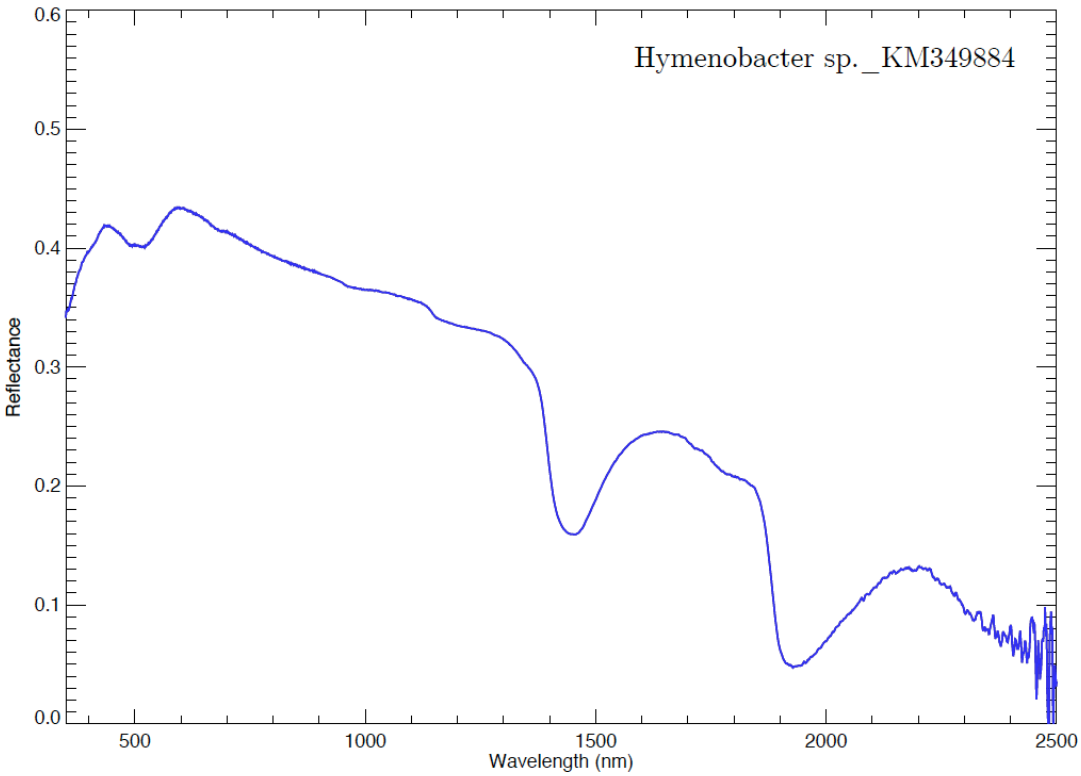

Isochrysis galbana

Sample name: *Isochrysis galbana*

Accession number for 16S rRNA partial gene sequence: Not available

Classification: Eukaryota; Haptophyta; Coccolithophyceae; Isochrysidales; Isochrysidaceae; Isochrysis

Metabolism: Autotrophic (oxygenic photosynthesis)

Origin: Marine sample, Society Islands, Tahiti

Collection: Kudela laboratory (UCSC, CA, USA)

Sample concentration: 4.06×10^5 cells/ml

Sample count on filter substrate: $4.06 \pm 0.41 \times 10^6$ cells

Laboratory growth conditions: 25 °C, up to 6 months

Culture medium: Enriched Seawater medium (f/2)

Sample photograph:

Sample micrograph:

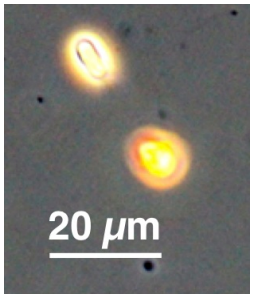

Sample reflectance spectrum:

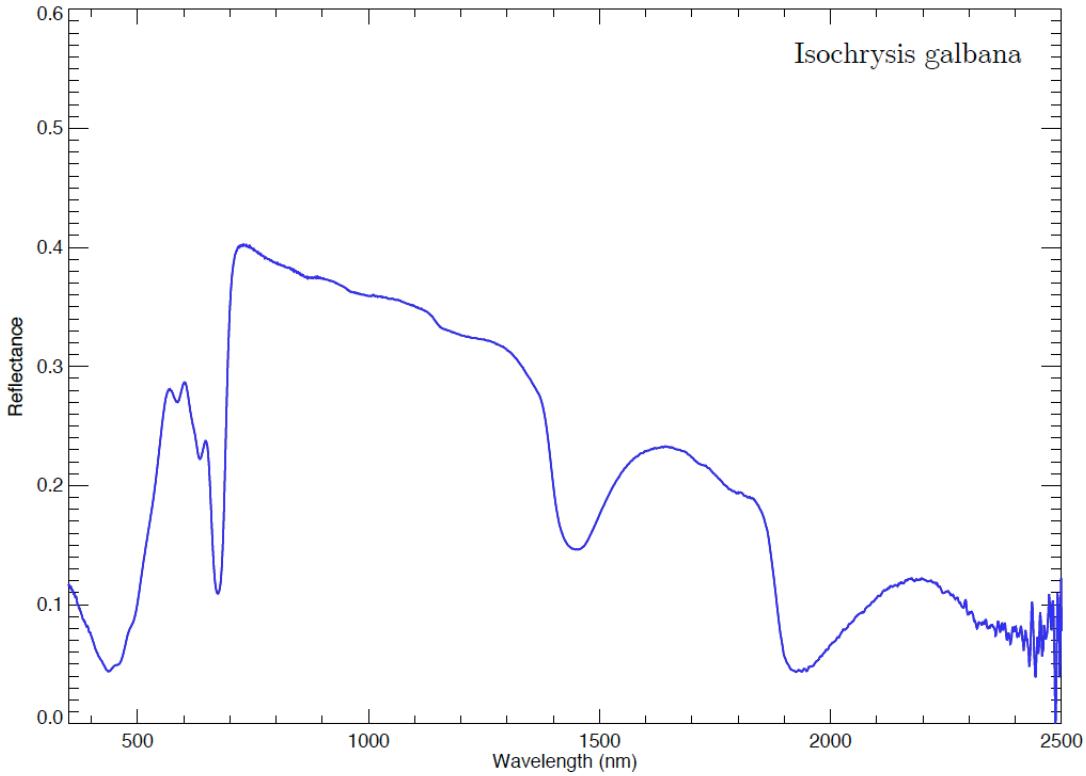

Kocuria sp._KM349888

Sample name: *Kocuria* sp.

Accession number for 16S rRNA partial gene sequence: KM349888

Classification: Bacteria; Actinobacteria; Actinobacteridae; Actinomycetales; Micrococcineae; Micrococcaceae; Kocuria

Metabolism: Heterotrophic

Origin: Atacama desert, Chile

Isolation: Ivan P. Lima (NPP at NASA Ames, CA, USA)

Sample concentration: 6.27×10^7 cells/ml

Sample count on filter substrate: $1.88 \pm 0.13 \times 10^8$ cells

Laboratory growth conditions: 30 °C, 180 rpm, 48 h

Culture medium: Reasoner's 2A (R2A)

Sample photograph:

Sample micrograph:

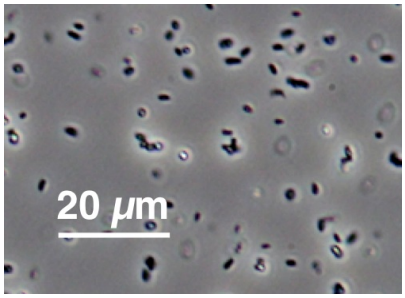

Sample reflectance spectrum:

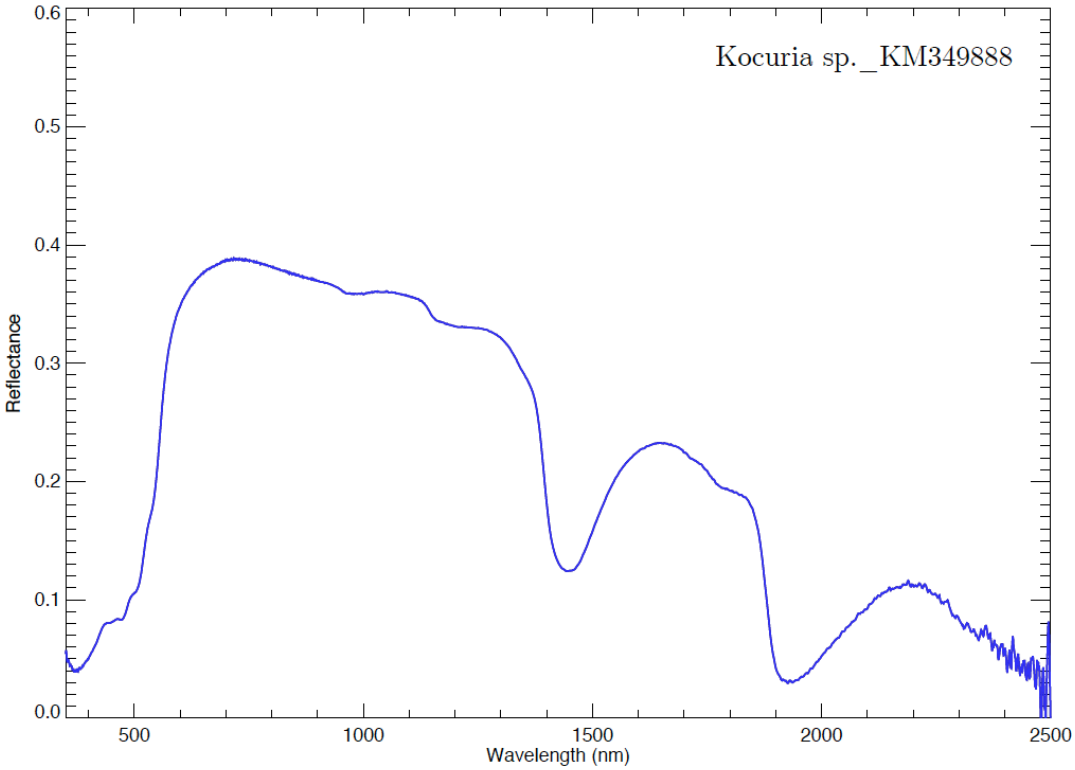

Kocuria sp._KM349891

Sample name: *Kocuria* sp.

Accession number for 16S rRNA partial gene sequence: KM349891

Classification: Bacteria; Actinobacteria; Actinobacteridae; Actinomycetales; Micrococcineae; Micrococcaceae; Kocuria

Metabolism: Heterotrophic

Origin: Atacama desert, Chile

Isolation: Ivan P. Lima (NPP at NASA Ames, CA, USA)

Sample concentration: 4.28×10^7 cells/ml

Sample count on filter substrate: $1.28 \pm 0.09 \times 10^8$ cells

Laboratory growth conditions: 30 °C, 180 rpm, 48 h

Culture medium: Marine Broth (MB)

Sample photograph:

Sample micrograph:

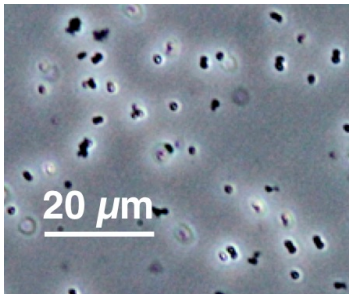

Sample reflectance spectrum:

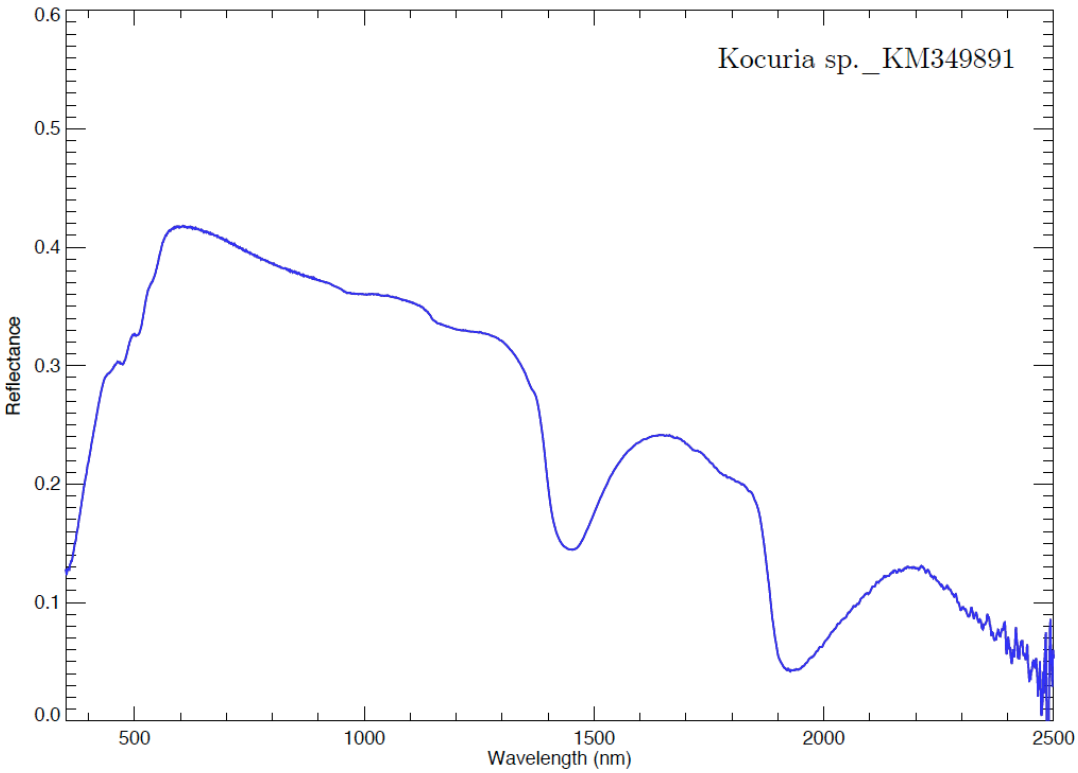

Kocuria sp._KM349896

Sample name: *Kocuria* sp.

Accession number for 16S rRNA partial gene sequence: KM349896

Classification: Bacteria; Actinobacteria; Actinobacteridae; Actinomycetales; Micrococcineae; Micrococcaceae; Kocuria

Metabolism: Heterotrophic

Origin: Atacama desert, Chile

Isolation: Ivan P. Lima (NPP at NASA Ames, CA, USA)

Sample concentration: 8.58×10^7 cells/ml

Sample count on filter substrate: $2.57 \pm 0.17 \times 10^8$ cells

Laboratory growth conditions: 30 °C, 180 rpm, 24 h

Culture medium: Reasoner's 2A (R2A)

Sample photograph:

Sample micrograph:

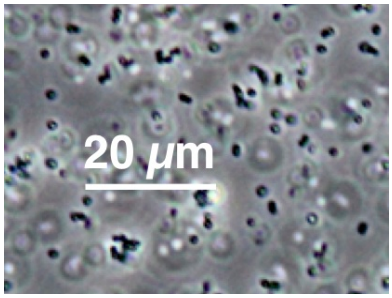

Sample reflectance spectrum:

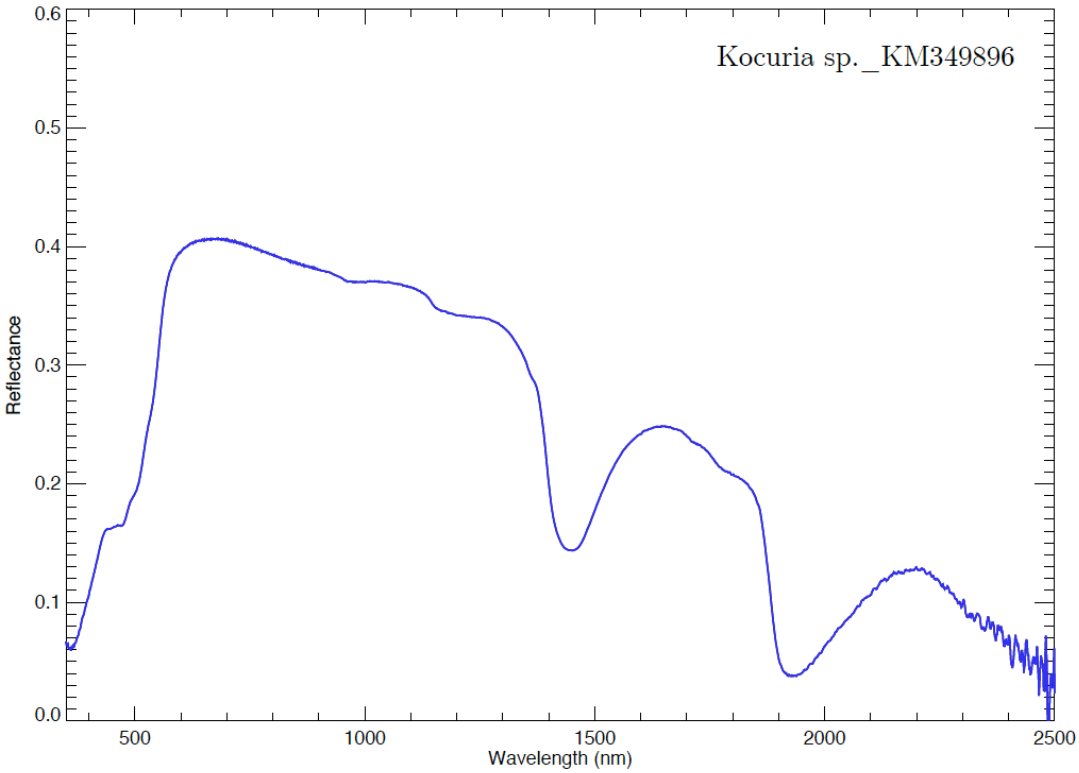

Kocuria sp._KM349900

Sample name: *Kocuria* sp.

Accession number for 16S rRNA partial gene sequence: KM349900

Classification: Bacteria; Actinobacteria; Actinobacteridae; Actinomycetales; Micrococcineae; Micrococcaceae; Kocuria

Metabolism: Heterotrophic

Origin: Atacama desert, Chile

Isolation: Ivan P. Lima (NPP at NASA Ames, CA, USA)

Sample concentration: 4.44 $\times$ 10^7 cells/ml

Sample count on filter substrate: 1.33 $\pm$ 0.09 $\times$ 10^8 cells

Laboratory growth conditions: 30 °C, 180 rpm, 24 h

Culture medium: Marine Broth (MB)

Sample photograph:

Sample micrograph:

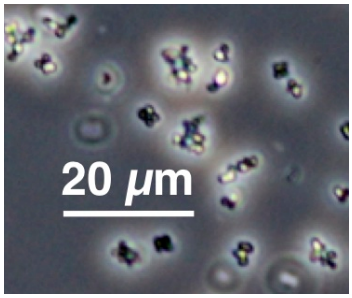

Sample reflectance spectrum:

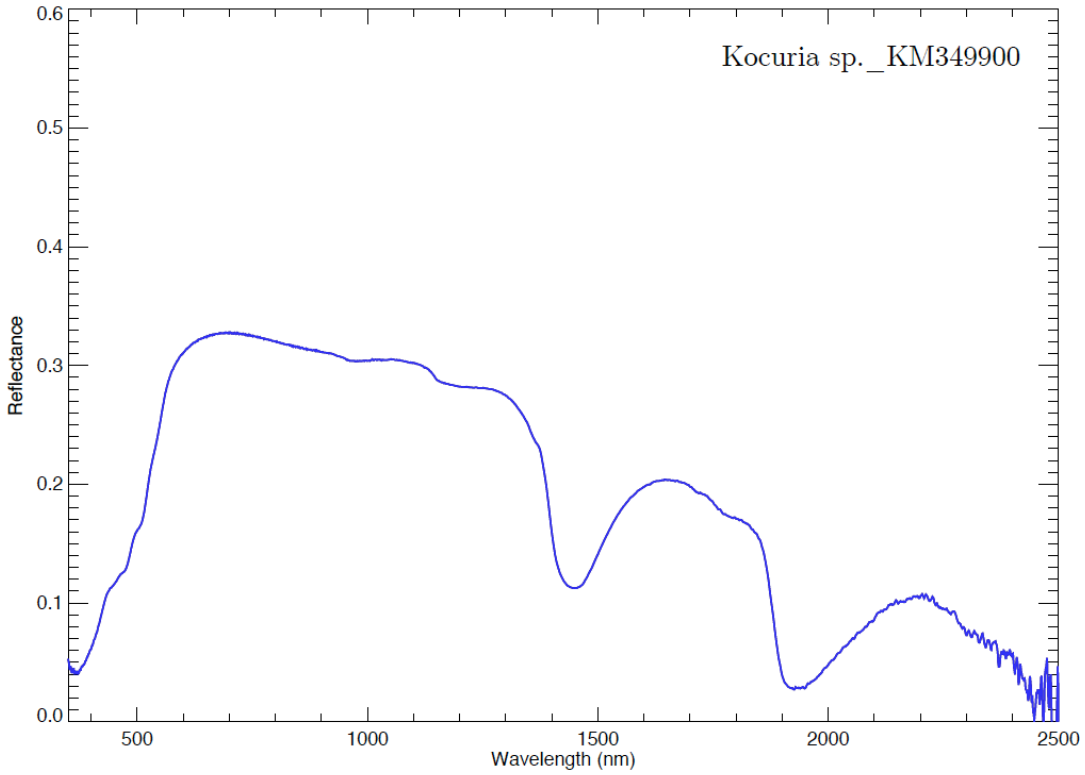

Kocuria sp._KM349907

Sample name: *Kocuria* sp.

Accession number for 16S rRNA partial gene sequence: KM349907

Classification: Bacteria; Actinobacteria; Actinobacteridae; Actinomycetales; Micrococcineae; Micrococcaceae; Kocuria

Metabolism: Heterotrophic

Origin: Sonoran desert, AZ, USA

Isolation: Ivan P. Lima (NPP at NASA Ames, CA, USA)

Sample concentration: 1.54×10^7 cells/ml

Sample count on filter substrate: $4.62 \pm 0.31 \times 10^7$ cells

Laboratory growth conditions: 30 °C, 180 rpm, 24 h

Culture medium: Marine Broth (MB)

Sample photograph:

Sample micrograph:

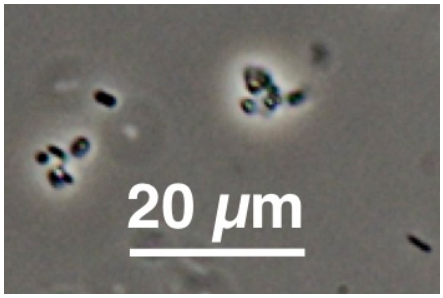

Sample reflectance spectrum:

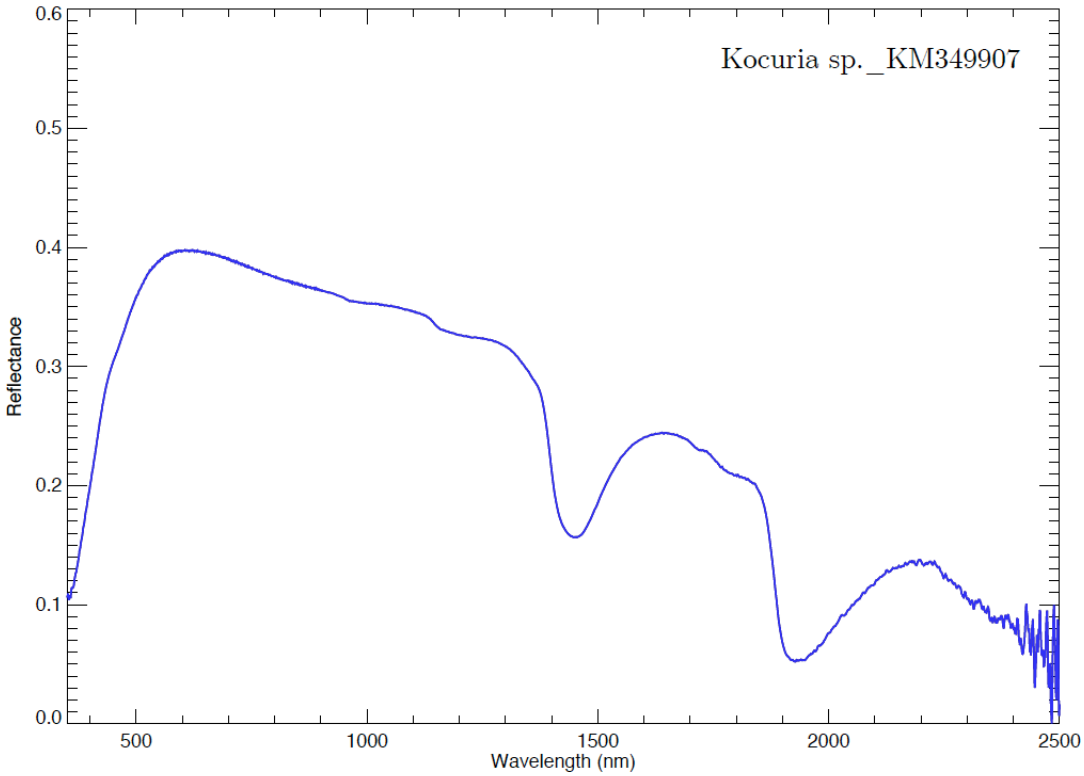

Kocuria sp._KM349908

Sample name: *Kocuria* sp.

Accession number for 16S rRNA partial gene sequence: KM349908

Classification: Bacteria; Actinobacteria; Actinobacteridae; Actinomycetales; Micrococcineae; Micrococcaceae; Kocuria

Metabolism: Heterotrophic

Origin: Sonoran desert, AZ, USA

Isolation: Ivan P. Lima (NPP at NASA Ames, CA, USA)

Sample concentration: 3.45×10^7 cells/ml

Sample count on filter substrate: $1.03 \pm 0.07 \times 10^8$ cells

Laboratory growth conditions: 30 °C, 180 rpm, 24 h

Culture medium: Marine Broth (MB)

Sample photograph:

Sample micrograph:

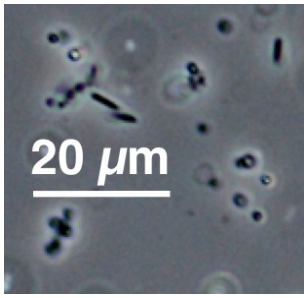

Sample reflectance spectrum:

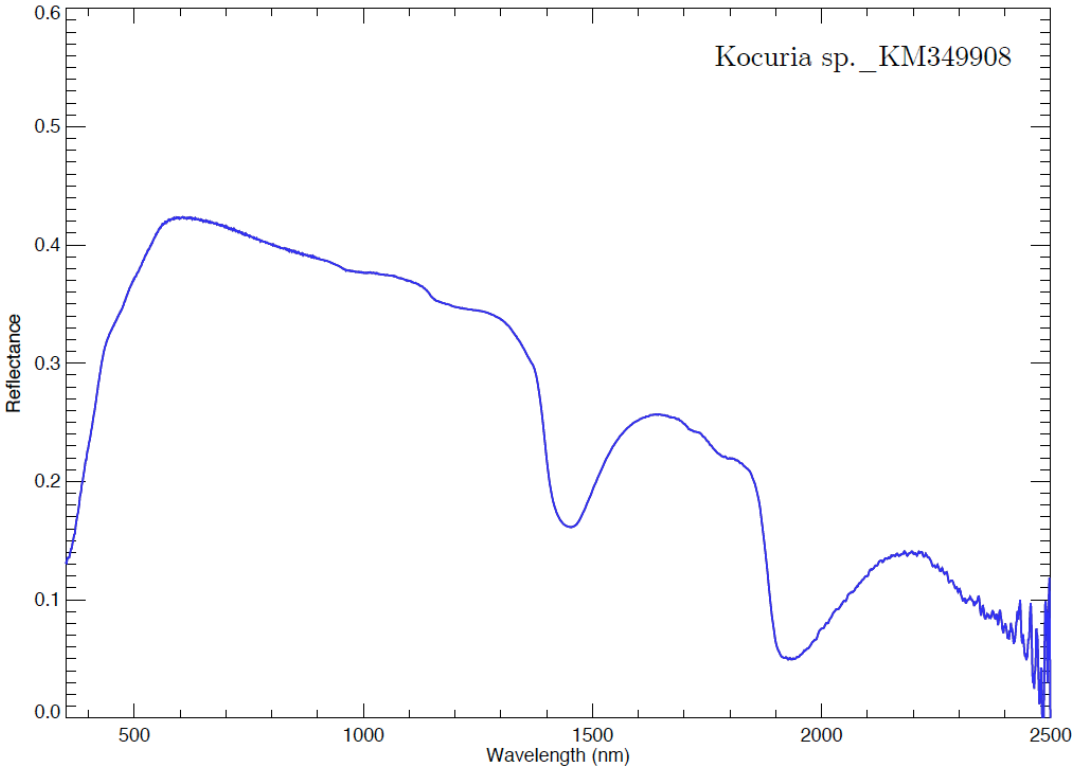

Kocuria sp._KM349909

Sample name: *Kocuria* sp.

Accession number for 16S rRNA partial gene sequence: KM349909

Classification: Bacteria; Actinobacteria; Actinobacteridae; Actinomycetales; Micrococcineae; Micrococcaceae; Kocuria

Metabolism: Heterotrophic

Origin: Sonoran desert, AZ, USA

Isolation: Ivan P. Lima (NPP at NASA Ames, CA, USA)

Sample concentration: 1.62×10^8 cells/ml

Sample count on filter substrate: $4.87 \pm 0.32 \times 10^8$ cells

Laboratory growth conditions: 30 °C, 180 rpm, 24 h

Culture medium: Marine Broth (MB)

Sample photograph:

Sample micrograph:

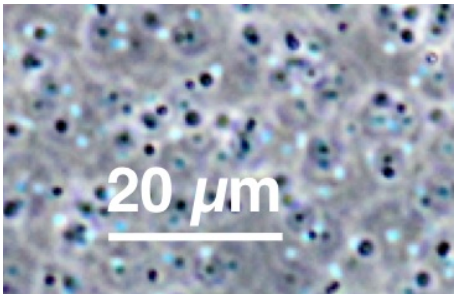

Sample reflectance spectrum:

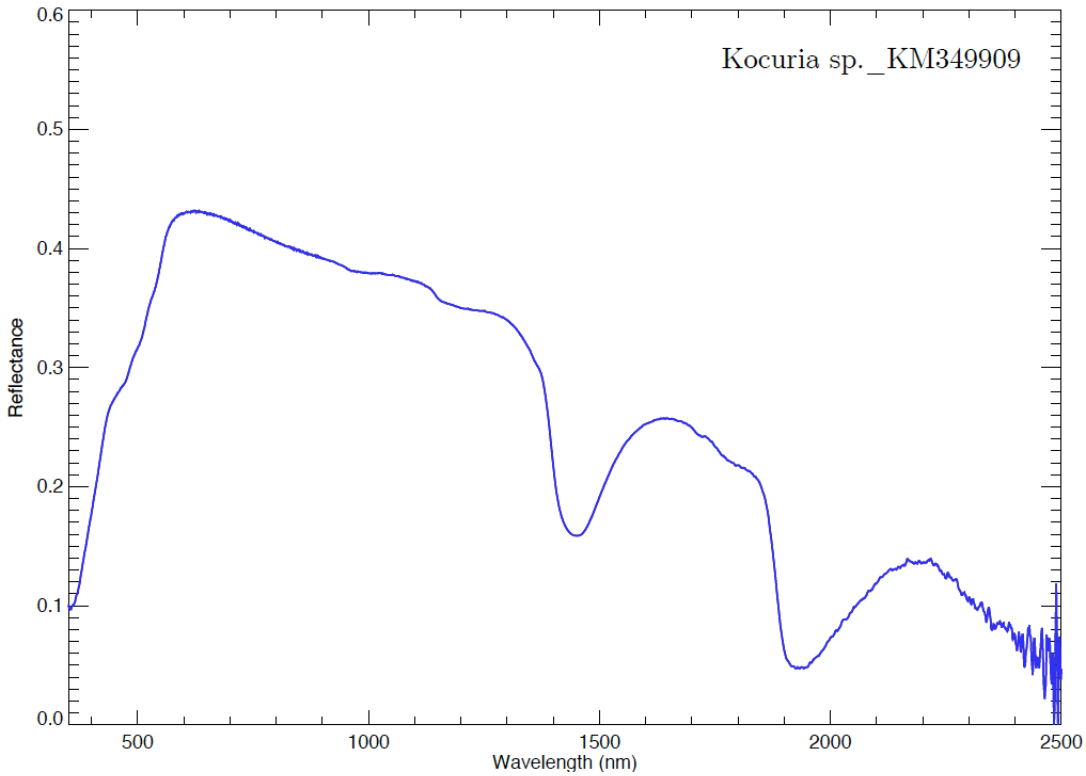

Kocuria sp._KM349917

Sample name: *Kocuria* sp.

Accession number for 16S rRNA partial gene sequence: KM349917

Classification: Bacteria; Actinobacteria; Actinobacteridae; Actinomycetales; Micrococcineae; Micrococcaceae; Kocuria

Metabolism: Heterotrophic

Origin: Sonoran desert, AZ, USA

Isolation: Ivan P. Lima (NPP at NASA Ames, CA, USA)

Sample concentration: 3.84×10^7 cells/ml

Sample count on filter substrate: $1.15 \pm 0.08 \times 10^8$ cells

Laboratory growth conditions: 30 °C, 180 rpm, 24 h

Culture medium: Marine Broth (MB)

Sample photograph:

Sample micrograph:

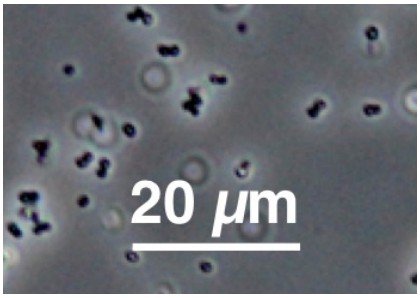

Sample reflectance spectrum:

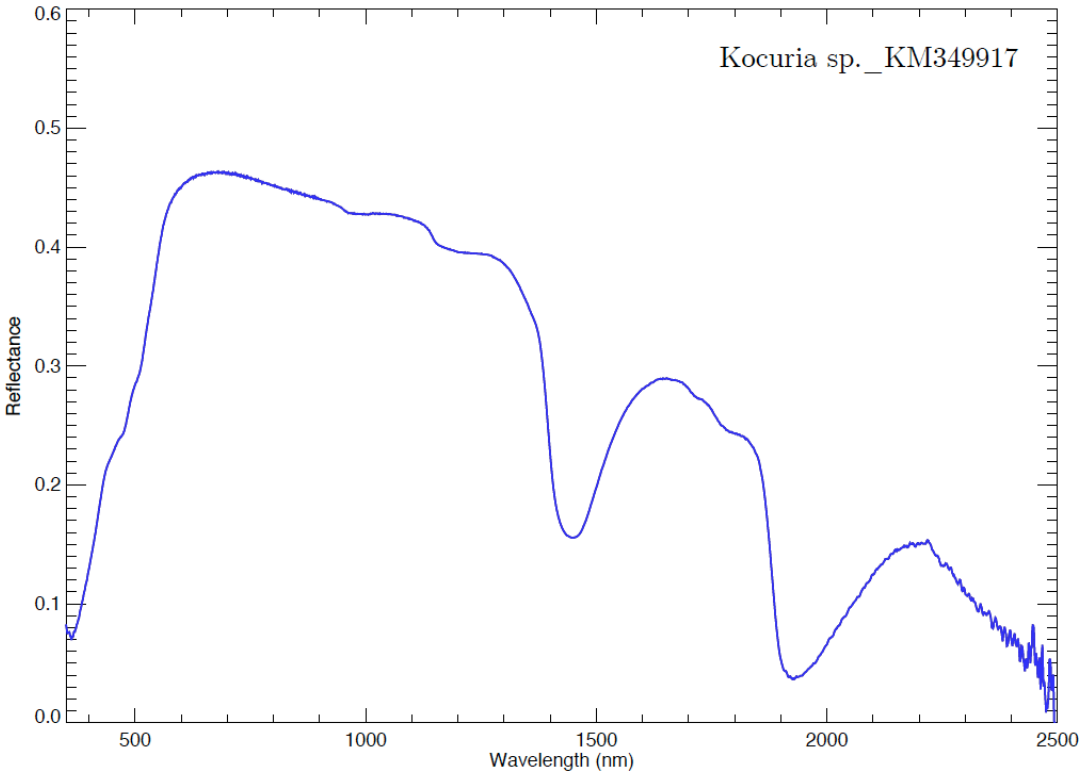

Kocuria sp._KM349920

Sample name: *Kocuria* sp.

Accession number for 16S rRNA partial gene sequence: KM349920

Classification: Bacteria; Actinobacteria; Actinobacteridae; Actinomycetales; Micrococcineae; Micrococcaceae; Kocuria

Metabolism: Heterotrophic

Origin: Sonoran desert, AZ, USA

Isolation: Ivan P. Lima (NPP at NASA Ames, CA, USA)

Sample concentration: 1.38×10^8 cells/ml

Sample count on filter substrate: $4.15 \pm 0.28 \times 10^8$ cells

Laboratory growth conditions: 30 °C, 180 rpm, 24 h

Culture medium: Marine Broth (MB)

Sample photograph:

Sample micrograph:

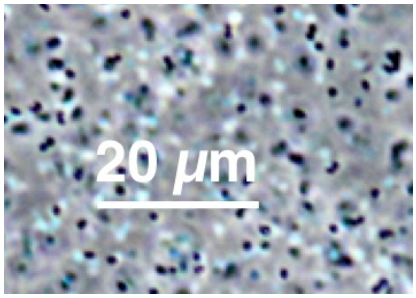

Sample reflectance spectrum:

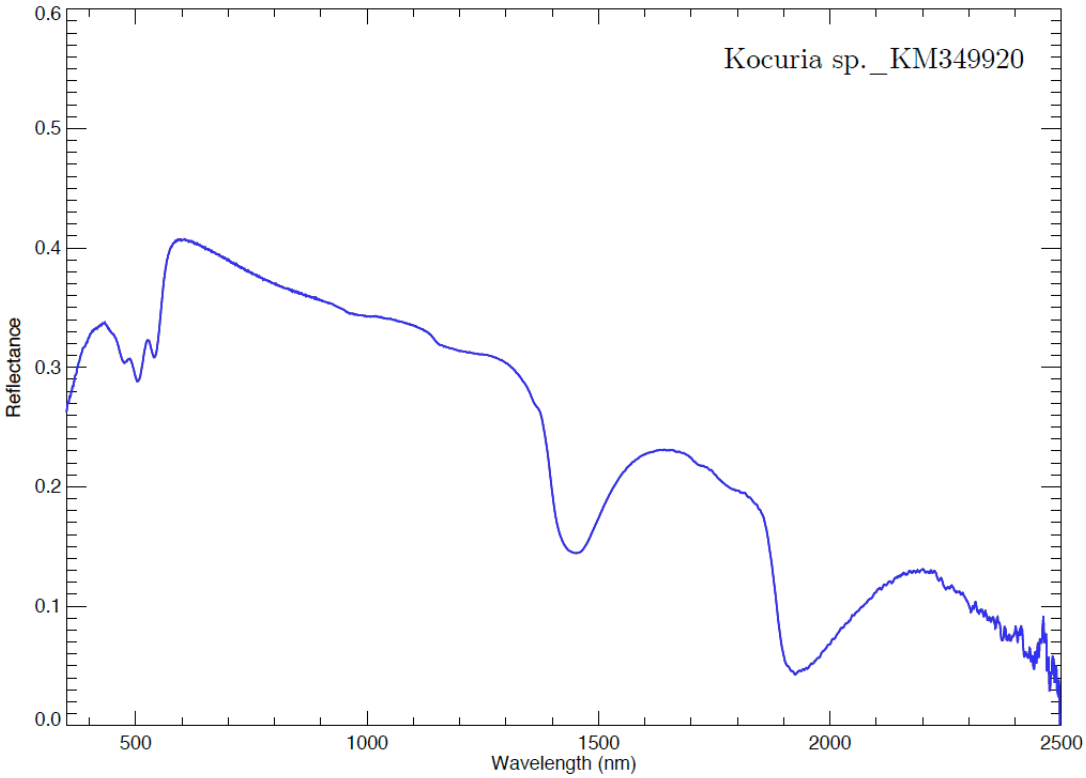

Kocuria sp._KM349926

Sample name: *Kocuria* sp.

Accession number for 16S rRNA partial gene sequence: KM349926

Classification: Bacteria; Actinobacteria; Actinobacteridae; Actinomycetales; Micrococcineae; Micrococcaceae; Kocuria

Metabolism: Heterotrophic

Origin: Sonoran desert, AZ, USA

Isolation: Ivan P. Lima (NPP at NASA Ames, CA, USA)

Sample concentration: 7.56×10^7 cells/ml

Sample count on filter substrate: $2.27 \pm 0.15 \times 10^8$ cells

Laboratory growth conditions: 30 °C, 180 rpm, 24 h

Culture medium: Lysogeny Broth (LB)

Sample photograph:

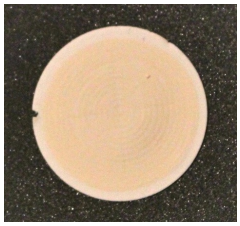

Sample micrograph:

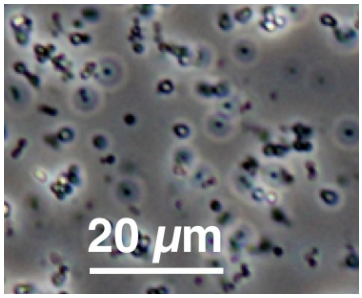

Sample reflectance spectrum:

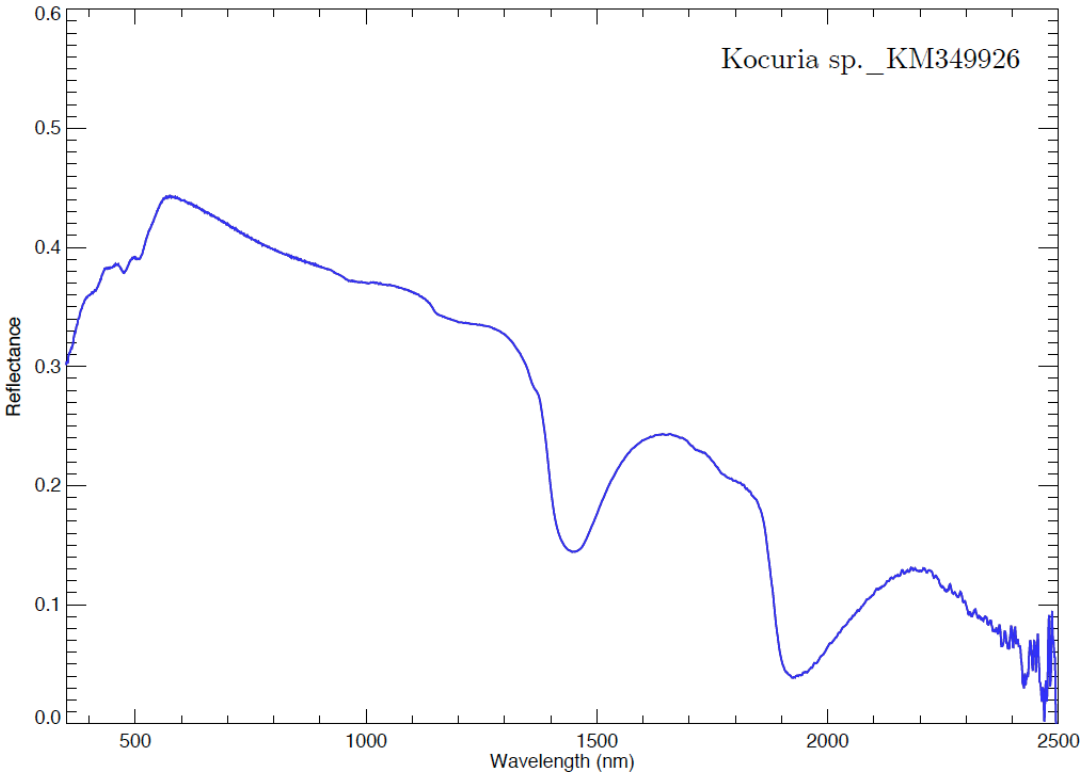

Kocuria sp._KM349935

Sample name: *Kocuria* sp.

Accession number for 16S rRNA partial gene sequence: KM349935

Classification: Bacteria; Actinobacteria; Actinobacteridae; Actinomycetales; Micrococcineae; Micrococcaceae; Kocuria

Metabolism: Heterotrophic

Origin: Atacama desert, Chile

Isolation: Ivan P. Lima (NPP at NASA Ames, CA, USA)

Sample concentration: 6.33×10^7 cells/ml

Sample count on filter substrate: $1.90 \pm 0.13 \times 10^8$ cells

Laboratory growth conditions: 30 °C, 180 rpm, 24 h

Culture medium: Marine Broth (MB)

Sample photograph:

Sample micrograph:

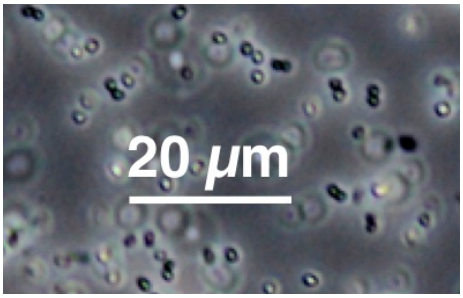

Sample reflectance spectrum:

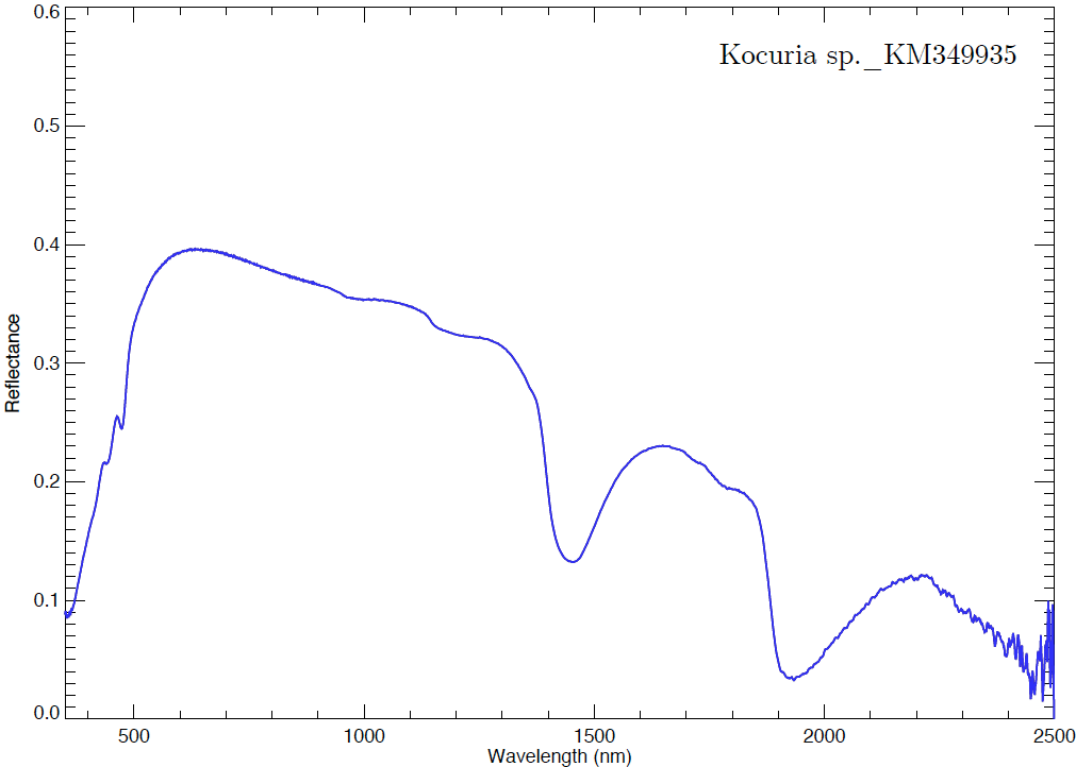

Kocuria sp._KM349964

Sample name: *Kocuria* sp.

Accession number for 16S rRNA partial gene sequence: KM349964

Classification: Bacteria; Actinobacteria; Actinobacteridae; Actinomycetales; Micrococcineae; Micrococcaceae; Kocuria

Metabolism: Heterotrophic

Origin: Atacama desert, Chile

Isolation: Ivan P. Lima (NPP at NASA Ames, CA, USA)

Sample concentration: 1.96 $\times$ 10^7 cells/ml

Sample count on filter substrate: 5.88 $\pm$ 0.39 $\times$ 10^7 cells

Laboratory growth conditions: 30 °C, 180 rpm, 48 h

Culture medium: Marine Broth (MB)

Sample photograph:

Sample micrograph:

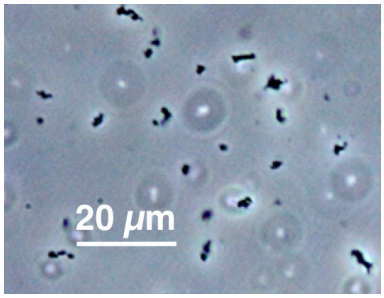

Sample reflectance spectrum:

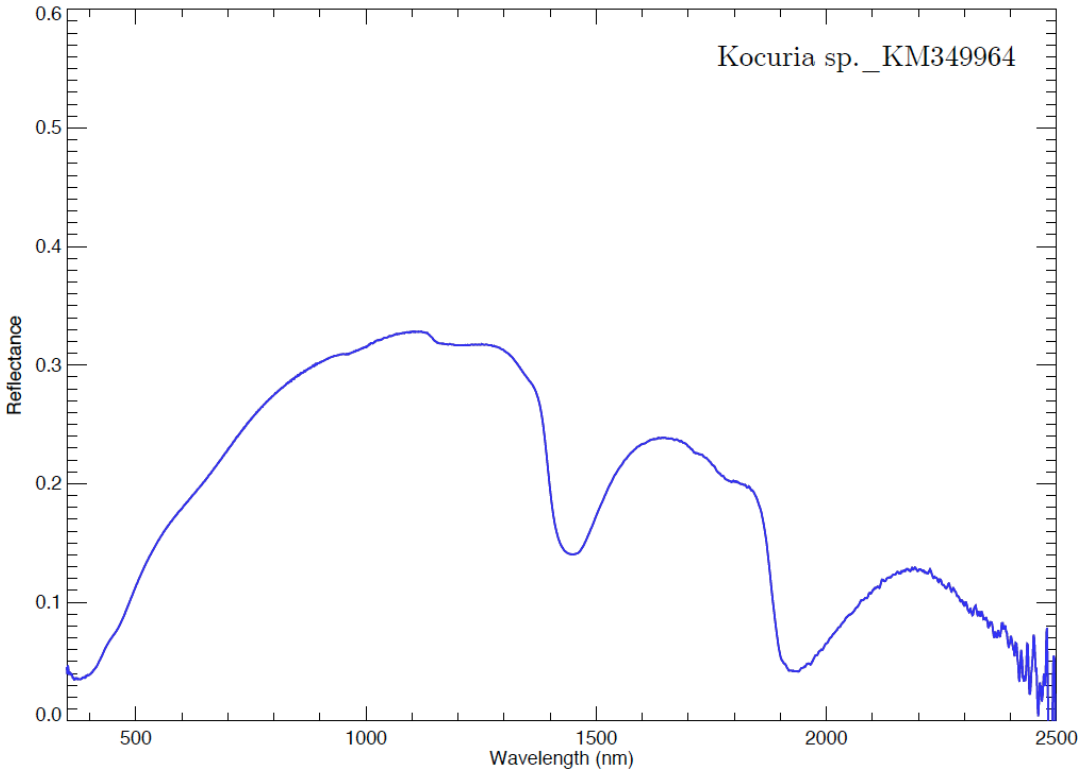

Lyngbya purpurem

Sample name: *Lyngbya purpurem*

Accession number for 16S rRNA partial gene sequence: Not available

Classification: Bacteria; Cyanobacteria; Cyanophyceae; Oscillatoriales; Oscillatoriaceae; Lyngbya

Metabolism: Autotrophic (oxygenic photosynthesis)

Origin: Freshwater species

Collection: UTEX (TX, USA)

Sample concentration: 3.26×10^7 cells/ml

Sample count on filter substrate: $3.26 \pm 0.33 \times 10^8$ cells

Laboratory growth conditions: 25 °C, up to 6 months

Culture medium: Bold 3N medium

Sample photograph:

Sample micrograph:

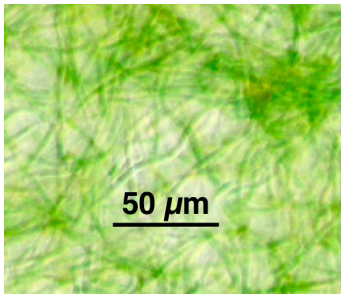

Sample reflectance spectrum:

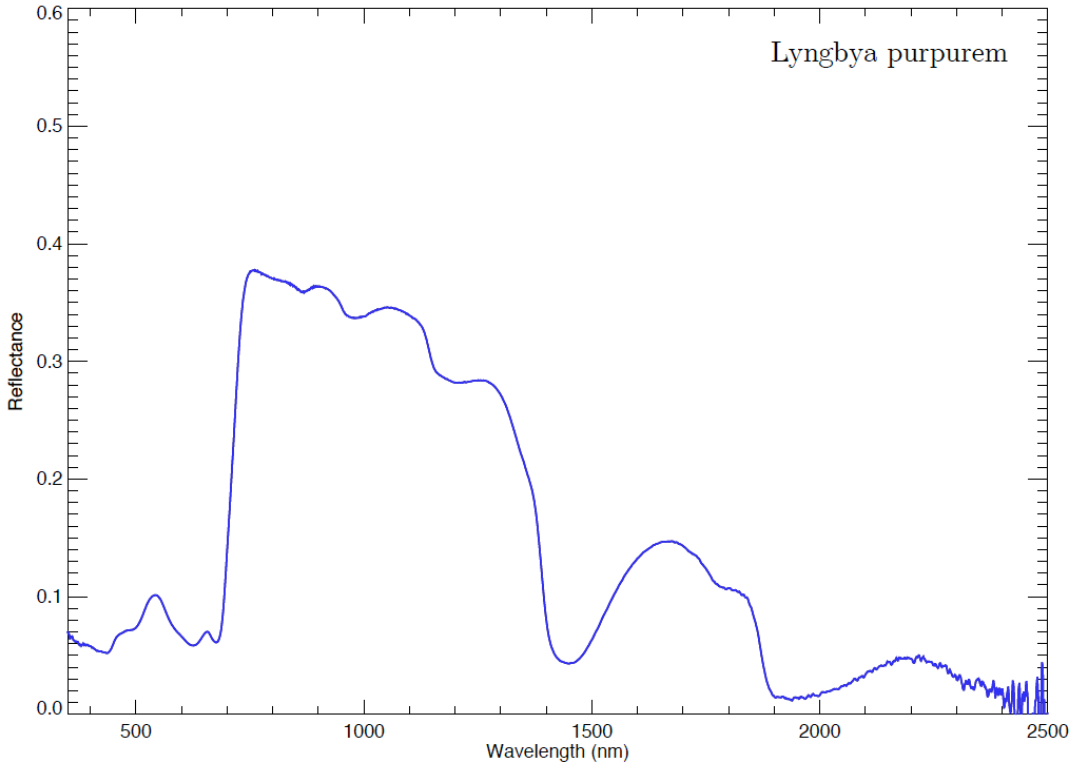

Methylobacterium sp._KM349880

Sample name: *Methylobacterium* sp.

Accession number for 16S rRNA partial gene sequence: KM349880

Classification: Bacteria; Proteobacteria; Alphaproteobacteria; Rhizobiales; Methylobacteriaceae; Methylobacterium

Metabolism: Heterotrophic

Origin: Moffett Field, CA, USA

Isolation: Ivan P. Lima (NPP at NASA Ames, CA, USA)

Sample concentration: 8.25×10^6 cells/ml

Sample count on filter substrate: $2.47 \pm 0.17 \times 10^7$ cells

Laboratory growth conditions: 30 °C, 180 rpm, 48 h

Culture medium: Reasoner's 2A (R2A)

Sample photograph:

Sample micrograph:

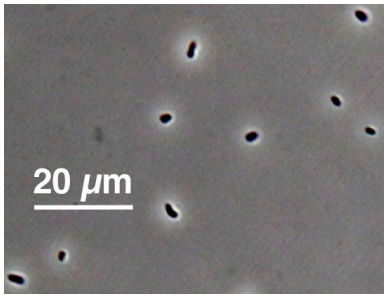

Sample reflectance spectrum:

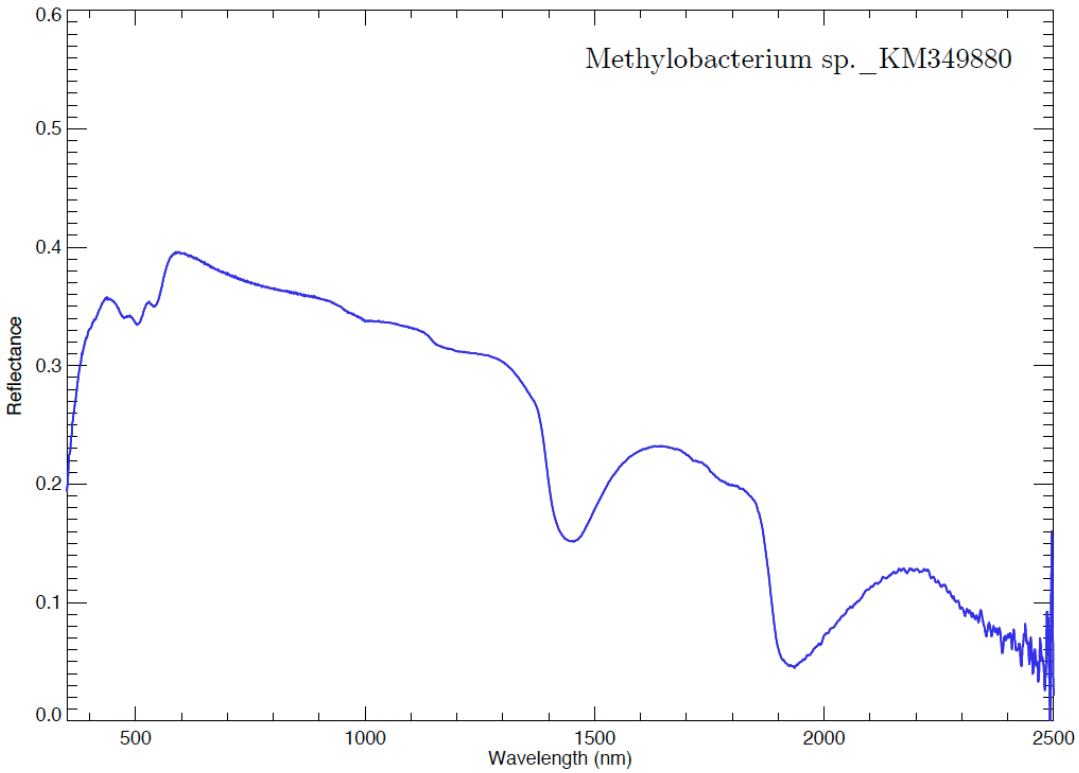

Methylobacterium sp._KM349881

Sample name: *Methylobacterium* sp.

Accession number for 16S rRNA partial gene sequence: KM349881

Classification: Bacteria; Proteobacteria; Alphaproteobacteria; Rhizobiales; Methylobacteriaceae; Methylobacterium

Metabolism: Heterotrophic

Origin: Moffett Field, CA, USA

Isolation: Ivan P. Lima (NPP at NASA Ames, CA, USA)

Sample concentration: 2.03 $\times$ 10^6 cells/ml

Sample count on filter substrate: 6.08 $\pm$ 0.41 $\times$ 10^6 cells

Laboratory growth conditions: 30 °C, 180 rpm, 48 h

Culture medium: Reasoner's 2A (R2A)

Sample photograph:

Sample micrograph:

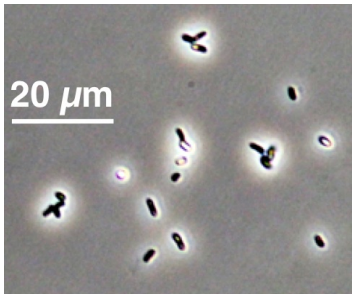

Sample reflectance spectrum:

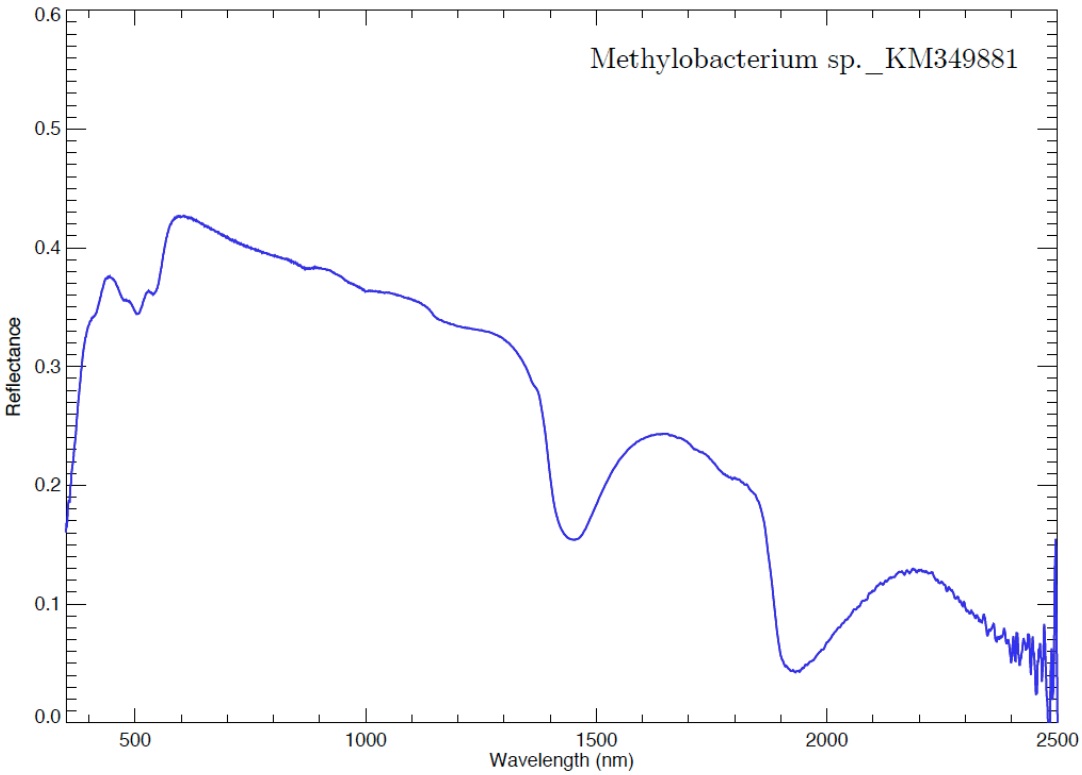

Methylobacterium sp._KM349885

Sample name: *Methylobacterium* sp.

Accession number for 16S rRNA partial gene sequence: KM349885

Classification: Bacteria; Proteobacteria; Alphaproteobacteria; Rhizobiales; Methylobacteriaceae; Methylobacterium

Metabolism: Heterotrophic

Origin: Atacama desert, Chile

Isolation: Ivan P. Lima (NPP at NASA Ames, CA, USA)

Sample concentration: 2.64 $\times$ 10^6 cells/ml

Sample count on filter substrate: 7.91 $\pm$ 0.53 $\times$ 10^6 cells

Laboratory growth conditions: 30 °C, 180 rpm, 48 h

Culture medium: Reasoner's 2A (R2A)

Sample photograph:

Sample micrograph:

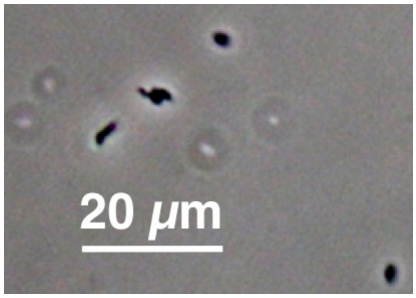

Sample reflectance spectrum:

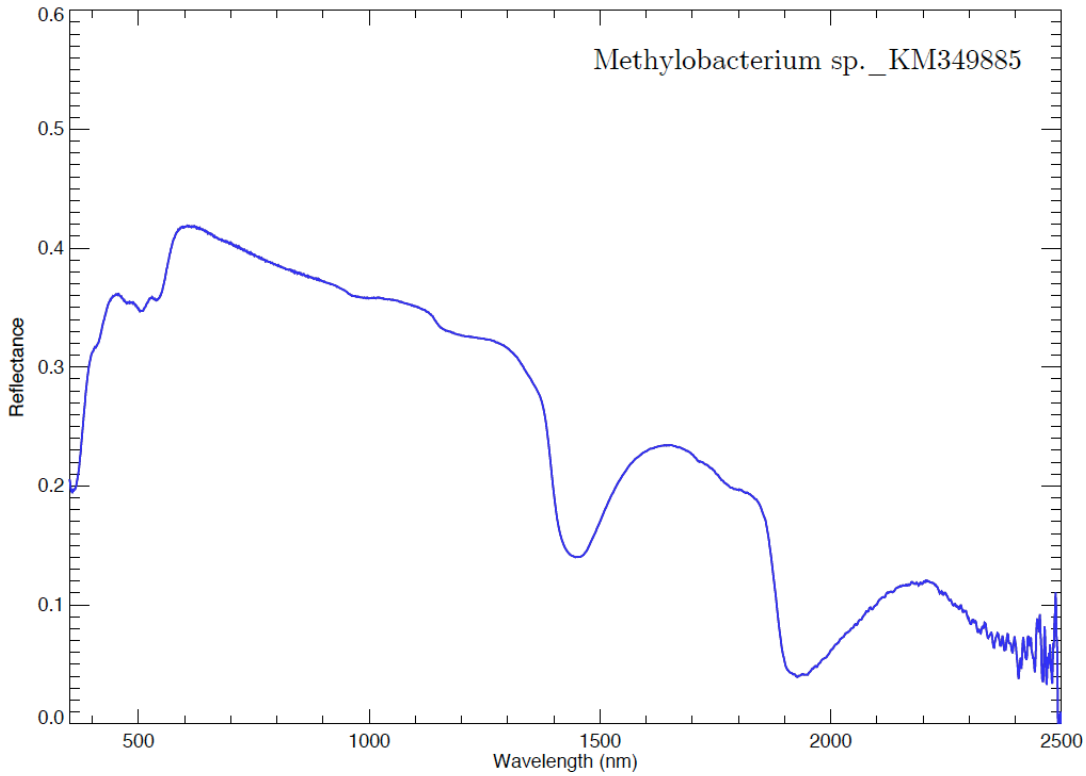

Microbacterium sp._KM349942

Sample name: *Microbacterium* sp.

Accession number for 16S rRNA partial gene sequence: KM349942

Classification: Bacteria; Actinobacteria; Actinobacteridae; Actinomycetales; Micrococcineae; Microbacteriaceae; Microbacterium

Metabolism: Heterotrophic

Origin: Atacama desert, Chile

Isolation: Ivan P. Lima (NPP at NASA Ames, CA, USA)

Sample concentration: 2.08×10^8 cells/ml

Sample count on filter substrate: $6.25 \pm 0.42 \times 10^8$ cells

Laboratory growth conditions: 30 °C, 180 rpm, 24 h

Culture medium: Marine Broth (MB)

Sample photograph:

Sample micrograph:

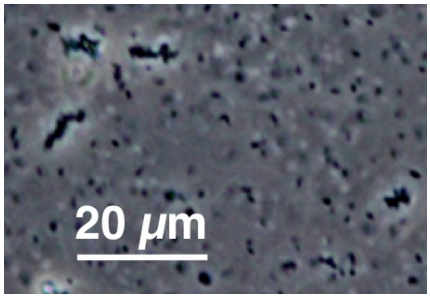

Sample reflectance spectrum:

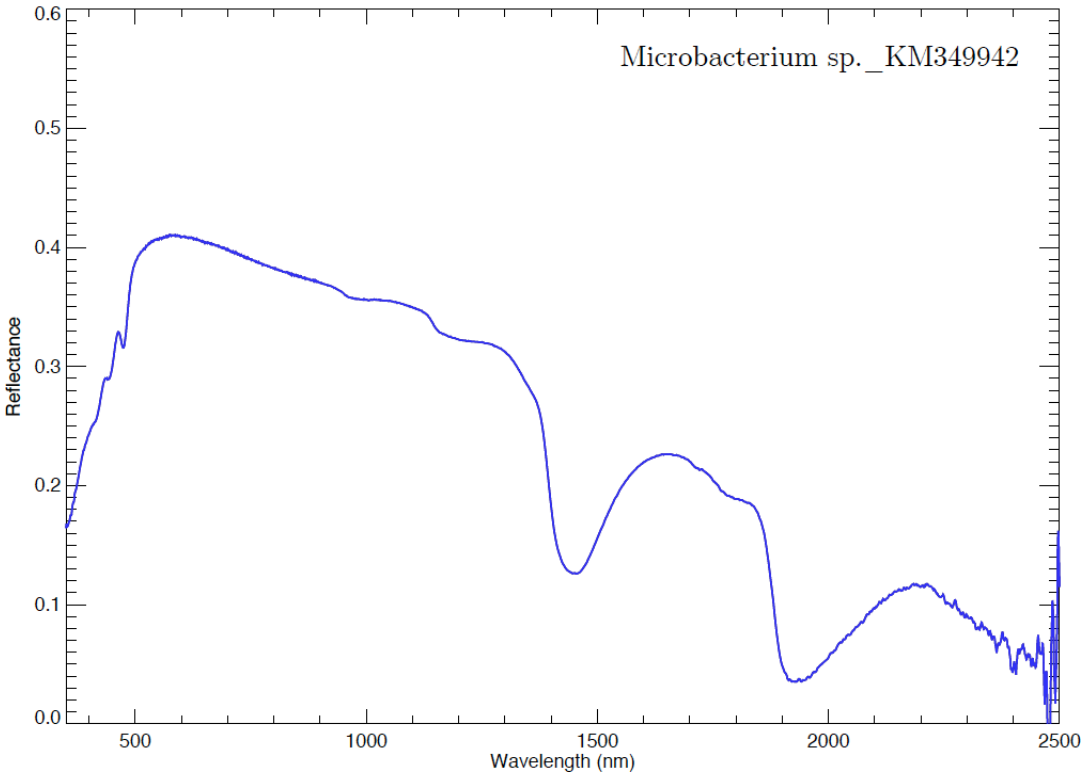

Micrococcaceae_KM349922

Sample name: Micrococcaceae

Accession number for 16S rRNA partial gene sequence: KM349922

Classification: Bacteria; Actinobacteria; Actinobacteridae; Actinomycetales; Micrococcineae; Micrococcaceae

Metabolism: Heterotrophic

Origin: Sonoran desert, AZ, USA

Isolation: Ivan P. Lima (NPP at NASA Ames, CA, USA)

Sample concentration: 4.03×10^7 cells/ml

Sample count on filter substrate: $1.21 \pm 0.08 \times 10^8$ cells

Laboratory growth conditions: 30 °C, 180 rpm, 24 h

Culture medium: Reasoner's 2A (R2A)

Sample photograph:

Sample micrograph:

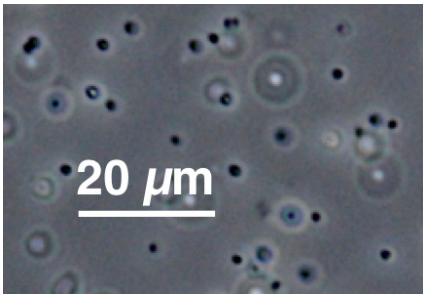

Sample reflectance spectrum:

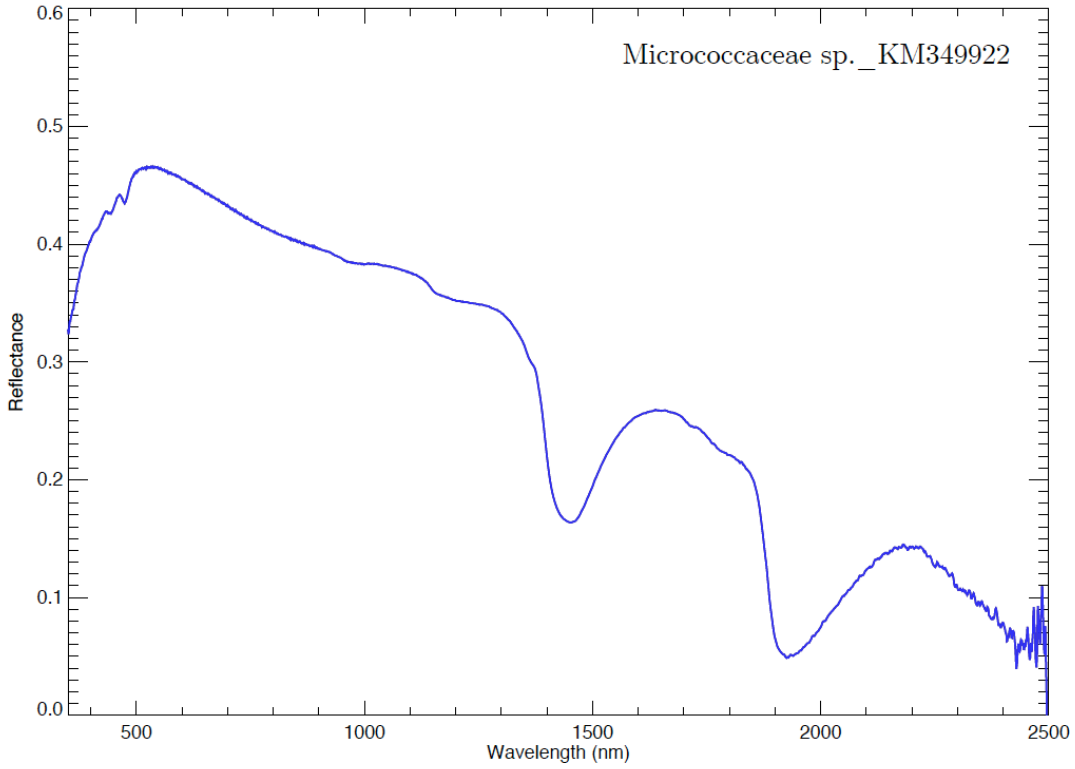

Nannochloropsis oculata

Sample name: *Nannochloropsis oculata*

Accession number for 16S rRNA partial gene sequence: Not available

Classification: Eukaryota; Ochrophyta; Eustigmatophyceae; Eustigmatales; Monodopsidaceae; Nannochloropsis

Metabolism: Autotrophic (oxygenic photosynthesis)

Origin: Brackish rockpool, Isle of Cumbrae, Scotland

Collection: UTEX (TX, USA)

Sample concentration: 6.62×10^6 cells/ml

Sample count on filter substrate: $6.62 \pm 0.66 \times 10^7$ cells

Laboratory growth conditions: 25 °C, up to 6 months

Culture medium: Artificial Seawater medium

Sample photograph:

Sample micrograph:

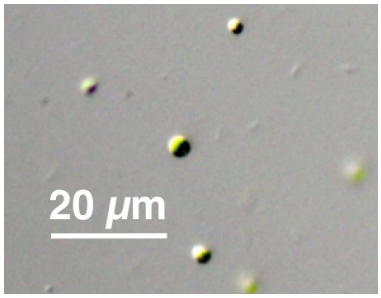

Sample reflectance spectrum:

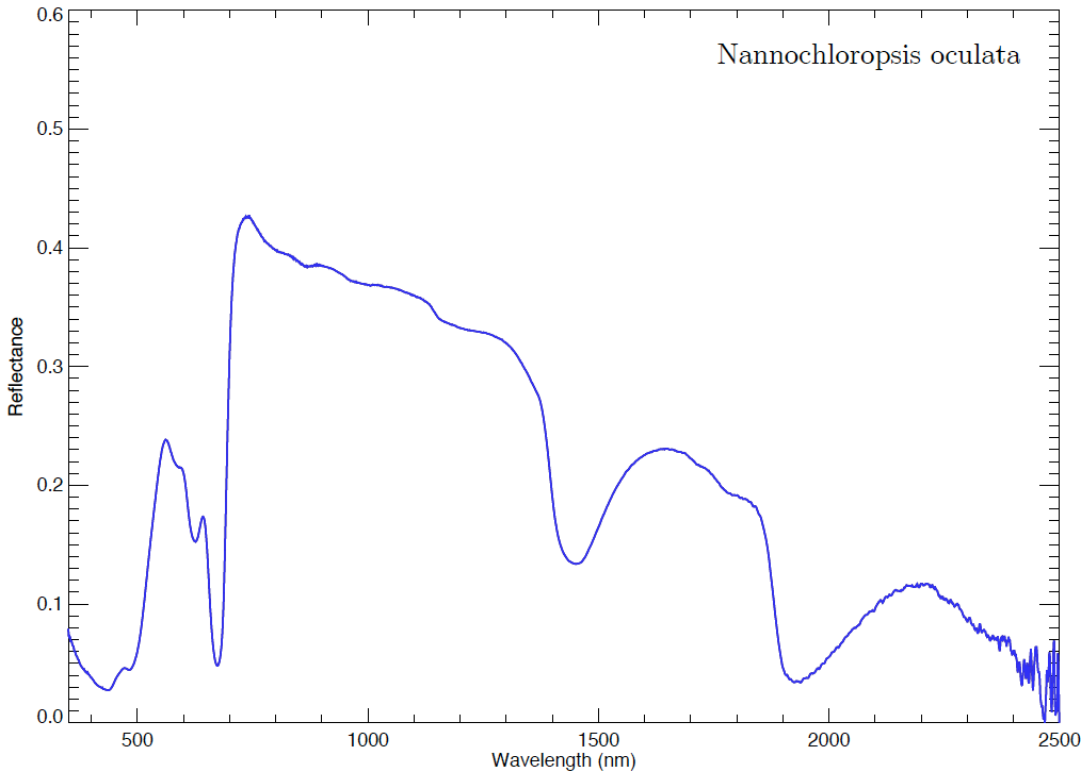

Nocardioides sp._KM349960

Sample name: *Nocardioides* sp.

Accession number for 16S rRNA partial gene sequence: KM349960

Classification: Bacteria; Actinobacteria; Actinobacteridae; Actinomycetales; Propionibacterineae; Nocardioidaceae; Nocardioides

Metabolism: Heterotrophic

Origin: Atacama desert, Chile

Isolation: Ivan P. Lima (NPP at NASA Ames, CA, USA)

Sample concentration: 5.04×10^7 cells/ml

Sample count on filter substrate: $1.51 \pm 0.10 \times 10^8$ cells

Laboratory growth conditions: 30 °C, 180 rpm, 24 h

Culture medium: Reasoner's 2A (R2A)

Sample photograph:

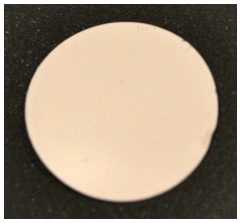

Sample micrograph:

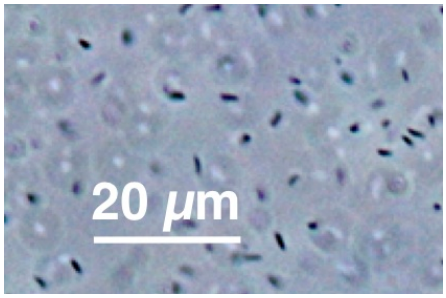

Sample reflectance spectrum:

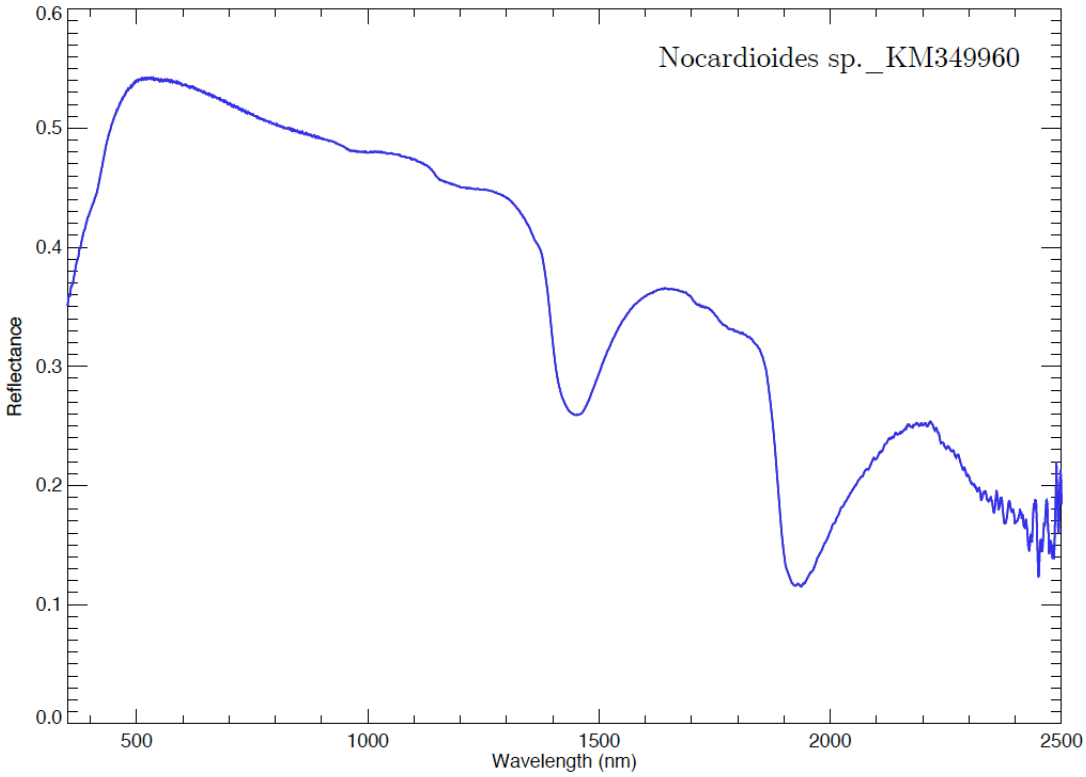

Oocystis minuta

Sample name: *Oocystis minuta*

Accession number for 16S rRNA partial gene sequence: Not available

Classification: Eukaryota; Chlorophyta; Trebouxiophyceae; Chlorellales; Oocystaceae; Oocystis

Metabolism: Autotrophic (oxygenic photosynthesis)

Origin: Oyster Pond, Martha's Vineyard, MA, USA

Collection: UTEX (TX, USA)

Sample concentration: 4.06×10^5 cells/ml

Sample count on filter substrate: $4.06 \pm 0.41 \times 10^6$ cells

Laboratory growth conditions: 25 °C, up to 6 months

Culture medium: Bold 3N medium

Sample photograph:

Sample micrograph:

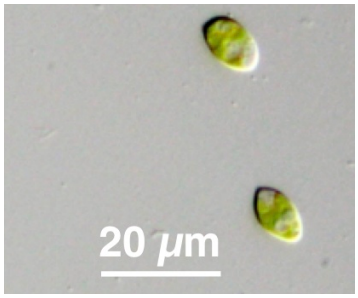

Sample reflectance spectrum:

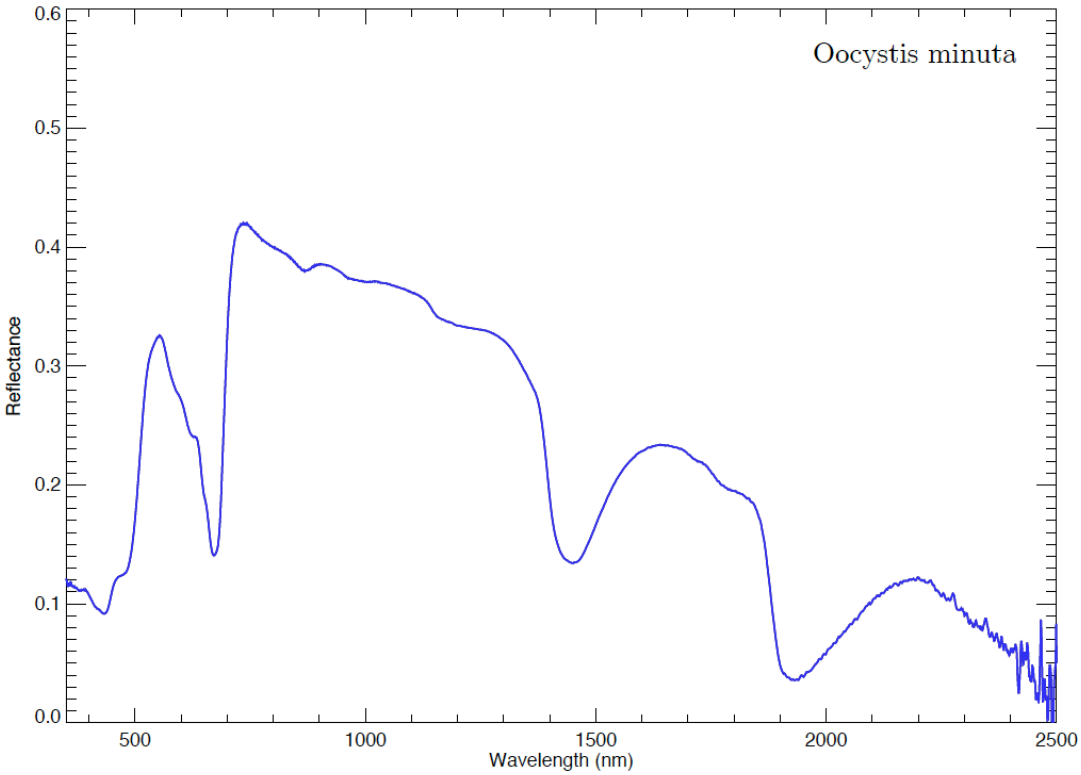

Paracoccus sp._KM349912

Sample name: *Paracoccus* sp.

Accession number for 16S rRNA partial gene sequence: KM349912

Classification: Bacteria; Proteobacteria; Alphaproteobacteria; Rhodobacterales; Rhodobacteraceae; Paracoccus

Metabolism: Heterotrophic

Origin: Sonoran desert, AZ, USA

Isolation: Ivan P. Lima (NPP at NASA Ames, CA, USA)

Sample concentration: 2.50×10^8 cells/ml

Sample count on filter substrate: $7.50 \pm 0.50 \times 10^8$ cells

Laboratory growth conditions: 30 °C, 180 rpm, 24 h

Culture medium: Marine Broth (MB)

Sample photograph:

Sample micrograph:

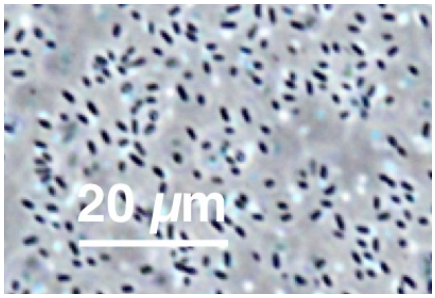

Sample reflectance spectrum:

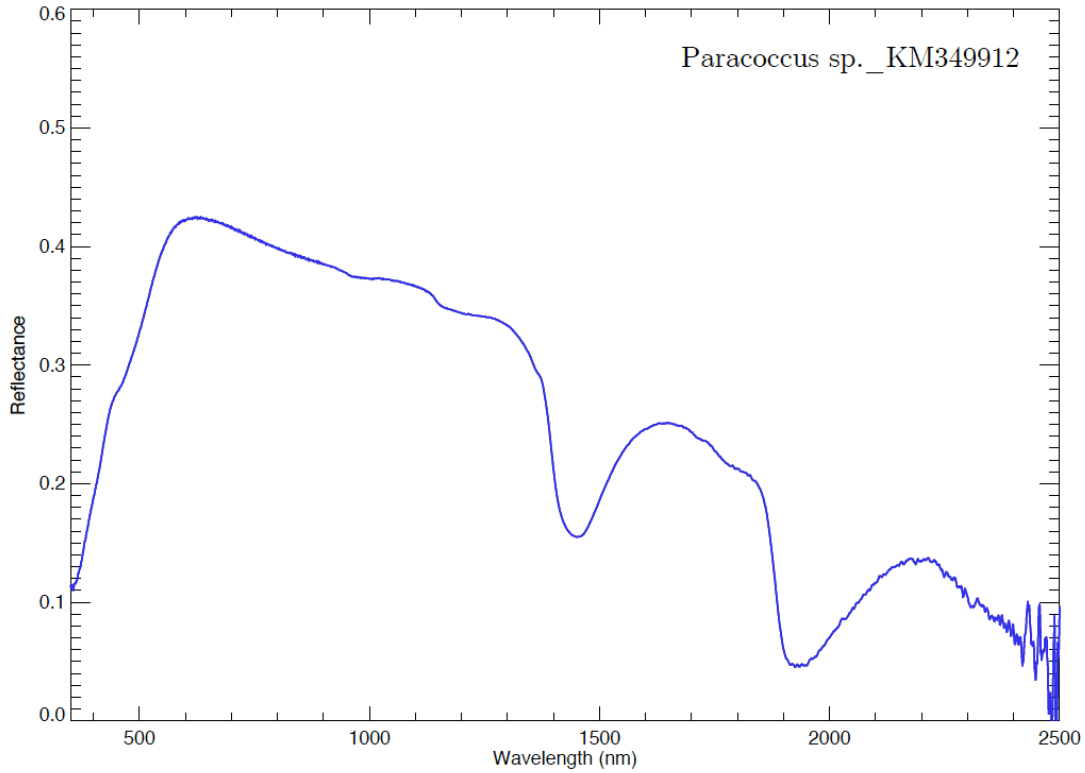

Pedobacter sp._KM349886

Sample name: *Pedobacter* sp.

Accession number for 16S rRNA partial gene sequence: KM349886

Classification: Bacteria; Bacteroidetes; Sphingobacteriia; Sphingobacteriales; Sphingobacteriaceae; Pedobacter

Metabolism: Heterotrophic

Origin: Atacama desert, Chile

Isolation: Ivan P. Lima (NPP at NASA Ames, CA, USA)

Sample concentration: 5.04×10^7 cells/ml

Sample count on filter substrate: $1.51 \pm 0.10 \times 10^8$ cells

Laboratory growth conditions: 30 °C, 180 rpm, 48 h

Culture medium: Lysogeny Broth (LB)

Sample photograph:

Sample micrograph:

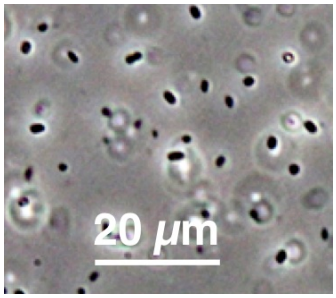

Sample reflectance spectrum:

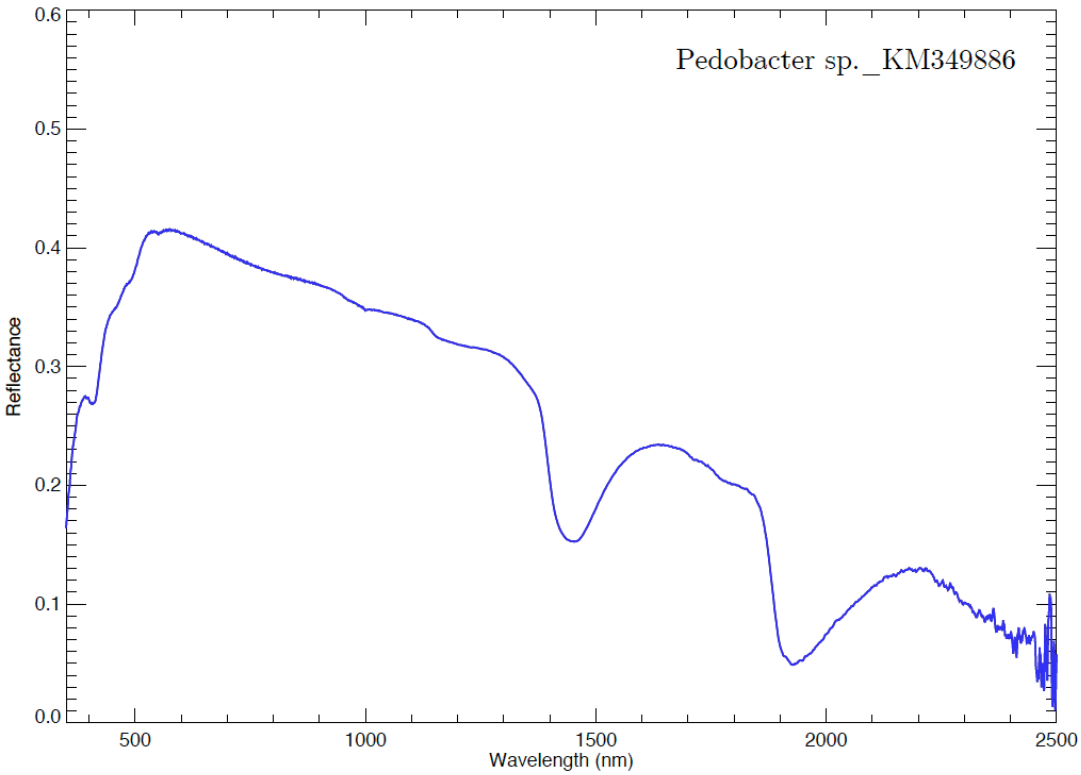

Phormidium inundatum

Sample name: *Phormidium inundatum*

Accession number for 16S rRNA partial gene sequence: Not available

Classification: Bacteria; Cyanobacteria; Cyanophyceae; Oscillatoriales; Phormidiaceae; Phormidium

Metabolism: Autotrophic (oxygenic photosynthesis)

Origin: Thermal water, France

Collection: UTEX (TX, USA)

Sample concentration: 1.42×10^6 cells/ml

Sample count on filter substrate: $1.42 \pm 0.14 \times 10^7$ cells

Laboratory growth conditions: 25 °C, up to 6 months

Culture medium: Modified Bold 3N medium

Sample photograph:

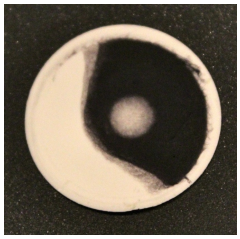

Sample micrograph:

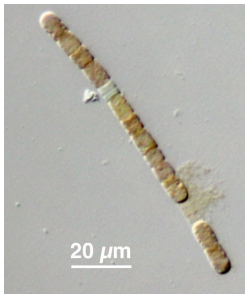

Sample reflectance spectrum:

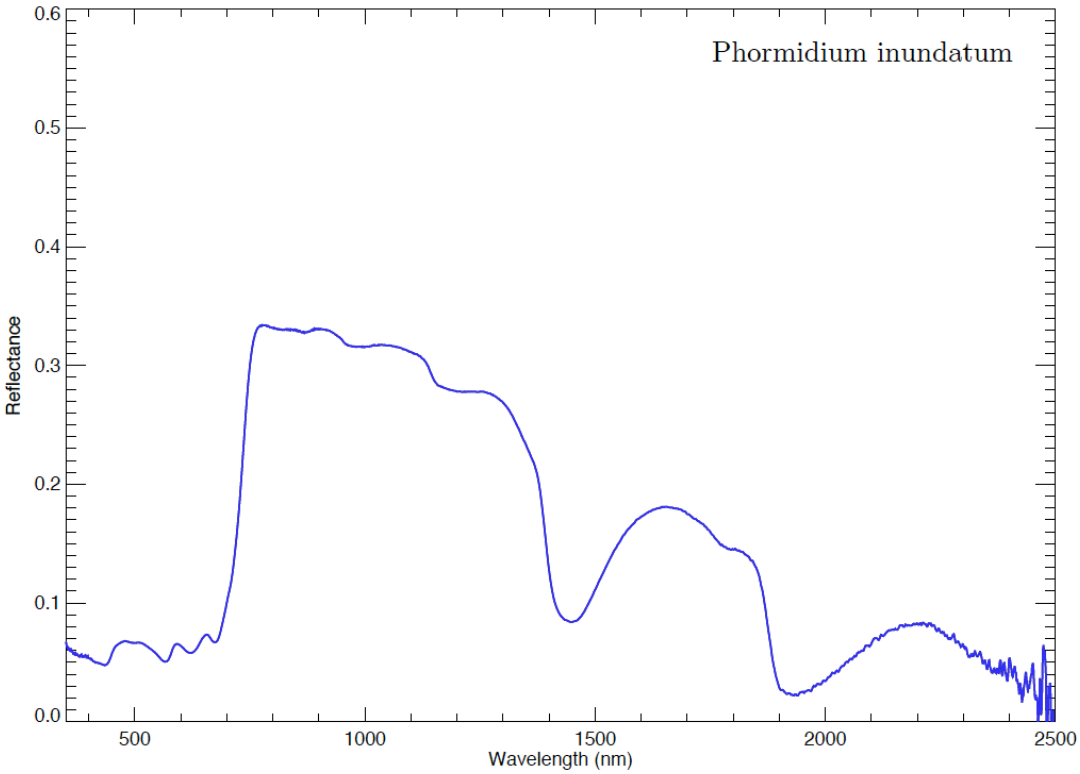

Phormidium sp.

Sample name: *Phormidium* sp.

Accession number for 16S rRNA partial gene sequence: Not available

Classification: Bacteria; Cyanobacteria; Cyanophyceae; Oscillatoriales; Phormidiaceae; Phormidium

Metabolism: Autotrophic (oxygenic photosynthesis)

Origin: Kamori Channel, Palau, W.C.I.

Collection: UTEX (TX, USA)

Sample concentration: 5.41×10^5 cells/ml

Sample count on filter substrate: $5.41 \pm 0.54 \times 10^6$ cells

Laboratory growth conditions: 25 °C, up to 6 months

Culture medium: Enriched Seawater medium

Sample photograph:

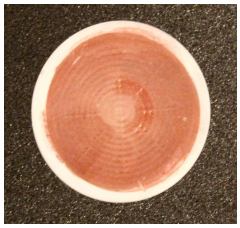

Sample micrograph:

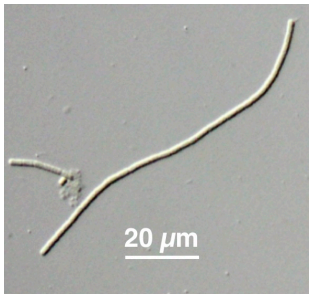

Sample reflectance spectrum:

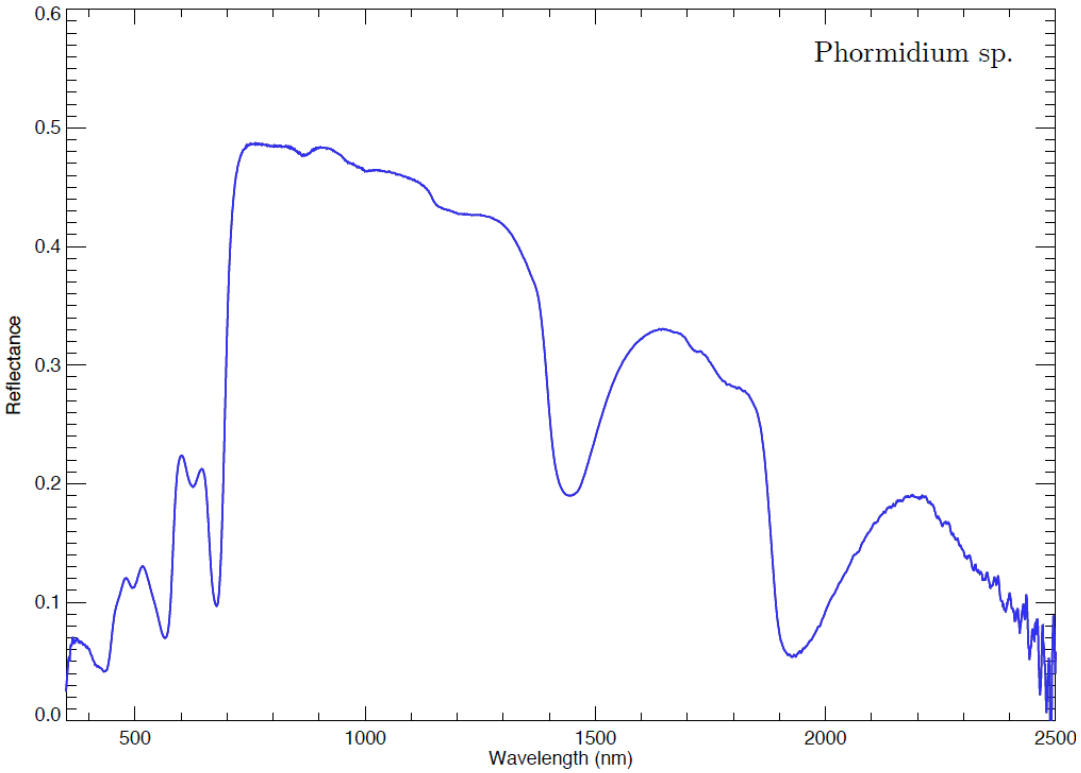

Planococcaceae_KM349897

Sample name: Planococcaceae

Accession number for 16S rRNA partial gene sequence: KM349897

Classification: Bacteria; Firmicutes; Bacilli; Bacillales; Planococcaceae

Metabolism: Heterotrophic

Origin: Atacama desert, Chile

Isolation: Ivan P. Lima (NPP at NASA Ames, CA, USA)

Sample concentration: 3.29 $\times$ 10^7 cells/ml

Sample count on filter substrate: 9.86 $\pm$ 0.66 $\times$ 10^7 cells

Laboratory growth conditions: 30 °C, 180 rpm, 24 h

Culture medium: Lysogeny Broth (LB)

Sample photograph:

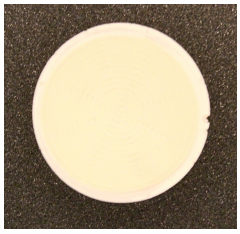

Sample micrograph:

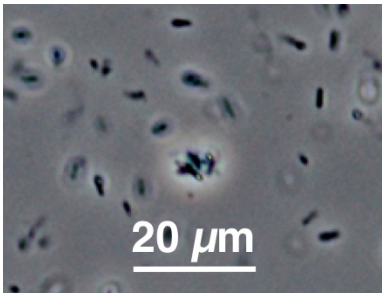

Sample reflectance spectrum:

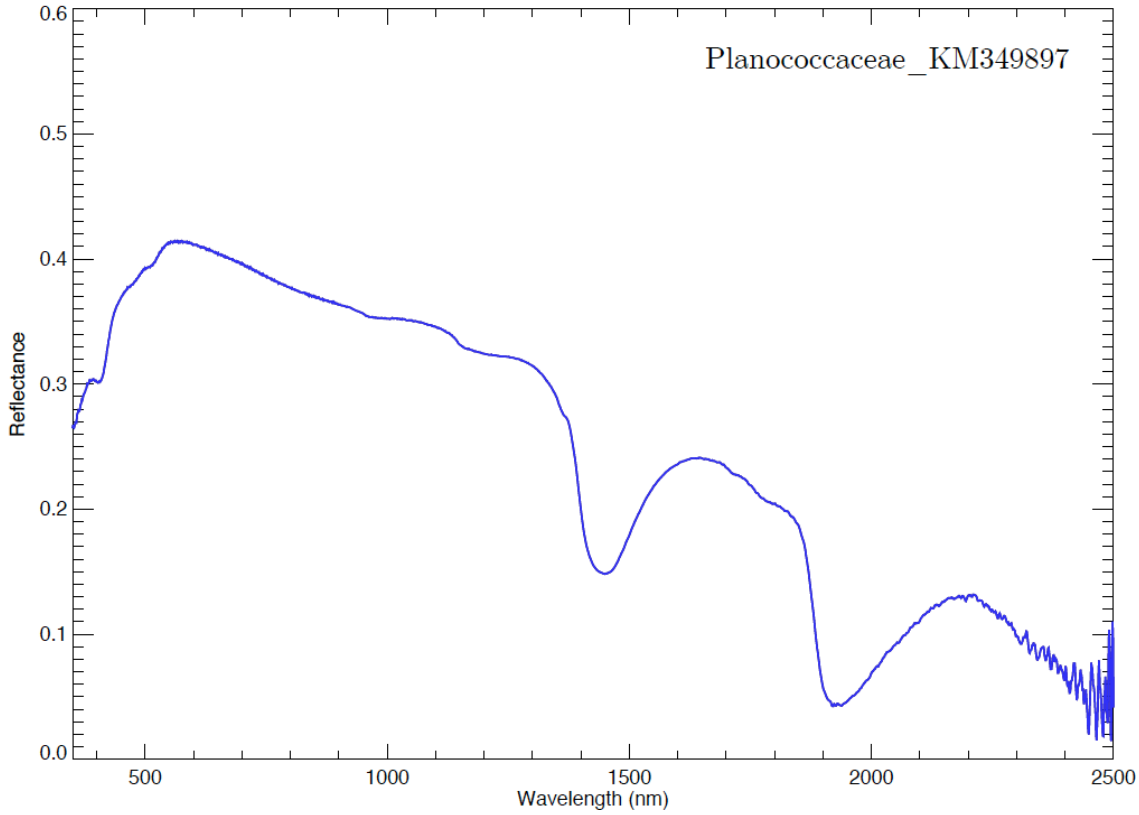

Planococcaceae_KM349910

Sample name: Planococcaceae

Accession number for 16S rRNA partial gene sequence: KM349910

Classification: Bacteria; Firmicutes; Bacilli; Bacillales; Planococcaceae

Metabolism: Heterotrophic

Origin: Sonoran desert, AZ, USA

Isolation: Ivan P. Lima (NPP at NASA Ames, CA, USA)

Sample concentration: 6.86 $\times$ 10^7 cells/ml

Sample count on filter substrate: 2.06 $\pm$ 0.14 $\times$ 10^8 cells

Laboratory growth conditions: 30 °C, 180 rpm, 24 h

Culture medium: Marine Broth (MB)

Sample photograph:

Sample micrograph:

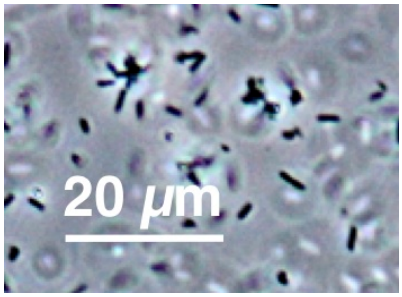

Sample reflectance spectrum:

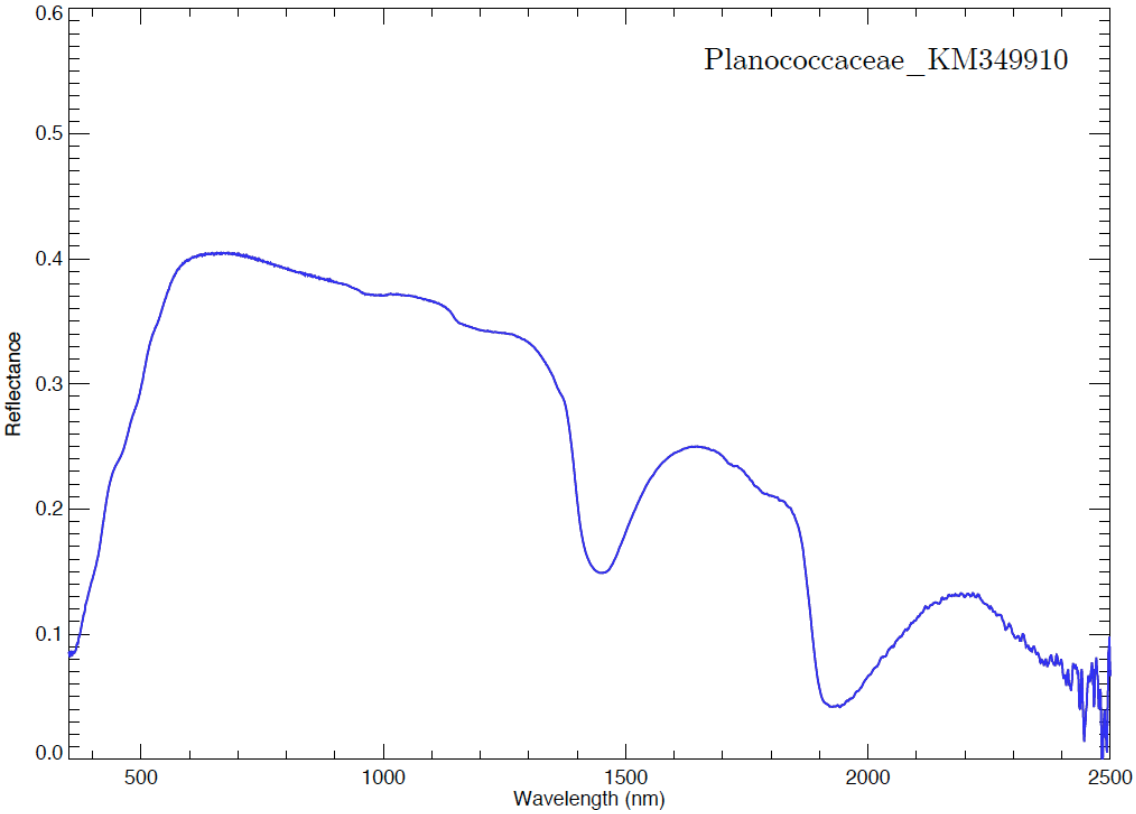

Planococcaceae_KM349932

Sample name: Planococcaceae

Accession number for 16S rRNA partial gene sequence: KM349932

Classification: Bacteria; Firmicutes; Bacilli; Bacillales; Planococcaceae

Metabolism: Heterotrophic

Origin: Atacama desert, Chile

Isolation: Ivan P. Lima (NPP at NASA Ames, CA, USA)

Sample concentration: 6.03 $\times$ 10^7 cells/ml

Sample count on filter substrate: 1.81 $\pm$ 0.12 $\times$ 10^8 cells

Laboratory growth conditions: 30 °C, 180 rpm, 24 h

Culture medium: Marine Broth (MB)

Sample photograph:

Sample micrograph:

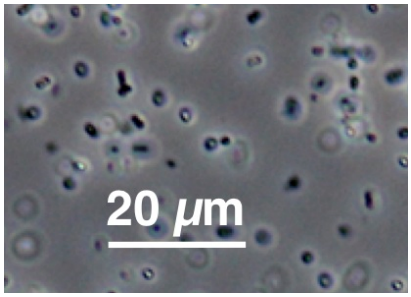

Sample reflectance spectrum:

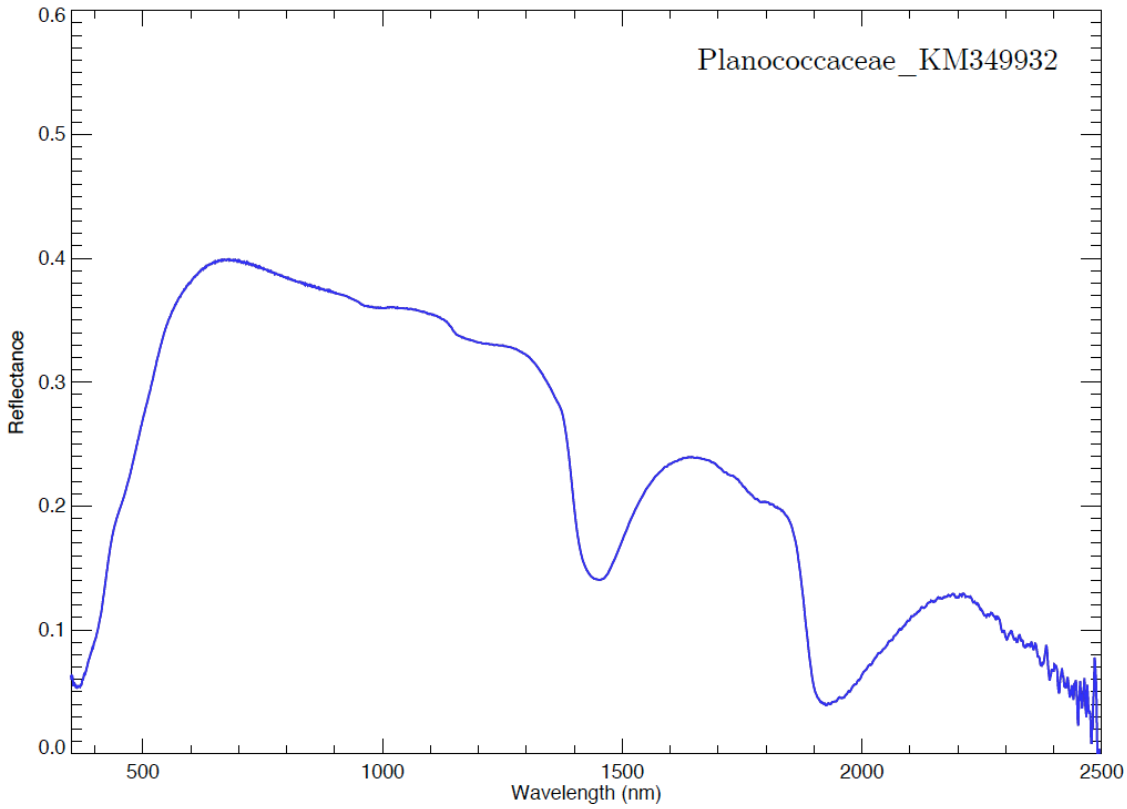

Planococcaceae_KM349933

Sample name: Planococcaceae

Accession number for 16S rRNA partial gene sequence: KM349933

Classification: Bacteria; Firmicutes; Bacilli; Bacillales; Planococcaceae

Metabolism: Heterotrophic

Origin: Atacama desert, Chile

Isolation: Ivan P. Lima (NPP at NASA Ames, CA, USA)

Sample concentration: 6.15×10^7 cells/ml

Sample count on filter substrate: $1.85 \pm 0.12 \times 10^8$ cells

Laboratory growth conditions: 30 °C, 180 rpm, 24 h

Culture medium: Marine Broth (MB)

Sample photograph:

Sample micrograph:

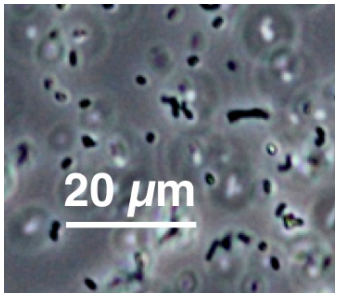

Sample reflectance spectrum:

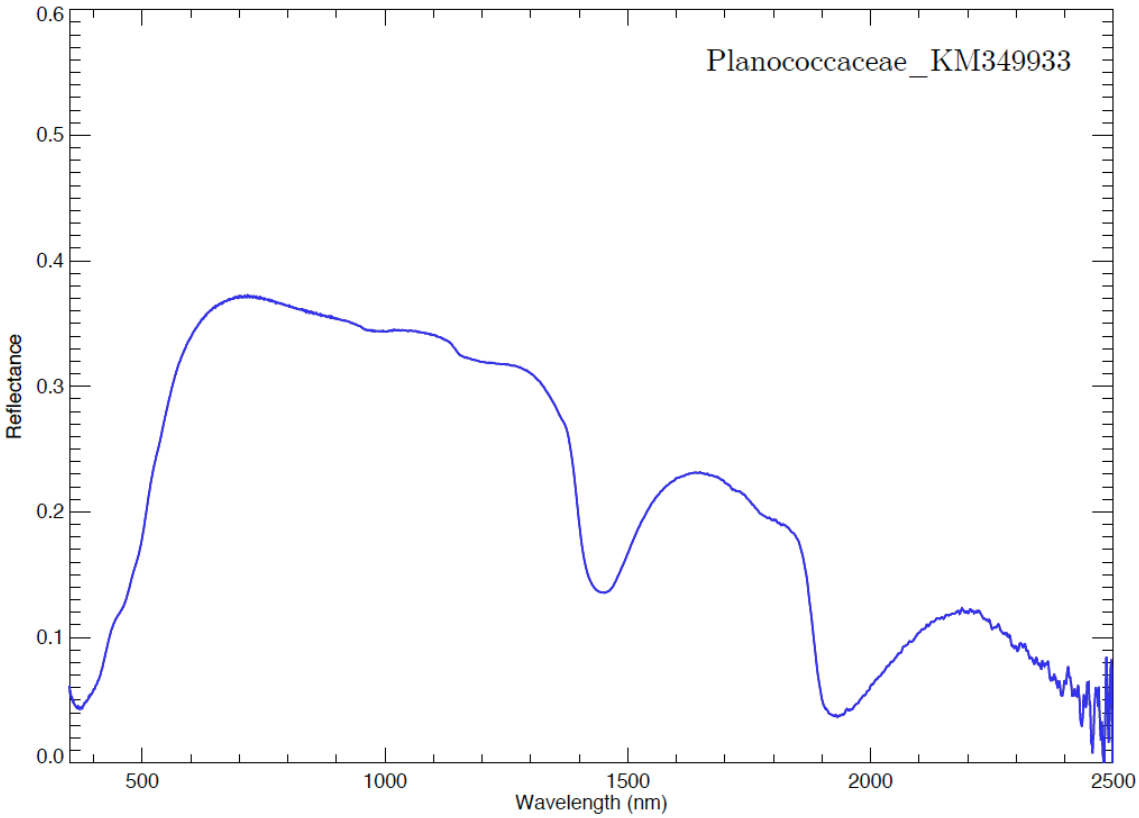

Planococcaceae_KM349955

Sample name: Planococcaceae

Accession number for 16S rRNA partial gene sequence: KM349955

Classification: Bacteria; Firmicutes; Bacilli; Bacillales; Planococcaceae

Metabolism: Heterotrophic

Origin: Atacama desert, Chile

Isolation: Ivan P. Lima (NPP at NASA Ames, CA, USA)

Sample concentration: 5.83×10^7 cells/ml

Sample count on filter substrate: $1.75 \pm 0.12 \times 10^8$ cells

Laboratory growth conditions: 30 °C, 180 rpm, 24 h

Culture medium: Marine Broth (MB)

Sample photograph:

Sample micrograph:

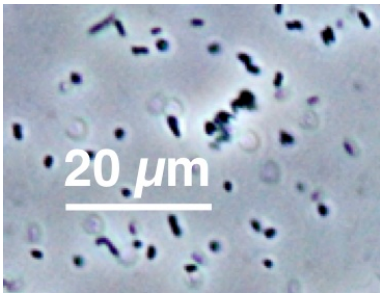

Sample reflectance spectrum:

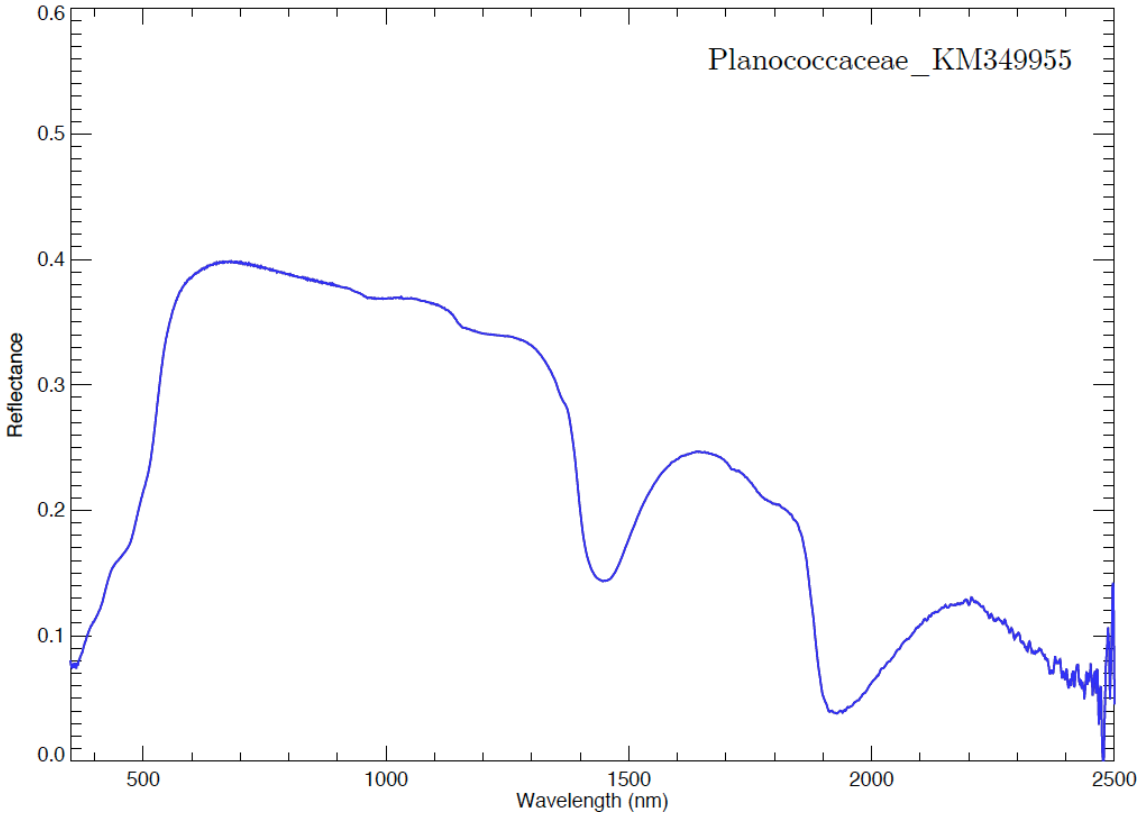

Planomicrobium sp._KM349904

Sample name: *Planomicrobium* sp.

Accession number for 16S rRNA partial gene sequence: KM349904

Classification: Bacteria; Firmicutes; Bacilli; Bacillales; Planococcaceae; Planomicrobium

Metabolism: Heterotrophic

Origin: Sonoran desert, AZ, USA

Isolation: Ivan P. Lima (NPP at NASA Ames, CA, USA)

Sample concentration: 6.31 $\times$ 10^7 cells/ml

Sample count on filter substrate: 1.89 $\pm$ 0.13 $\times$ 10^8 cells

Laboratory growth conditions: 30 °C, 180 rpm, 24 h

Culture medium: Marine Broth (MB)

Sample photograph:

Sample micrograph:

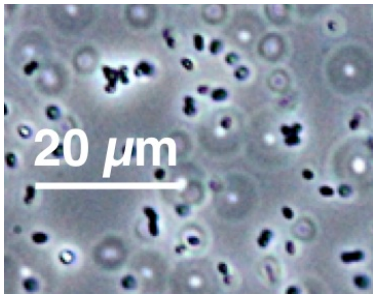

Sample reflectance spectrum:

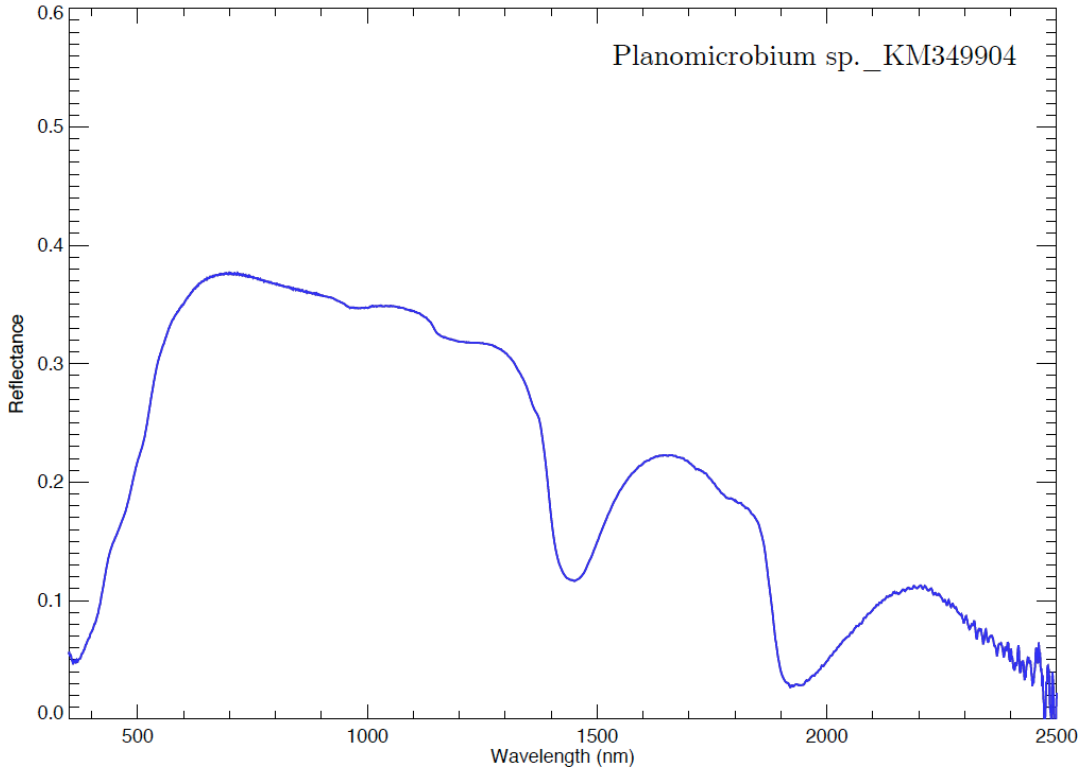

Pontibacter sp._KM349890

Sample name: *Pontibacter* sp.

Accession number for 16S rRNA partial gene sequence: KM349890

Classification: Bacteria; Bacteroidetes; Cytophagia; Cytophagales; Cytophagaceae; Pontibacter

Metabolism: Heterotrophic

Origin: Atacama desert, Chile

Isolation: Ivan P. Lima (NPP at NASA Ames, CA, USA)

Sample concentration: 2.14 $\times$ 10^7 cells/ml

Sample count on filter substrate: 6.43 $\pm$ 0.43 $\times$ 10^7 cells

Laboratory growth conditions: 30 °C, 180 rpm, 24 h

Culture medium: Marine Broth (MB)

Sample photograph:

Sample micrograph:

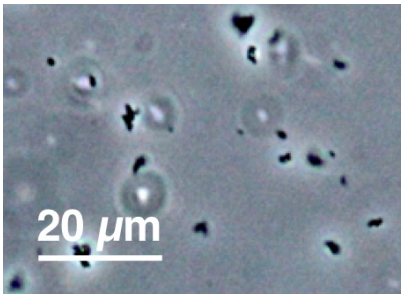

Sample reflectance spectrum:

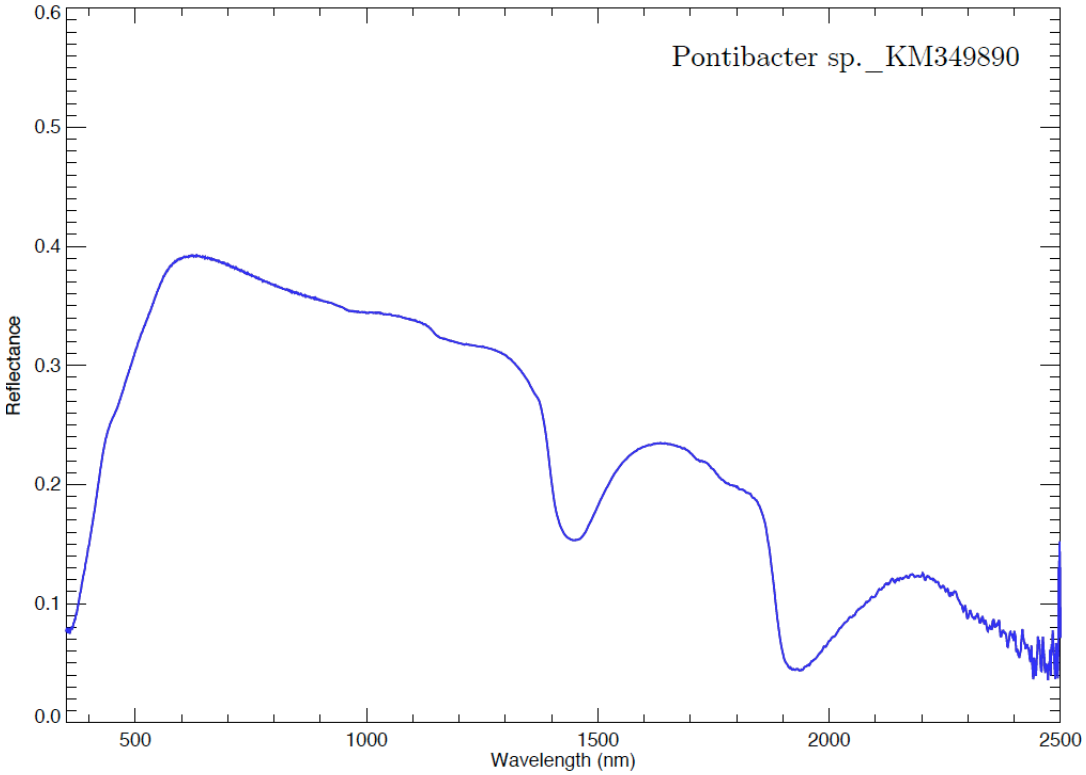

Pontibacter sp._KM349894

Sample name: *Pontibacter* sp.

Accession number for 16S rRNA partial gene sequence: KM349894

Classification: Bacteria; Bacteroidetes; Cytophagia; Cytophagales; Cytophagaceae; Pontibacter

Metabolism: Heterotrophic

Origin: Atacama desert, Chile

Isolation: Ivan P. Lima (NPP at NASA Ames, CA, USA)

Sample concentration: 1.73 $\times$ 10^7 cells/ml

Sample count on filter substrate: 5.19 $\pm$ 0.35 $\times$ 10^7 cells

Laboratory growth conditions: 30 °C, 180 rpm, 24 h

Culture medium: Reasoner's 2A (R2A)

Sample photograph:

Sample micrograph:

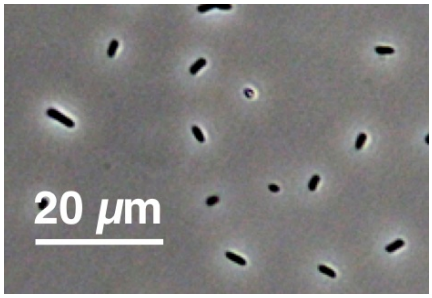

Sample reflectance spectrum:

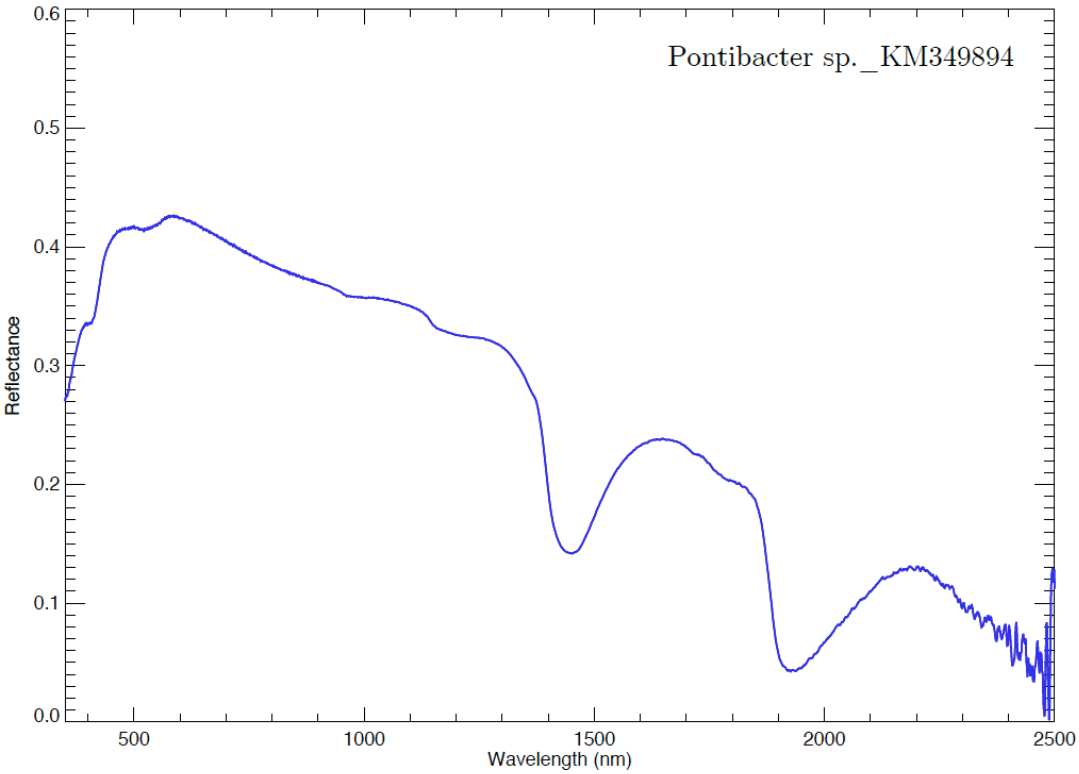

Porphyridium purpureum

Sample name: *Porphyridium purpureum*

Accession number for 16S rRNA partial gene sequence: Not available

Classification: Eukaryota; Rhodophyta; Porphyridiophyceae; Porphyridiales; Porphyridiaceae; Porphyridium

Metabolism: Autotrophic (oxygenic photosynthesis)

Origin: Old woodwork at salt spring, Boone's Lick State Park, MO, USA

Collection: UTEX (TX, USA)

Sample concentration: 1.49 $\times$ 10^6 cells/ml

Sample count on filter substrate: 1.49 $\pm$ 0.15 $\times$ 10^7 cells

Laboratory growth conditions: 25 °C, up to 6 months

Culture medium: Bold 1NV:Erdshreiber (1:1)

Sample photograph:

Sample micrograph:

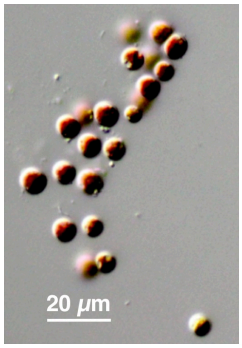

Sample reflectance spectrum:

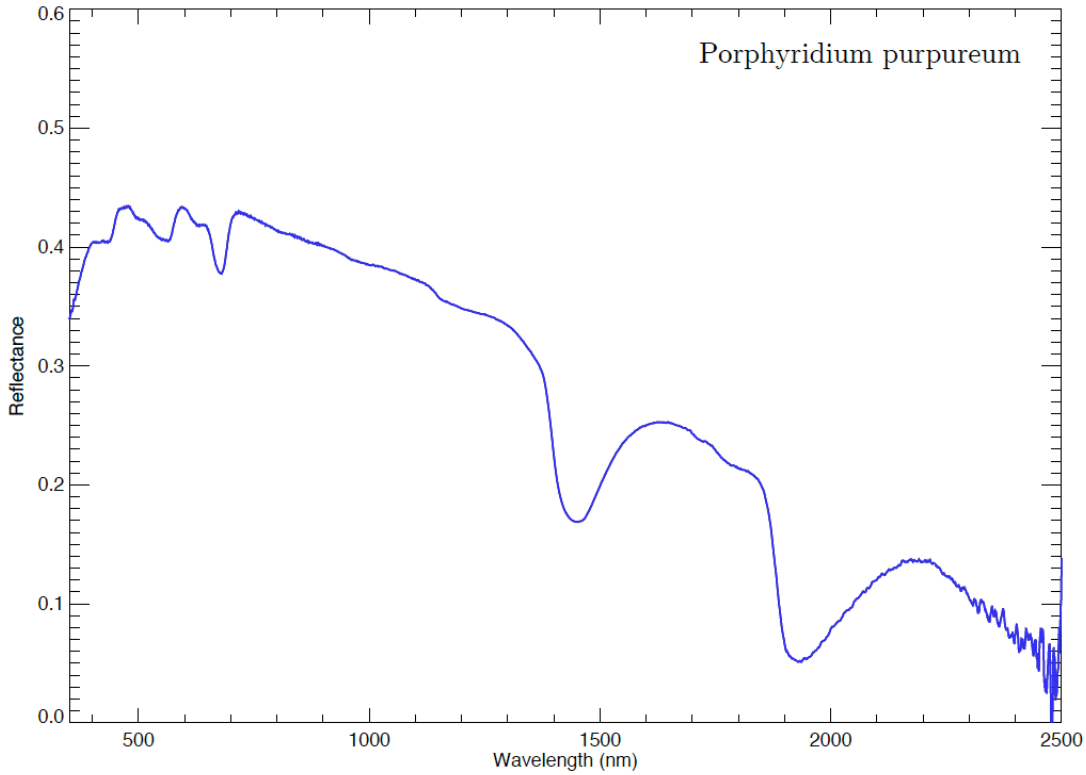

Prorocentrum micans

Sample name: *Prorocentrum micans*

Accession number for 16S rRNA partial gene sequence: Not available

Classification: Eukaryota; Dinophyta; Dinophyceae; Prorocentrales; Prorocentraceae; Prorocentrum

Metabolism: Autotrophic (oxygenic photosynthesis)

Origin: Santa Cruz Wharf, CA, USA

Collection: Kudela laboratory (UCSC, CA, USA)

Sample concentration: 6.76×10^4 cells/ml

Sample count on filter substrate: $6.76 \pm 0.68 \times 10^5$ cells

Laboratory growth conditions: 25 °C, up to 6 months

Culture medium: Enriched Seawater medium (L1)

Sample photograph:

Sample micrograph:

Sample reflectance spectrum:

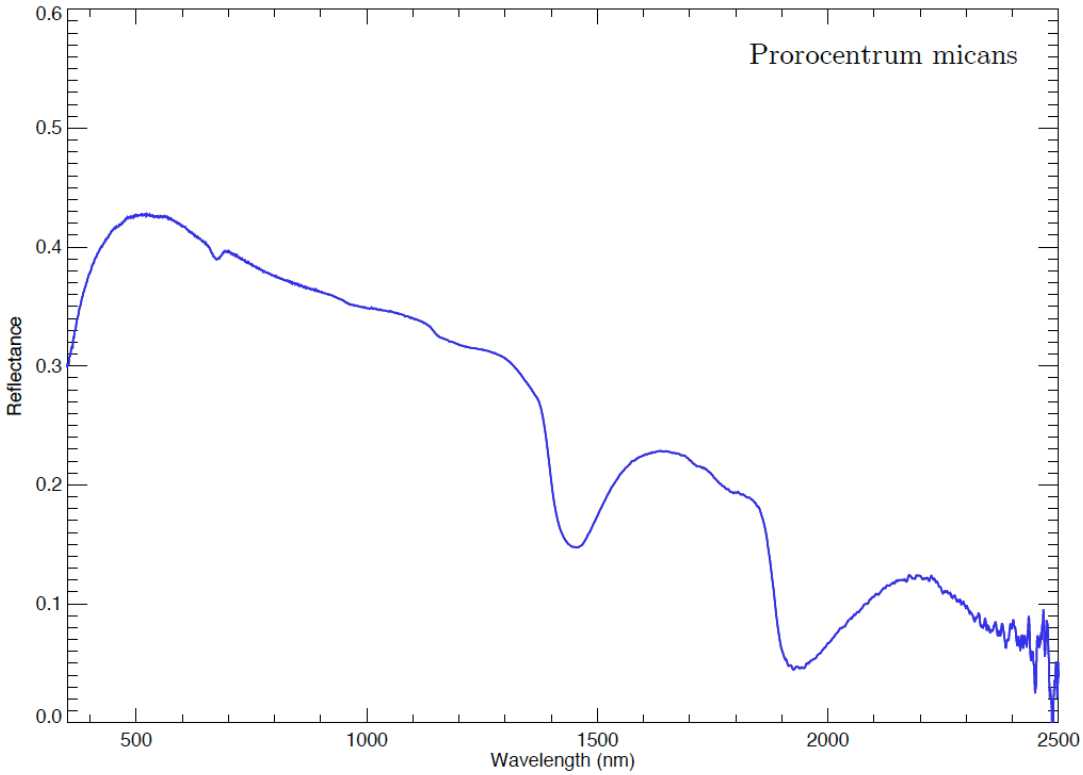

Ramlibacter sp._KM349961

Sample name: *Ramlibacter* sp.

Accession number for 16S rRNA partial gene sequence: KM349961

Classification: Bacteria; Proteobacteria; Betaproteobacteria; Burkholderiales; Comamonadaceae; Ramlibacter

Metabolism: Heterotrophic

Origin: Atacama desert, Chile

Isolation: Ivan P. Lima (NPP at NASA Ames, CA, USA)

Sample concentration: 5.55×10^7 cells/ml

Sample count on filter substrate: $1.66 \pm 0.11 \times 10^8$ cells

Laboratory growth conditions: 30 °C, 180 rpm, 24 h

Culture medium: Reasoner's 2A (R2A)

Sample photograph:

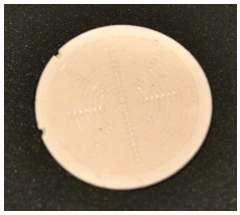

Sample micrograph:

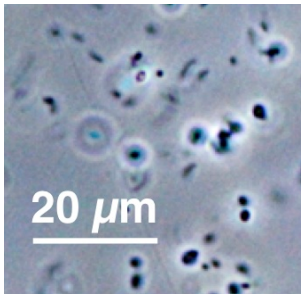

Sample reflectance spectrum:

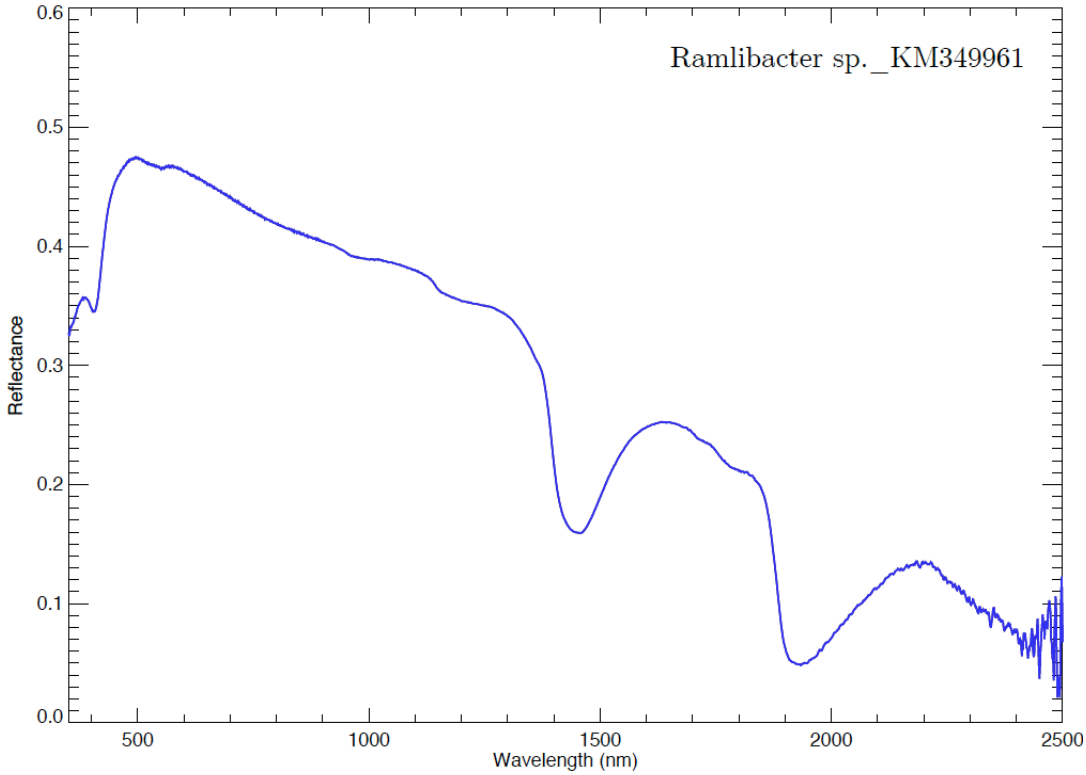

Rhodococcus sp._KM349949

Sample name: *Rhodococcus* sp.

Accession number for 16S rRNA partial gene sequence: KM349949

Classification: Bacteria; Actinobacteria; Actinobacteridae; Actinomycetales; Corynebacterineae; Nocardiaceae; Rhodococcus

Metabolism: Heterotrophic

Origin: Atacama desert, Chile

Isolation: Ivan P. Lima (NPP at NASA Ames, CA, USA)

Sample concentration: 2.43 $\times$ 10^7 cells/ml

Sample count on filter substrate: 7.30 $\pm$ 0.49 $\times$ 10^7 cells

Laboratory growth conditions: 30 °C, 180 rpm, 48 h

Culture medium: Lysogeny Broth (LB)

Sample photograph:

Sample micrograph:

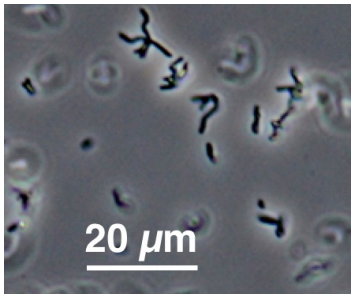

Sample reflectance spectrum:

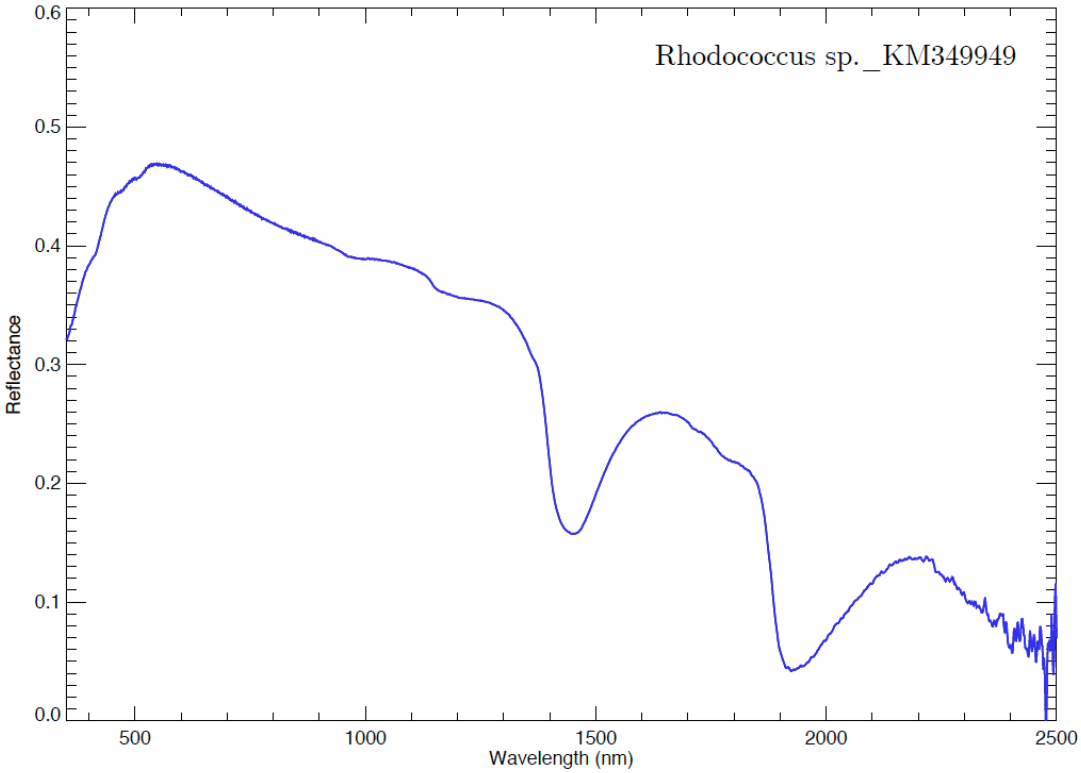

Rhodosorus marinus

Sample name: *Rhodosorus marinus*

Accession number for 16S rRNA partial gene sequence: Not available

Classification: Eukaryota; Rhodophyta; Stylonematophyceae; Stylonematales; Stylonemataceae; Rhodosorus

Metabolism: Autotrophic (oxygenic photosynthesis)

Origin: Seawater culture, Hawaii, USA

Collection: UTEX (TX, USA)

Sample concentration: 8.79×10^6 cells/ml

Sample count on filter substrate: $8.79 \pm 0.88 \times 10^7$ cells

Laboratory growth conditions: 25 °C, up to 6 months

Culture medium: Erdschreiber's medium

Sample photograph:

Sample micrograph:

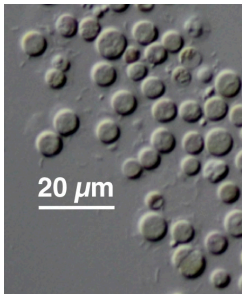

Sample reflectance spectrum:

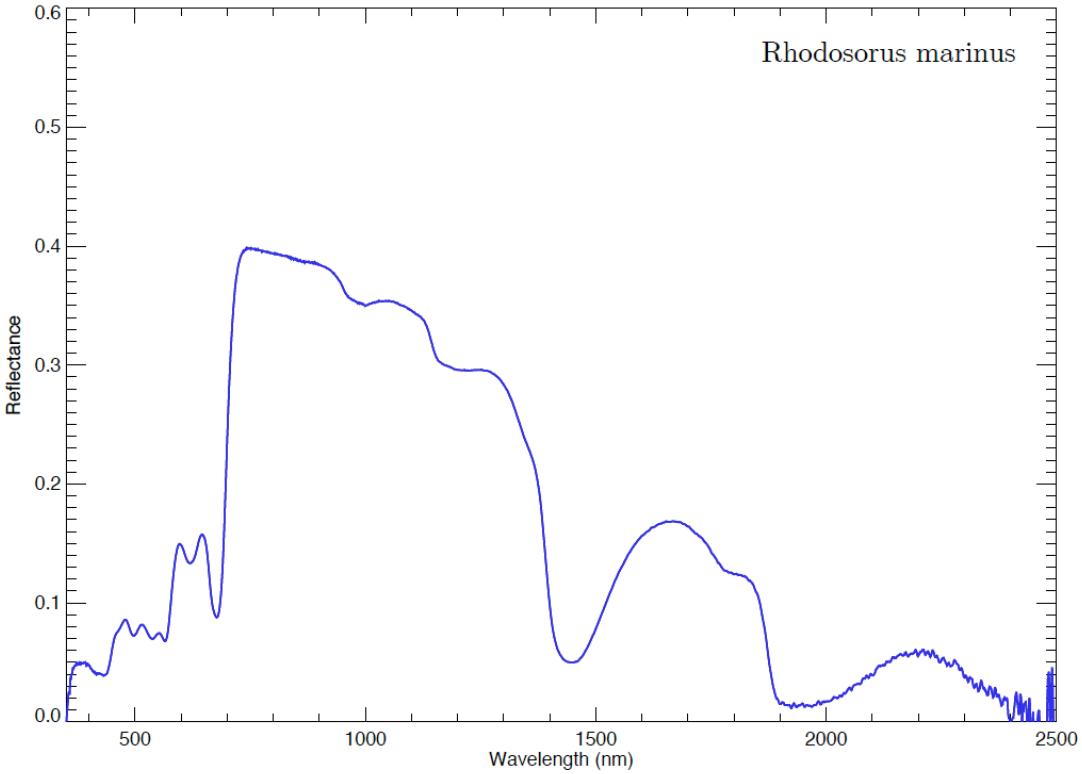

Spirulina platensis

Sample name: *Spirulina platensis*

Accession number for 16S rRNA partial gene sequence: Not available

Classification: Bacteria; Cyanobacteria; Cyanophyceae; Chroococcales; Spirulinaceae; Spirulina

Metabolism: Autotrophic (oxygenic photosynthesis)

Origin: Del Mar Slough, San Diego, CA, USA

Collection: Kudela laboratory (UCSC, CA, USA)

Sample concentration: 1.42×10^7 cells/ml

Sample count on filter substrate: $1.42 \pm 0.14 \times 10^8$ cells

Laboratory growth conditions: 25 °C, up to 6 months

Culture medium: Enriched Seawater medium (f/2-Si)

Sample photograph:

Sample micrograph:

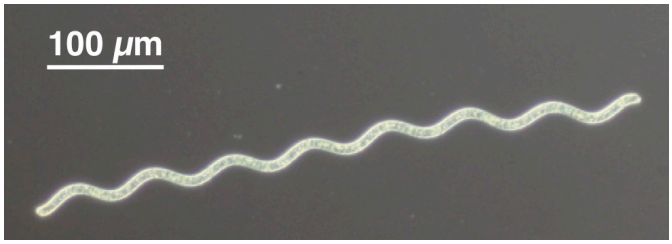

Sample reflectance spectrum:

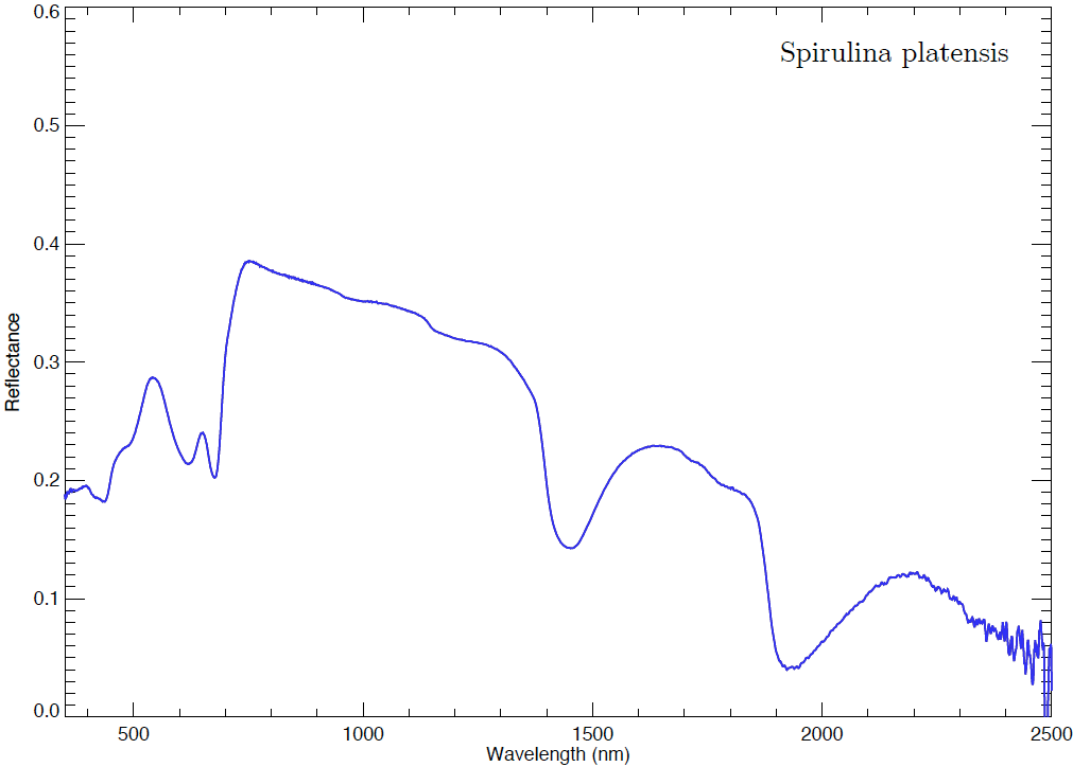

Sporidiobolales_KM349951

Sample name: Sporidiobolales

Accession number for 16S rRNA partial gene sequence: KM349951

Classification: Eukaryota; Fungi; Dikarya; Basidiomycota; Pucciniomycotina; Microbotryomycetes; Sporidiobolales; unclassified Sporidiobolales

Metabolism: Heterotrophic

Origin: Atacama desert, Chile

Isolation: Ivan P. Lima (NPP at NASA Ames, CA, USA)

Sample concentration: 2.19 $\times$ 10^7 cells/ml

Sample count on filter substrate: 6.57 $\pm$ 0.44 $\times$ 10^7 cells

Laboratory growth conditions: 30 °C, 180 rpm, 48 h

Culture medium: Lysogeny Broth (LB)

Sample photograph:

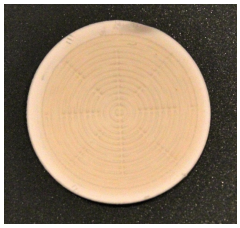

Sample micrograph:

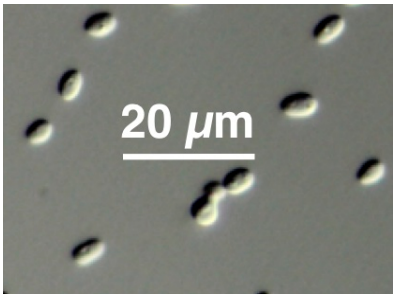

Sample reflectance spectrum:

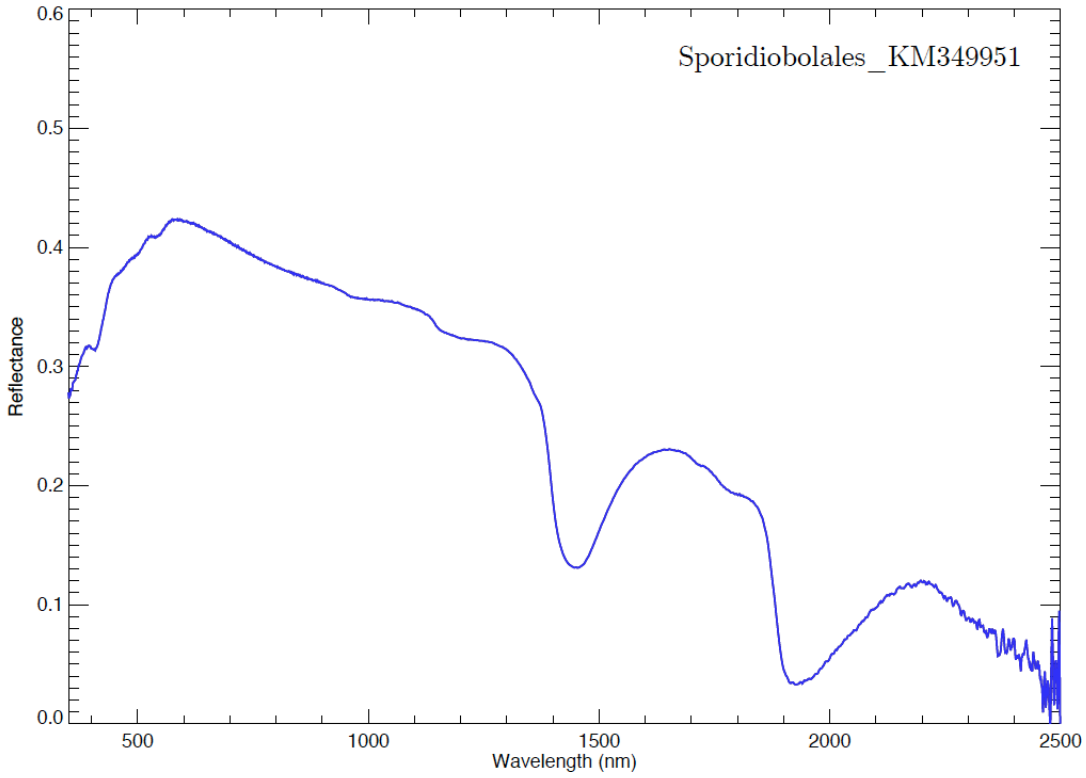

Sporidiobolales_KM349953

Sample name: Sporidiobolales

Accession number for 16S rRNA partial gene sequence: KM349953

Classification: Eukaryota; Fungi; Dikarya; Basidiomycota; Pucciniomycotina; Microbotryomycetes; Sporidiobolales; unclassified Sporidiobolales

Metabolism: Heterotrophic

Origin: Atacama desert, Chile

Isolation: Ivan P. Lima (NPP at NASA Ames, CA, USA)

Sample concentration: 2.04 $\times$ 10^7 cells/ml

Sample count on filter substrate: 6.12 $\pm$ 0.41 $\times$ 10^7 cells

Laboratory growth conditions: 30 °C, 180 rpm, 48 h

Culture medium: Reasoner's 2A (R2A)

Sample photograph:

Sample micrograph:

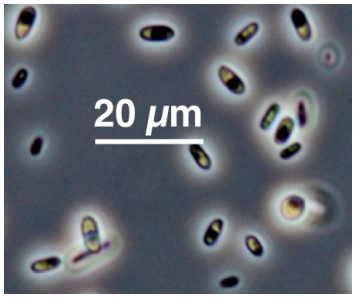

Sample reflectance spectrum:

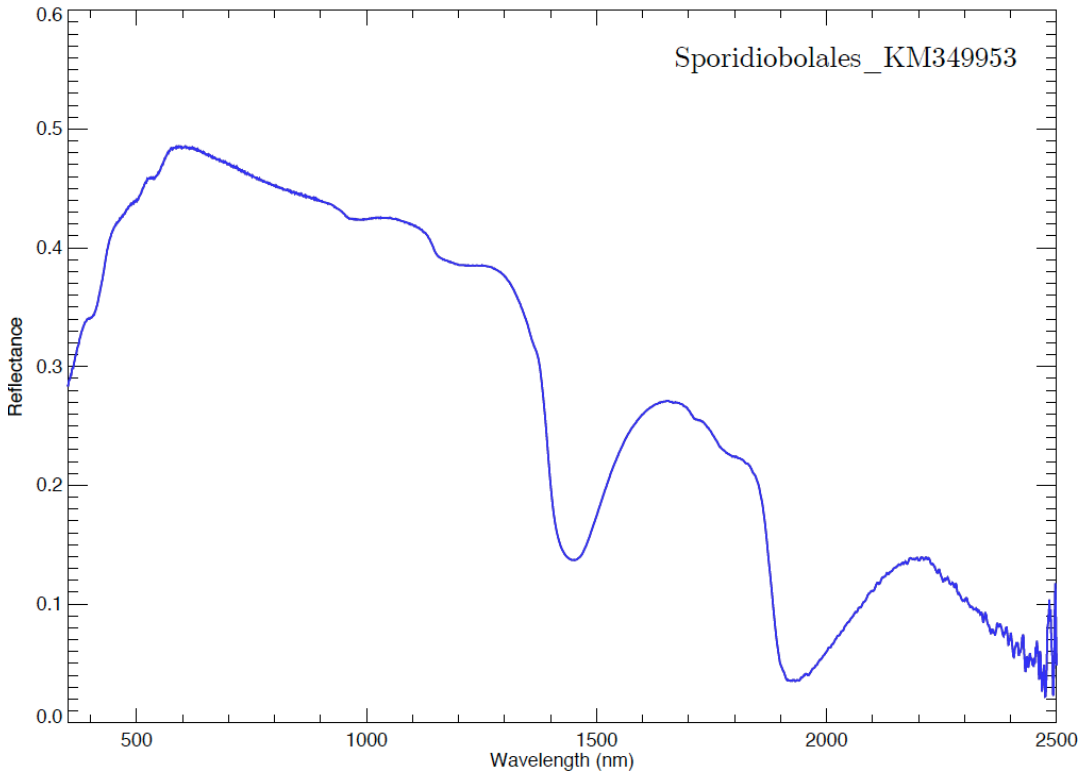

Sporidiobolales_KM349954

Sample name: Sporidiobolales

Accession number for 16S rRNA partial gene sequence: KM349954

Classification: Eukaryota; Fungi; Dikarya; Basidiomycota; Pucciniomycotina; Microbotryomycetes; Sporidiobolales; unclassified Sporidiobolales

Metabolism: Heterotrophic

Origin: Atacama desert, Chile

Isolation: Ivan P. Lima (NPP at NASA Ames, CA, USA)

Sample concentration: 3.24 $\times$ 10^6 cells/ml

Sample count on filter substrate: 9.73 $\pm$ 0.65 $\times$ 10^6 cells

Laboratory growth conditions: 30 °C, 180 rpm, 48 h

Culture medium: Reasoner's 2A (R2A)

Sample photograph:

Sample micrograph:

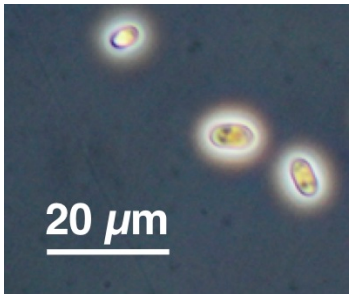

Sample reflectance spectrum:

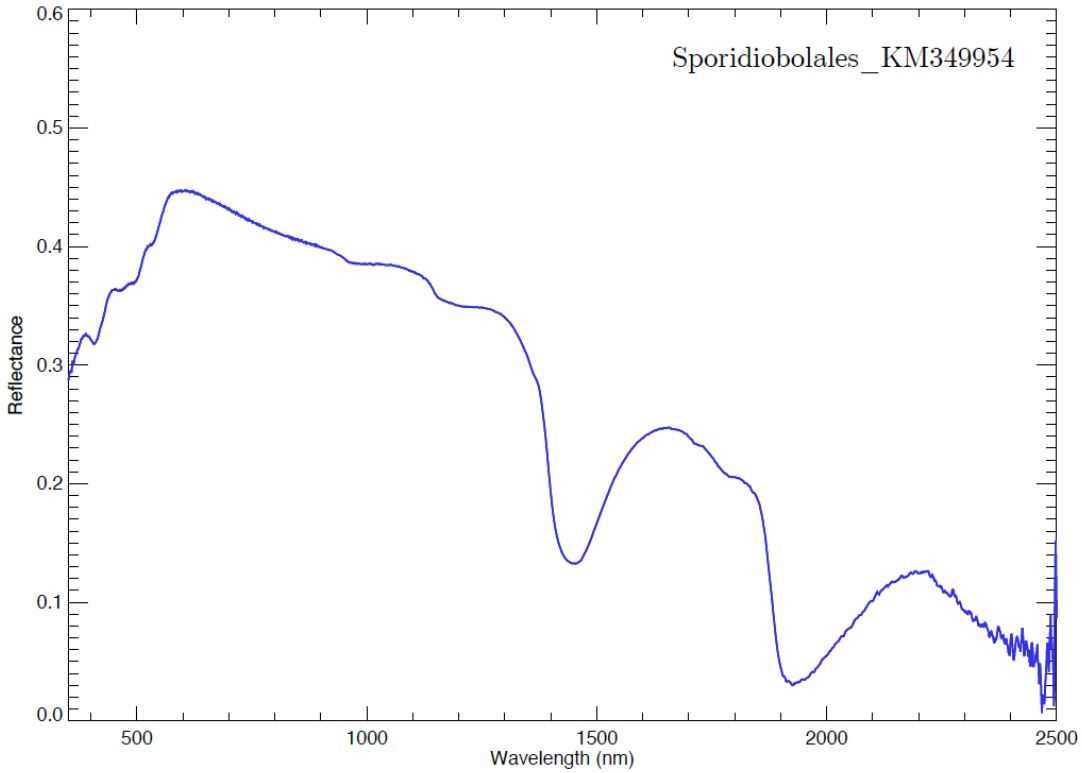

Sporosarcina sp._KM349905

Sample name: *Sporosarcina* sp.

Accession number for 16S rRNA partial gene sequence: KM349905

Classification: Bacteria; Firmicutes; Bacilli; Bacillales; Planococcaceae; Sporosarcina

Metabolism: Heterotrophic

Origin: Sonoran desert, AZ, USA

Isolation: Ivan P. Lima (NPP at NASA Ames, CA, USA)

Sample concentration: 3.15 $\times$ 10^7 cells/ml

Sample count on filter substrate: 9.45 $\pm$ 0.63 $\times$ 10^7 cells

Laboratory growth conditions: 30 °C, 180 rpm, 24 h

Culture medium: Marine Broth (MB)

Sample photograph:

Sample micrograph:

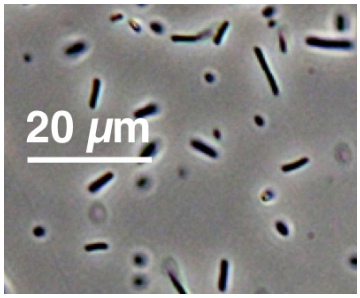

Sample reflectance spectrum:

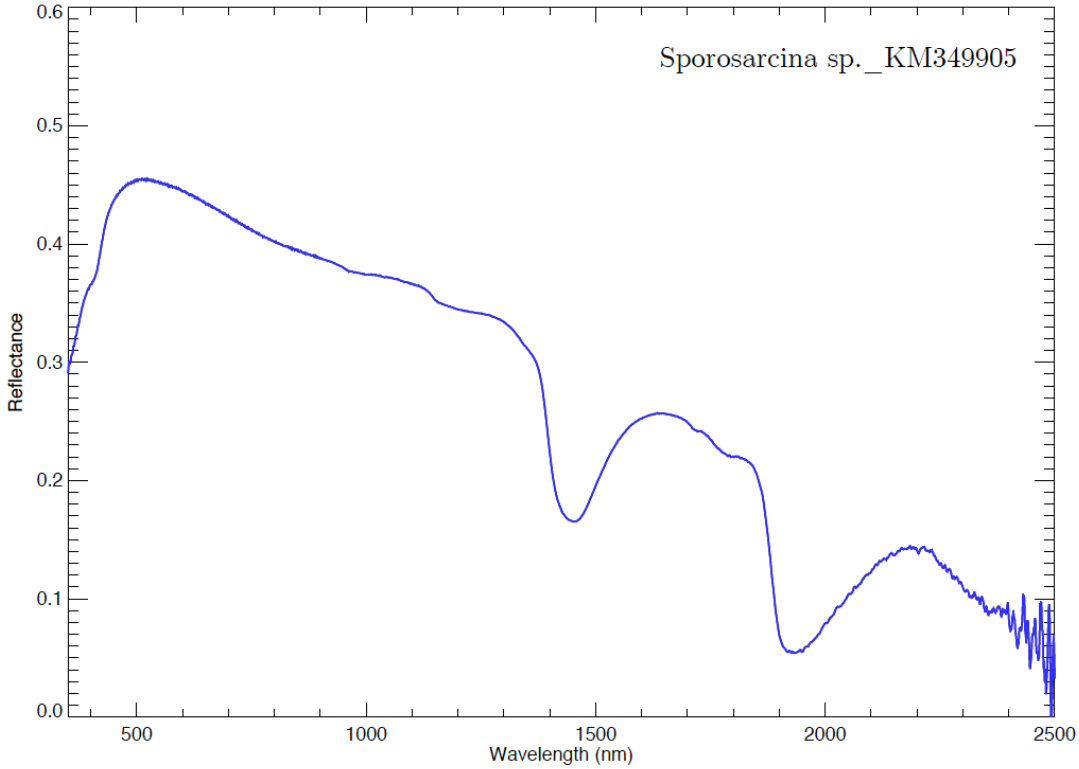

Streptomyces sp._KM349862

Sample name: *Streptomyces* sp.

Accession number for 16S rRNA partial gene sequence: KM349862

Classification: Bacteria; Actinobacteria; Actinobacteridae; Actinomycetales; Streptomycineae; Streptomycetaceae; Streptomyces

Metabolism: Heterotrophic

Origin: Sonoran desert, AZ, USA

Isolation: Ivan P. Lima (NPP at NASA Ames, CA, USA)

Sample concentration: 2.47×10^7 cells/ml

Sample count on filter substrate: $7.42 \pm 0.50 \times 10^7$ cells

Laboratory growth conditions: 30 °C, 180 rpm, 24 h

Culture medium: Marine Broth (MB)

Sample photograph:

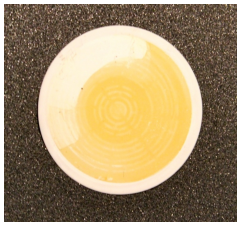

Sample micrograph:

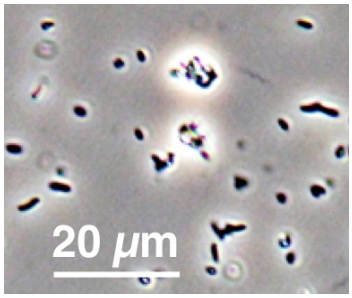

Sample reflectance spectrum:

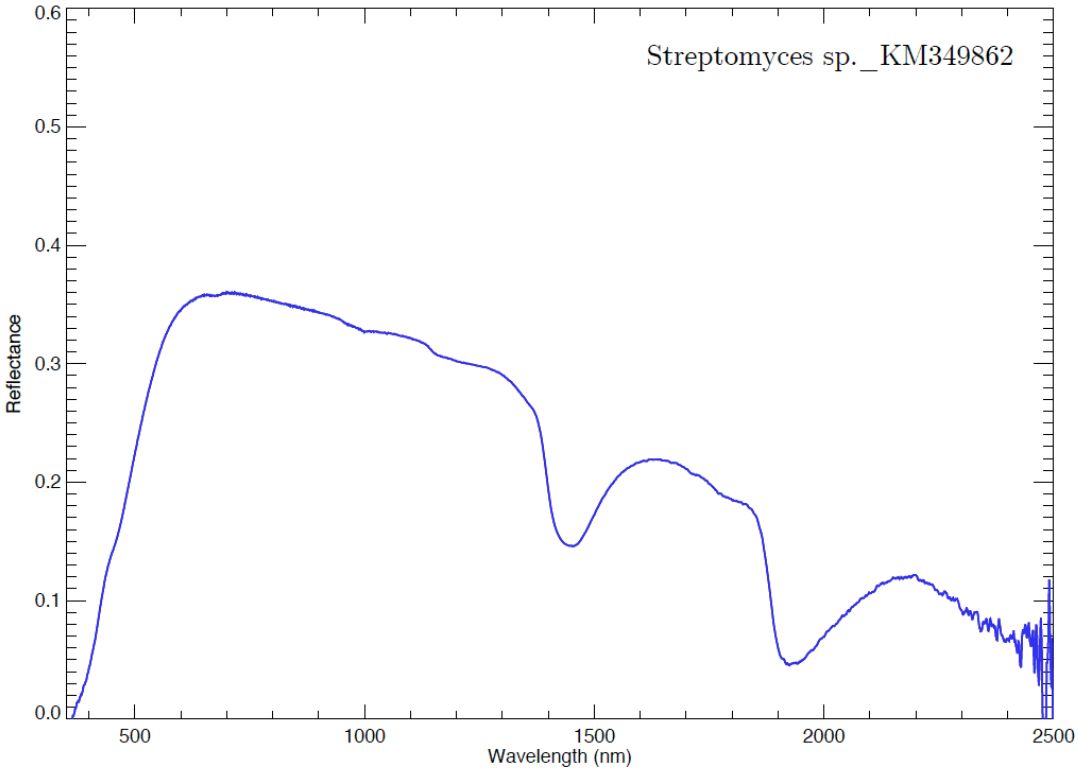

Streptomyces sp._KM349965

Sample name: *Streptomyces* sp.

Accession number for 16S rRNA partial gene sequence: KM349965

Classification: Bacteria; Actinobacteria; Actinobacteridae; Actinomycetales; Streptomycineae; Streptomycetaceae; Streptomyces

Metabolism: Heterotrophic

Origin: Atacama desert, Chile

Isolation: Ivan P. Lima (NPP at NASA Ames, CA, USA)

Sample concentration: 3.69×10^7 cells/ml

Sample count on filter substrate: $1.11 \pm 0.07 \times 10^8$ cells

Laboratory growth conditions: 30 °C, 180 rpm, 72 h

Culture medium: Marine Broth (MB)

Sample photograph:

Sample micrograph:

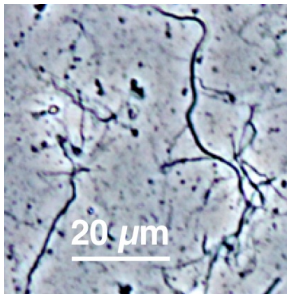

Sample reflectance spectrum:

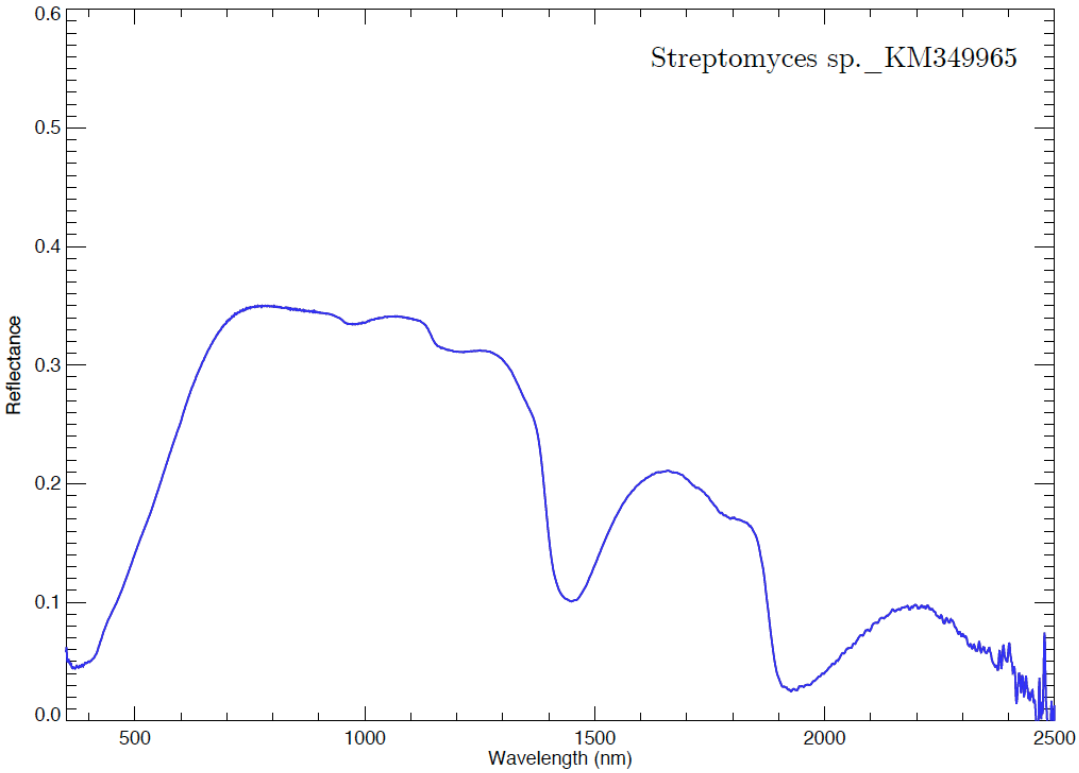

Synechococcus leopoliensis

Sample name: *Synechococcus leopoliensis*

Accession number for 16S rRNA partial gene sequence: Not available

Classification: Bacteria; Cyanobacteria; Cyanophyceae; Synechococcales; Synechococcaceae; Synechococcus

Metabolism: Autotrophic (oxygenic photosynthesis)

Origin: Waller Creek, Austin, TX, USA

Collection: UTEX (TX, USA)

Sample concentration: 5.84×10^7 cells/ml

Sample count on filter substrate: $5.84 \pm 0.58 \times 10^8$ cells

Laboratory growth conditions: 25 °C, up to 6 months

Culture medium: Blue-Green medium (BG-11)

Sample photograph:

Sample micrograph:

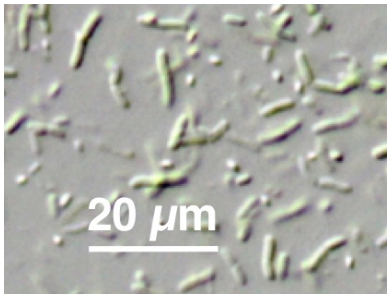

Sample reflectance spectrum:

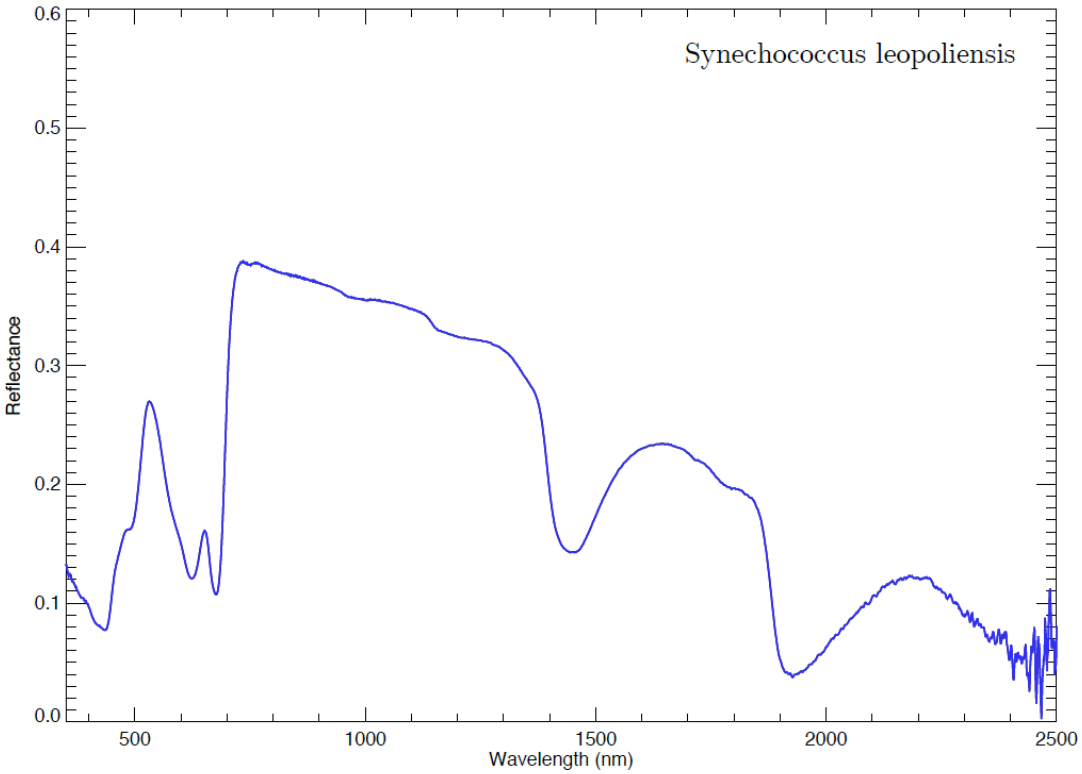

Synechococcus sp.

Sample name: *Synechococcus* sp.

Accession number for 16S rRNA partial gene sequence: Not available

Classification: Bacteria; Cyanobacteria; Cyanophyceae; Synechococcales; Synechococcaceae; Synechococcus

Metabolism: Autotrophic (oxygenic photosynthesis)

Origin: Marine sample, Belize

Collection: Kudela laboratory (UCSC, CA, USA)

Sample concentration: 2.70×10^6 cells/ml

Sample count on filter substrate: $2.70 \pm 0.27 \times 10^7$ cells

Laboratory growth conditions: 25 °C, up to 6 months

Culture medium: Enriched Seawater medium (f/2)

Sample photograph:

Sample micrograph:

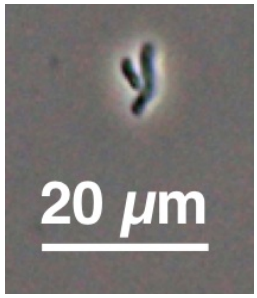

Sample reflectance spectrum:

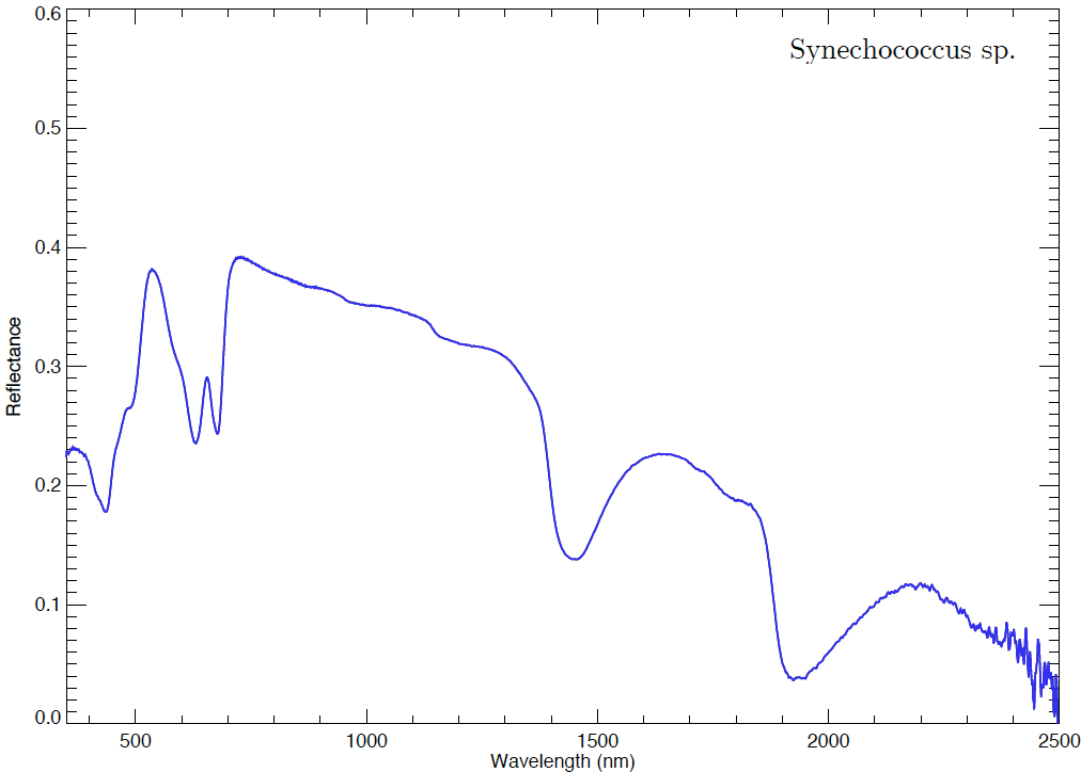

Synechococcus sp. with reduced phycocyanin

Sample name: *Synechococcus* sp. with reduced phycocyanin

Accession number for 16S rRNA partial gene sequence: Not available

Classification: Bacteria; Cyanobacteria; Cyanophyceae; Synechococcales; Synechococcaceae; Synechococcus

Metabolism: Autotrophic (oxygenic photosynthesis)

Origin: Santa Cruz Wharf, CA, USA

Collection: Kudela laboratory (UCSC, CA, USA)

Sample concentration: 5.41×10^5 cells/ml

Sample count on filter substrate: $5.41 \pm 0.54 \times 10^6$ cells

Laboratory growth conditions: 25 °C, up to 6 months

Culture medium: Enriched Seawater medium (f/2)

Sample photograph:

Sample micrograph:

Sample reflectance spectrum:

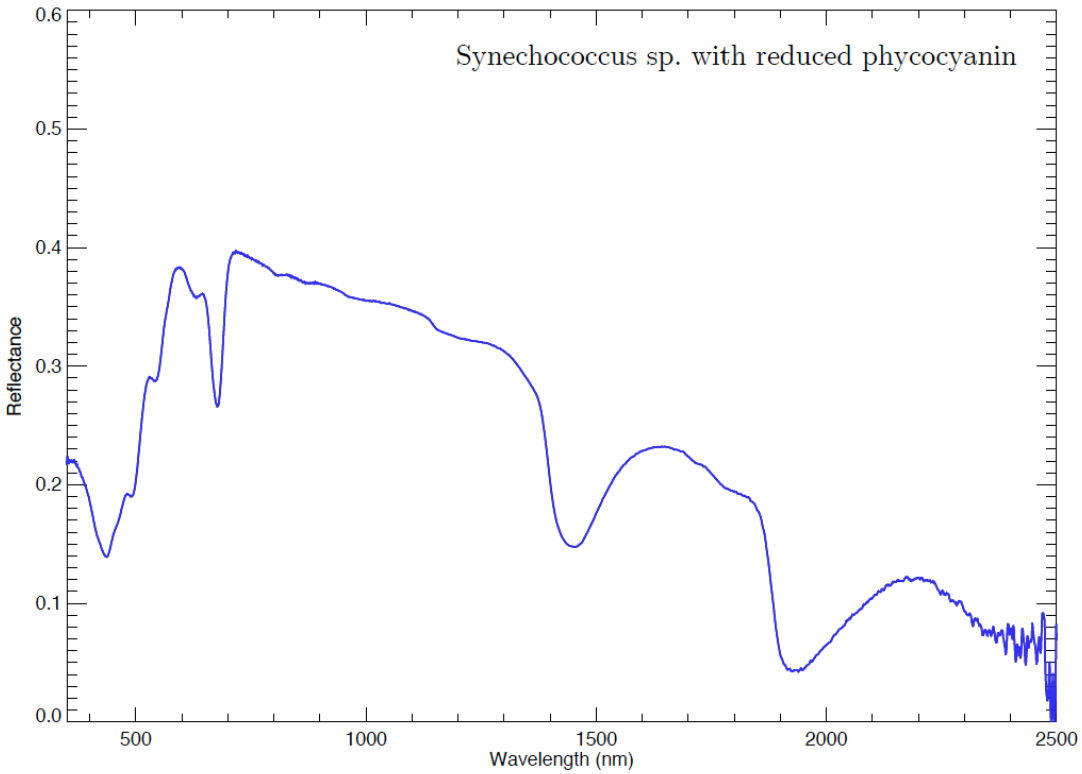

Bibliography

Anglada-Escudé, G., Arriagada, P., Vogt, S. S., Rivera, E. J., Butler, R. P., Crane, J. D., Shectman, S. A., Thompson, I. B., Minniti, D., Haghighipour, N., Carter, B. D., Tinney, C. G., Wittenmyer, R. A., Bailey, J. A., O'Toole, S. J., Jones, H. R. A., & Jenkins, J. S. (2012), "A planetary system around the nearby M dwarf GJ 667C with at least one super-Earth in its habitable zone", *Astrophysical Journal Letters*, vol. 751, L16.

Arnold, L., Gillet, S., Lardière, O., Riaud, P., & Schneider, J. (2002), "A test for the search for life on extrasolar planets - Looking for the terrestrial vegetation signature in the Earthshine spectrum", *Astronomy & Astrophysics*, vol. 392, no. 1, pp. 231-237.

Baldridge, A. M., Hook, S. J., Grove, C. I., & Rivera, G. (2009), "The ASTER spectral library version 2.0", *Remote Sensing of Environment*, vol. 113, no. 4, pp. 711-715. http://speclib.jpl.nasa.gov/

Batalha, N.M., (2014), "Exploring exoplanet populations with NASA's Kepler Mission", *Proc Natl Acad Sci USA*, **111**:12647–12654.

Batalha, N. M., Borucki, W. J., Bryson, S. T., Buchhave, L. A., Caldwell, D. A., Christensen-Dalsgaard, J., Ciardi, D., Dunham, E. W., Fressin, F., Gautier III, T. N., Gilliland, R. L., Haas, M. R., Howell, S. B., Jenkins, J. M., Kjeldsen, H., Koch, D. G., Latham, D. W., Lissauer, J. J., Marcy, G. W., Rowe, J. F., Sasselov, D. D., Seager, S., Steffen, J. H., Torres, G., Basri, G. S., Brown, T. M., Charbonneau, D., Christiansen, J., Clarke, B., Cochran, W. D., Dupree, A., Fabrycky, D. C., Fischer, D., Ford, E. B., Fortney, J., Girouard, F. R., Holman, M. J., Johnson, J., Isaacson, H., Klaus, T. C., Machalek, P., Moorehead, A. V., Morehead, R. C., Ragozzine, D., Tenenbaum, P., Twicken, J., Quinn, S., VanCleve, J., Walkowicz, L. M., Welsh, W. F., DeVore, E., & Gould, A. (2011), "Kepler's First Rocky Planet: Kepler-10b", *Astrophysical Journal*, vol. 729, no. 1.

Batalha, N. M., Rowe, J. F., Bryson, S. T., Barclay, T., Burke, C. J., Caldwell, D. A., Christiansen, J. L., Mullally, F., Thompson, S. E., Brown, T. M., Dupree, A. K., Fabrycky, D. C., Ford, E. B., Fortney, J. J., Gilliland, R. L., Isaacson, H., Latham, D. W., Marcy, G. W., Quinn, S., Ragozzine, D., Shporer, A., Borucki, W. J., Ciardi, D. R., Gautier III, T. N., Haas, M. R., Jenkins, J. M., Koch, D. G., Lissauer, J. J., Rapin, W., Basri, G. S., Boss, A. P., Buchhave, L. A., Charbonneau, D., Christensen-Dalsgaard, J., Clarke, B. D., Cochran, W. D., Demory, B. O., DeVore, E., Esquerdo, G. A., Everett, M., Fressin, F., Geary, J. C., Girouard, F. R., Gould, A., Hall, J. R., Holman, M. J., Howard, A. W., Howell, S. B., Ibrahim, K. A., Kinemuchi, K., Kjeldsen, H., Klaus, T. C., Li, J., Lucas, P. W., Morris, R. L., Prsa, A., Quintana, E., Sanderfer, D. T., Sasselov, D., Seader, S. E., Smith, J. C., Steffen, J. H., Still, M., Stumpe, M. C., Tarter, J. C., Tenenbaum, P., Torres, G., Twicken, J. D., Uddin, K., Van Cleve, J., Walkowicz, L., & Welsh, W. F. (2012), "Planetary Candidates Observed by Kepler, III: Analysis of the First 16 Months of Data", *Astrophysical Journal* (submitted). *arXiv:1202.5852*.

Battista, J. R. (1997), "Against all odds: The survival strategies of Deinococcus radiodurans", *Annual Review of Microbiology*, vol. 51, pp. 203-224.

Björn, L. O. (ed.) (2008), "Spectral tuning in biology", in *Photobiology: The Science of Life and Light*, 2nd edn, Springer, pp. 155-196.

Bonfils, X., Delfosse, X., Udry, S., Forveille, T., Mayor, M., Perrier, C., Bouchy, F., Gillon, M., Lovis, C., Pepe, F., Queloz, D., Santos, N. C., Ségransan, D., & Bertaux, J. L. (2011), "The HARPS search for southern extra-solar planets XXXI. The M-dwarf sample", *Astronomy & Astrophysics* (submitted). *arXiv:1111.5019*.

Bonfils X., et al. (2013), "The HARPS search for southern extra-solar planets XXXI", TheM-dwarf sample. arXiv:1111.5019v2.

Borucki, W. J., Koch, D. G., Basri, G., Batalha, N., Brown, T. M., Bryson, S. T., Caldwell, D., Christensen-Dalsgaard, J., Cochran, W. D., DeVore, E., Dunham, E. W., Gautier III, T. N., Geary, J. C., Gilliland, R., Gould, A., Howell, S. B., Jenkins, J. M., Latham, D. W., Lissauer, J. J., Marcy, G. W., Rowe, J., Sasselov, D., Boss, A., Charbonneau, D., Ciardi, D., Doyle, L., Dupree, A. K., Ford, E. B., Fortney, J., Holman, M. J., Seager, S., Steffen, J. H., Tarter, J., Welsh, W. F., Allen, C., Buchhave, L. A., Christiansen, J. L., Clarke, B. D., Das, S., Désert, J. M., Endl, M., Fabrycky, D., Fressin, F., Haas, M., Horch, E., Howard, A., Isaacson, H., Kjeldsen, H., Kolodziejczak, J., Kulesa, C., Li, J., Lucas, P. W., Machalek, P., McCarthy, D., MacQueen, P., Meibom, S., Miquel, T., Prsa, A., Quinn, S. N., Quintana, E. V., Ragozzine, D., Sherry, W., Shporer, A., Tenenbaum, P., Torres, G.,

Twicken, J. D., Van Cleve, J., Walkowicz, L., Witteborn, F. C., & Still, M. (2011), "Characteristics of Planetary Candidates Observed by Kepler, II. Analysis of the First Four Months of Data", *Astrophysical Journal*, vol. 736, no. 1.

Borucki, W. J., Koch, D. G., Batalha, N., Bryson, S. T., Rowe, J., Fressin, F., Torres, G., Caldwell, D., Christensen-Dalsgaard, J., Cochran, W. D., DeVore, E., Gautier III, T. N., Geary, J. C., Gilliland, R., Gould, A., Howell, S. B., Jenkins, J. M., Latham, D. W., Lissauer, J. J., Marcy, G. W., Sasselov, D., Boss, A., Charbonneau, D., Ciardi, D., Kaltenegger, L., Doyle, L., Dupree, A. K., Ford, E. B., Fortney, J., Holman, M. J., Steffen, J. H., Mullally, F., Still, M., Tarter, J., Ballard, S., Buchhave, L. A., Carter, J., Christiansen, J. L., Demory, B. O., Désert, J. M., Dressing, C., Endl, M., Fabrycky, D., Fischer, D., Haas, M., Henze, C., Horch, E., Howard, A., Isaacson, H., Kjeldsen, H., Johnson, J. A., Klaus, T., Kolodziejczak, J., Barclay, T., Li, J., Meibom, S., Prsa, A., Quinn, S. N., Quintana, E. V., Robertson, P., Sherry, W., Shporer, A., Tenenbaum, P., Thompson, S. E., Twicken, J. D., Van Cleve, J., Welsh, W. F., Basu, S., Chaplin, W., Miglio, A., Kawaler, S. D., Arentoft, T., Stello, D., Metcalfe, T. S., Verner, G. A., Karoff, C., Lundkvist, M., Lund, M. N., Handberg, R., Elsworth, Y., Hekker, S., Huber, D., Bedding, T. R., & Rapin, W. (2012), "Kepler-22b: A 2.4 Earth-radius Planet in the Habitable Zone of a Sun-like Star", *Astrophysical Journal*, vol. 745.

Canganella, F. & Wiegel, J. (2011), "Extremophiles: from abyssal to terrestrial ecosystems and possibly beyond", *Naturwissenschaften*, vol. 98, no. 4, pp. 253-279.

Canuto, V. M., Levine, J. S., Augustsson, T. R., & Imhoff, C. L. (1982), "UV radiation from the Young Sun and Oxygen and Ozone Levels in the Prebiological Paleoatmosphere", *Nature*, vol. 296, no. 5860, pp. 816-820.

Carroll, S. B. (2001), "Chance and necessity: the evolution of morphological complexity and diversity", *Nature*, vol. 409, no. 6823, pp. 1102-1109.

Cavicchioli, R. (2002), "Extremophiles and the search for extraterrestrial life", *Astrobiology*, vol. 2, no. 3, pp. 281-292.

Clark, R. N. (1993), "SPECtrum Processing Routines User's Manual Version 3 (program SPECPR)", *U.S.Geological Survey Open File Report* pp. 93-595. http://speclab.cr.usgs.gov/

Clark, R. N., Swayze, G. A., Wise, R., Livo, E., Hoefen, T., Kokaly, R., & Sutley, S. J. (2007), "USGS digital spectral library splib06a", *U.S. Geological Survey, Digital Data Series 231.* http://speclab.cr.usgs.gov/

Cloud, P. (1972), "A Working Model of the Primitive Earth", *American Journal of Science*, vol. 272, no. 6, pp. 537-548.

Cockell, C. S. (2000), "The ultraviolet history of the terrestrial planets - implications for biological evolution", *Planetary and Space Science*, vol. 48, no. 2-3, pp. 203-214.

Cockell, C. S., Kaltenegger, L., & Raven, J. A. (2009), "Cryptic Photosynthesis-Extrasolar Planetary Oxygen Without a Surface Biological Signature", *Astrobiology*, vol. 9, no. 7, pp. 623-636.

Cowan, N. B., Agol, E., Meadows, V. S., Robinson, T., Livengood, T. A., Deming, D., Lisse, C. M., A'Hearn, M. F., Wellnitz, D. D., Seager, S., & Charbonneau, D. (2009), "Alien Maps of An Ocean-Bearing World", *Astrophysical Journal*, vol. 700, no. 2, pp. 915-923.

Cowan, N. B., Robinson, T., Livengood, T. A., Deming, D., Agol, E., A'Hearn, M. F., Charbonneau, D., Lisse, C. M., Meadows, V. S., Seager, S., Shields, A. L., & Wellnitz, D. D. (2011), "Rotational Variability of Earth's Polar Regions: Implications for Detecting Snowball Planets", *Astrophysical Journal*, vol. 731, no. 1.

Crow, C. A., McFadden, L. A., Robinson, T., Meadows, V. S., Livengood, T. A., Hewagama, T., Barry, R. K., Deming, L. D., Lisse, C. M., & Wellnitz, D. (2011), "Views from EPOXI: Colors in Our Solar System As An Analog for Extrasolar Planets", *Astrophysical Journal*, vol. 729, no. 2.

Dalton, J. B., Mogul, R., Kagawa, H. K., Chan, S. L., & Jamieson, C. S. (2003), "Near-infrared detection of potential evidence for microscopic organisms on Europa", *Astrobiology*, vol. 3, no. 3, pp. 505-529.

Demain, A. L. (1998), "Induction of microbial secondary metabolism", *International Microbiology*, vol. 1, pp. 259-264.

Des Marais, D. J., Harwit, M. O., Jucks, K. W., Kasting, J. F., Lin, D. N. C., Lunine, J. I., Schneider, J., Seager, S., Traub, W. A., & Woolf, N. J. (2002), "Remote sensing of planetary properties and biosignatures on extrasolar terrestrial planets", *Astrobiology*, vol. 2, no. 2, pp. 153-181.

Dressing C.D., Charbonneau D. (2013), "The occurrence rate of small planets around Small Stars", *Astrophys J*, 767(1):95.

Ferreira, A. C., Nobre, M. F., Moore, E., Rainey, F. A., Battista, J. R., & da Costa, M. S. (1999), "Characterization and radiation resistance of new isolates of Rubrobacter radiotolerans and Rubrobacter xylanophilus", *Extremophiles*, vol. 3, no. 4, pp. 235-238.

Ford, E. B., Seager, S., & Turner, E. L. (2001), "Characterization of extrasolar terrestrial planets from diurnal photometric variability", *Nature*, vol. 412, no. 6850, pp. 885-887.

Fressin F., et al. (2013), "The false positive rate of Kepler and the occurrence of planets", *Astrophys J*, 766(2):81.

Fujii, Y., Kawahara, H., Suto, Y., Fukuda, S., Nakajima, T., Livengood, T. A., & Turner, E. L. (2011), "Colors of a Second Earth II. Effects of Clouds on Photometric Characterization of Earth-like Exoplanets", *Astrophysical Journal*, vol. 738, no. 2.

Gaidos E. (2013), "Candidate planets in the habitable zones of Kepler stars", *Astrophys J*, 770:.

Geissler, P., Thompson, W. R., Greenberg, R., Moersch, J., McEwen, A., & Sagan, C. (1995), "Galileo Multispectral Imaging of Earth", *Journal of Geophysical Research-Planets*, vol. 100, no. E8, pp. 16895-16906.

Graham, L.E. and Wilcox, L.W. (2000), *Algae*, Prentice-Hall, Upper Saddle River, NJ.

Halldal, P. (1968), "Photosynthetic Capacities and Photosynthetic Action Spectra of Endozoic Algae of Massive Coral Favia", *Biological Bulletin*, vol. 134, no. 3, p. 411-424.

Hegde, S. & Kaltenegger, L. (2013), "Colors of Extreme Exo-Earth Environments", *Astrobiology*, vol. 13, no. 1, pp. 47-56.

Hegde, S. et al., (2014), "Surface biosignatures of exo-Earths: Remote detection of extraterrestrial life", *Proc Natl Acad Sci USA*: In Review.

Holland, H. D. (1994), "Early Proterozoic atmospheric change", in *Early Life on Earth*, S. Bengtson, ed., Columbia University Press, New York, pp. 237-244.

Holland, H. D. (2006), "The oxygenation of the atmosphere and oceans", *Philosophical Transactions of the Royal Society B-Biological Sciences*, vol. 361, no. 1470, pp. 903-915.

Howard, A. W. (2013), "Observed properties of Extrasolar Planets", *Science*, vol. 340, pp. 572-576.

Igamberdiev, A. U. & Lea, P. J. (2006), "Land plants equilibrate O-2 and CO2 concentrations in the atmosphere", *Photosynthesis Research*, vol. 87, no. 2, pp. 177-194.

Irvine, W.H., Simon, T., Menzel, D. H., Charon, J., Lecomte, G., Griboval, P., Young, A. T., (1968a), "Multicolor Photoelectric Photometry of the Brighter Planets. II. Observations from Le Houga Observatory", *Astron. J.*, 73, 251.

Irvine, W.H., Simon, T., Menzel, D. H., Pikoos, C., Young, A. T., (1968b), "Multicolor Photoelectric Photometry of the Brighter Planets. III. Observations from Boyden Observatory", *Astron. J.*, 73, 807.

Kaltenegger, L., Traub, W. A., & Jucks, K. W. (2007), "Spectral evolution of an Earth-like planet", *Astrophysical Journal*, vol. 658, no. 1, pp. 598-616.

Kaltenegger, L., Selsis, F., Fridlund, M., Lammer, H., Beichman, C., Danchi, W., Eiroa, C., Henning, T., Herbst, T., Léger, A., Liseau, R., Lunine, J., Paresce, F., Penny, A., Quirrenbach, A., Röttgering, H., Schneider, J., Stam, D., Tinetti, G., & White, G. J. (2010), "Deciphering Spectral Fingerprints of Habitable Exoplanets", *Astrobiology*, vol. 10, no. 1, pp. 89-102.

Kaltenegger, L. & Sasselov, D. (2011), "Exploring the Habitable Zone for Kepler Planetary Candidates", *Astrophysical Journal Letters*, vol. 736, no. 2.

Karkoschka, E. (1998), "Methane, ammonia, and temperature measurements of the Jovian planets and Titan from CCD-spectrophotometry", *Icarus*, 133, 134-146.

Kasting, J. F. & Catling, D. (2003), "Evolution of a habitable planet", *Annual Review of Astronomy and Astrophysics*, vol. 41, pp. 429-463.

Kiang, N. Y., Siefert, J., Govindjee, & Blankenship, R. E. (2007a), "Spectral signatures of photosynthesis. I. Review of Earth organisms", *Astrobiology*, vol. 7, no. 1, pp. 222-251.

Kiang, N. Y., Segura, A., Tinetti, G., Govindjee, Blankenship, R. E., Cohen, M., Siefert, J., Crisp, D., & Meadows, V. S. (2007b), "Spectral signatures of photosynthesis. II. Coevolution with other stars and the atmosphere on extrasolar worlds", *Astrobiology*, vol. 7, no. 1, pp. 252-274.

Knacke, R. F. (2003), "Possibilities for the detection of microbial life on extrasolar planets", *Astrobiology*, vol. 3, no. 3, pp. 531-541.

Kopparapu R.K. (2013), "A revised estimate of the occurrence rate of terrestrial planets in the habitable zones around Kepler M-dwarfs", *Astrophys J Lett*, 767(1):L8.

Kopparapu R.K., et al. (2014), "Habitable zones around main sequence stars: Dependence on planetary mass", *Astrophys J Lett,* 787(2):L29.

Kranner, I., Cram, W. J., Zorn, M., Wornik, S., Yoshimura, I., Stabentheiner, E., & Pfeifhofer, H. W. (2005), "Antioxidants and photoprotection in a lichen as compared with its isolated symbiotic partners", *Proceedings of the National Academy of Sciences of the United States of America*, vol. 102, no. 8, pp. 3141-3146.

Kubelka, P. & Munk, F. (1931), "Ein Beitrag zur Optik der Farbanstriche", *Z.Tech.Phys.*, vol. 12, p. 593.

Lederberg, J. (1965), "Signs of Life - Criterion-System of Exobiology", *Nature*, vol. 207, no. 4992, p. 9-13.

Léger, A., Rouan, D., Schneider, J., Barge, P., Fridlund, M., Samuel, B., Ollivier, M., Guenther, E., Deleuil, M., Deeg, H. J., Auvergne, M., Alonso, R., Aigrain, S., Alapini, A., Almenara, J. M., Baglin, A., Barbieri, M., Bruntt, H., Bordé, P., Bouchy, F., Cabrera, J., Catala, C., Carone, L., Carpano, S., Csizmadia, S., Dvorak, R., Erikson, A., Ferraz-Mello, S., Foing, B., Fressin, F., Gandolfi, D., Gillon, M., Gondoin, P., Grasset, O., Guillot, T., Hatzes, A., Hébrard, G., Jorda, L., Lammer, H., Llebaria, A., Loeillet, B., Mayor, M., Mazeh, T., Moutou, C., Pätzold, M., Pont, F., Queloz, D., Rauer, H., Renner, S., Samadi, R., Shporer, A., Sotin, C., Tingley, B., Wuchterl, G., Adda, M., Agogu, P., Appourchaux, T., Ballans, H., Baron, P., Beaufort, T., Bellenger, R., Berlin, R., Bernardi, P., Blouin, D., Baudin, F., Bodin, P., Boisnard, L., Boit, L., Bonneau, F., Borzeix, S., Briet, R., Buey, J. T., Butler, B., Cailleau, D., Cautain, R., Chabaud, P. Y., Chaintreuil, S., Chiavassa, F., Costes, V., Parrho, V. C., Fialho, F. D., Decaudin, M., Defise, J. M., Djalal, S., Epstein, G., Exil, G. E., Fauré, C., Fenouillet, T., Gaboriaud, A., Gallic, A., Gamet, P., Gavalda, P., Grolleau, E., Gruneisen, R., Gueguen, L., Guis, V., Guivarc'h, V., Guterman, P., Hallouard, D., Hasiba, J., Heuripeau, F., Huntzinger, G., Hustaix, H., Imad, C., Imbert, C., Johlander, B., Jouret, M., Journoud, P., Karioty, F., Kerjean, L., Lafaille, V., Lafond, L., Lam-Trong, T., Landiech, P., Lapeyrere, V., Larqué, T., Laudet, P., Lautier, N., Lecann, H., Lefevre, L., Leruyet, B., Levacher, P., Magnan, A., Mazy, E., Mertens, F., Mesnager, J. M., Meunier, J. C., Michel, J. P., Monjoin, W., Naudet, D., Nguyen-Kim, K., Orcesi, J. L., Ottacher, H., Perez, R., Peter, G., Plasson, P., Plesseria, J. Y., Pontet, B., Pradines, A., Quentin, C., Reynaud, J. L., Rolland, G., Rollenhagen, F., Romagnan, R., Russ, N., Schmidt, R., Schwartz, N., Sebbag, I., Sedes, G., Smit, H., Steller, M. B., Sunter, W., Surace, C., Tello, M., Tiphène, D., Toulouse, P., Ulmer, B., Vandermarcq, O., Vergnault, E., Vuillemin, A., & Zanatta, P. (2009), "Transiting exoplanets from the CoRoT space mission VIII. CoRoT-7b: the first super-Earth with measured radius", *Astronomy & Astrophysics*, vol. 506, no. 1, pp. 287-302.

Lovelock, J. E. (1965), "A Physical Basis for Life Detection Experiments", *Nature*, vol. 207, no. 4997, p. 568-570.

Marion, G. M., Fritsen, C. H., Eicken, H., & Payne, M. C. (2003), "The search for life on Europa: Limiting environmental factors, potential habitats, and Earth analogues", *Astrobiology*, vol. 3, no. 4, pp. 785-811.

Mattimore, V. & Battista, J. R. (1996), "Radioresistance of Deinococcus radiodurans: Functions necessary to survive ionizing radiation are also necessary to survive prolonged desiccation", *Journal of Bacteriology*, vol. 178, no. 3, pp. 633-637.

Mayor, M., Bonfils, X., Forveille, T., Delfosse, X., Udry, S., Bertaux, J. L., Beust, H., Bouchy, F., Lovis, C., Pepe, F., Perrier, C., Queloz, D., & Santos, N. C. (2009), "The HARPS search for southern extra-solar planets XVIII. An Earth-mass planet in the GJ 581 planetary system", *Astronomy & Astrophysics*, vol. 507, no. 1, pp. 487-494.

Mayor, M., Marmier, M., Lovis, C., Udry, S., Ségransan, D., Pepe, F., Benz, W., Bertaux, J. L., Bouchy, F., Dumusque, X., LoCurto, G., Mordasini, C., Queloz, D., & Santos, N. C. (2011), "The HARPS search for southern extra-solar planets XXXIV. Occurrence, mass distribution and orbital properties of super-Earths and Neptune-mass planets", *Astronomy & Astrophysics* (submitted). *arXiv:1109.2497*.

Mayor, M., Queloz, D. (1995), "A Jupiter-mass companion to a solar-type star", *Nature*, 378(6555), pp. 355-359.

Montañés-Rodríguez, P., Pallé, E., Goode, P. R., & Martin-Torres, F. J. (2006), "Vegetation signature in the observed globally integrated spectrum of Earth considering simultaneous cloud data: Applications for extrasolar planets", *Astrophysical Journal*, vol. 651, no. 1, pp. 544-552.

Montero-Calasanz, M. D. et al. (2014), "Geodermatophilus poikilotrophi sp nov.: A Multitolerant Actinomycete Isolated from Dolomitic Marble", *Biomed Research International*, Article ID 914767, 11 pages.

Normand, P. (2006), "Geodermatophilaceae fam. nov., a formal description", *International Journal of Systematic and Evolutionary Microbiology*, vol. 56, pp. 2277-2278.

O'Malley-James, J. T., Raven, J. A., Cockell, C. S., & Greaves, J. S. (2012), "Light and Life: Exotic Photosynthesis in Binary Star Systems", *Astrobiology*, vol. 12, no. 2.

Pallé, E., Ford, E. B., Seager, S., Montañés-Rodríguez, P., & Vazquez, M. (2008), "Identifying the rotation rate and the presence of dynamic weather on extrasolar earth-like planets from photometric observations", *Astrophysical Journal*, vol. 676, no. 2, pp. 1319-1329.

Pavlov, A. A., Brown, L. L., & Kasting, J. F. (2001), "UV shielding of NH3 and O-2 by organic hazes in the Archean atmosphere", *Journal of Geophysical Research-Planets*, vol. 106, no. E10, pp. 23267-23287.

Pepe, F., Lovis, C., Ségransan, D., Benz, W., Bouchy, F., Dumusque, X., Mayor, M., Queloz, D., Santos, N. C., & Udry, S. (2011), "The HARPS search for Earth-like planets in the habitable zone I. Very low-mass planets around HD 20794, HD 85512, and HD 192310", *Astronomy & Astrophysics*, vol. 534.

Petigura E.A., Howard A.W., Marcy G.W. (2013), "Prevalence of Earthsize planets orbiting Sun-like stars", *Proc Natl Acad Sci USA*, 110(48): 19273–19278.

Pikuta, E. V., Hoover, R. B., & Tang, J. (2007), "Microbial extremophiles at the limits of life", *Critical Reviews in Microbiology*, vol. 33, no. 3, pp. 183-209.

Rauer, H., et al. 2014, *Experimental Astronomy*, in press, arXiv:1310.0696.

Ricker, G. R., et al. 2014, in *SPIE Conference Series*, vol. 9143, 20.

Rothschild, L. J. & Mancinelli, R. L. (2001), "Life in extreme environments", *Nature*, vol. 409, no. 6823, pp. 1092-1101.

Rothschild, L. J. (2008), "The evolution of photosynthesis... again?", *Philosophical Transactions of the Royal Society B-Biological Sciences*, vol. 363, no. 1504, pp. 2787-2801.

Rothschild, L. J. (2009), "A biologist's guide to the solar system", in *Exploring the Origin, Extent, and Future of Life: Philosophical, Ethical, and Theological Perspectives*, C. Bertka, ed., Cambridge University Press, pp. 113-142.

Roy, P. S. (1989), "Spectral Reflectance Characteristics of Vegetation and Their Use in Estimating Productive Potential", *Proceedings of the Indian Academy of Sciences-Plant Sciences*, vol. 99, no. 1, pp. 59-81.

Sagan, C., Thompson, W. R., Carlson, R., Gurnett, D., & Hord, C. (1993), "A Search for Life on Earth from the Galileo Spacecraft", *Nature*, vol. 365, no. 6448, pp. 715-721.

Saunderson, J. L. (1942), "Calculation of the color of pigmented plastics", *Journal of the Optical Society of America*, vol. 32, no. 12, pp. 727-736.

Schopf, J.W. (1999), *Cradle of Life, The Discovery of the Earth's Oldest Fossils*, Princeton University Press, Princeton, NJ.

Schroeder, W. A. & Johnson, E. A. (1993), "Antioxidant Role of Carotenoids in *Phaffia rhodozyma*", *Journal of General Microbiology*, vol. 139, pp. 907-912.

Seager, S., Turner, E. L., Schafer, J., & Ford, E. B. (2005), "Vegetation's red edge: A possible spectroscopic biosignature of extraterrestrial plants", *Astrobiology*, vol. 5, no. 3, pp. 372-390.

Seager, S., (2013), "Exoplanet Habitability", *Science*, vol. 340, pp. 577-581.

Segura, A., Krelove, K., Kasting, J. F., Sommerlatt, D., Meadows, V., Crisp, D., Cohen, M., & Mlawer, E. (2003), "Ozone concentrations and ultraviolet fluxes on Earth-like planets around other stars", *Astrobiology*, vol. 3, no. 4, pp. 689-708.

Segura, A., Meadows, V. S., Kasting, J., Cohen, M., & Crisp, D. (2007), "Abiotic production of O2 and O3 on high CO2 terrestrial atmospheres", *Astrobiology*, vol. 7, no. 3, pp. 494-495.

Selsis, F., Kasting, J. F., Levrard, B., Paillet, J., Ribas, I., & Delfosse, X. (2007), "Habitable planets around the star Gliese 581?", *Astronomy & Astrophysics*, vol. 476, no. 3, pp. 1373-1387.

Sims, D. A. & Gamon, J. A. (2002), "Relationships between leaf pigment content and spectral reflectance across a wide range of species, leaf structures and developmental stages", *Remote Sensing of Environment*, vol. 81, no. 2-3, pp. 337-354.

Singaravelan, N. et al. (2008), "Adaptive Melanin Response of the Soil Fungus *Aspergillus niger* to UV Radiation Stress at 'Evolution Canyon', Mount Carmel, Israel", *Plos One*, vol. 3, no. 8.

Southam, G., Rothschild, L. J., & Westall, F. (2007), "The geology and habitability of terrestrial planets: Fundamental requirements for life", *Space Science Reviews*, vol. 129, no. 1-3, pp. 7-34.

Tinetti, G., Meadows, V. S., Crisp, D., Fong, W., Fishbein, E., Turnbull, M., & Bibring, J. P. (2006), "Detectability of planetary characteristics in disk-averaged spectra. I: The Earth model", *Astrobiology*, vol. 6, no. 1, pp. 34-47.

Traub, W. A. & Jucks, K. W. (2002), "A Possible Aeronomy of Extrasolar Terrestrial Planets", in *Atmospheres in the Solar System: Comparative Aeronomy*, Geophysical Monograph 130 edn, M. Mendillo, A. Nagy, & J. H. Waite, eds., American Geophysical Union, p. 369.

Traub, W. A. (2003a), "The Colors of Extrasolar Planets", *Scientific Frontiers in Research on Extrasolar Planets, ASP Conference Series*, vol. 294, pp. 595-602.

Traub, W. A. (2003b), "Extrasolar planet characteristics in the visible wavelength range", *In: Proceedings of the Conference on Towards Other Earths: DARWIN/TPF and the Search for Extrasolar Terrestrial Planets, 22-25 April 2003, Heidelberg, Germany.* pp. 231-239.

Traub, W. A. (2012), "Terrestrial, Habitable-Zone Exoplanet Frequency from Kepler", *ApJ*, 745, 20.

Udry, S., Bonfils, X., Delfosse, X., Forveille, T., Mayor, M., Perrier, C., Bouchy, F., Lovis, C., Pepe, F., Queloz, D., & Bertaux, J. L. (2007), "The HARPS search for southern extra-solar planets - XI. Super-Earths (5 and 8 M_Earth) in a 3-planet system", *Astronomy & Astrophysics*, vol. 469, no. 3, p. L43-L47.

Venkateswaran, A., McFarlan, S. C., Ghosal, D., Minton, K. W., Vasilenko, A., Makarova, K., Wackett, L. P., & Daly, M. J. (2000), "Physiologic determinants of radiation resistance in Deinococcus radiodurans", *Applied and Environmental Microbiology*, vol. 66, no. 6, pp. 2620-2626.

Wolszczan, A., Frail, D. A. (1992), "A planetary system around the millisecond pulsar PSR1257+12", *Nature*, 355(6356), pp. 145-147.

Woolf, N. J., Smith, P. S., Traub, W. A., & Jucks, K. W. (2002), "The spectrum of earthshine: A pale blue dot observed from the ground", *Astrophysical Journal*, vol. 574, no. 1, pp. 430-433.